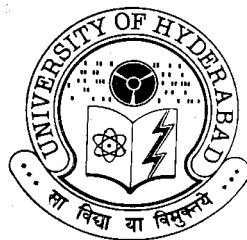


HETEROSYNTHONS IN CRYSTAL ENGINEERING

**A Thesis
Submitted for the Degree of
Doctor of Philosophy**

**By
PEDDY VISHWESHWAR**



**School of Chemistry
University of Hyderabad
Hyderabad 500 046
India**

July 2003

STATEMENT

I hereby declare that the matter embodied in this thesis entitled "**Heterosynthons in Crystal Engineering**" is the result of investigations carried out by me in the School of Chemistry, University of Hyderabad under the supervision of Prof. Ashwini Nangia.

In keeping with the general practice of reporting scientific observations due acknowledgements have been made wherever the work described is based on the findings of other investigators.

Hyderabad
July 2003

Peddy Vishweshwar

CERTIFICATE

Certified that the work "**Heterosynthons in Crystal Engineering**" has been carried out by **Peddy Vishweshwar** under my supervision and that the same has not been submitted elsewhere for a degree.

Dean

School of Chemistry

Prof. Ashwini Nangia

Thesis Supervisor

ACKNOWLEDGEMENT

I wish to express my deep sense of gratitude and profound thanks to my supervisor, **Prof. Ashwini Nangia** for introducing me to this fascinating multi-faceted field of research. I have been able to learn a great deal from him and consider my association with him to be a rewarding experience.

It is my pleasure to thank Prof. Gautam R. Desiraju for his helpful guidance and constant encouragement throughout my Ph.D. tenure. I have been fortunate to have inspiring discussions with him.

I would like to thank Dr. Vincent M. Lynch, University of Texas, Austin, U.S.A., Prof. Roland Boese, University of Essen, Germany, Prof. Mariusz Jaskólski, A. Mickiewicz University, Poland, Prof. Judy Flippen–Anderson, Naval Research Laboratory, Washington DC, U.S.A., for assistance with X-ray data collection on the various crystals studied in this thesis. I also thank Prof. Judith A.K. Howard, University of Durham, U.K. and Dr. Sax A. Mason, Institut Laue Langevin, France, for extending the ILL facility to collect variable temperature neutron diffraction on the tetra-acid studied in Chapter 4. I thank Dr. J.A.R.P. Sarma, gvk bioSciences Pvt. Ltd., Hyderabad and Dr. B. Gopalakrishnan, Tata consultancy services, Hyderabad for helpful discussions.

I thank the former Deans and the present Dean, School of Chemistry, Prof. E.D. Jemmis, and all the faculty members of the School for their cooperation on various occasions.

I also thank all the staff of the School of Chemistry and the Computer Centre for their kind help during various occasions.

I wish to thank my friendly and cooperative labmates Drs. P.S. Chandrakala, V.R. Thalladi, A. Anthony, N.N.L. Madhavi, T. Ram, S.S. Kuduva, R.K.R. Jetti, A.K. Varma, S. Sarkhel, V.S.S. Kumar and P.K. Thallapally, Messrs. V. Venu, G.

Sumod, K.V.V.M. Sairam, P. Narender, Sreenivas Reddy, Balakrishna, Srinivas, Srinivasulu, Binoy, Malla Reddy, Rahul, Aparna, Sunil, Dinabandhu, Archan, Prashanth, Ravi and Jeevan for creating a cheerful work atmosphere. My stay on this campus has been pleasant with the association of Drs. Srinivas, Rajesh, Dharmarao, Bandaru, Giribabu, Messrs. Phani, Shiva, Sastri, Raghu, Sampath, Jagan, Bhanu, Rajashekar, Kommana, Jayapal, Srivardhan, Bhasker, Raghavaiah, Ashok, Vamsee, Shankaran, Mahipal, Pavan, Mrs. Subbalakshmi and Aruna.

I wish to thank my M.Sc. friends Srihari, Rajender, Radhakishan, Naveen, Sreedhar, Ch. Srinivas, Khanna for their encouragement.

I wish to record my grateful thanks to CSIR, New Delhi for fellowship support. I thank the DST for providing National Single Crystal X-ray Diffractometer facility at University of Hyderabad.

I am very thankful to Dr. T. Ram for his support and encouragement.

A special note of thanks to Phani, Senthil, Praveen, Venu and Sairam for their support and pleasant company during my research tenure.

It would be too formal to thank my bosom friends Messrs. Venu, Ravi and Giri for their encouragement.

The blessings and best wishes of my parents, brother, sister, brother-in-law and sister-in-law have made me what I am and I owe everything to them. Last, but certainly not the least, my nieces Vinni, Hanni and Shiva deserve a word of thanks for their smiles.

Vishu

PREFACE

Crystal engineering, the design of organic solids, has emerged as an important cross-disciplinary field of basic and applied endeavour. Recently, three specialized journals, *Crystal Engineering*, *CrystEngComm* and *Crystal Growth & Design*, established by Elsevier Science, Royal Society of Chemistry and American Chemical Society respectively, are entirely devoted to this area of research. Manuscripts specific to crystal engineering are being published on an increasingly regular basis dealing with strategies for synthesis, control of packing and prediction of crystal structures.

Crystal engineering deals with rationalization and synthesis of crystal structures. An organic crystal is the ultimate supermolecule and therefore crystal engineering is a supramolecular equivalent of organic synthesis. The supramolecular synthon concept plays a significant role in crystal design. The utility of the synthon concept, especially heterosynthons in crystal engineering, is illustrated in Chapter 1 and this theme is the crux of this thesis.

Chapter 2 deals with the robust and recurring carboxylic acid–pyridine supramolecular heterosynthon in isomeric methylpyrazine monocarboxylic acids. The persistence of this heterosynthon compared to the more common acid–acid homodimer in these crystal structures has been explained by synthon energy computations. Pyrazine dicarboxylic acids and tetra acid crystallize as dihydrate through $\text{O}_{\text{acid}}\text{--H}\cdots\text{O}_{\text{water}}$ hydrogen bond, a recurring pattern in these acids.

Crystal chemistry of a family of isomeric methylpyrazine carboxamides and pyrazine-2,3-dicarboxamide are examined in Chapter 3. The structure of 5-methylpyrazine-2-carboxamide is isostructural to the α -polymorph of pyrazinamide. A stair case network has been identified in the crystal structure of pyrazine-2,3-dicarboxamide.

A very short $O_{\text{acid}}\text{--H}\cdots O_{\text{water}}$ hydrogen bond in pyrazine-2,3,5,6-tetracarboxylic acid dihydrate is ascribed to the cumulative stabilization from σ - and π -bond cooperativity. This novel hydrogen bond shortening phenomenon is further validated by the variable temperature neutron diffraction study, discussed in Chapter 4.

A proper understanding of the factors that direct hydrogen-bonding motifs when other functional groups are also present in the molecule is discussed in Chapter 5. Five α,ω -alkanedicarboxylic acids (oxalic acid, malonic acid, succinic acid, glutaric acid and adipic acid) crystallize with isonicotinamide in 1:2 stoichiometry according to hierarchy rules of hydrogen bonding. However, glutaric acid and adipic acid also crystallize in 1:1 ratio. Synthon energy computations have been utilized to explain why 1:1 co-crystals are obtained for the weaker acids.

Chapter 6 describes supramolecular synthons in co-crystals of four phenols with isonicotinamide. The hydroxyl group hydrogen bonds to the pyridine nitrogen and the amide group self-assembles as $\text{N--H}\cdots\text{O}$ dimer.

Network structures of cyclohexane-1, 3*cis*, 5*cis*-tricarboxylic acid hydrate and its complex with 4,4'-bipyridine are discussed in Chapter 7. There is a striking similarity of these hydrogen-bonded networks to those found in the crystal structures of trimesic acid and its complex with 4,4'-bipyridine.

Salient crystallographic details of the crystal structures discussed in this thesis are listed in Appendix section. A full list of atomic coordinates has been deposited with University of Hyderabad and can be obtained from Prof. Ashwini Nangia (ansc@uohyd.ernet.in).

Hyderabad

Peddy Vishweshwar

July 2003

CONTENTS

Statement	v
Certificate	vii
Acknowledgement	ix
Preface	xi

CHAPTER ONE

CRYSTAL ENGINEERING

1.1	Introduction	1
1.2	Intermolecular Interactions	4
1.3	Supramolecular Synthons and their Probability of Formation	5
1.4	Hydrogen Bond Rules	8
1.5	Molecular Complexes	10
1.6	Design of Network Structures with Heterosynthons	14
1.7	Supramolecular Synthesis of Functionalised Solids	18
1.7.1	NLO Materials	18
1.7.2	Porous Solids	19
1.8	Polymorphism	20
1.9	References and Notes	21

CHAPTER TWO

CARBOXYLIC ACID–PYRIDINE SUPRAMOLECULAR SYNTHON

2.1	Introduction	27
2.2	Complementarity of Carboxylic Acid with Pyridine Functional Group	29
2.3	Advantages of Single Component Over Binary System	30

2.4	Objective of the Study	31
2.5	5-Methylpyrazine-2-Carboxylic Acid, 2	31
2.6	3-Methylpyrazine-2-Carboxylic Acid, 3	35
2.7	6-Methylpyrazine-2-Carboxylic Acid, 4	35
2.8	Pyrazine-2,5-Dicarboxylic Acid, 11	38
2.9	Hierarchy in Acid–Pyridine Recognition	39
2.10	Supramolecular Synthons in Pyridine and Pyrazine mono and di- Carboxylic Acids: Synthon V vs VII	40
2.11	Restricted Hartree Fock Computation of Charge and Energy	42
2.12	Networks	45
2.12.1	Coordination Polymer and Organic T-Modules: Recent Literature	45
2.12.2	Herringbone Network in 5-Methylpyrazine-2-Carboxylic Acid, 2	48
2.13	Database Analysis	50
2.14	Conclusions	51
2.15	Experimental Section	52
2.16	References and Notes	55

CHAPTER THREE

SUPRAMOLECULAR SYNTHONS IN PYRAZINE CARBOXAMIDES

3.1	Introduction	61
3.2	5-Methylpyrazine-2-Carboxamide, 2	64
3.3	3-Methylpyrazine-2-Carboxamide, 3	68
3.4	6-Methylpyrazine-2-Carboxamide, 4	68
3.5	Staircase Network in Pyrazine-2,3-Dicarboxamide, 5	70
3.6	Cambridge Structural Database Study	73
3.7	Conclusions	74

3.8	Experimental Section	74
3.9	References and Notes	76

CHAPTER FOUR

A VERY SHORT O–H···O HYDROGEN BOND: A NEUTRON STUDY

4.1	Introduction	81
4.2	Cooperativity	84
4.2.1	σ -Bond Cooperativity	84
4.2.2	π -Bond Cooperativity or Resonance Assisted Hydrogen Bonding (RAHB)	86
4.3	A Very Short O–H···O Hydrogen Bond in 1	88
4.4	5,6-Dimethylpyrazine-2,3-Dicarboxylic Acid Dihydrate, 3	93
4.5	X-ray vs Neutron Diffraction	95
4.6	Variable Temperature ND Structures of Tetra Acid, 1	96
4.7	Conclusions	99
4.8	Experimental Section	100
4.9	References and Notes	103

CHAPTER FIVE

HYDROGEN BONDING IN CARBOXYLIC ACID–ISONICOTINAMIDE COMPLEXES

5.1	Introduction	107
5.2	Hierarchic Hydrogen Bonding	109
5.3	Co-crystallization of Isonicotinamide with α,ω -Aliphatic Dicarboxylic Acids	110
5.4	(Oxalic Acid)•(Isonicotinamide) ₂	111
5.4.1	<i>syn</i> -Planar Conformation of Oxalic Acid in OA•(IN) ₂	112

5.5	(Malonic Acid)•(Isonicotinamide) ₂	118
5.6	(Succinic Acid)•(Isonicotinamide) ₂	119
5.7	(Glutaric Acid)•(Isonicotinamide) ₂	120
5.8	(Adipic Acid)•(Isonicotinamide) ₂	121
5.9	(Glutaric Acid)•(Isonicotinamide)	121
5.10	(Adipic Acid)•(Isonicotinamide)	122
5.11	Results and Discussion	123
5.11.1	Synthon Energy Computations	124
5.12	Melting Point Alternation	128
5.13	Conclusions	131
5.14	Experimental Section	132
5.15	References and Notes	134

CHAPTER SIX

HYDROGEN BOND SYNTHONS IN PHENOL–ISONICOTINAMIDE COMPLEXES

6.1	Introduction	139
6.2	(Hydroquinone) _{0.5} •(Isonicotinamide), 1	141
6.3	(Resorcinol)•(Isonicotinamide) ₂ , 2	144
6.4	(Phloroglucinol)•(Isonicotinamide) ₂ •(H ₂ O) ₂ , 3	145
6.5	(4-Hydroxybenzoic Acid)•(Isonicotinamide), 4	147
6.6	Conclusions	150
6.7	Experimental Section	150
6.8	References and Notes	152

CHAPTER SEVEN

HYDROGEN BOND NETWORKS IN CYCLOHEXANE-1, 3*cis*, 5*cis*-TRICARBOXYLIC ACID

7.1	Introduction	157
7.2	A Pseudo-Honeycomb Network in CTA•H ₂ O	159
7.3	Super Pseudo-Honeycomb Network of (CTA) ₂ •(4,4'-bipyridine) ₃ •H ₂ O	166
7.4	Conclusions	170
7.5	Experimental Section	170
7.6	References and Notes	171

Appendix	173
-----------------	-----

About the Author

List of Publications

CHAPTER ONE

CRYSTAL ENGINEERING

1.1 Introduction

Molecules can be simply regarded as a collection of atoms connected by strong covalent bonds (50–100 kcal/mol) that result from partial overlap between atomic orbitals. In chemical reactions, different molecules “interact” with one another by the stepwise breaking and making of covalent bonds. These are relatively slow processes that usually have high kinetic barriers. For more than a century organic chemists have been studying chemical reactions in a systematic way, leading ultimately to the development of a wealth of synthetic methods. Virtually every chemical transformation can nowadays be achieved, and this renders the total synthesis of structurally very complex molecules with molecular weight ≤ 1000 Da, such as taxol or palytoxin, possible.¹ However, the synthesis of molecular structures with molecular weights ≥ 1000 Da through the stepwise formation of covalent bonds generates a formidable challenge with the exception of synthesis of polymeric structures, which uses repetitive reaction sequences. The field of covalent synthesis has perhaps reached the limit of what is synthetically achievable in terms of time requirements and yields.

Molecules can also “interact” with other molecules through weak interactions (0.2–10 kcal/mol), such as hydrogen bonding, van der Waals or dispersive forces, which are collectively known as non-covalent interactions. Such interactions play a key role in fundamental biological processes, such as protein folding or the expression and transfer of genetic information. The universal importance of molecular recognition phenomenon observed in biological systems seriously started to fascinate synthetic chemists in the early 1970s. Inspired by the accidental but inspired discovery of the crown ethers by Pedersen in 1967, the research groups of

Lehn and Cram started to explore the chemistry of synthetic receptors for small charged and neutral molecules. Subsequently, these and other groups (Atwood, Vögtle, Gokel *etc.*) have extended this work to synthetic receptors involving hydrogen bonding and other non-covalent interactions. This novel synthetic approach, also known as “non-covalent synthesis² or supramolecular synthesis” deals with the self-assembly of supermolecules using non-covalent interactions. In supramolecular synthesis, supermolecules are synthesized through the self-assembly of intermolecular interactions in a single step whereas traditional covalent synthesis of complex molecules requires multiple steps. Supramolecular chemistry has grown around Lehn’s analogy³ that “*supermolecules are to molecules and the intermolecular bond what molecules are to atoms and the covalent bond*”. Important characteristics of covalent and non-covalent synthesis are summarized in Table 1.

Table 1. Characteristics of covalent and non-covalent synthesis.

	Covalent Synthesis	Non-covalent Synthesis
Building block	Atoms	Molecules, ions
Target	Molecules	Supermolecule, Crystal
Molecular weight	1–1000 Da	1–100 kDa
Bond type	Covalent	Ionic, hydrophobic, metal coordination, hydrogen bond
Bond energy	50–135 kcal/mol	2–20 kcal/mol
Reaction path	Reactant → Transition state → Product	Molecule → Crystal nucleus → Crystal
Kinetic Stability	High	Low
Components	$\Delta H \gg T\Delta S$	$\Delta H \approx T\Delta S$
Solvent effects	Secondary	Primary
Characteristics	–	Cooperativity

Supramolecular chemistry has developed into two distinct branches: the study of supermolecules in solution and the study of crystals that is solid-state structures. The concepts and principles of recognition and the nature of the interactions that mediate supramolecular construction are nearly the same in solution and in the solid state. However, a distinction does take place in the early stages of development of these two branches, with studies of solution supermolecules being referred to as molecular recognition and those in the solid state as crystal engineering.⁴ Solid-state supramolecular chemistry has taken advantage from X-ray crystallography even as it is well recognized that a crystal is the perfect supermolecule: according to Dunitz, ‘a supermolecule *par excellence*’, an assembly of millions of molecules self-crafted by mutual recognition at an ‘amazing level of precision’.⁵ The concept of crystal engineering was introduced briefly by Pepinsky⁶ in 1955 but conceptualized and elaborated by Schmidt during the period 1950–1971 in the context of organic solid-state photochemical reactions of cinnamic acids and amides.⁷ A broad definition of crystal engineering was suggested by Desiraju in 1989 as “*the understanding of intermolecular interactions in the context of crystal packing and in the utilization of such understanding in the design of new solids with desired physical and chemical properties*”.⁸ The aim of crystal engineering is to establish rigorous connections between molecular and supramolecular structure *via* intermolecular interaction. Crystal engineering is a rapidly growing field because it lies at the intersection of ‘top down’ and ‘bottom up’ technologies for supramolecular materials.⁹

Analysis and design are the two principal components of crystal engineering. Analysis means examination of various intermolecular interactions that govern the crystal packing. This is mainly carried out by the analysis of structural data archived in the Cambridge Structural Database (CSD)¹⁰ and through computational methods. Design involves utilization of the knowledge thus gained in the synthesis of new structures. Crystal engineering is an interdisciplinary field that seeks to develop

protocols for predicting and controlling the structure and thus functional properties of solids. Such properties range from the commonplace (colour, melting point) to those of great relevance to materials scientists and physicists (polarity, porosity, conductivity) and pharmaceutical development (active drug form, bioavailability). Some of the key research areas under the purview of crystal engineering include:¹¹ catalysis, optical materials, conducting and magnetic materials, nanotechnology, electronic materials and sensors, protein-receptor binding, nano and microporous materials, supramolecular devices, molecular modeling and drug design.

1.2 Intermolecular Interactions

The crystal structure of a molecule is the free energy minimum resulting from the optimization of attractive and repulsive intermolecular interactions with varying strengths, directional preferences and distance-dependence properties. Hence, understanding the nature and strength of intermolecular interactions is of fundamental importance in supramolecular chemistry. Intermolecular interactions in organic compounds can be classified as isotropic, medium-range forces, which define molecular shape, size and close packing; and anisotropic, long-range forces, which are electrostatic and involve heteroatom interactions.¹² In general, isotropic forces include $C\cdots C$, $C\cdots H$ and $H\cdots H$ interactions and anisotropic interactions include ionic forces, strongly directional hydrogen bonds ($O-H\cdots O$, $N-H\cdots O$),¹³ weakly directional hydrogen bonds ($C-H\cdots O$, $C-H\cdots N$, $C-H\cdots X$, where X is a halogen, and $O-H\cdots \pi$)¹⁴ and other weak heteroatom interactions¹⁵ such as halogen \cdots halogen, nitrogen \cdots halogen, sulfur \cdots halogen and so on. The observed three-dimensional architecture in the crystal is the result then of the interplay between the isotropic van der Waals forces whose magnitude is proportional to the size of the molecule, and the anisotropic hydrogen bond interactions whose strength are related to the donor atom acidities and acceptor group basicities.

1.3 Supramolecular Synthons and their Probability of Formation

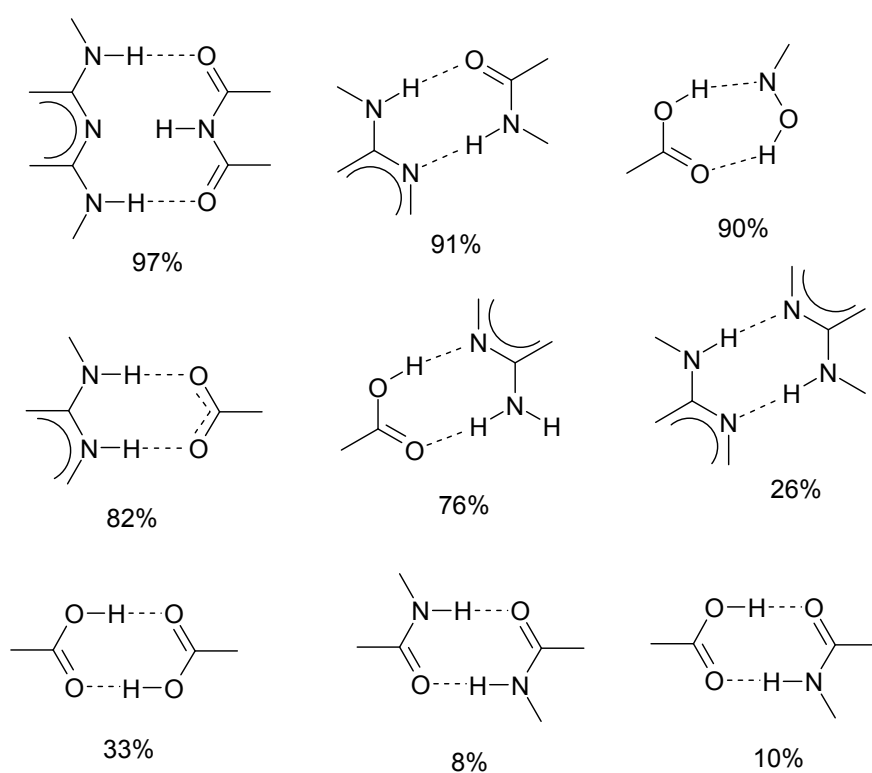
Analysis of individual structures leads to the identification of intermolecular interactions pertaining to a specific structure. The geometrical attributes of intermolecular interactions and their chemical characteristics can be studied reliably by statistical methods. Statistical analysis of a particular interaction in a group of crystal structures lead to useful chemical conclusions.¹⁶ A search of packing motifs that are common to crystal structures of molecules possessing functional groups of interest would be to provide information on molecular association in solids. Implicit in the statistical approach to crystal engineering is an insight into the various ways in which the interactions can be grouped together to form substructural units. These substructural units have been variously termed as motifs, patterns, building blocks or supramolecular synthons. The supramolecular synthon was defined by Desiraju as “*a structural unit within supermolecules, which can be formed and/or assembled by known or conceivable synthetic operations involving intermolecular interactions*”.¹⁷ Knowledge about supramolecular synthon is clearly as important to crystal engineering as is an understanding of reaction mechanisms and reagents in conventional covalent synthesis. It is the smallest structural unit containing the maximum structural information. Accordingly, the supramolecular synthon consists of chemical and geometrical information necessary for the molecular recognition and for the generation of supermolecules.

It is difficult to predict whether or not a hydrogen bond between a potential donor X–H and a potential acceptor A in a given system will actually be formed. One can only define a probability of formation, that is, the fraction of X–H...A hydrogen bonds among the number of such hydrogen bonds that could be formed in principle. This is a global property of the sample, averaged overall chemical and structural situations. Nevertheless, the probability of formation is important for judging if a given type of hydrogen bond is general or exotic. Only if a hydrogen bond or an array

of hydrogen bonds has a reasonably high probability of formation can it be used in rational crystal design. Hydrogen bonds that are formed occasionally will be very difficult to control.

Probabilities of formation can be determined for single hydrogen bonds, as well as for hydrogen bond arrays. From a survey of the CSD, Allen and co-workers¹⁸ have classified 75 bimolecular supramolecular synthons comprising ≤ 20 atoms formed with conventional O–H \cdots O, O–H \cdots N, N–H \cdots O and N–H \cdots N interactions occurring in >12 organic structures. Some of the supramolecular synthons with their probabilities of formation are shown in scheme 1. Recently Steiner studied the formation of hydrogen bonds by the carboxylic acid functional group.¹⁹ Only 33 % of all carboxylic acid groups in crystals donate a hydrogen bond to carboxylic acid acceptors, mostly forming the carboxylic acid dimer. The remaining 67 % form hydrogen bonds with a variety of acceptors. The “relative success” of an alternative acceptor A competing with carboxylic acceptor can be defined as $\text{succ}(A) = n(\text{O} \cdots \text{H} \cdots A) / [n(\text{O} \cdots \text{H} \cdots A) + n(\text{O} \cdots \text{H} \cdots \text{O}_{\text{carboxyl}})]$. Most types of O and N acceptors are more successful in competing for the strong donor than the carboxyl group itself. The success rate was found to be over 90 % for the strongest acceptors like COO^- , $\text{P}=\text{O}$, $\text{N}(\text{Pyridine})$, F^- *etc.* Water is also a very strong competitor with a success rate of 84 %. The probability of formation increases with the number of hydrogen bonds constituting a motif. Whereas “two-point recognition” normally operates only moderately well, three-point recognition is better, and four-point recognition is highly successful.²⁰ The success rates are plotted against mean distances D for O acceptors in Figure 1. There is clear correlation between these quantities, and it should be noticed that even weak acceptors like C–O–C (13 %) and $-\text{NO}_2$ (2 %) have modest chances of attracting the strong carboxylic acid donor. This weakens the general applicability of rules for predicting hydrogen bond modes from hierarchies of donor and acceptor strengths. These studies indicate that the engineering of carboxylic acid

dimer clearly requires the absence of successful competitors. For example, when pyridyl-N atom is present as a competitor; it is much more likely that a carboxylic acid–pyridine heterosynthon is formed (with success rate of 91 %) than a carboxylic acid dimer or catemer. Robustness and recurrence of this heterosynthon is analyzed in Chapter 2 and 5.



Scheme 1. Some examples of supramolecular synthons with their probability of formation (P_m) in crystals.

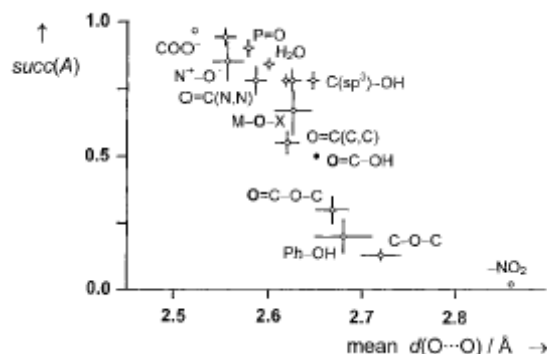


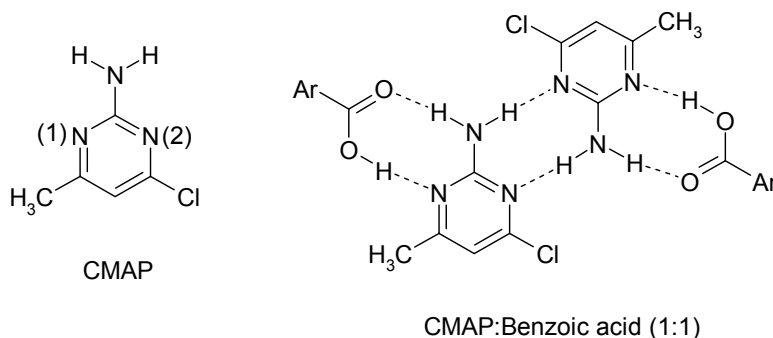
Figure 1. Correlation of the relative success of hydrogen bond acceptors competing for the carboxylic acid donor versus the mean hydrogen bond length. This plot indicates that shorter hydrogen bonds have better chances of being formed in competitive situations.

1.4 Hydrogen-Bond Rules

Elaborating on earlier studies by Robertson and Donohue, three hydrogen bond rules were proposed by Etter for predicting crystal structures of organic molecules. In the case of reasonably strongly hydrogen-bonded systems, in which there is a single interaction that dominates the crystal packing of regularly shaped small molecules, it is possible to make some predictions about the resulting crystal structures. A fundamental rule is that “*all acidic hydrogens available in a molecule will be used in hydrogen bonding in the crystal structure of that compound.*”²¹ A second rule, corresponding to the first one, is that “*all good proton acceptors will be used in hydrogen bonding when there are available hydrogen-bond donors.*”²² The third rule is that “*the best hydrogen-bond donor and the best hydrogen acceptor will preferentially form hydrogen bonds to one another.*”²³ A general rule is that if six-membered ring intramolecular hydrogen bonds can form, they will usually do so in preference to forming intermolecular hydrogen bonds. The hydrogen bond rules provide useful information about the preferred connectivity patterns, hydrogen bond

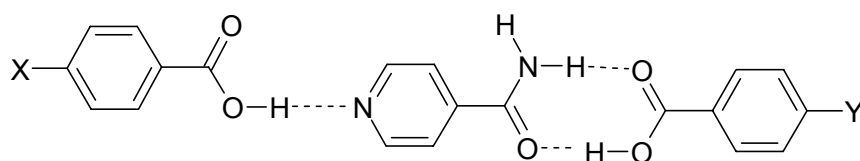
selectivity, and stereoelectronic properties of hydrogen bonds for a particular functional group or for sets of functional groups.

The methods of ranking solid-state hydrogen bond preferences are based on functional group competitions in homomeric crystals or heteromeric co-crystals. The procedure involves analyzing which donors are selected by a limited number of acceptors or *vice versa* during crystallization. For example, it was found that 4-phenyl pyridine and ethyl isonicotinate are both capable of completely separating the acid of lower pK_a value from the one with higher pK_a by co-crystallization. Neutral hydrogen bonded co-crystal form with acid–pyridine synthon between the carboxylic acid and pyridine components.^{23b} It has been also observed that when benzoic acid is co-crystallized with 2-amino-4-chloro-6-methylpyrimidine (CMAP), the best donor, carboxylic acid O–H, preferentially bonded to the best acceptor N(1), whose electron density is enhanced by the electron donating adjacent methyl group. The electron density on N(2) is decreased by the electron withdrawing nature of chlorine atom. Hence, the second best donor, the amine N–H hydrogen bonded to the second best acceptor N(2), thus following the hierarchy of hydrogen bonding.^{23b}



Based on the third postulate, *i.e.*, best donor preferentially hydrogen bonds to the best acceptor followed by second best donor to the second best acceptor, Aakeröy and co-workers have synthesized three ternary co-crystals by offering two different carboxylic acids to the isonicotinamide molecule.²⁴ The stronger acid (lower pK_a , best

donor) interacted preferentially with the best acceptor (the pyridine nitrogen atom) through acid–pyridine recognition and the weaker acid (higher pK_a , second best donor) formed a heteromeric acid–amide motif with the second best acceptor amide carbonyl oxygen.



Best donor.....Best acceptor Second-best acceptor.....Second-best donor
(Stronger acid) (Weaker acid)

They also synthesized around fifteen co-crystals of mono- and di- carboxylic acids with isonicotinamide based on hierarchy of hydrogen bonding.²⁵ However, expected or typical hydrogen-bond patterns may not occur when there are multiple competitive hydrogen bond sites are present. Some of these issues will be discussed in Chapter 5 and 6.

1.5 Molecular Complexes

The current interest in the structural aspects of hydrogen bonds stems from their specificity and directionality. This leads to interactions between different molecular species with well-defined stoichiometry and structure. The complementary of hydrogen bonding functional groups may be utilized for the design of materials with desired physical, chemical or biological properties. Co-crystal is a crystal that contains two or more different molecular species also referred to as molecular complexes. The process of obtaining co-crystals may be thought of as contrary to the general experience that crystallization of a mixture of soluble compounds is an effective method of purification of the components, not a means for obtaining ordered

crystals with a stoichiometry relationship between two or more compounds. Co-crystals have free energy that is lower than that of the individual pure components. Once this condition is fulfilled, there is a driving force for the spontaneous formation of co-crystals. The presence of two compounds with different functional groups can provide the opportunity for the formation of hydrogen bonds between components, which are energetically more favorable than those between like molecules of either component. Intermolecular interactions between different molecules are the basis for the formation of molecular complexes. The analysis of single component crystal structure is useful for studying the structures of ensemble of molecules after association has taken place, while molecular complexation studies are useful for monitoring competitive interactions that determine the selectivity of recognition processes. In other words, molecular complexes generally contain stronger or more specific interactions than does either of the starting materials. A substantial amount of work has been done in this area and some of these studies are particularly relevant in the design of one-, two- and three-dimensional hydrogen bonded networks.

Co-crystals are generally formed by evaporation of solution containing stoichiometric moles of the components, although sublimation and growth from the melt are also used. They can also be prepared by grinding the two solid reagents together. Depending on the rate and vigour of grinding, particle size, and vapor pressures of the reagents, a complete conversion to the new hydrogen-bonded co-crystal phase can be accomplished in the solid state. More often than not, the phase that is obtained is identical with that obtained from the solution crystal growth, implying that solvent is not necessary to direct molecules with strong directional intermolecular interactions into their preferred crystal form. For example, recently Jones and co-workers²⁶ synthesized the molecular complex of cyclohexane-1, 3*cis*, 5*cis*-tricarboxylic acid (CTA) and hexamethylene tetramine (HMTA) simply by grinding both the components in ball mill (mechanochemistry). However, co-

crystallization by simple grinding is not always successful. There was only partial reaction in case of CTA and 4,4'-bipyridine. However, with addition of very small amounts of methanol, co-crystallization is found to be significantly accelerated such that complete conversion is achieved within few minutes. The enhancement in kinetics might be rationalized by the additional degrees of orientational and conformational freedom open to molecules at the various interfaces as well as the enhancement of opportunities for molecular collisions. In addition, tiny co-crystal seeds may be envisaged to form within the solvent during the grinding process so that the rate of co-crystallization can be increased.

The one consistent feature in solid-state co-crystallization is that the two components form stronger hydrogen bonds to one another than to themselves. For example, the carboxylic acid–pyridine heterosynthon has been extensively studied through many binary crystallization experiments.²⁷ Recently our research group^{27a} has shown that this robust heterosynthon can be utilized in the expansion of pseudohoneycomb network of CTA monohydrate using 1,2-*bis*(4,4'-bipyridyl)ethane as a spacer between the acid dimers (Figure 2). The molecular complex forms a parallel triply interpenetrated 2D network.

MacGillivray and his co-workers²⁸ have shown that the co-crystallization technique can be exploited for the photodimerization of olefins. Co-crystallization of 1,8-naphthalenedicarboxylic acid (1,8-nap) with *trans*-1-(3-pyridyl)-2-(4-pyridyl)ethylene (3,4-bpe) gave a discrete molecular solid-state assembly, (3,4-bpe)₂·(1,8-nap)₂, that is held together by acid–pyridine synthon wherein the diacid directs a regiocontrolled [2 + 2] photodimerization, the reaction occurs by way of a single-crystal-to-single-crystal transformation.

Very recently Boese *et. al.*,²⁹ have shown that when gas is cooled in the presence of a solvent under elevated pressure, co-crystals may form in which the

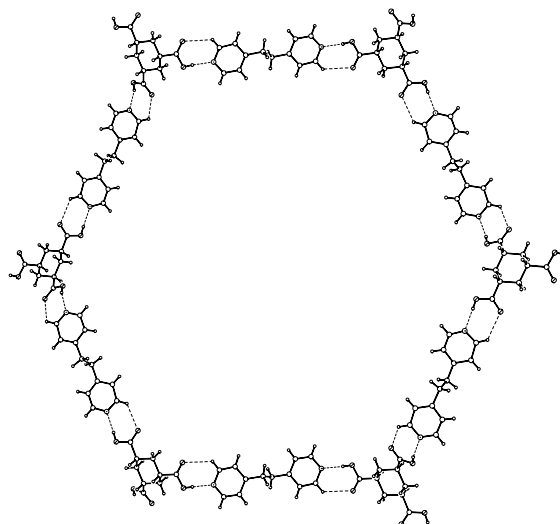


Figure 2. Super honeycomb network of $(\text{CTA})_2 \cdot (1,2\text{-bis}(4,4'\text{-bipyridyl})\text{ethane})_3$ complex built from acid–pyridine heterosynthon. The dimension of the cavity is $36.7 \times 34.1 \text{ \AA}$.

gas molecules act as guests in the lattice of the host solvent molecules. Acetylene gas has been co-crystallized with acetone and dimethyl sulfoxide through *in situ* method. Acetylene and acetone co-crystals have two concomitant phases namely, α and β . In the α -phase the ratio of acetylene and acetone is 1:2, the structure indicates a three-component molecular complex with a dumbbell shape and two almost linear $\text{C-H}\cdots\text{O}$ hydrogen bonds. In the crystal structure these complexes are arranged in a herringbone fashion (Figure 3a). In the β -phase the ratio of acetylene to acetone is 1:1. The molecules are arranged in a zigzag chain with two hydrogen bonds to the oxygen atom of each acetone molecule (Figure 3b). In the molecular complex of acetylene with DMSO, the stoichiometry of acetylene to DMSO is 2:1. The crystal structure shows that it has two-dimensional pseudohoneycomb network of triple acetylene-bridged oxygen atoms is rather open so that neighboring layers can interlock and still leave for a third molecule of acetylene that does not form any

hydrogen bonding. Bond³⁰ also studied the molecular recognition between the low-melting solids, pyrazine and alkanemonocarboxylic acids using *in situ* technique. The co-crystallization method has been exploited to study recognition between multifunctional groups and design of network structures are highlighted in Chapters 5, 6 and 7.

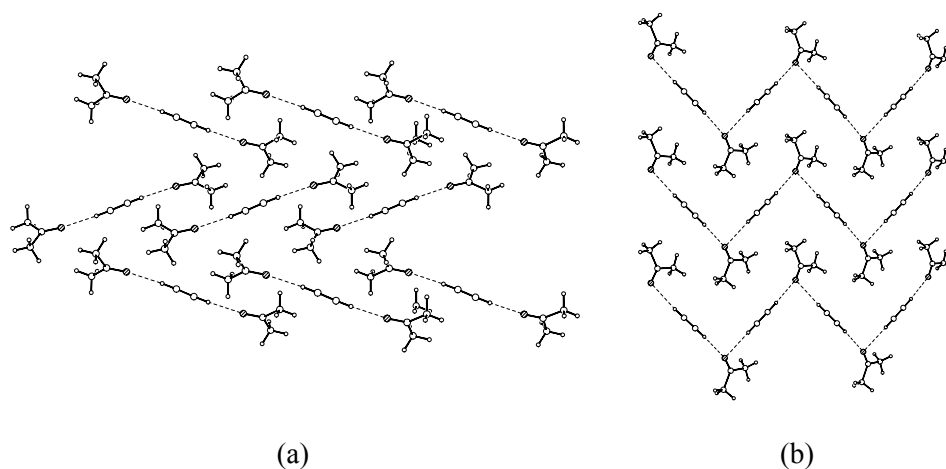


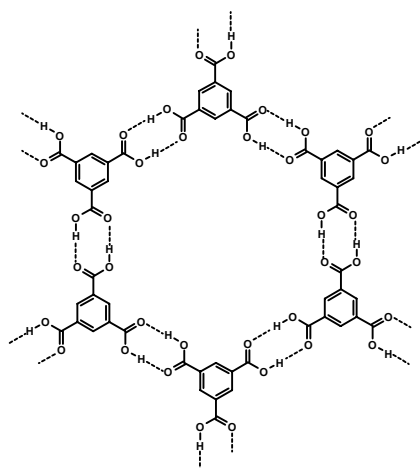
Figure 3. Crystal structures of acetylene and acetone cocrystals. (a) 1:2. (b) 1:1.

1.6 Design of Network Structures with Heterosynthons

The description of crystal structures in terms of networks is one of the most promising of systematic approaches to communicate structural information in a precise fashion.³¹ One conceptual approach to building networks can be carried out by representing molecules as nodes and the intermolecular interactions connecting the molecules as node connectors.³² This method has been applied to understand many organic structures and is very useful in elucidating relationships between different structures.

Hydrogen bonded 2D networks are exemplified by organic molecular networks that are constituted from organic moieties with multiple complementary

terminal functional groups that necessarily assemble into 2D arrays because of their geometric dispositions. For example, benzene-1,3,5-tricarboxylic acid (trimesic acid, TMA) is an important building block in crystal engineering due its predictable 2D honeycomb formation in the crystal. The α -polymorph of trimesic acid³³ contains hexagonal rings made of TMA molecules with a dimensions of approximately 14×14 Å (Scheme 2). An open framework of TMA much like “chicken wire” comprising rings of six molecules of trimesic acid hydrogen bonded together through carboxylic acid dimer. However, the network of TMA results in large holes must be filled if satisfactory packing is to be attained. The filling is accomplished through a mutual interpenetration of different chicken-wire frameworks. Through each hole of one framework pass, at an angle of about 70° , three parallel six-molecule rings of other frameworks, in turn, the original framework is one of three arrays that pass through the holes in the second set of frameworks. In other words, it has four-fold inclined interpenetration. γ -polymorph of TMA also has 4-fold inclined interpenetration³⁴ (Figure 4).



Scheme 2. Schematic diagram of hexagonal network structure with 14×14 Å cavity of TMA.

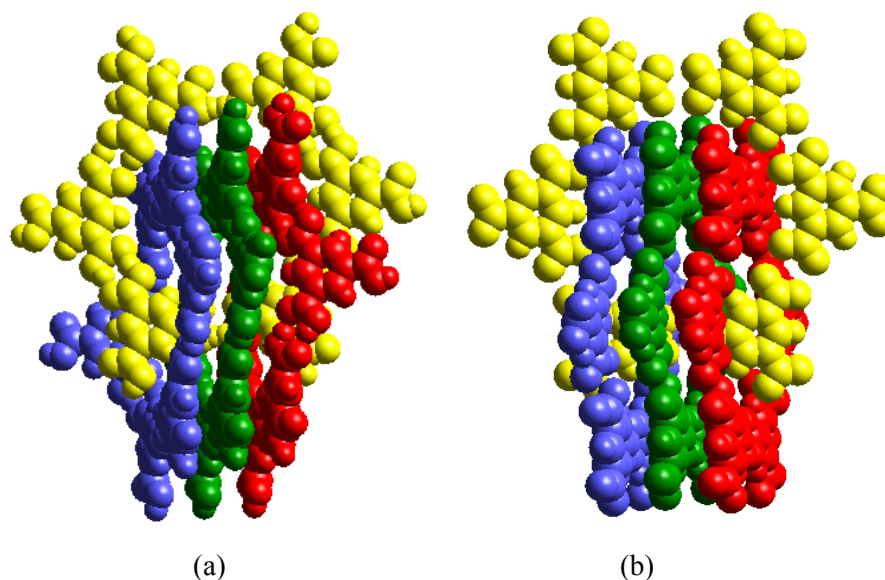


Figure 4. Four-fold inclined interpenetration in TMA. (a) α -polymorph. (b) γ -polymorph.

Zaworotko *et. al.*,³⁵ have reported the crystal structure of TMA–4,4'-bipyridine (2:3) complex, expected to exist as an expanded form of trimesic acid honeycomb network since the carboxylic acid–pyridine heterosynthon is more pronounced than carboxylic acid dimer itself. The bipyridine spacer extends the acid dimer linearly with acid–pyridine heterosynthon from $14 \times 14 \text{ \AA}$ size cavity of TMA network to $35 \times 26 \text{ \AA}$ dimension (Figure 5). However, these large cavities are filled by the three-fold parallel interpenetration of the independent networks, thereby affording a close-packed structure (Figure 6). Chapter 7 describes network structures of cyclohexane-1, 3*cis*, 5*cis*-tricarboxylic acid and its complex with 4,4'-bipyridine. The mode of interpenetration in these crystal structures follow that of the corresponding TMA structures in most respects.

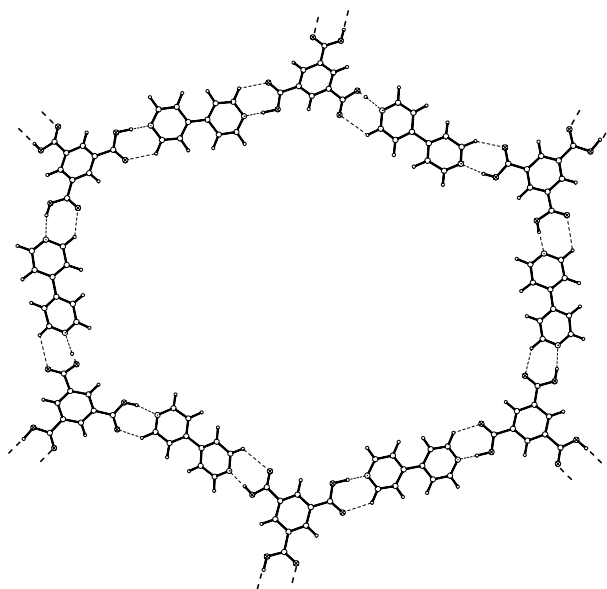


Figure 5. The distorted hexagonal network in TMA•4,4'-bipyridine complex. The cavity size is $35 \times 26 \text{ \AA}$.

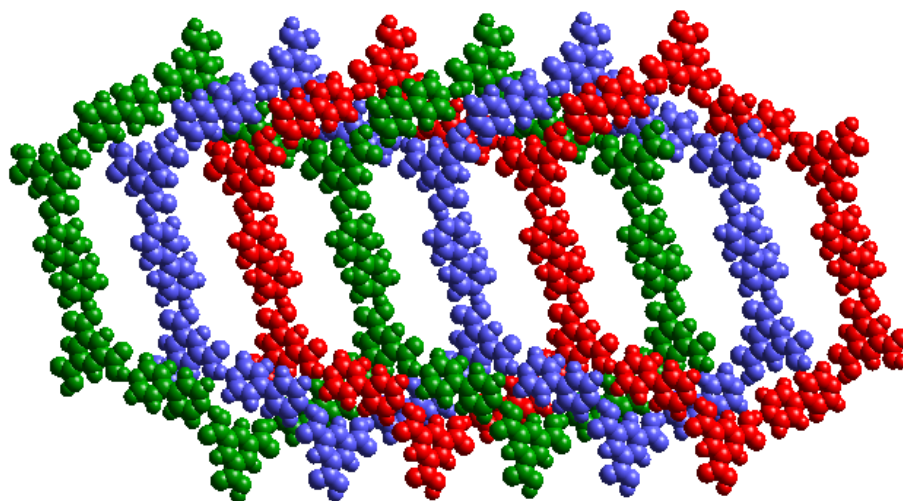


Figure 6. Three-fold two-dimensional chicken-wire networks of TMA•4,4'-bipyridine (2:3).

1.7 Supramolecular Synthesis of Functionalised Solids

The ultimate goal in crystal engineering today is not only the design of specific structures but also engineering functional materials for practical applications³⁶ such as NLO, magnetic materials, microporous solids, telecommunication devices, material for information processing, optical lasers and drug discovery.

1.7.1 NLO Materials

During the last few years, the non-linear optical (NLO) materials have generated great interest for their wide range of applications: second-harmonic generation, frequency mixing, electro-optic modulation, optical parametric oscillation, optical bistability, optical signal processing and optical communications. One of the necessary conditions for second-order nonlinear optical properties is that the bulk materials have no center of symmetry. This property is very difficult to control because the high ground state dipole moment of conjugated molecules tends to align molecules in an anti-parallel fashion and therefore more than 74 % of all organic crystals crystallize in centrosymmetric space groups. To overcome such problem, Lin's group³⁷ have suggested that the diamondoid networks represent an interesting structural motif for the construction of non-centrosymmetric/polar solids because they are not predisposed to pack in centrosymmetric space groups owing to the lack of inversion centers on each tetrahedral connecting point. An intrinsically non-centrosymmetric diamond net will arise if unsymmetrical bridging ligands are used to like tetrahedrally connected metal centers. Furthermore, the use of unsymmetrical bridging ligands also introduces the electronic asymmetry (push-pull effects) that is essential for second-order optical non-linearity. In another approach, Hulliger's group suggested that channel-type inclusion compounds of PHTP hold considerable promise in the design of solids that possess tunable bulk property.³⁸

1.7.2 Porous Solids

The design of organic and inorganic porous solids with controlled sizes and shapes and chemical environments using the principles of crystal engineering has generated enormous interest in recent years because such designer solids may be exploited for separations, shape selective catalysis, and optoelectronic applications.³⁹ The design of porous solids is based on crystal engineering strategies, molecular symmetry carry-over through rigid directional forces, hydrogen bonds or metal coordination bonds such that open porous networks may result. One of the main drawbacks of such an approach is that the open frameworks often tend to interpenetrate.⁴⁰ One way to prevent interpenetration is to build macrocyclic compounds whose covalently closed rings cannot concatenate.⁴¹ New approaches have been identified to overcome the problem of the interpenetration of open networks or close-packing based on the principles that dense or thick two-dimensional sheets cannot interpenetrate and must therefore lie in parallel layers.⁴² One approach has been to use molecules with clumsy shapes that cannot close pack by themselves. Wheel-and-axle or dumb-bell-shaped host with a variable length acetylene 'axle' and adamantane 'wheels', was shown to include a variety of guest species in the open pores.⁴³ For example, Nangia *et. al.*, have designed a new organic host, with the axle built supramolecularly through acid dimer synthon rather than with C–C covalent bonds. Crystallization of *p*-tritylbenzoic acid, form a variety of aromatic solvents, such as xylene, mesitylene, chlorobenzene afford clathrate structures with channels of cross-sectional area 42 and 71 Å². The pore size could be tuned through a large number of edge-to-face and offset face-to-face recognition motifs between the phenyl rings of trityl groups.⁴⁴ The corresponding amide derivative also show host-guest properties.⁴⁵

1.8 Polymorphism

Polymorphism is defined as the phenomenon wherein the same chemical substance exists in different crystal forms.⁴⁶ Mitscherlich recognized the phenomenon of polymorphism in 1822.⁴⁷ Polymorphism gives a clear idea about different ways in which molecules can be arranged to give different crystal structures. Polymorphs have different crystal structures and hence different physical and chemical properties.⁴⁸ The existence of polymorphism implies that kinetic factors are important during crystal nucleation and growth.⁴⁹ Getting the right polymorph is of the utmost importance in drugs, pharmaceuticals, explosives, dyes, pigments, flavors and confectionery products.⁵⁰ The existence of polymorphism implies that free energy differences between different crystalline forms are small (<10 kJ/mol).⁵¹ McCrone states “*the number of forms known for a given compound is proportional to the time and money spent in research on that compound*”.⁵² However, the generality of McCrone’s statement remains unclear despite indications that polymorphism is more general than expected from the CSD. A recent survey of the CSD shows that only 5 % of compounds are classified as polymorphic.⁵³ Desiraju and Sarma demonstrated that the frequency of occurrence of polymorphism modifications is not necessarily uniform in all categories of substances and the phenomenon is probably more common with molecules that have conformational flexibility and/or multiple functional groups capable of hydrogen bonding. Though the phenomenon is well known, it is still difficult to define the idea precisely because of the existence of several sub-classes, such as pseudopolymorphism, conformational polymorphs or tautomeric polymorphs.⁵⁴ When polymorphs crystallize simultaneously in the same flask under identical crystal growth conditions from the same solvent, they are termed as concomitant polymorphs. Polymorphism is a major hurdle in crystal engineering and is a not fully understood phenomenon at the fundamental level. A better understanding of this phenomenon will certainly improve crystal engineering design

strategies. Rationalization of different polymorphs based on the number of possible synthons that a functional group can form is a practical approach to understand this phenomenon. This synthon concept has been utilized to explain the existence of polymorphism in pyrazine carboxamide⁵⁵ and also in 6-amino-2-phenylsulfonylimino-1,2-dihydropyridine.⁵⁶ Chapter 3 describes some features common to the polymorphs of pyrazinamide are observed in the methyl isomers of pyrazinecarboxamide.

1.9 References and Notes

1. (a) K.C. Nicolaou, *Angew. Chem., Int. Ed. Engl.*, **1996**, *35*, 589. (b) J.J. Masters, J.T. Link, L.B. Synder, W.B. Young and S.J. Danishefsky, *Angew. Chem., Int. Ed. Engl.*, **1995**, *34*, 1723. (c) K.C. Nicolaou and R.K. Guy, *Angew. Chem., Int. Ed. Engl.*, **1995**, *34*, 2079. (d) K.C. Nicolaou, D. Vourloumis, N. Winssinger and P.S. Baran, *Angew. Chem., Int. Ed.*, **2000**, *39*, 44. (e) E.J. Corey and X.-M. Cheng, *The Logic of Chemical Synthesis*, Wiley, New York, **1989**. (f) K.C. Nicolaou and E.J. Sorensen, *Classics in Total Synthesis*, VCH, Weinheim, **1995**. (g) S.J. Danishefsky and J.R. Allen, *Angew. Chem., Int. Ed.*, **2000**, *39*, 836.
2. (a) G.M. Whitesides, E.E. Simanek, J.P. Mathias, C.T. Seto, D.N. Chin, M. Mammen and D.M. Gordon, *Acc. Chem. Res.*, **1995**, *28*, 37. (b) M.C.T. Fyfe and J.F. Stoddart, *Acc. Chem. Res.*, **1997**, *30*, 393.
3. J.-M. Lehn, *Supramolecular Chemistry*, VCH, Weinheim, **1995**.
4. G.R. Desiraju and C.V.K. Sharma, *Crystal Engineering and Molecular Recognition. Twin facets of Supramolecular Chemistry. Perspectives in Supramolecular Chemistry, The Crystal as a Supramolecular Entity*, ed. G.R. Desiraju, Wiley, Chichester, **1995**, Vol. 2, 31.
5. J.D. Dunitz, *Pure Appl. Chem.*, **1991**, *63*, 177.
6. R. Pepinsky, *Phys. Rev.*, **1955**, *100*, 971.

7. G.M.J. Schmidt, *Pure Appl. Chem.*, **1971**, 27, 647.
8. G.R. Desiraju, *Crystal Engineering: The Design of Organic Solids*, Elsevier: Amsterdam, **1989**.
9. (a) M.A. Hillmeyer and J.S. Moore, *J. Phys. Org. Chem.*, Special Issue on Materials for the 21st Century, **2000**, 13, 765–879. (b) D.N. Reinhoudt (ed.), *Perspectives in Supramolecular Chemistry*, Vol. 4, Supramolecular Materials and Technologies, Wiley, Chichester, **1999**. (c) M.R. Bryce (ed.), *J. Mater. Chem.*, Special Issue on Molecular Assemblies and Nanochemistry, **1997**, 7, 1069–1290.
10. (a) F.H. Allen, *Acta Crystallogr., Sect. B*, **2002**, 58, 380. (b) A. Nangia, *CrystEngComm*, **2002**, 4, 93.
11. (a) I. Weissbuch, M. Lahav and L. Leiserowitz, *Cryst. Growth Des.*, **2003**, 3, 125. (b) C.V.K. Sharma, *Cryst. Growth Des.*, **2002**, 2, 465.
12. A.I. Kitaigorodski, “*Molecular Crystals and Molecules*,” Academic Press, New York, **1973**.
13. (a) G.A. Jeffrey, *An Introduction to Hydrogen Bonding*, Oxford University Press, Oxford, **1997**. (b) G.A. Jeffrey and W. Saenger, *Hydrogen Bonding in Biological Structures*, Springer, Berlin, **1991**.
14. (a) G.R. Desiraju and T. Steiner, *The Weak Hydrogen Bond in Structural Chemistry and Biology*, Oxford University Press, Oxford, **1999**. (b) G.R. Desiraju, *Acc. Chem. Res.*, **2002**, 35, 565. (c) T. Steiner, *Angew. Chem., Int. Ed.*, **2002**, 41, 48.
15. (a) A. Crihfield, J. Hartwell, D. Phelps, R.B. Walsh, J.L. Harris, J.F. Payne, W.T. Pennington and T. W. Hanks, *Cryst. Growth Des.*, **2003**, 3, 313. (b) E. Bosch and C.L. Branes, *Cryst. Growth Des.*, **2002**, 2, 299. (c) R.B. Walsh, C.W. Padgett, P. Metrangolo, G. Resnati, T.W. Hanks and W.T. Pennington, *Cryst. Growth Des.*, **2001**, 1, 165. (d) Q. Chu, Z. Wang, Q. Huang, C. Yan and S. Zhu, *J. Am. Chem. Soc.*, **2001**, 123, 11069. (e) J.M.A. Robinson, D. Philp, K.D.M. Harris and B.M.

- Kariuki, *New J. Chem.*, **2000**, 24, 799. (f) O. Navon, J. Bernstein and V. Khodorkovsky, *Angew. Chem., Int. Ed. Engl.*, **1997**, 36, 601.
16. F.H. Allen, O. Kennard and R. Taylor, *Acc. Chem. Res.*, **1983**, 16, 146.
 17. G.R. Desiraju, *Angew. Chem., Int. Ed. Engl.*, **1995**, 34, 2311.
 18. F.H. Allen, W.D.S. Motherwell, P.R. Raithby, G.P. Shields and R. Taylor, *New J. Chem.*, **1999**, 23, 25.
 19. T. Steiner, *Acta Crystallogr., Sect. B*, **2001**, 57, 103.
 20. (a) F.H. Beijer, H. Kooijman, A.L. Spek, R.P. Sijbesma and E.W. Meijer, *Angew. Chem., Int. Ed.*, **1998**, 37, 75. (b) C. Schmuck and W. Wienand, *Angew. Chem., Int. Ed.*, **2001**, 40, 4363.
 21. J. Donohue, *J. Phys. Chem.*, **1952**, 56, 502.
 22. M.C. Etter, *J. Am. Chem. Soc.*, **1982**, 104, 1095.
 23. (a) M.C. Etter, *Acc. Chem. Res.*, **1990**, 23, 120. (b) M.C. Etter, *J. Phys. Chem.*, **1991**, 95, 4601.
 24. C.B. Aakeröy, A.M. Beatty and B.A. Helfrich, *Angew. Chem., Int. Ed.*, **2001**, 40, 3240.
 25. (a) C.B. Aakeröy, A.M. Beatty and B.A. Helfrich, *J. Am. Chem. Soc.*, **2002**, 124, 14425. (b) C.B. Aakeröy, A.M. Beatty, B.A. Helfrich and M. Nieuwenhuyzen, *Cryst. Growth Des.*, **2003**, 3, 159.
 26. N. Shan, F. Toda and W. Jones, *Chem. Commun.*, **2002**, 2372.
 27. (a) B.R. Bhogala and A. Nangia, *Cryst. Growth Des.*, **2003**, 3, 547. (b) J.F. Remenar, S.L. Morissette, M.L. Peterson, B. Moulton, J.M. MacPhee, H.R. Guzmán and Ö. Almarsson, *J. Am. Chem. Soc.*, **2003**, 125, 8456. (c) R.D.B. Walsh, M.W. Bradner, S. Fleischman, L.A. Morales, B. Moulton, N. Rodriguez-Hornedo and M.J. Zaworotko, *Chem. Commun.*, **2003**, 186. (d) N. Shan, A.D. Bond and W. Jones, *Cryst. Eng.*, **2002**, 5, 9.

28. D.B. Varshney, G.S. Papaefstathiou and L.R. MacGillivray, *Chem. Commun.*, **2002**, 1964.
29. R. Boese, M.T. Kirchner, W.E. Billups and L.R. Norman, *Angew. Chem., Int. Ed.*, **2003**, 42, 1961.
30. A.D. Bond, *Chem. Commun.*, **2003**, 250.
31. (a) M. Eddaoudi, D.B. Moler, H. Li, B. Chen, T.M. Reineke, M. O'keffe and O.M. Yaghi, *Acc. Chem. Res.*, **2001**, 34, 319. (b) B. Moulton and M.J. Zaworotko, *Chem. Rev.*, **2001**, 101, 1629. (c) S.R. Batten, *CrystEngComm*, **2001**, 18, 1. (d) S.R. Batten and R. Robson, *Angew. Chem., Int. Ed. Engl.*, **1998**, 37, 1460.
32. (a) G.R. Desiraju, *Chem. Commun.*, **1997**, 1475. (b) M.J. Zaworotko, *Chem. Commun.*, **2001**, 1.
33. (a) D.J. Duchamp and R.E. Marsh, *Acta Crystallogr., Sect. B*, **1969**, 25, 5. (b) F.H. Herbstein, in *Comprehensive Supramolecular Chemistry*, eds., D.D. MacNicol, F. Toda and R. Bishop, Pergamon, Oxford, **1996**, Vol. 6, pp. 61–83.
34. F.H. Herbstein, M. Kapon and G.M. Reisner, *Acta Crystallogr., Sect. B*, **1985**, 41, 348.
35. C.V.K. Sharma and M.J. Zaworotko, *Chem. Commun.*, **1996**, 2655.
36. (a) K.T. Holman, A.M. Pivovar, J.A. Swift and M.D. Ward, *Acc. Chem. Res.*, **2001**, 34, 107. (b) M.J. Zaworotko, *Angew. Chem., Int. Ed.*, **2000**, 39, 220. (c) P.J. Langley and J. Hulliger, *Chem. Soc. Rev.*, **1999**, 28, 279. (d) T.J. Barton, L.M. Bull, W.G. Klemperer, D.A. Loy, B. McEnaney, M. Misono, P.A. Monson, G. Pez, G.W. Scherer, J.C. Vartuli and O.M. Yaghi, *Chem. Mater.*, **1999**, 11, 2633. (e) J. Zyss and J.-F. Nicoud, *Curr. Opin. Solid State Mater. Sci.*, **1996**, 1, 533. (f) O. Kahn, *Curr. Opin. Solid State Mater. Sci.*, **1996**, 1, 547. (g) N. Bowden, A. Rerfort, J. Carbeck and G.M. Whitesides, *Science*, **1997**, 276, 233. (h) C.F.V. Nostrum and R.J.M. Nottle, *Chem. Commun.*, **1996**, 2385.

37. O.R. Evans and W. Lin, *Chem. Mater.*, **2001**, *13*, 2705.
38. J. Hulliger, P. Robin, A. Quintel, P. Rechsteiner, O. König and M. Wubbenhorst, *Adv. Mater.*, **1997**, *9*, 662.
39. (a) O.R. Evans and W. Lin, *Acc. Chem. Res.*, **2002**, *35*, 511. (b) M. Eddaoudi, D.B. Moler, H. Li, B. Chen, T.M. Reineke, M. O'Keeffe and O.M. Yaghi, *Acc. Chem. Res.*, **2001**, *34*, 319. (c) K.T. Holman, A.M. Pivovar, J.A. Swift and M.D. Ward, *Acc. Chem. Res.*, **2001**, *34*, 107. (d) A. Nangia, *Curr. Opin. Solid State Mater. Sci.*, **2001**, *5*, 115. (e) S.T. Nguyen, D.L. Gin, J.T. Hupp and X. Zhang, *PNAS*, **2001**, *98*, 11849.
40. S.R. Batten and R. Robson, *Angew. Chem., Int. Ed.*, **1998**, *37*, 1460.
41. D. Venkataraman, S. Lee, J. Zhang and J.S. Moore, *Nature*, **1994**, *371*, 1941.
42. V.A. Russell, C.C. Evans, W. Li and M.D. Ward, *Science*, **1997**, *276*, 575.
43. T. Müller, J. Hulliger, W. Seichter, E. Weber, T. Weber and M. Wubbenhorst, *Chem. Eur. J.*, **2000**, *6*, 54.
44. R.K.R. Jetti, F. Xue, T.W.S. Mak and A. Nangia, *J. Chem. Soc., Perkin Trans. 2*, **2000**, 1223.
45. C.M. Reddy, A. Nangia, C. Lam and T.C.W. Mak, *CrystEngComm*, **2002**, *4*, 323.
46. (a) J. Bernstein, *Polymorphism in Molecular Crystals*, Clarendon Press, Oxford, **2002**. (b) R.J. Davey, *Chem. Commun.*, **2003**, 1463. (c) J. Bernstein, R.J. Davey and J.-O. Henck, *Angew. Chem., Int. Ed.*, **1999**, *38*, 3440. (d) T.L. Threllfall, *Analyst*, **1995**, *120*, 2435.
47. E. Mitscherlich, *Ann. Chim. Phys.*, **1822**, *19*, 350.
48. T. Siegrist, C. Kloc, J.H. Schön, B. Batlogg, R.C. Haddon, S. Berg and G.A. Thomas, *Angew. Chem., Int. Ed.*, **2001**, *40*, 1732.
49. M.R. Caira, *Top. Curr. Chem.*, **1998**, *198*, 164–208.

50. (a) G. Klebe, F. Graser, E. Hädicke and J. Berndt, *Acta Crystallogr., Sect. B*, **1989**, 45, 69. (b) I. Bar and J. Bernstein, *J. Pharm. Sci.*, **1985**, 74, 255. (c) S.R. Byrn, *Solid State Chemistry of Drugs*, Academic Press, New York, **1982**, 79.
51. A. Gavezzotti and G. Fillippini, *J. Am. Chem. Soc.*, **1995**, 117, 12299.
52. W.C. McCrone, *Polymorphism in Physics and Chemistry of the Organic Solid State*; eds. D. Fox, M.M. Labes and A. Weisemberg, Interscience, New York, **1965**, 726.
53. J.A.R.P. Sarma and G.R. Desiraju, *Crystal Engineering: The Design and Application of Functional Solids*; eds., M.J. Zaworotko and K.R. Seddon, Kluwer: Dordrecht, **1999**, 325.
54. (a) V.S.S. Kumar, S.S. Kuduva and G.R. Desiraju, *J. Chem. Soc., Perkin Trans. 2*, **1999**, 1069. (b) V.S. Kumar, A. Addlagatta, A. Nangia, W.T. Robinson, C.K. Broder, R. Mondal, I.R. Evans, J.A.K. Howard and F.H. Allen, *Angew. Chem., Int. Ed.*, **2002**, 41, 3848.
55. G.R. Desiraju, *Science*, **1997**, 278, 404.
56. R.K.R. Jetti, R. Boese, J.A.R.P. Samra, L.S. Reddy, P. Vishweshwar and G.R. Desiraju, *Angew. Chem., Int. Ed.*, **2003**, 42, 1963.

CHAPTER TWO

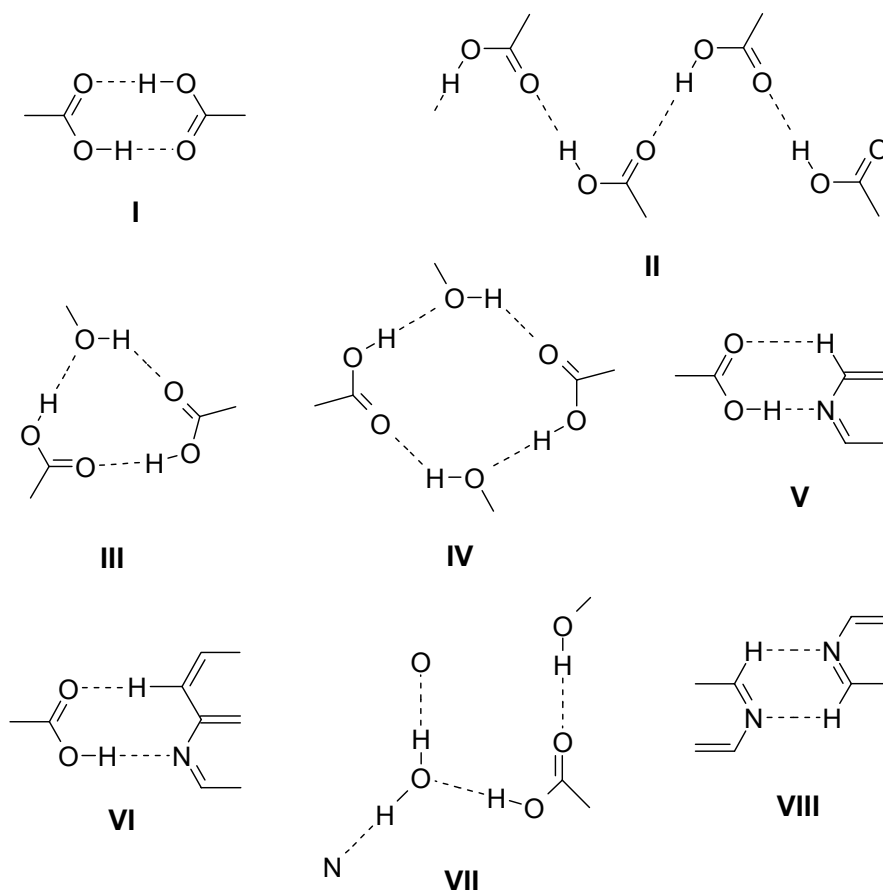
CARBOXYLIC ACID–PYRIDINE SUPRAMOLECULAR SYNTHON

2.1 Introduction

Crystal engineering is the design and construction of target crystal structures from molecular components.¹ It is a type of non-covalent synthesis of target crystal structures with hydrogen bonding as the key recognition element between molecules.² A crystal structure may be analyzed in terms of supramolecular synthons³ and crystal engineering carried out by the identification of a molecular skeleton with specific functional groups that will predictably and persistently lead to robust synthons and therefore to the desired crystal structure. The repeating array in a crystal structure may be a single interaction, a small pattern, or a larger pattern. The subjective distinction between a pattern and a supramolecular synthon is based on its frequency of occurrence and is thus related to its reliability as an indicator of crystal packing. If a pattern appears repeatedly enough, then it may more confidently be termed as a synthon. The more often a synthon occurs within a family or across families of compounds, the more robust and useful it is in crystal design.

Carboxylic acids are among the most common hydrogen bond functionalities in crystal engineering.⁴ The crystal packing patterns of various carboxylic acids have been examined in depth and thus they are considered as the most important building blocks in deliberate crystal design. Since they possess a hydrogen bond donor as well as an acceptor site, carboxylic acids are well-known to form centrosymmetric dimer **I** as the dominant recognition motif; however, hydrogen bond catemer **II**, and singly/doubly bridged aggregation motifs **III** and **IV** incorporating one or two alcohol (or water) molecules are also known (scheme 1).^{4b}

Formation of motif **I** is not very reliable and in competitive situations, it is often displaced by other hydrogen bond configurations. In a recent database analysis,



Scheme 1. Hydrogen bond synthons of carboxylic acid discussed in this chapter.

Allen *et.al.* determined the global probabilities of formations of 75 bimolecular hydrogen bonded ring synthons in organic crystal structures.⁵ Carboxylic acids are the second most common category of molecules archived in the Cambridge Crystallographic Database (CSD). For the carboxylic acid dimer motif **I**, the probability of formation is found to be *only* 33 % averaged over all competitive situations and this relatively low probability is explained by competition with other hydrogen bonded acceptors (*e.g.* COO^- , pyridine N, S=O , P=O). However, the

probability increases to 96 % in mono-carboxylic acids when competing donor and acceptor groups are absent, making synthon **I** a robust and reliable crystal design element.

2.2 Complementarity of Carboxylic Acid with Pyridine Functional Group

Many of the best-known supramolecular synthons rely on the complementarity of two hydrogen-bonding groups. Such complementarity of two motifs has been utilized to synthesise many supramolecular architectures. A perusal of supramolecular synthon schemes^{3,5,6} shows that there are examples of bimolecular motifs with two strong hydrogen bonds or with two weak hydrogen bonds, but motifs with one strong and one weak bond are rare. However, as more crystal structures are deposited in the CSD new hydrogen bond patterns are discovered. A recent database study by Steiner⁷ on carboxyl donors shows that recognition of CO₂H with pyridine is 9 times favoured through O–H⋯N hydrogen bond compared to dimer **I** and catemer **II** motifs with itself. The participation of weak C–H⋯O hydrogen bond between pyridine and acid results in heterodimer ring motif **V**. The study indicates that the acid–acid dimer motif **I** does not generally form when a better acceptor is present in the system. Thus crystal design may be implemented by exploiting robust recognition in a heterosynthon. The carboxylic acid–pyridine synthon is the most reliable supramolecular motif and exploited in crystal engineering to obtain desirable architectures.⁸ Synthon **V** has been used to design liquid-crystalline materials, two-dimensional β -networks and to expand the trimesic acid (TMA) honeycomb network. Furthermore, depending on the pK_a of carboxylic acid and pyridine, O–H⋯N hydrogen bonding will result when $\Delta pK_a < 3.75$ and proton transfer when $\Delta pK_a > 3.75$.^{8f,9} The pK_a of pyrazinic acid **1** is 2.92¹⁰ and pyridine 5.23 giving ΔpK_a of 2.31, a value that is in agreement with O–H⋯N hydrogen bonding observed in these crystal structures. For example, adducts of formic acid with pyridine crystallize as 1:1

molecular complex and also as a 4:1 ionic salt.¹¹ Cyclohexane-1, 3*cis*, 5*cis*-tricarboxylic acid (CTA) forms O–H···N hydrogen bond with 4,4'-bipyridine and 1,2-*bis*(4-pyridyl)ethane whereas proton transfer occurs with 1,2-*bis*(4-pyridyl)ethylene and *trans*-1,4-*bis*(2-(4-pyridyl)ethenyl)benzene.¹² In a variation to synthon V, and containing one strong (O–H···N) and one weak (C–H···O) hydrogen bond, supramolecular assemblies of predictable one- and two-dimensional arrays were constructed using co-crystals of carboxylic acids with phenazine (synthon VI).¹³

2.3 Advantages of Single Component Over Binary System

While binary crystals are excellent systems to study new synthons and their robustness, difficulties in obtaining a particular co-crystal because of mismatched solubility between the two components is a vexing problem. For example, Jones and co-workers^{13b} were interested in mixed crystals of terephthalic acid with phenazine to synthesise molecular tapes but instead had to use malonic acid because solubility considerations favoured complexation with the latter acid. Recently our research group have identified, *trans*-1,4-dithiane-1,4-dioxide as a new spacer ligand for carboxylic acids.¹⁴ The molecule is highly soluble in water but almost insoluble in organic solvents. Only four co-crystals were isolated among a large number of acids used in crystallization experiments even though the acid–sulfoxide synthon is calculated to be more stable than acid–acid and sulfoxide–sulfoxide recognition. This could be because the sulfoxide is strongly hydrogen bonded to water molecules and so it does not form complexes readily. Generally, the more soluble component dictates the choice of complementary molecules in co-crystallization experiments. On the other hand, single component crystals can be recrystallized from a wide variety of solvents depending on the solubility profile of that particular molecule. Therefore one can systematically study crystal-packing characteristics in a family of structures with the same functional group (*e.g.* CO₂H, CONH₂, OH) and different substituents (*e.g.*

alkyl, phenyl, halogen), or with the same substituent in isomeric positions. Crystal engineering studies that deal with functional group \leftrightarrow supramolecular synthon correlation in closely related structures continue to elicit interest from organic and supramolecular chemists.¹⁵ By modifying the nature of donor and acceptor groups in a graded manner through chemical synthesis, it is possible to probe the supramolecular behaviour of a particular synthon in the crystal. The idea in these studies is to find out the extent to which one can perturb the molecule and yet obtain the same or similar crystal packing, and also the limit at which a different hydrogen bond pattern is adopted.

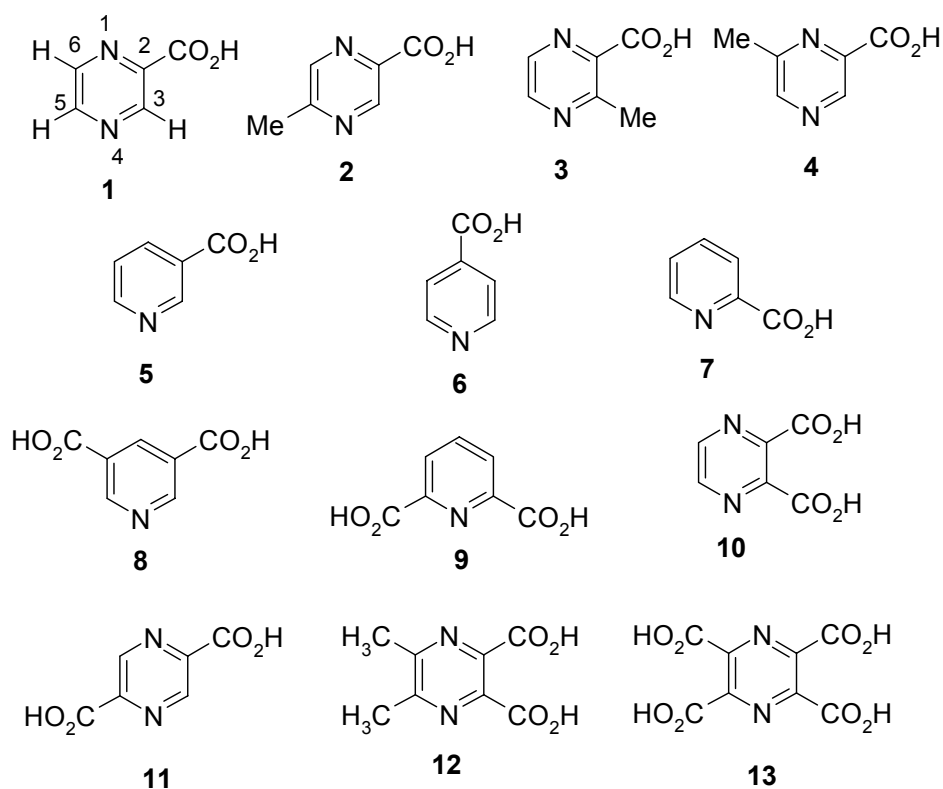
2.4 Objective of the Study

Pyrazine carboxylic acids are exemplified by pyrazinic acid, **1** (scheme 2) a rare category of molecules in the CSD.¹⁶ The crystal structures of acids **2–4** and diacid **11** were determined by single crystal X-ray diffraction with the following objectives: (1) To find out the occurrence of heterosynthon **V** in the family of substituted pyrazinic acids. (2) To examine the formation of O–H \cdots N and C–H \cdots O hydrogen bonds in competing situations of donor acidity and acceptor basicity in the same crystal structure. (3) To calculate the energy of heterodimer **V** and homodimer **I** in order to explain the preference for synthon **V** in the crystal structures of pyridine and pyrazine mono-carboxylic acids. (4) The crystal structure of pyrazine-2,5-dicarboxylic acid **11** contains synthon **VII**, a new motif common to pyrazine di- and tetracarboxylic acids.

2.5 5-Methylpyrazine-2-Carboxylic Acid, **2**

5-Methylpyrazine-2-carboxylic acid, **2** crystallizes in the monoclinic crystal system (space group $P2_1/n$, $Z = 4$). Screw axis related molecules form a zigzag, hydrogen bonded tape along $[0\ 1\ 0]$ with synthon **V**. The metrics of O–H \cdots N and C–

H \cdots O hydrogen bonds are 1.70 Å, 174.3° and 2.49 Å, 129.9°. The hydrogen bonded tapes of synthon **V** are connected through C–H \cdots N dimer¹⁷ **VIII** (2.43 Å, 122.7°) and C–H \cdots O bonds to produce a lamellar structure in the (10 $\bar{2}$) plane (Figure 1). It is likely that the layered structure of **2** is stabilised by a combination of synthon **V** and C–H \cdots O/N hydrogen bonds; the sheets are in turn stacked with slight offset through van der Waals interactions. Six molecules of **2** assemble in a brick-shaped array, with the hydrophobic core occupied by methyl groups of inversion related molecules. The metrics of intermolecular distances are shown in Table 1.



Scheme 2. Pyridine and pyrazine carboxylic acids analyzed in this chapter.

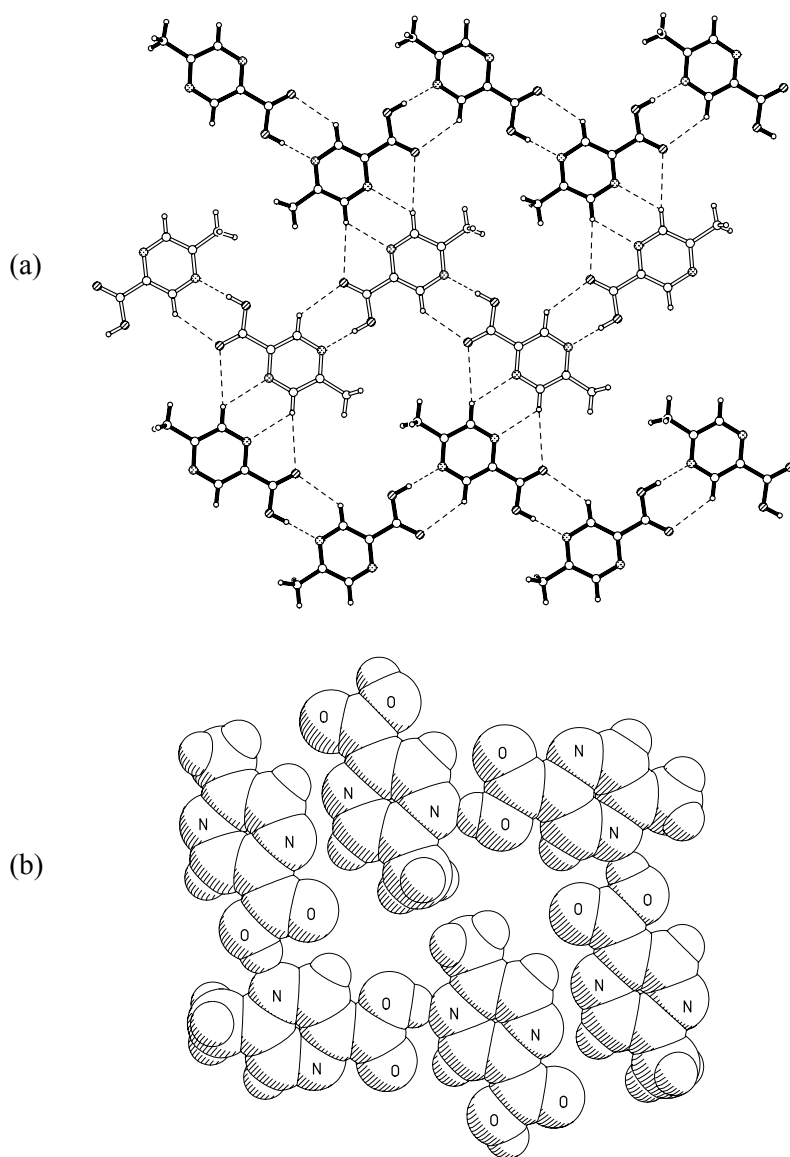


Figure 1. (a) Zigzag hydrogen bonded tapes mediated by synthon **V** along [010] in 5-methylpyrazine-2-carboxylic acid **2**. Inversion related tapes (shaded differently) are connected by C–H···O/N hydrogen bonds (synthon **VIII**). (b) Space-filling representation of six molecules of **2** to show the rectangular array of 12.8×7.4 Å. Methyl groups fill the internal hydrophobic core.

Table 1. Geometrical parameters of selected intermolecular interactions.

Acid	Interaction	d (Å) ^a	D (Å)	θ (°)
1 ^b	O–H \cdots N ^c	1.68	2.66	173.4
	C3–H \cdots O ^c	2.32	3.10	127.2
	C5–H \cdots O	2.33	3.16	132.7
	C6–H \cdots O	2.76	3.68	143.2
	C5–H \cdots N	2.51	3.53	157.2
2	O–H \cdots N ^c	1.70	2.683(1)	174.3
	C3–H \cdots O ^c	2.49	3.294(2)	129.9
	C6–H \cdots O	2.72	3.805(2)	172.1
	C6–H \cdots N	2.43	3.158(2)	122.7
3	O–H \cdots N ^c	1.67	2.655(1)	176.4
	C5–H \cdots O ^c	2.42	3.227(1)	130.1
	C6–H \cdots O	2.37	3.458(1)	175.5
	(Me)C7–H \cdots O	2.76	3.633(1)	137.5
	C6–H \cdots N	2.53	3.224(1)	120.6
4	O–H \cdots N ^c	1.69	2.680(2)	177.5
	C3–H \cdots O ^c	2.39	3.225(2)	132.3
	(Me)C7–H \cdots O	2.54	3.540(2)	152.9
	(Me)C7–H \cdots O	2.49	3.536(2)	160.1
	C5–H \cdots N	2.62	3.658(2)	158.4
11	O–H \cdots O(H ₂ O) ^d	1.54	2.514(1)	170.3
	(H ₂ O)O–H \cdots O ^d	1.88	2.802(1)	153.5
	(H ₂ O)O–H \cdots N ^d	1.88	2.849(2)	165.8
	C3–H \cdots O	2.49	3.452(2)	146.3
12 ^e	O–H \cdots O(H ₂ O) ^d	1.55	2.527(1)	167.2
	(H ₂ O)O–H \cdots O ^d	1.92	2.874(1)	162.4
	(H ₂ O)O–H \cdots N ^d	1.97	2.896(1)	155.1
13 ^e	O–H \cdots O(H ₂ O) ^d	1.50	2.479(1)	170.3
	(H ₂ O)O–H \cdots O ^d	1.74	2.701(1)	162.6
	(H ₂ O)O–H \cdots N ^d	2.01	2.939(2)	156.1

^a O–H and C–H distances are neutron-normalized to 0.983 and 1.083 Å. ^b Ref. 18. ^c Hydrogen bonds in synthon **V**. ^d Hydrogen bonds in synthon **VII**. ^e Ref. 19.

2.6 3-Methylpyrazine-2-Carboxylic Acid, **3**

3-Methylpyrazine-2-carboxylic acid, **3** crystallizes in the monoclinic system with one molecule in the asymmetric unit (space group $P2_1/c$, $Z = 4$). Screw related molecules are assembled with linear tapes of acid–pyridine synthon **V** (1.67 Å, 176.4°; 2.42 Å, 130.1°) along $[1\ 0\ -1]$ direction which are in turn connected by weak centrosymmetric C–H \cdots N dimer motif **VIII** and C–H \cdots O hydrogen bonds (Figure 2). Compared to the brick pattern of **2**, hydrogen bonded molecules of **3** produce a pseudo-hexagonal core that is occupied by methyl groups.

2.7 6-Methylpyrazine-2-Carboxylic Acid, **4**

6-Methylpyrazine-2-carboxylic acid, **4** crystallizes in the polar space group $Pca2_1$ with one molecule in the asymmetric unit ($Z = 4$). Zigzag tapes of 2_1 -related molecules connected by synthon **V** (1.69 Å, 177.5°; 2.39 Å, 132.3°) along $[0\ 0\ 1]$ extend into a pleated sheet through (pyrazine)C–H \cdots N and (methyl)C–H \cdots O hydrogen bonds (Figure 3). Cyclic C–H \cdots N synthon **VIII** is not possible in **4** because *ortho*-substituents flank the second N-atom. (Me)C–H \cdots O and (pyrazine)C–H \cdots N hydrogen bond chains run in opposite directions within a pleated layer. Significantly, adjacent layers stack in a parallel fashion resulting in the non-centrosymmetric, polar crystal structure. In centrosymmetric structures **2** and **3**, the layers stack with the more common anti-parallel alignment. The arrangement of molecules and hydrogen bonding motifs in **4** are similar to the crystal structure of pyrazinic acid **1** ($Pna2_1$, $Z = 4$).¹⁸

In the structure **1**, C5–H is involved in a bifurcated C–H \cdots O/N motif while C6–H makes a long contact (Table 1, Figure 4). In methyl-substituted acid **4**, C5–H is engaged in a C–H \cdots N interaction and C6 position is occupied by methyl group. Thus, replacement of H with Me at the position on the pyrazine ring that is only weakly C–H \cdots O bonded results in minimal structural perturbation. A minor difference between

these structures is that the layer is flat in **1** but pleated in **4**, a structural adjustment that accommodates the bulkier Me group in place of H atom. The above analysis also explains why crystal structures of isomeric acids **2** and **3** are very different and adopt centrosymmetric packing in $P2_1/n$ and $P2_1/c$ space groups. Replacement of H with Me at C3 or C5 position of **1** results in global structural changes because these H atoms are intimately involved in hydrogen bonding.

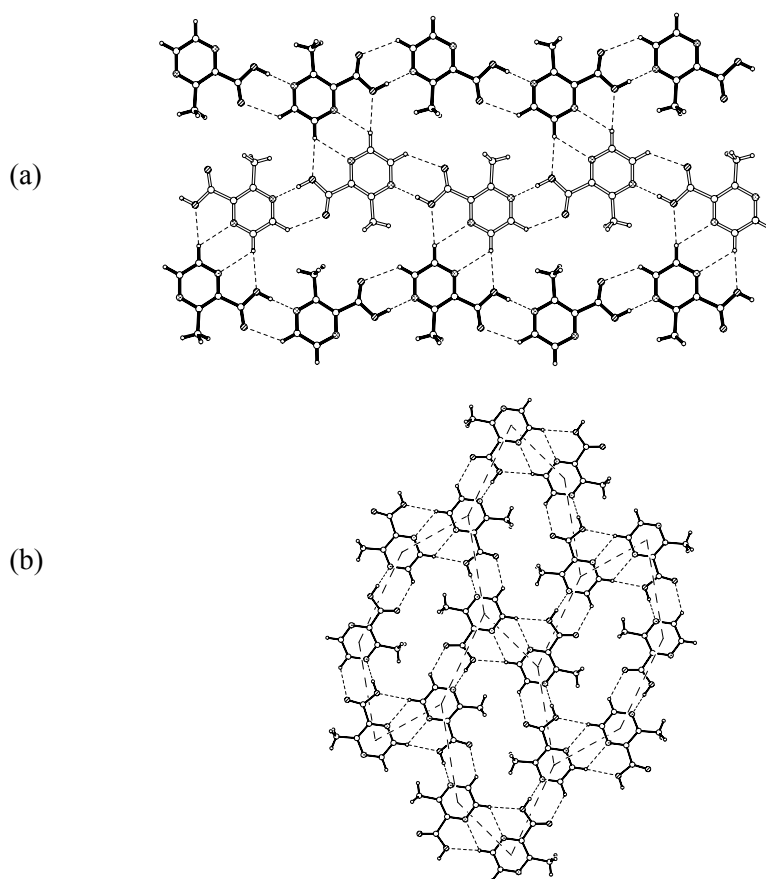


Figure 2. (a) Linear tapes of synthon **V** in 3-methylpyrazine-2-carboxylic acid **3**. Inversion related tapes produce the layer structure in (101). (b) Pseudo-hexagonal network of **3**.

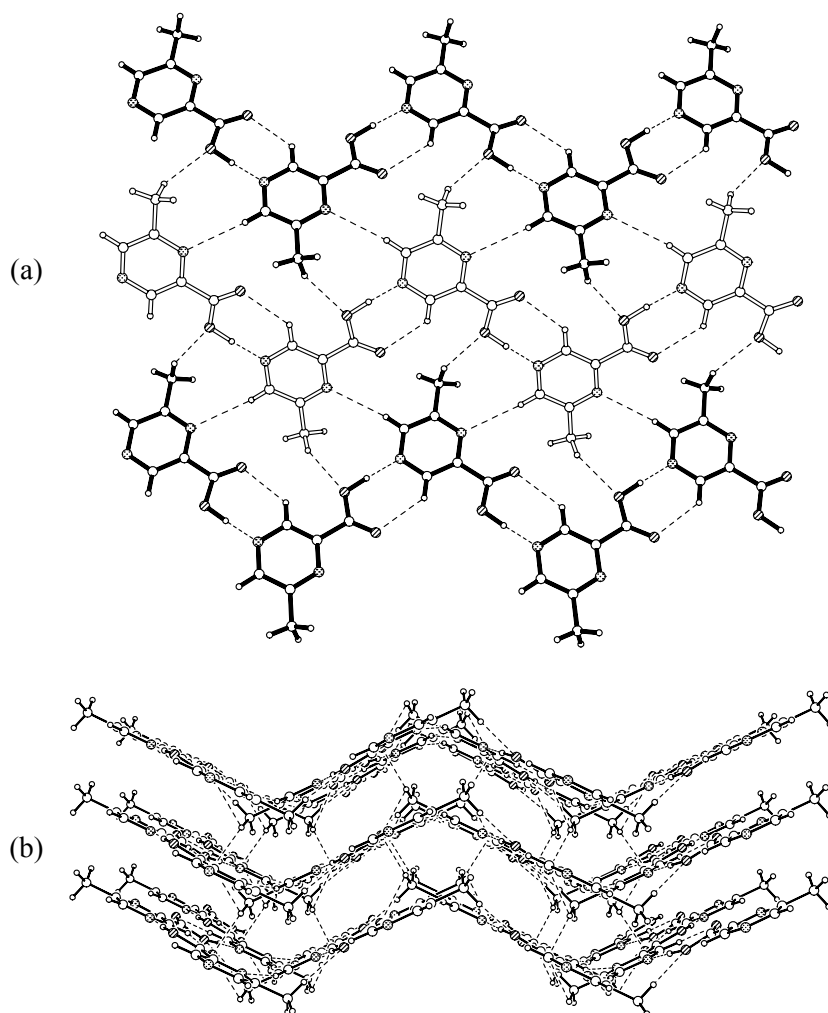


Figure 3. (a) Zigzag tapes of 6-methylpyrazine-2-carboxylic acid **4** assembled with synthon **V** along [001]. Translation related tapes are connected by C–H...O/N hydrogen bonds into a pleated sheet structure. Notice that synthon **VIII** is not possible here. (b) Stacking of pleated sheets with (Me)C–H...O interactions between the layers.

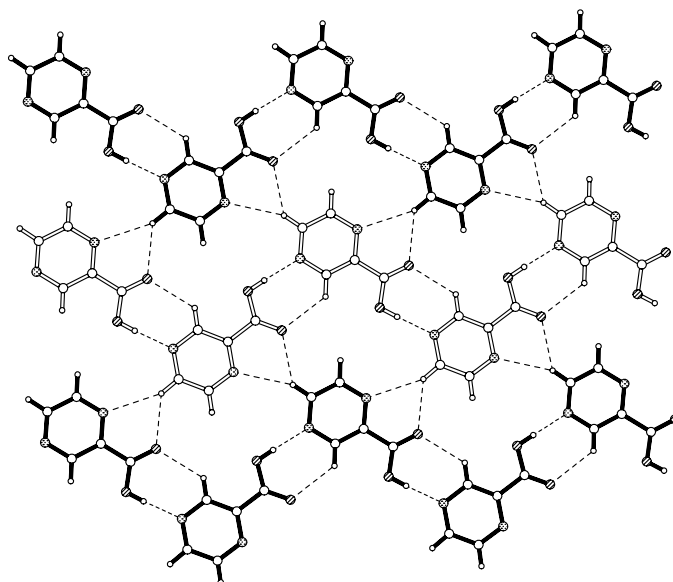


Figure 4. Laminated sheet parallel to (001) in pyrazinecarboxylic acid **1**. Note the similarity with Figure 3. The layer in **1** is flat while it is pleated in **4**.

2.8 Pyrazine-2,5-Dicarboxylic Acid, **11**

Pyrazine-2,5-dicarboxylic acid, **11** crystal structure is analysed in order to compare this structure with the 2,3-diacid. Pyrazine-2,5-diacid crystallizes as a dihydrate, **11**•2(H₂O) (space group $P\bar{1}$). The structure contains a short (carboxyl)O–H···O(water) hydrogen bond (1.54 Å, 170.3°) that is part of motif **VII**. The carbonyl oxygen accepts hydrogen bond from a water molecule (O–H···O=C: 1.88 Å, 153.5°) and the water molecule is polarised because it donates to the pyrazine N-atom (1.88 Å, 165.8°), resulting in a cyclic cooperative array (Figure 5).

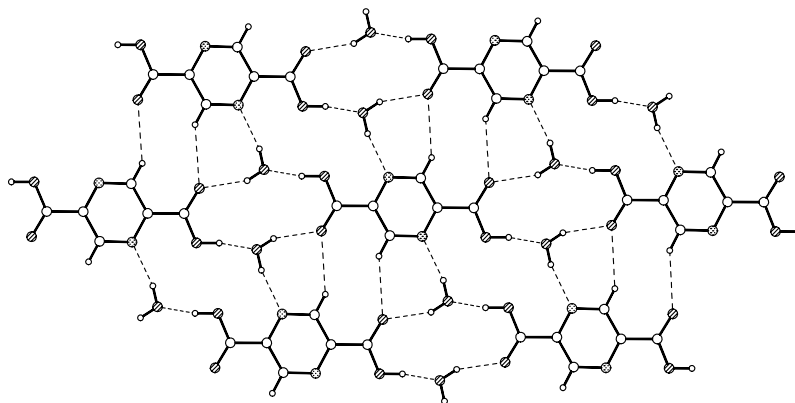
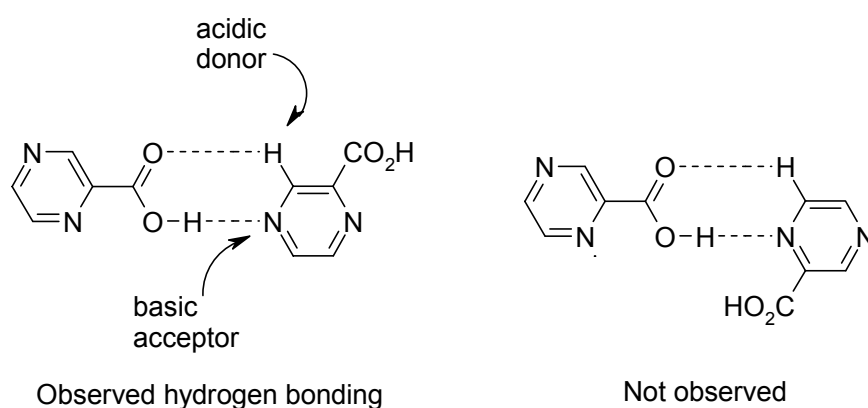


Figure 5. Lamellar structure parallel to $(1\bar{2}1)$ mediated by synthon **VII** in pyrazine-2,5-dicarboxylic acid **11**. The extended hydrogen bond array $\text{O}-\text{H}\cdots\text{O}=\text{C}-\text{O}-\text{H}\cdots\text{OH}_2\cdots\text{O}/\text{N}$ is stabilized through cooperativity and polarisation resulting in the strong (carboxyl) $\text{O}-\text{H}\cdots\text{O}(\text{water})$ hydrogen bond.

2.9 Hierarchy in Acid–Pyridine Recognition

The recurrence of synthon **V** in crystal structure of pyrazinic acids, **1–4** confirms the robustness of this recognition motif. Since synthon **V** can result from more than one $\text{O}-\text{H}\cdots\text{N}$ hydrogen bond orientation in pyrazinic acids, the nature of acceptor group in these crystal structures are scrutinized. It is known that hydrogen bond strength increases with acidity of the donor atom and basicity of the acceptor group.²⁰ Predictable target architectures result from hydrogen bond hierarchy rules formulated by Etter:²¹ the best donor hydrogen bonds to the best acceptor and the second best donor and acceptor groups hydrogen bond next. In acids, **1–4** the carboxyl $\text{O}-\text{H}$ bonds to the more basic pyridine moiety, namely the N-atom adjacent to the H/Me group, and not the N-atom *ortho*- to the electron-withdrawing CO_2H group. Furthermore, this preference is observed even for the weak $\text{C}-\text{H}\cdots\text{O}$ hydrogen bond in pyrazinic acids **1** and **4**. C3–H donor, activated by the *ortho*- CO_2H group, forms the $\text{C}-\text{H}\cdots\text{O}$ bond that is part of synthon **V**, and not C5–H. Thus, both the CO_2H group and the $\text{H}-\text{C}=\text{N}$ moiety form the best combination of $\text{O}-\text{H}\cdots\text{N}$ and $\text{C}-$

H \cdots O hydrogen bonds (synthon **V**) in pyrazinic acids **1–4** (Scheme 3). These results imply that not only the strong O–H \cdots N (7–8 kcal/mol) but also the weak C–H \cdots O (1–2 kcal/mol) hydrogen bond contribute to the stability of synthon **V**. This issue is substantiated by computation of charges on donor/acceptor atoms in pyrazinic acid, **1** and energies of synthons **I**, **V** and **VIII** later in this chapter.

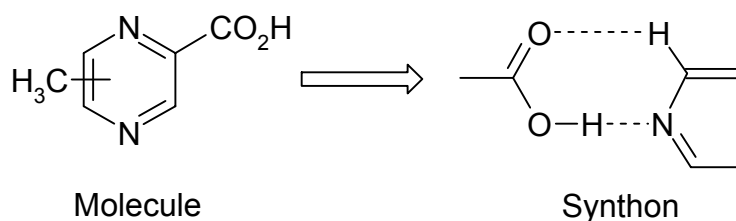


Scheme 3. Selectivity in hydrogen bonding between CO₂H group and chemically different H–C=N moiety.

2.10 Supramolecular Synthons in Pyridine and Pyrazine mono and di-Carboxylic Acids: Synthon **V** vs **VII**

A comparison of hydrogen bonding in closely related crystal structures gives an idea of the molecular features that favour the recurrence of a particular synthon and also of the factors that result in different crystal packing motifs. Crystal structures of pyrazinic acids **1–4** were compared with pyridine and pyrazine mono and dicarboxylic acids. Crystal packing in some simple pyridine and pyrazine mono- and dicarboxylic acids may be summarised as follows: pyrazine mono carboxylic acids **1–4**, nicotinic acid **5**,²² isonicotinic acid **6**,²³ and dinicotinic acid **8**,²⁴ contain synthon **V**; dipicolinic acid **9**,²⁵ pyrazine-2,3-dicarboxylic acid **10**,²⁶ pyrazine-2,5-dicarboxylic

acid **11**, 5,6-dimethylpyrazine-2,3-dicarboxylic acid **12** and pyrazine-2,3,5,6-tetracarboxylic acid **13** crystallize as dihydrates *via* motif **VII**. Picolinic acid **7**²⁷ has a complex hydrogen-bonding network between neutral and zwitterionic molecules. Crystals of **10** and **11**, as well as related compounds diacid **12** and tetraacid **13**,¹⁹ are hydrated because these molecules are rich in hydrogen bond acceptor groups (CO₂H, N-atom). The inclusion of water, a donor rich molecule, compensates this imbalance and completes the hydrogen bond network in these crystal structures.²⁸ The (carboxyl)O–H···O(water) hydrogen bond is short and linear compared to isolated hydrogen bonds of synthon **VII** (Table 1). A reason for the absence of synthon **V** in **10–13** could be either the inclusion of water molecule that opens the possibility for strong (carboxyl)O–H···O(water) motif, and/or because the *ortho*- CO₂H group deactivates the pyrazine N-atom as the O–H···N acceptor. A very short (carboxyl)O–H···O(water) hydrogen bond in the crystal structure of **13** is attributed to the cumulative stabilization from σ - and π - bond cooperativity, a phenomenon that will be discussed in Chapter 4. In any case, acid–acid homodimer **I** is not formed either in pyrazine mono- or di-carboxylic acids. Acid–pyridine synthon **V** is a recurring (robust) structural pattern in pyridine and pyrazine mono-carboxylic acids while di- and tetra-acids adopt motif **VII** in hydrate crystal structures (Table 2). Such a molecule \rightarrow synthon correlation is an essential exercise for the rational supramolecular synthesis of target crystal structures from functionalised molecules.⁵ While establishing such relationships it may be noted that carboxylic acids participate in a variety of hydrogen bond motifs depending on the presence of other functional groups,^{4b} activated C–H donor,^{13b} and heterocyclic ring.²⁹ Therefore, reliable correlation is possible only within families of homogeneous crystal structures. As the structural diversity is expanded to cover the entire database,⁶ the probability of occurrence of the synthon is reduced.

**Table 2.** Dominant synthon in some pyridine and pyrazine carboxylic acids

Molecule	Synthon	Molecule	Synthon
1	V	8	V
2	V	9	VII
3	V	10	VII
4	V	11	VII
5	V	12	VII
6	V	13	VII

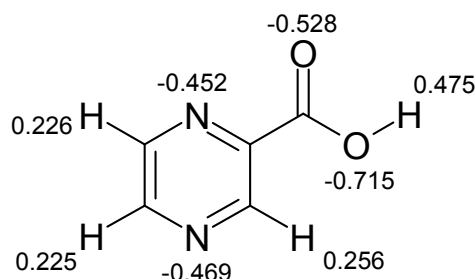
2.11 Restricted Hartree Fock Computation of Charge and Energy

The synthon energy³⁰ of acid–acid **I**, acid–pyridine **V** and pyridine dimer **VIII** were calculated in Restricted Hartree Fock (RHF) with 6-31G* basis set using Spartan program.³¹ The molecules selected for energy calculation are the 1:1 CH₃CO₂H–pyridine adduct and isonicotinic acid **6** so that energies of these synthons may be compared in two types of chemical systems, molecular complex and single molecule. Energy of the synthon was computed by calculating the difference between the minimised energy of the hydrogen bonded complex and that of the isolated molecules. For example, energy of synthon **V** was calculated by minimizing the energy of CH₃CO₂H–pyridine complex and subtracting from this value the energy of CH₃CO₂H and pyridine. The computed energy of synthons **I**, **V** and **VIII** is listed in Table 3. The hydrogen bond geometry in the minimized configuration is in the

normal distance–angle range for these interactions. From these data it is clear that crystallization through heterodimer **V** ($2 \times -9.97 = -19.94$ kcal/mol) is energetically favoured compared to a combination of O–H \cdots O and C–H \cdots N homosynthons **I** and **VIII** [$-(15.62 + 2.67) = -18.29$ kcal/mol] by -1.65 kcal/mol in isonicotinic acid **6**. Similarly acid–pyridine molecular complex formation is favoured over acid–acid and pyridine–pyridine hydrogen bonded aggregates by -1.86 kcal/mol. Thus, the recurrence of mixed strong–weak hydrogen bonded synthon **V** in crystal structures is explained on energy considerations. Recently our research group have shown that the acid–sulfoxide recognition is favoured over acid–acid and sulfoxide–sulfoxide dimer synthon by -4.7 kcal/mol.¹⁴ A possible reason why crystal structures with combination of strong and weak hydrogen bond synthons are formed in preference to strong–strong and weak–weak hydrogen bonding is that propagation in crystal nuclei into larger aggregates and then to stable crystal is more likely in the former case. Crystal structures with isoenergetic combination of strong–strong and weak–weak hydrogen bonding motifs presumably dissociate at the weak–weak interface prior to reaching the final stages of crystallization. The calculated Mulliken charge (RHF/6-31G*) on donor/acceptor atoms in pyrazinic acid **1** is displayed in Scheme 4. It is clear that the more basic N-acceptor (electronegative) and the more acidic C–H donor (electropositive) participate in the hydrogen bonds of synthon **V**. These charges are in agreement with the selectivity for synthon formation summarised in Scheme 3.

Table 3. Energy of synthons calculated in RHF/6-31G* (in kcal/mol)

Synthon	Isonicotinic acid	CH ₃ CO ₂ H–pyridine
I	–15.62	–15.54
V	–9.97	–9.95
VIII	–2.67	–2.50



Scheme 4. Mulliken charges on donor and acceptor atoms in pyrazine carboxylic acid **1**.

Aakeröy has suggested in a recent paper³² that formation of acid–pyridine synthon **V** may be rationalised by the formation of O–H···N hydrogen bond between the best donor (CO₂H) and best acceptor (pyridine N atom) in the crystal, based on the hydrogen bond rules formulated by Etter. The electronegativity of the C=O oxygen is moderately better than the pyridine nitrogen in **1** based on Mulliken charge (−0.528 e, −0.469 e). Computations suggest that hydrogen bonding of carboxylic acid O–H group is equally likely with both C=O oxygen and pyridine N for electrostatic and basicity reasons. However, self-assembly of molecules in the crystal is favoured *via* heterosynthon **V** compared to homosynthon **I** because of energetic factors. Since different atoms in different chemical environments are the potential acceptors, namely C=O and pyridine-N, the final outcome in terms of O–H···O *vs* O–H···N hydrogen bonding is determined by a combination of electronegativity and basicity factors. A hydrogen bond is a three-centre four-electron multi-component interaction and a dissection of the various contributions to the total energy is non-trivial. The issue of hydrogen bonding in competitive situations is discussed in more detail in chapter 5.

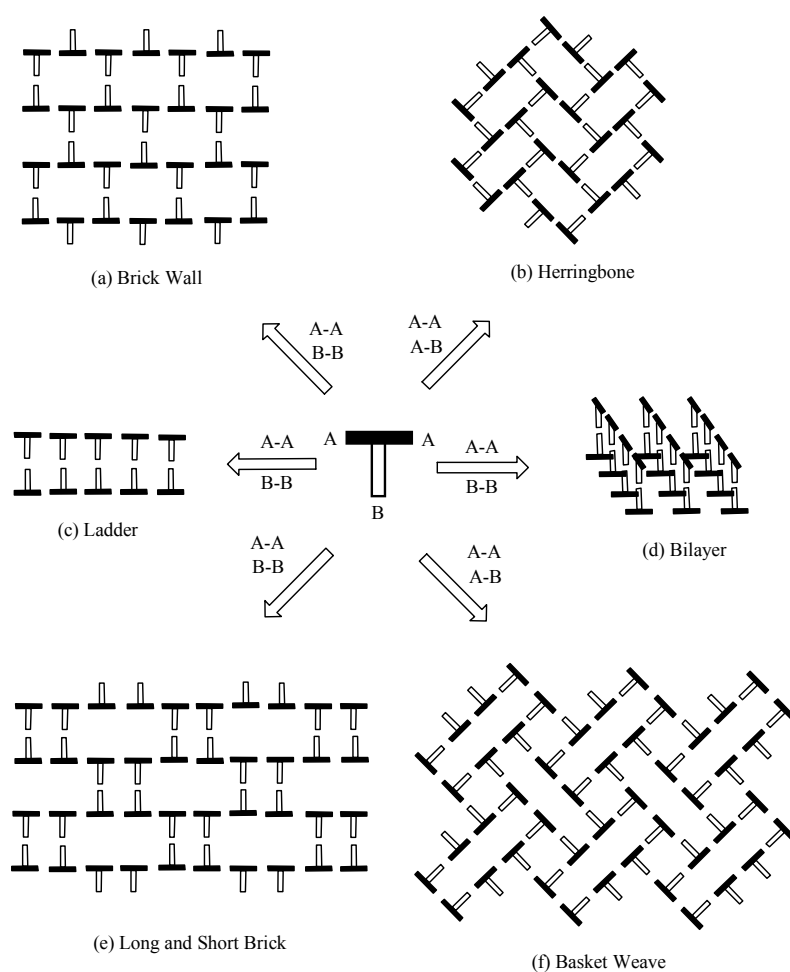
2.12 Networks

The description of crystal structures as networks may be carried out by representing the molecules as points or nodes and the intermolecular interactions connecting the molecules as node connectors.³³ The network representation facilitates in the understanding of 3D architectures and in the comparison of structures assembled with the same or different molecular constituents. The network topology in coordination polymers can be usually designed by selecting the coordination geometry of metal and the chemical structure of organic ligand. A metal geometry of particular interest because of its potential range of network structures is simple and prototypal “T-shaped” module. The T-shape node has thus far produced examples of 1D, 2D and 3D networks. Self-assembly of T-node molecules with three recognition sites can produce ladder, brick wall, herringbone or bilayer networks in crystal structures as shown in Scheme 5. 2D brick wall and herringbone networks are topologically identical to the honeycomb grid because these are (6,3) nets. Ladder, brick wall, herringbone, and bilayer networks are relatively common in coordination polymers,³⁴ *i.e.*, crystal structures assembled with metal-ligand and hydrogen bonds. However, examples of organic structures in these network categories are rare.³⁵

2.12.1 Coordination Polymer and Organic T-Modules: Recent Literature

The T-node coordination polymers that produce network structures with (6,3) topology may be obtained with a 1:1.5 ratio of metal ions to a linear spacer ligands (such as 4,4'-bipyridine, 4,4'-azopyridine, 1,2-dipyridyl ethane *etc.*). For example, the metal complex $[\text{Cd}_2(\text{azpy})_3(\text{NO}_3)_4]$ **14**^{34f} was obtained by reaction of cadmium(II)nitrate and 4,4'-azopyridine (azpy) in ethanol/acetone (2:3 ratio). The cadmium has distorted pentagonal bipyramidal geometry with three pyridyl nitrogen atoms and four oxygen atoms of two bidentate nitrate anions. A T-shaped module is recognized from the geometry. The two pyridine rings of the azpy B are nearly

coplanar, while the two pyridine rings of the azpy A is not coplanar with dihedral angle of 65° . **14** exhibits a herringbone type 2D network, (Figure 6) which is comprised of rectangular cavities with dimensions of $23 \times 11 \text{ \AA}$. Such networks are triply interpenetrated. Despite the interpenetration, there are channels (about 5×5) in the sheets, which include acetone molecules.



Scheme 5. Self-assembly of a T-module into (a) Brick Wall, (b) Herringbone, (c) Ladder, (d) Bilayer, (e) Long and short brick, (f) Basket Weave. Motifs (e) and (f) are yet to be realized.

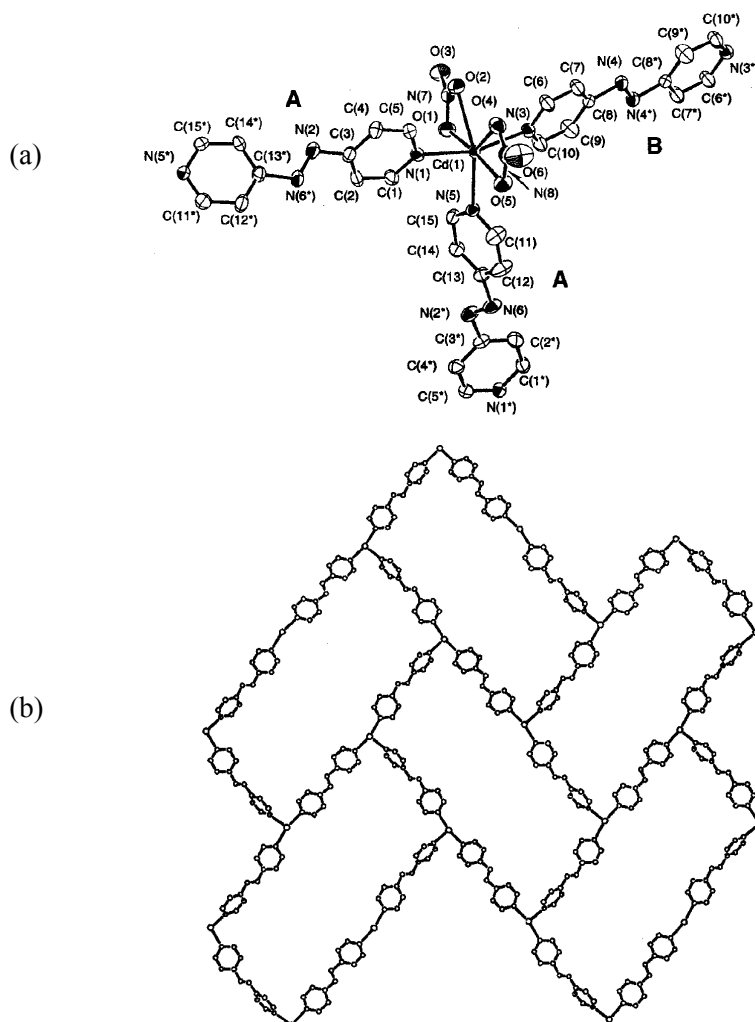


Figure 6. (a) ORTEP plot of T-shaped molecule **14** to show the A, A and B sites. (b) Herringbone 2D network formed by one A–A and two A–B type Cd \cdots N interactions.

The factors that should be considered for the crystal engineering of organic networks with T-modules are: (i) a T-geometry at the metal centre is easily achieved in square planar, octahedral and trigonal bipyramidal coordination with appropriate ligands, but it is difficult to design a T-shaped organic molecule given that the

standard angles at carbon are 109°, 120° or 180°; (ii) in coordination polymer networks, the metal atom acts as the node and the ligands serve as the node connectors, whereas in organic networks the molecule is the node and hydrogen bonds are the node connectors; (iii) metal–ligand coordination bonds are strong and directional (40–80 kcal/mol), whereas hydrogen bonds (2–15 kcal/mol) exhibit moderate directionality in crystals. Very recently, 5-nitrosalicylic acid was identified as an organic T-node molecule in our research group, with three hydrogen bonding recognition sites on its molecular periphery (Figure 7).^{35a} If the T-module is viewed as having two A and one B type hydrogen bond sites, then recognition *via* two A⋯A and one B⋯B interactions results in the brick wall architecture as shown in Figure 8.

2.12.2 Herringbone Network in 5-Methylpyrazine-2-Carboxylic Acid, **2**

Self-assembly of a T-module with recognition sites A, A and B produces a herringbone network through one A–A and two A–B type metal–ligand or through hydrogen bonding in the case of an organic molecule. In the nomenclature of Scheme 5, acid **2** may be viewed as a T-shaped molecule (Figure 9a) with pyridyl groups making A type hydrogen bonding and carboxylic acid representing B type recognition site. In the crystal structure of **2**, two acid–pyridine synthons **V** and one pyridine dimer **VIII** at each molecule (node) produce the herringbone network in the $(10\bar{2})$ -plane (Figure 9b). It may be noted that Cd⋯N bonding with A and B type azpy ligands in **14**•2Me₂CO is replaced by synthons **V** and **VIII** in **2**. In effect, the 2D network formed by an organic molecule and a metal–organic clathrate is identical. Such topological comparison of crystal structures and their connectivity is possible only through the network representation. Acid **2** is the first example of an organic crystal structure with a herringbone network.

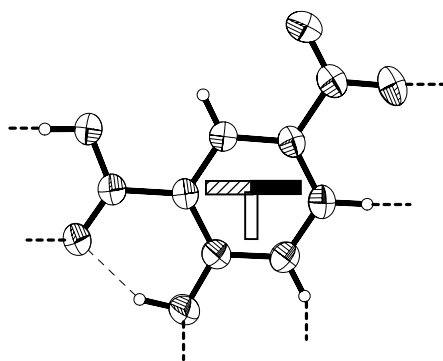


Figure 7. T-shaped 5-nitrosalicylic acid with O-H...O, C-H...O and C-H...O hydrogen bond donors that furnish T-shape to the molecule.

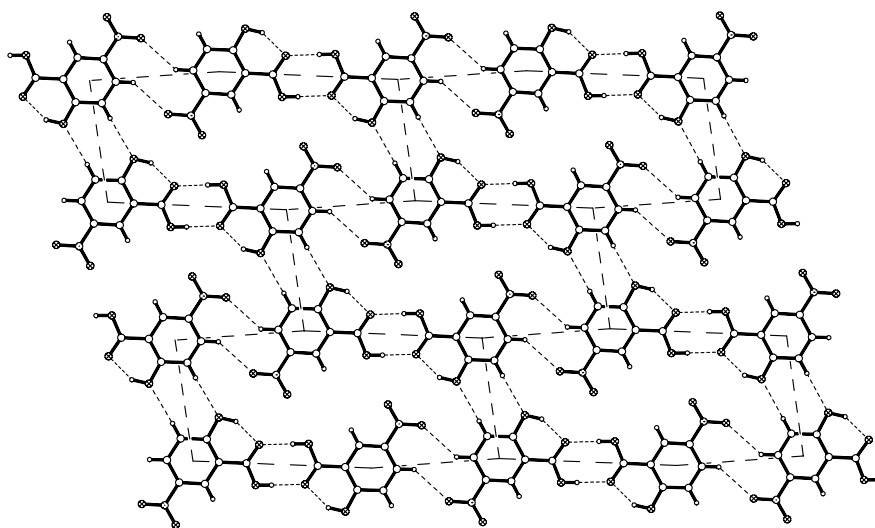


Figure 8. Crystal structure of 5-nitrosalicylic acid to show the brick wall network. Note the self-assembly of T-module *via* like recognition, A...A and B...B produces the brick wall architecture.

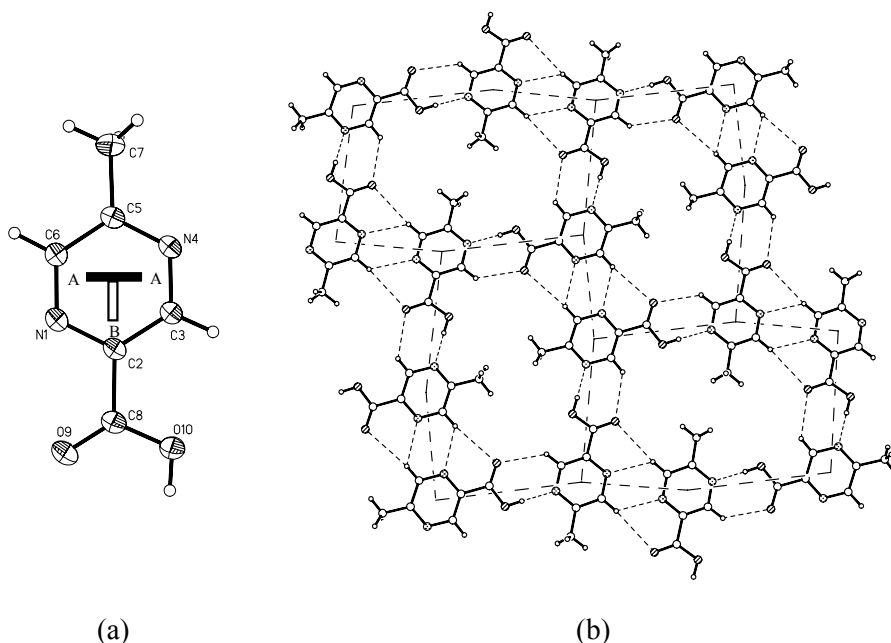


Figure 9. (a) ORTEP plot of 5-methylpyrazine-2-carboxylic acid **2** to show the A, A and B hydrogen bonding sites. (b) Self-assembly of the T-shaped molecule **2** into a 2D herringbone network *via* two A–B (synthon **V**) and one A–A (synthon **VIII**) type interactions.

2.13 Database Analysis

The significance of C–H \cdots O hydrogen bonds in supramolecular synthon **V** has been analyzed using the Cambridge Crystallographic Database (CSD, Version 5.24, 272066 entries). A sub-data base (110 hits) of organic structures that contain CO₂H and pyridine moiety with at least one *ortho*-H atom (no disorder, 3D coordinates present, no errors, no ions, not polymorphic, and with R factor <0.1 constraints were applied) was created in the O–H \cdots N distance and angle range: 1.5–2.4 Å, 130–180°. Of these, 64 compounds were found to exhibit C–H \cdots O hydrogen bonds (C–H \cdots O: 2.0–3.0 Å, 110–180°) with mean C \cdots O distance and angle of 3.36 Å and 125° respectively. The 46 compounds that do not exhibit these interactions are

engaged in other strong/weak hydrogen bonds (4 O–H \cdots O, 31 N–H \cdots O and 11 C–H \cdots O) which compete with the weak C–H \cdots O hydrogen bond formation or motif **V**. This observation suggests that C–H \cdots O interactions afford additional stability and rigidity to synthon **V** and the generality of this interaction is further supported by the existence of this interaction in crystal structures **1–4**.

2.14 Conclusions

Hydrogen bonding supramolecular synthons in a family of crystalline pyrazine carboxylic acids have been studied with X-ray diffraction. The present study reveals that heterosynthon **V**, assembled by (carboxyl)O–H \cdots N(pyridine) and (pyridine)C–H \cdots O(carbonyl) hydrogen bonds, is a robust recognition motif that is largely insensitive to the substitution and placement of functional groups in pyridine and pyrazine mono-carboxylic acids. However, a pyridyl N with an *ortho*-CO₂H group is sufficiently deactivated that it does not form synthon **V**. Both the O–H \cdots N and C–H \cdots O hydrogen bonds in synthon **V** result from activated acidic donor and basic acceptor atoms in **1–4**. Pyridine and pyrazine dicarboxylic acids crystallize as dihydrates with (carboxyl)O–H \cdots O(water) hydrogen bond as the strong and dominant interaction in synthon **VII**. The structural analysis shows that pyrazine mono- and dicarboxylic acids exhibit distinct hydrogen bonding patterns. The recurrence of acid–pyridine heterodimer **V** compared to the more common acid–acid homodimer **I** in these crystal structures of pyridine and pyrazine monocarboxylic acids is supported by *ab initio* computations. The lamellar and pleated architectures of pyrazinic acids discussed in this chapter provide a novel system for the design of nanostructures from tailored molecules. The study on pyrazine mono- and dicarboxylic acids examines crystal packing in complex and competing chemical environments and hence provides a better understanding of a useful supramolecular synthon in crystal engineering.

2.15 Experimental Section

Synthesis

The pyrazinecarboxylic acids were synthesized and characterized by IR and ^1H -NMR spectroscopy. IR spectra were recorded on a Jasco 5300 spectrophotometer and ^1H -NMR was recorded at 200 MHz on a Bruker ACF instrument.

1. Synthesis of 5-methylpyrazine-2-carboxylic acid, 2

This compound was synthesized in three steps. First step involves the preparation of methyl quinoxaline and oxidation to pyrazine dicarboxylic acid followed by decarboxylation to mono acid.

(a) 2-Methyl Quinoxaline:³⁶ 5.5 g (51 mmol) of o-phenylene diamine was dissolved in 90 ml of water, and the solution was heated to 70 °C. With stirring, a solution of 8.6 ml of 40 % methyl glyoxal (50 mmol) in 65 ml of hot water was added to the o-phenylene diamine solution. The mixture was allowed to stand for 15 minutes and then was cooled to room temperature. 21 g of sodium carbonate monohydrate was added to the mixture. Methyl quinoxaline was extracted with three 15 ml portions of diethyl ether solvent. The combined extracts were dried over anhydrous MgSO_4 , filtered, and concentrated. The residual liquid, consisting of almost pure methyl quinoxaline was collected. Yield: 5.4 g (74 %). ^1H -NMR (DMSO-d_6): δ 8.7 (s, 1H), 8.04-7.99 (m, 2H), 7.74-7.69 (m, 2H), 2.77 (s, 3H). IR (neat): 3435, 3063, 3016, 1637, 1560, 1493, 1437, 1410, 1369 cm^{-1} .

(b) 5-Methylpyrazine-2,3-dicarboxylic acid:³⁷ To 2 g (14 mmol) of methyl quinoxaline, 50 ml of water was added and heated to 80 °C. With rapid stirring a saturated aqueous solution of 12.8 g (81 mmol) of KMnO_4 was added, stirred for 30 minutes and filtered the reaction mixture to remove MnO_2 . The filtrate (about 150 ml) was evaporated under reduced pressure to about 50 ml. The solution was stirred gently while 7 ml of conc. HCl was cautiously added. Evaporation under reduced

pressure was then continued until a moist cake of solid KCl and the product remained in the flask. Some water and 25 ml of acetone was added to the solid material and the mixture was boiled under reflux for 15 minutes, then cooled to room temperature and filtered. The acetone filtrate was distilled to obtain the product 5-methylpyrazine-2,3-dicarboxylic acid. Yield: 1.5 g (60 %). M.p.: 171–176 °C. $^1\text{H-NMR}$ ($\text{DMSO-}d_6$): δ 8.72 (s, 1H), 2.59 (s, 3H). IR (KBr): 2847, 1712, 1577, 1421, 1234, 1194, 1097, 794, 760 cm^{-1} .

(c) 5-Methylpyrazine-2-carboxylic acid:³⁷ 250 mg (1.4 mmol) of 5-methylpyrazine-2,3-dicarboxylic acid was placed in a vacuum sublimation apparatus and was decarboxylated by heating to 175–185 °C at 2 mm of Hg, resulted in the formation of 5-methylpyrazine-2-carboxylic acid. Yield: 134 mg (71 %). M.p.: 134–137 °C. $^1\text{H-NMR}$ ($\text{DMSO-}d_6$): δ 9.06 (s, 1H), 8.69 (s, 1H), 2.60 (s, 3H). IR (KBr): 1894, 1728, 1379, 1336, 1307, 1275, 1184, 1045 cm^{-1} .

2. 3-Methylpyrazine-2-carboxylic acid, **3**³⁸

To 1 ml (9.3 mmol) of 2,3-dimethylpyrazine in 10 ml water at 70–75 °C, 3.3 g (21 mmol) of KMnO_4 was added in 50 ml of water. After decolourisation of purple colour, the MnO_2 cake was filtered and washed with water several times. The filtrate was acidified to pH 1.5 with HNO_3 , the solution heated to 50 °C, cooled to room temperature and extracted with EtOAc. Work up afforded 350 mg (28 %) of acid **3**. M.p.: 170–171 °C. $^1\text{H-NMR}$ ($\text{DMSO-}d_6$): δ 2.65 (s, 3H), 2.66 (s, 1H), 2.75 (s, 1H). IR (KBr): 3749, 1684, 1508, 1413, 1288, 1103 cm^{-1} .

3. 6-Methylpyrazine-2-carboxylic acid, **4**

Prepared in 21 % yield using the above procedure starting from 2,6-dimethylpyrazine. M.p.: 200–201 °C. $^1\text{H-NMR}$ ($\text{DMSO-}d_6$): δ 2.59 (s, 3H), 8.85 (s, 1H), 9.05 (s, 1H). IR (KBr): 3435, 1732, 1383, 1296, 1257, 1018 cm^{-1} .

Pyrazine-2,5-dicarboxylic acid, 11 (dihydrate) was purchased from Acros Chemicals and used as such for crystallization without further purification.

Crystallization

Diffraction quality single crystals were obtained by recrystallizing compound **2** from 4:1 EtOH/H₂O, **3** and **4** from *n*-hexane/EtOAc and **11** from 20 % aqueous HCl.

X-ray Data Collection and Crystal Structure Determinations

X-ray data for acid **2** was collected at H.C.U. on Enraf-Nonius CAD-4 diffractometer. Data for acids **3**, **4** and **11** were collected by Dr. Vincent M. Lynch (University of Texas, Austin, U.S.A.) by Nonius Kappa CCD diffractometer. The incident radiation is Mo-K α X-ray ($\lambda = 0.71073\text{\AA}$) on both instruments. Data on crystal of **2** was collected at 293 K whereas crystals of **3**, **4** and **11** were cooled with Oxford Cryostream device attached to the CCD machine. Data reduction was performed using Xtal 3.5 (CAD-4) and DENZO-SMN (CCD).³⁹ Structures were solved by direct methods using SHELXS-97⁴⁰ and refined by full-matrix least-squares refinement on F^2 with anisotropic displacement parameters for the non-H atoms using SHELXL-97. Geometrical analysis was carried out in PLATON⁴¹ on Silicon Graphics Octane2 workstation.

2.16 References and Notes

1. (a) G.R. Desiraju, *Crystal Engineering: The Design of Organic Solids*, Elsevier: Amsterdam, **1989**. (b) A. Anthony, G.R. Desiraju, R.K.R. Jetti, S.S. Kuduva, N.N.L. Madhavi, A. Nangia, R. Thaimattam and V.R. Thalladi, *Cryst. Eng.*, **1998**, *1*, 1.
2. (a) J.L. Prins, D.N. Reinhoudt and P. Timmerman, *Angew. Chem., Int. Ed.*, **2001**, *40*, 2382. (b) A. Nangia, *Curr. Opin. Solid State Mater. Sci.*, **2001**, *5*, 115. (c) M.C.Y. Fyfe and J.F. Stoddart, *Acc. Chem. Res.*, **1997**, *30*, 393. (d) G.M. Whitesides, E.E. Simanek, J.P. Mathias, C.T. Seto, D.N. Chin, M. Mammen and D.M. Gordon, *Acc. Chem. Res.*, **1995**, *28*, 37.
3. G.R. Desiraju, *Angew. Chem., Int. Ed. Engl.*, **1995**, *34*, 2311.
4. (a) S.S. Kuduva, D.C. Craig, A. Nangia and G.R. Desiraju, *J. Am. Chem. Soc.*, **1999**, *121*, 1936. (b) S.V. Kolotuchin, E.E. Fenlon, S.R. Wilson, C.J. Loweth and S.C. Zimmerman, *Angew. Chem., Int. Ed. Engl.*, **1995**, *34*, 2654. (c) J. Bernstein, M.C. Etter and L. Leiserowitz, in *Structure Correlation*, Vol. 2, eds. H.-B. Bürgi and J.D. Dunitz, VCH: Weinheim, **1994**. (d) Z. Berkovitch-Yellin and L. Leiserowitz, *J. Am. Chem. Soc.*, **1982**, *104*, 4052. (e) L. Leiserowitz, *Acta Crystallogr., Sect. B*, **1976**, *32*, 775. (f) L. Leiserowitz and G.M.J. Schmidt, *J. Chem. Soc. A*, **1969**, 2372.
5. F.H. Allen, W.D.S. Motherwell, P.R. Raithby, G.P. Shields and R. Taylor, *New J. Chem.*, **1999**, *23*, 25.
6. A. Nangia and G.R. Desiraju, *Top. Curr. Chem.*, **1998**, *198*, 57.
7. T. Steiner, *Acta Crystallogr., Sect. B*, **2001**, *57*, 103.
8. (a) R.D.B. Walsh, M.W. Bradner, S. Fleischman, L.A. Morales, B. Moulton, N. Rodriguez-Hornedo and M.J. Zaworotko, *Chem. Commun.*, **2003**, 186. (b) A.D. Bond, *Chem. Commun.*, **2003**, 250. (c) B.R. Bhogala, P. Vishweshwar and A. Nangia, *Cryst. Growth Des.*, **2002**, *2*, 325. (d) N. Shan, A.D. Bond and W. Jones,

- Cryst. Eng.*, **2002**, 5, 9. (e) C.B. Aakeröy, A.M. Beatty, M. Tremayne, D.M. Rowe and C.C. Seaton, *Cryst. Growth Des.*, **2001**, 1, 377. (f) D.E. Lynch and I. McClenaghan, *Acta Crystallogr., Sect. C*, **2001**, 57, 830. (g) H. Ishida, B. Rahman and S. Kashino, *Acta Crystallogr., Sect. C*, **2001**, 57, 876. (h) A.J. Lough, P.S. Wheatley, G. Ferguson and C. Glidewell, *Acta Crystallogr., Sect. B*, **2000**, 56, 261. (i) G.T.R. Palmore and M.T. McBride, *Chem. Commun.*, **1998**, 145. (j) G. Ferguson, C. Glidewell, G.D. McManus and P.R. Meehan, *Acta Crystallogr., Sect. C*, **1998**, 55, 418. (k) V.R. Pedireddi, S. Chatterjee, A. Ranganathan and C.N.R. Rao, *Tetrahedron*, **1998**, 54, 9457. (l) C.V.K. Sharma and M.J. Zaworotko, *Chem. Commun.*, **1996**, 2655.
9. S.L. Johnson and K.A. Rumon, *J. Phys. Chem.*, **1965**, 69, 74.
 10. The Merck Index, 11th ed., Merck & Co., Rahway, **1989**, p. 1266.
 11. D. Wiechert and D. Mootz, *Angew. Chem., Int. Ed.*, **1999**, 38, 1974.
 12. B.R. Bhogala and A. Nangia, *Cryst. Growth Des.*, **2003**, 3, 547.
 13. (a) E. Batchelor, J. Klinowski and W. Jones, *J. Mater. Chem.*, **2000**, 10, 839. (b) V.R. Pedireddi, W. Jones, A.P. Chorlton and R. Docherty, *Chem. Commun.*, **1996**, 997.
 14. V.S.S. Kumar, A. Nangia, A.K. Katz and H.L. Carrell, *Cryst. Growth Des.*, **2002**, 2, 313.
 15. (a) S.S. Kuduva, D. Bläser, R. Boese and G.R. Desiraju, *J. Org. Chem.*, **2001**, 66, 1621. (b) P. Bhyrappa, S.R. Wilson and K.S. Suslick, *J. Am. Chem. Soc.*, **1997**, 119, 8492. (c) K.E. Schwiebert, D.N. Chin, J.C. MacDonald and G.M. Whitesides, *J. Am. Chem. Soc.*, **1996**, 118, 4018.
 16. The CSD (November 2002, 272066 entries) was searched for synthon V from good quality ($R < 0.10$, 3D coordinates present) organic crystal structures in the normal distance–angle range: O–H \cdots N (1.4–2.3 Å, 130–180°), C–H \cdots O (2.0–3.0 Å, 110–180°), O–H and C–H distance was neutron-normalized. Out of the 82 hits

retrieved, 17 structures are single component crystals and 65 are molecular complexes. The only example of a pyrazine carboxylic acid with synthon **V** in the database is **1**.

17. V.R. Thalladi, A. Gehrke and R. Boese, *New J. Chem.*, **2000**, 24, 463.
18. F. Takusagawa, T. Higuchi, A. Shimada, C. Tamura and Y. Sasada, *Bull. Chem. Soc. Jpn.*, **1974**, 47, 1409.
19. P. Vishweshwar, A. Nangia and V.M. Lynch, *Chem. Commun.*, **2001**, 179.
20. (a) G.R. Desiraju and T. Steiner, *The Weak Hydrogen Bond in Structural Chemistry and Biology*, OUP, Oxford, **1999**, pp. 50–56. (b) Ref. 5b, pp. 11–16.
21. (a) M.C. Etter, *J. Phys. Chem.*, **1991**, 95, 4601. (b) M.C. Etter, *Acc. Chem. Res.*, **1990**, 23, 120.
22. A. Kutoglu and C. Scherlinger, *Acta Crystallogr., Sect. C*, **1983**, 39, 232.
23. F. Takusagawa and A. Shimada, *Acta Crystallogr., Sect. B*, **1976**, 32, 1925.
24. F. Takusagawa, K. Hirotsu and A. Shimada, *Bull. Chem. Soc. Jpn.*, **1973**, 46, 2292.
25. F. Takusagawa, K. Hirotsu and A. Shimada, *Bull. Chem. Soc. Jpn.*, **1973**, 46, 2020.
26. F. Takusagawa and A. Shimada, *Chem. Lett.*, **1973**, 1121.
27. H. Hamazaki, H. Hosomi, S. Takeda, H. Kataoka and S. Ohba, *Acta Crystallogr., Sect. C*, **1988**, 54, e49.
28. (a) P. Vishweshwar, A. Nangia and V.M. Lynch, *Acta Crystallogr., Sect. C*, **2000**, 56, 1512. (b) T.M. Krygowski, S.J. Grabowski and J. Konarski, *Tetrahedron*, **1998**, 54, 11311. (c) G.R. Desiraju, *J. Chem. Soc., Chem. Commun.*, **1991**, 426.
29. Pyrazole-4-carboxylic acid forms ribbons of O–H···N and N–H···O hydrogen bonds in the solid state. C. Foces-Foces, A. Echevarría, N. Jagerovic, I. Alkorta, J. Elguero, U. Langer, O. Klein, M. Minguet-Bonvenhí and H.-H. Limbach, *J. Am. Chem. Soc.*, **2001**, 123, 7898.

30. For recent papers on hydrogen bond energy computations, see: (a) N. Kobko, L. Paraskevas, E. del Rio and J.J. Dannenberg, *J. Am. Chem. Soc.*, **2001**, *123*, 4348. (b) F.M. Raymo, M.D. Bartberger, K.N. Houk and J.F. Stoddart, *J. Am. Chem. Soc.*, **2001**, *123*, 9264. (c) R. Vargas, J. Garza, D.A. Dixon and B.P. Hay, *J. Am. Chem. Soc.*, **2000**, *122*, 4750.
31. *Spartan Pro 1.0*. Wave function Inc., 18401 von Karman Aveue, Suite 370, Irvine CA 92612, USA.
32. C.B. Aakeröy, A.M. Beatty and B.A. Helfrich, *Angew. Chem., Int. Ed.*, **2001**, *40*, 3240.
33. (a) M.J. Zaworotko, *Chem. Commun.*, **2001**, 1. (b) G.R. Desiraju, *Chem. Commun.*, **1997**, 1475.
34. (a) Y. Diskin-Posner, G.K. Patra and I. Goldberg, *Chem. Commun.*, **2002**, 1420. (b) Z.-Y. Fu, X.-T. Wu, J.-C. Dai, S.-M. Hu and W.-X. Du, *New J. Chem.*, **2002**, *26*, 978. (c) E.-Q. Gao, Z.-M. Wang, C.-S. Liao and C.-H. Yan, *New J. Chem.*, **2002**, *26*, 1096. (d) P. Gamez, P. de Hoog, O. Roubeau, M. Lutz, W.L. Driessen, A.L. Spek and J. Reedijk, *Chem. Commun.*, **2002**, 1488. (e) S.R. Batten, B.F. Hoskins and R. Robson, *Chem. Eur. J.*, **2000**, *6*, 156. (f) M. Kondo, M. Shimamura, S. Noro, S. Minakoshi, A. Asami, K. Seki and S. Kitagawa, *Chem. Mater.*, **2000**, *12*, 1288. (g) H. Gudbjarston, K. Biradha, K.M. Poirier and M.J. Zaworotko, *J. Am. Chem. Soc.*, **1999**, *121*, 2599. (h) Y.-B. Dong, R.C. Layland, N.G. Pschirer, M.D. Smith, U.H.F. Bunz and H.-C. Loye, *Chem. Mater.*, **1999**, *11*, 1413. (i) L. Carlucci, G. Ciani and D.M. Proserpio, *J. Chem. Soc., Dalton Trans.*, **1999**, 1799. (j) R. Masse, J.-F. Nicoud, M. Bagieu-Beucher and C. Bourgogne, *Chem. Phys.*, **1999**, *245*, 365. (k) M. A. Withersby, A.J. Blake, N.R. Champness, P.A. Coole, P. Hubberstey and M. Schröder, *New J. Chem.*, **1999**, *23*, 573.

35. (a) V.S.S. Kumar, A. Nangia, M.T. Kirchner and R. Boese, *New J. Chem.*, **2003**, 224. (b) S. Aitipamula, P.K. Thallapally, R. Thaimattam, M. Jaskólski and G.R. Desiraju, *Org. Lett.*, **2002**, 4, 921. (c) L.R. MacGillivray, J.L. Reid and J.A. Ripmeester, *Chem. Commun.*, **2001**, 1034. (d) Y. Zhang, C.D. Kim and P. Coppens, *Chem. Commun.*, **2000**, 2299.
36. R.G. Jones and K.C. McLaughlin, *Organic Synthesis*, Coll. Vol. 4, **1963**, 824.
37. F. Leonard and P.E. Spoerri, *J. Am. Chem. Soc.*, **1946**, 68, 526.
38. D. Pitre, S. Boveri and E.B. Grabitz, *Chem. Ber.*, **1966**, 99, 364.
39. (a) *Xtal3.5*. Reference Manual, University of Western Australia, Australia, Geneva, Switzerland and Maryland, U.S.A., eds. S.R. Hall, H.D. Flack and J.M. Stewart, **1995**. (b) *DENZO-SMN*. Z. Otwinowski and W. Minor, *Methods in Enzymology*, Vol. 276, Macromolecular Crystallography, Part A, eds. C.W. Carter Jr. and R.M. Sweets, Academic Press: New York, **1997**.
40. *SHELX-97*. G.M. Sheldrick, Program for the Refinement and Solution of Crystal Structures, University of Göttingen, Germany, **1997**.
41. *PLATON*. A.L. Spek, Bijvoet Centre for Biochemical Research, Vakgroep Kristal-en Structure-Chemie, University of Utrecht, The Netherlands.

CHAPTER THREE

SUPRAMOLECULAR SYNTHONS IN PYRAZINE CARBOXAMIDES

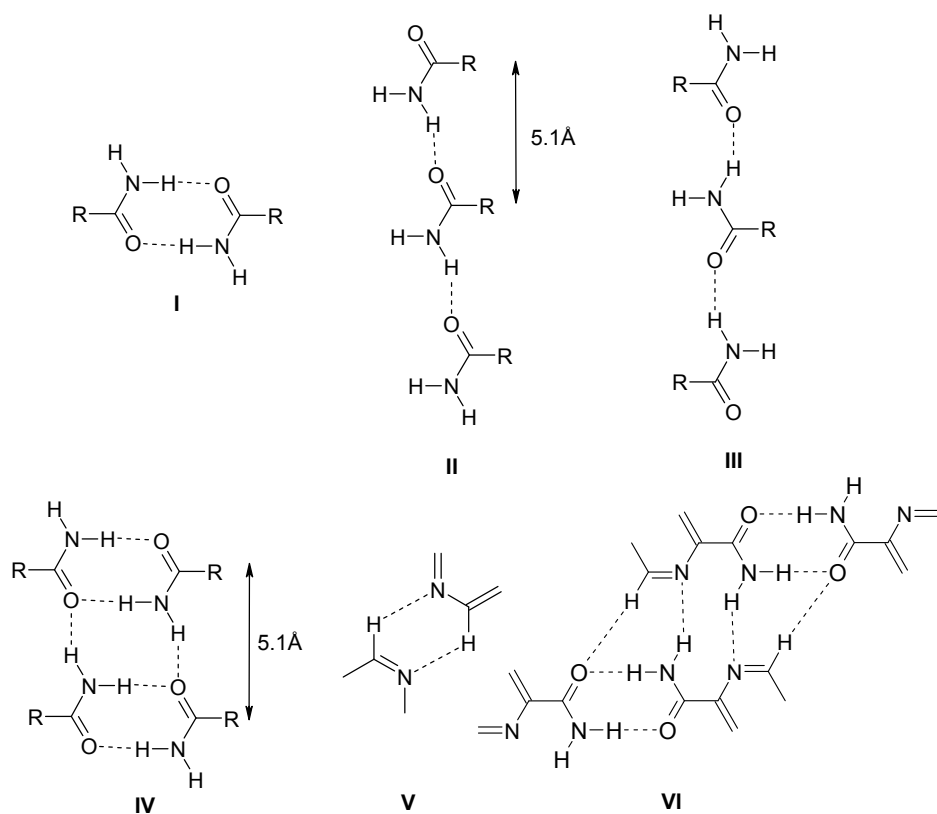
3.1 Introduction

Hydrogen bonding in amides is an important non-covalent interaction in determining recognition, geometry and modes of association between biological molecules.¹ In 1939 Pauling first introduced the importance of hydrogen bonding in amides.² Hydrogen bonding in amides played a key role in understanding the structure and biological function of the α -helix and the β -pleated sheet of proteins,³ as well as the Watson–Crick base-pairing in DNA double-helix.⁴ Amides have been used successfully to form a wide variety of supramolecular nanoscale architectures that are described as capsules,⁵ spheres,⁶ rosettes,⁷ rods,⁸ helices,⁹ tapes,¹⁰ ribbons,¹¹ tubes,¹² channels,¹³ and sheets or layers.¹⁴ In addition, amides have been used to create three-dimensional motifs that generate long-range order (*e.g.*, diamondoid lattices¹⁵ in crystals and liquid crystals¹⁶).

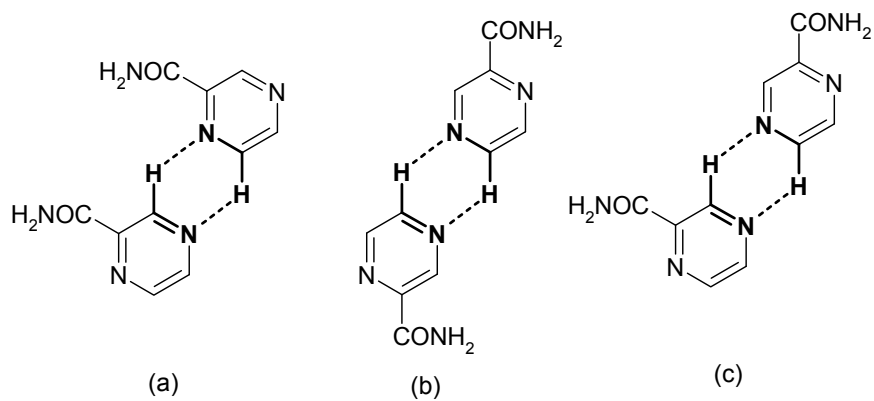
The role of the carboxamide functional group in crystal packing and molecular recognition was well studied by Leiserowitz.¹⁷ The geometry of the two hydrogen atoms on primary amides determines the type of structure that is formed through self-aggregation. Leiserowitz defines the orientation of these hydrogen atoms as having either *syn*- or *anti*- geometry, depending on whether the hydrogen atom is located on the same or the opposite side of the C–N bond as the carbonyl group. The hydrogen bond formed by amide N–H donors and C=O acceptors is strong and directional. Therefore amides assemble predictably into large and complex structures.¹⁸ The amide group generally forms centrosymmetric dimer synthon **I** with the *syn*-oriented N–H donor. This motif is analogous to the ring motif formed between two carboxylic acids. The *anti*-oriented N–H group forms hydrogen bonds according to one of the two motifs. (a) a linear pattern **II** in which succeeding

molecules are related by a 5.1 Å translation, or (b) a linear pattern **III** where adjacent molecules are related by a glide plane or a 2_1 axis. The 5.1 Å translation is generally preferred over the glide/screw motifs and, in combination with synthon **I**, leads to the commonly found translation ribbon synthon **IV** (scheme 1). In a recent survey of the CSD for bimolecular motifs in organic crystal structures, Allen *et. al.* noted that the eight-membered carboxamide dimer synthon **I** occurs only 8 % structures in the global database.¹⁹ This is because of competition from other strong donors and acceptors. However, formation of synthon **I** rises to 83 % for mono and 95 % for diamides in the absence of competitors.

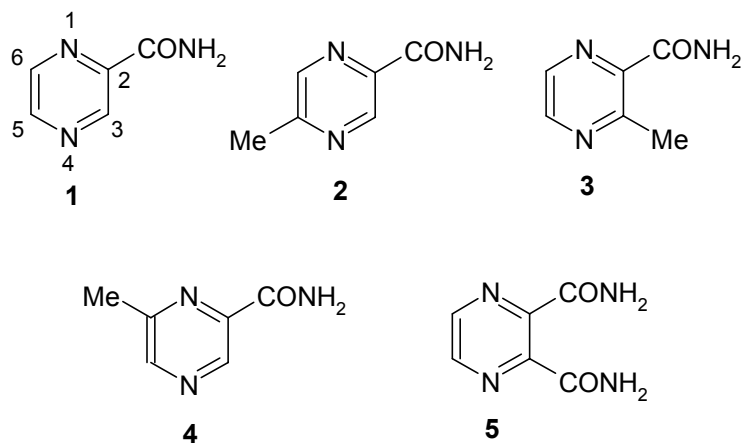
Active pharmaceutical ingredients (APIs) like pyrazine-2-carboxamide, **1** are of great interest for both fundamental and applied reasons. APIs are essentially predisposed for self-assembly since their utility is normally the result of the presence of one or more exofunctional supramolecular synthons. However, the crystal packing of APIs tends to be even less predictable than that of other organics because they often have multiple avenues for self-assembly and are therefore predisposed to exhibit polymorphism. Pyrazine-2-carboxamide, an antituberculosis drug, is a rare example of a compound with four (possibly five) different polymorphic forms.²⁰ Polymorphism is the phenomenon wherein the same chemical substance exists in different crystalline forms.²¹ The occurrence of polymorphism can also be explained in terms of supramolecular synthons. If a functional group can form more than one synthon this would lead to the possibility of polymorphism. In pyrazine carboxamide the same dimer synthon **V**, is formed from chemically distinct locations of the molecule leading to polymorphism (scheme 2).²² It is interesting to note that the three modifications of **1** include the same supramolecular synthon **V**.



Scheme 1. Supramolecular synthons discussed in this chapter.



Scheme 2. The $\text{C}-\text{H}\cdots\text{N}$ hydrogen-bonded supramolecular synthon **V** is optimized in the polymorphs of pyrazinamide **1** in alternative arrangements (a) through (c).



In this chapter, crystal chemistry of a family of methyl isomers of pyrazinecarboxamides, **2–4** and staircase network in pyrazine-2,3-dicarboxamide, **5** is studied. This is the follow-up of the earlier chapter on methyl isomers of pyrazinecarboxylic acids.²³

3.2 5-Methylpyrazine-2-Carboxamide, **2**

5-Methylpyrazine-2-carboxamide, **2** crystallizes in the monoclinic system with one molecule in asymmetric unit (space group $P2_1/n$). The carboxamide group is nearly co-planar with the heterocyclic pyrazine ring (torsion N–C–C–N: 1.2°). The N–H_s donor of carboxamide group forms a centrosymmetric N–H \cdots O (1.90 Å, 2.9136(15) Å, 176.8°) dimer **I**. However such dimers are not connected *via* the more common 5.1 Å short axis, and instead the N–H_a group of amide forms N–H \cdots N (2.26 Å, 3.0831(16) Å, 137.4°) hydrogen bonds with the pyrazine nitrogen atom and is supported by a C6–H \cdots O hydrogen bond (synthon **VI**), resulting in the formation of tape along [1 $\bar{1}$ 0] direction (Figure 1). The distance between the translated amide dimers is 7.7 Å. Such tapes are in turn connected by weak (methyl)C–H \cdots N(pyrazine) hydrogen bonds (Figure 2). Metrics of hydrogen bonds are shown in Table 1. It is

interesting to note that crystal structure of **2** is isostructural to the α -polymorph of pyrazine-2-carboxamide, **1**.

Kálmán²⁴ has suggested two parameters, which estimate the extent of isostructurality, or likeness between two similar structures, *the unit cell similarity index* (Π) and *the isostructurality index* [$I_i(n)$]. In unit cell similarity index (Π), a , b , c and a' , b' , c' are orthogonalized lattice parameters of the related crystal structures. Ideally, for a pair of completely isostructural structures Π should be close to zero.

$$\Pi = \left| \frac{a + b + c}{a' + b' + c'} - 1 \right| \cong 0$$

The isostructurality index, [$I_i(n)$] is a measure of the degree of internal isostructuralism, where n is the number of distance differences (ΔR_i) between the absolute coordinates of identical non-hydrogen atoms within the same section of asymmetric units of related (A and B) structures. Ideally, [$I_i(n)$] should be close to 100 % for isostructural crystals.

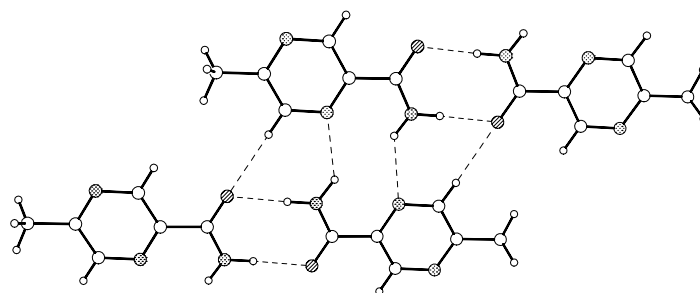
$$I_i(n) = \left[1 - \left(\frac{\sum_i \Delta R_i^2}{n} \right)^{1/2} \right] \times 100$$

The α -polymorph of pyrazinamide **1** and methylpyrazinamide **2** have almost identical a and b cell dimensions (α -polymorph of **1**: $a = 3.73$ Å, $b = 6.73$ Å; for **2**: $a = 3.77$ Å, $b = 6.75$ Å) whereas the c cell length is slightly higher for **2** (23.07 Å and 25.28 Å for α -polymorph of **1** and **2**, respectively). This is because (pyrazine)C5–H that is involved in C–H \cdots N (2.48 Å, 175.33°) hydrogen bond in α -polymorph of **1** is replaced by (methyl)C–H \cdots N in **2**. Crystal structure of α -polymorph of **1** is shown in Figure 3. The unit cell similarity index (Π) for the pair of α -polymorph of **1** and **2** is 0.07 suggesting near identity.

Table 1. Geometrical parameters of hydrogen bonds of amides **2–5**

Amide	H-bond	<i>d</i> (Å) ^a	<i>D</i> (Å)	θ (°)
2	N–H···O	1.09	2.913(2)	176.8
	N–H···N	2.26	3.083(2)	137.4
	C–H···O	2.29	3.360(2)	167.7
	C–H···N	2.59	3.581(2)	151.6
3	N–H···O	1.90	2.904(3)	172.6
	N–H···O	1.93	2.939(3)	175.8
	N–H···N	2.21	3.089(4)	143.5
	N–H···N	2.27	3.119(4)	141.0
	C–H···O	2.23	3.292(3)	166.4
	C–H···O	2.37	3.440(4)	168.7
	C–H···O	2.64	3.377(4)	124.3
	C–H···N	2.60	3.609(5)	154.6
4	N–H···O	1.91	2.899(2)	166.1
	N–H···N	2.26	3.090(2)	138.3
	C–H···O	2.53	3.584(3)	163.5
	C–H···O	2.54	3.448(3)	140.3
	C–H···O	2.61	3.663(2)	162.3
5	N–H···O	1.91	2.918(2)	177.3
	N–H···O	1.99	2.876(2)	144.2
	N–H···O	2.16	3.096(2)	153.8
	N–H···O	2.25	3.152(2)	147.3
	N–H···O	2.29	3.079(2)	133.5
	C–H···N	2.39	3.325(2)	142.7
	C–H···N	2.63	3.545(2)	141.7

^a O–H, N–H and C–H distances are neutron normalized to 0.983, 1.009 and 1.083, respectively.

**Figure 1.** Supramolecular synthon **VI** in the crystal structure of 5-methylpyrazine-2-carboxamide, **2**.

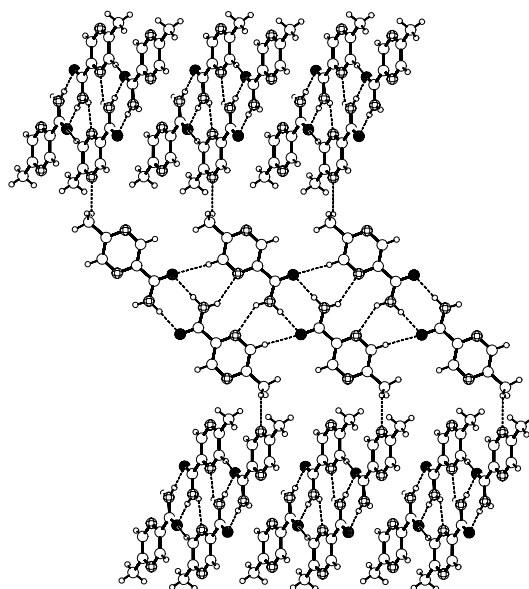


Figure 2. Crystal structure of 5-methylpyrazine-2-carboxamide, **2**.

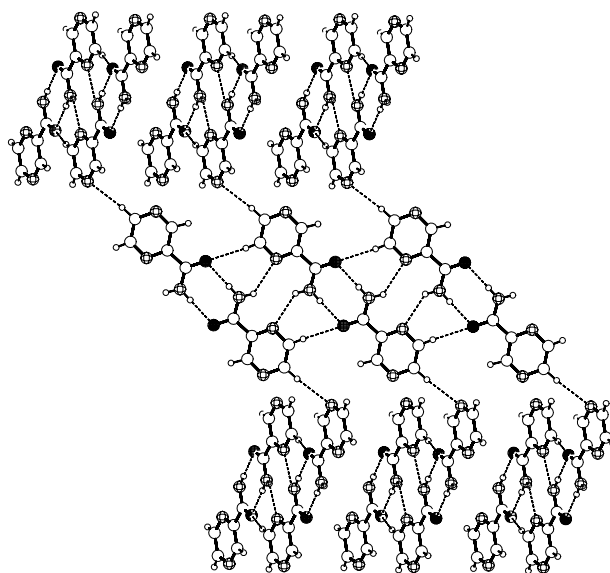


Figure 3. Crystal structure of α -polymorph of pyrazinamide, **1**. Notice the similarities between Figure 2 and 3.

3.3 3-Methylpyrazine-2-Carboxamide, **3**

The *ortho*-methyl isomer 3-methylpyrazine-2-carboxamide, **3** crystallizes in the monoclinic system with two molecules in the asymmetric unit (space group $P2_1/c$). The carboxamide groups are almost in the plane of the pyrazine ring (torsions N–C–C–N: 11.5 and 15.6°). Both the carboxamide groups form the centrosymmetric amide synthon **I** through *syn*-N–H \cdots O bonds. Such dimers are connected by *anti*-N–H \cdots N (synthon **VI**) hydrogen bonds along *c*-axis. C6–H donor forms C–H \cdots O bond with the carbonyl oxygen of amide group of the next layer (Figure 4). Such tapes are in turn connected by weak (methyl) C–H \cdots N hydrogen bonds (Figure 5). Metrics of hydrogen bonds are listed in Table 1. It is notable that such tapes are also observed in the crystal structure of **2**.

3.4 6-Methylpyrazine-2-Carboxamide, **4**

6-Methylpyrazine-2-carboxamide, **4** crystallizes in the orthorhombic crystal system with one molecule in the asymmetric unit (space group $Pna2_1$). In this structure also the carboxamide group is co-planar with the heterocyclic pyrazine ring (torsion N–C–C–N: 1.3°). However, the *syn*-N–H forms a N–H \cdots O hydrogen bonded catemer parallel to the *c*-axis. Such chains are in turn connected through N–H \cdots N(pyrazine) and C5–H \cdots O hydrogen bonds in a herringbone fashion (Figure 6). The metrics of the hydrogen bonds are shown in Table 1.

In the crystal structures **2** and **3**, amide groups form dimer synthon **I** but the catemer is formed in **4**. In amides **2** and **3** C6–H donor involved in C–H \cdots O hydrogen bonding, is a part of multipoint synthon **VI**. In amide **4** methyl group is present at the C6 atom. Hence, synthon **VI** is not possible because the N–H \cdots N hydrogen bonds cannot form with bulky *ortho*-pyridyl N-atom. Replacement of H with Me at C6 position therefore results in global structural changes because it disrupts stronger hydrogen bonding elsewhere in the crystal. The structure **2** and **4** indicates that the

structural changes are minimum when a methyl group replaces the single contact hydrogen-bonded proton, but results in different packing when hydrogen is part of the multipoint synthon. It is interesting to note that in all the pyrazinecarboxamides **2–4**, the *anti*-N–H of amide is hydrogen bonded to the pyrazine nitrogen not to the carbonyl oxygen of amide.

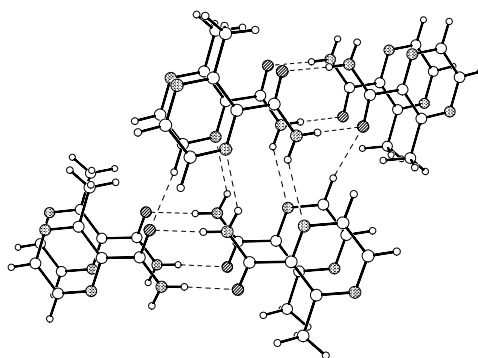


Figure 4. Supramolecular synthon **VI** in the crystal structure of 3-methylpyrazine-2-carboxamide, **3**.

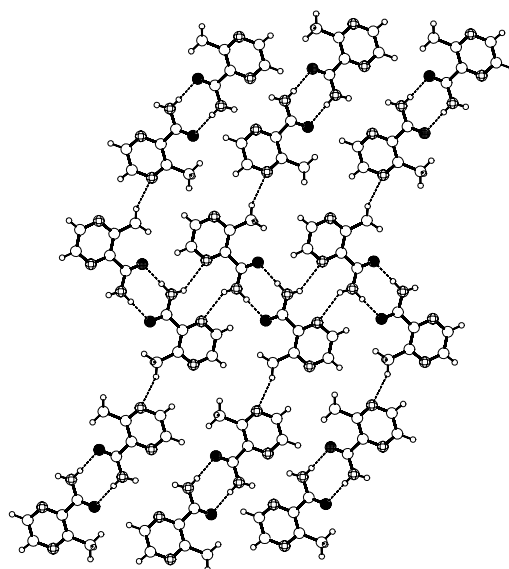


Figure 5. Crystal structure of 3-methylpyrazine-2-carboxamide, **3**.

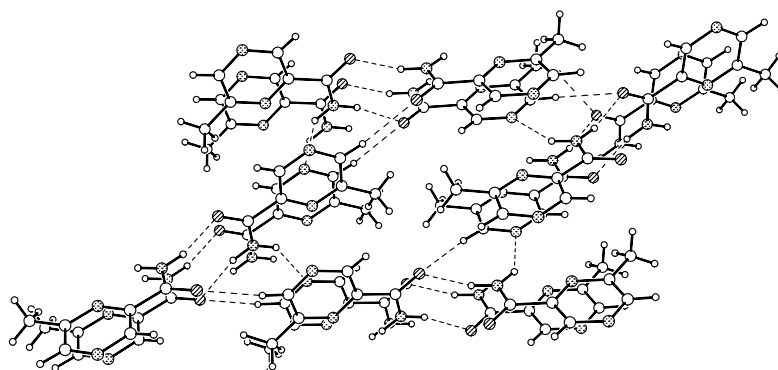


Figure 6. Crystal structure of 6-methylpyrazine-2-carboxamide, **4**.

3.5 Staircase Network in Pyrazine-2,3-Dicarboxamide, **5**

Pyrazine-2,3-dicarboxamide, **5** crystallizes in the triclinic system with one molecule in the asymmetric unit (space group $P\bar{1}$). The molecular geometry of **5** is shown in Figure 7. One of the carboxamide groups (C10) is in the plane of the heterocyclic pyrazine ring (torsion N–C–C–N: 6.8°) whereas the other (C7) is out of the plane (torsion N–C–C–N: 62.3°). The carboxamide group that is coplanar with the pyrazine ring (C10) forms centrosymmetric N–H_s⋯O dimers, which extend in a linear tape along $[2\ 0\ 1]$ via C–H⋯N dimers. In the normal 5.1 Å packing, translation related amide dimers are connected by N–H_a⋯O bonds to produce a sheet-like structure, as in benzamide. In **5**, however, the *anti*-N–H of the C10 carboxamide is bonded to the oxygen atom of the out of plane C7 carboxamide group, connecting the tapes mentioned above by translation along b -axis. This produces a staircase-like pattern, with the tape along $[2\ 0\ 1]$ constituting the flat step and the N–H_a⋯O bond along $[0\ 1\ 0]$ giving the height to the staircase (Figure 8). The C7 amide N–H donors connects the staircase networks via N–H⋯O hydrogen bonds (Figure 9). Such a molecular staircase motif was also identified recently in the crystal structure of the complex of benzene-1,2,4,5-tetracarboxylic acid and hexamethylenetetramine (Figure

10).²⁵ Very recently Bishop and coworkers have shown the staircase inclusion compounds formed by tetrahalodiquinoline hosts.²⁶

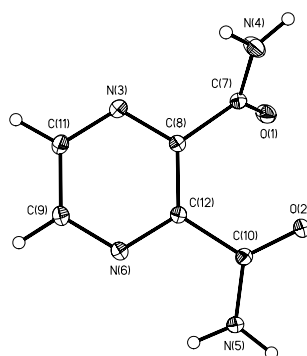


Figure 7. ORTEP plot of diamide **5**. Displacement ellipsoids are drawn at 50 % probability level for non-hydrogen atoms. Notice that C7 amide is out-of-plane of pyrazine ring whereas C10 amide is almost co-planar with the pyrazine.

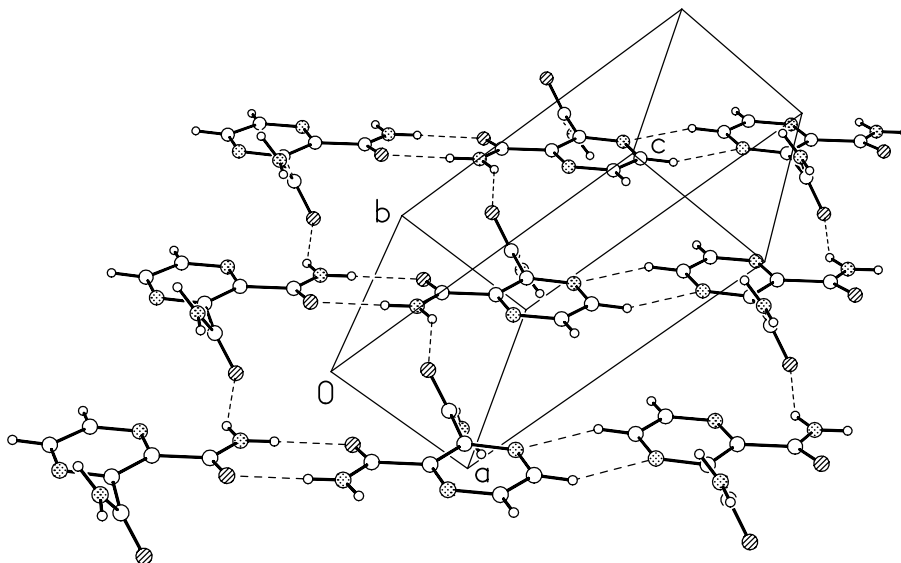


Figure 8. The crystal structure of diamide **5**, showing the molecular staircase. The linear tapes of N-H_s...O and C-H...N dimers **I** and **V** form the steps of the staircase and the N-H_a...O bonds along [0 1 0] build the network upwards.

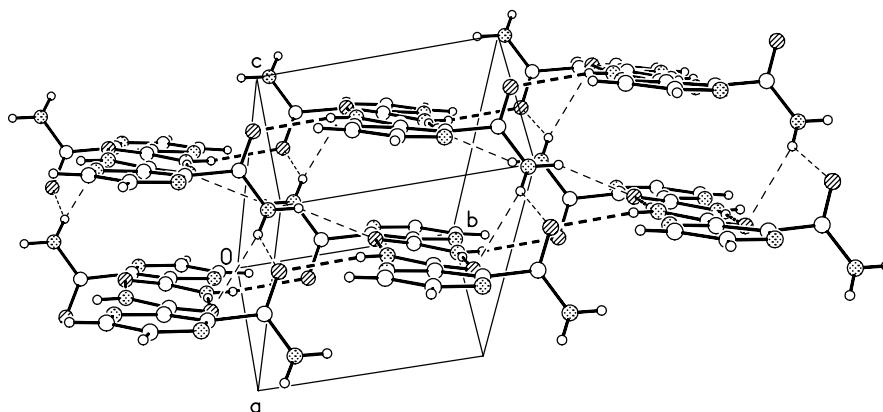


Figure 9. A side view of the molecular staircase network in **5**. The C7 carboxamide NH_2 groups connects the staircase networks *via* $\text{N-H}\cdots\text{O}$ hydrogen bonds.

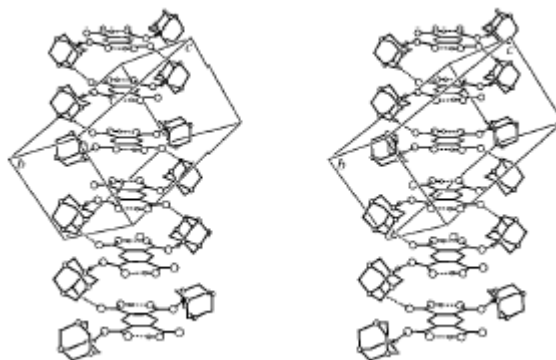


Figure 10. Stereoview of crystal structure of benzene-1,2,4,5-tetracarboxylic acid and hexamethylenetetramine, showing the molecular staircase.

In the structure **5**, hydrogen bonding in both the amide groups is satisfied because the number of strong donors (four, two NH_2 groups) and acceptors (four, two C=O groups) are matched. The weak C-H donors are bonded to the heterocyclic pyrazine nitrogen atoms. The crystal structure may therefore be rationalized *via* the preferred combinations of hydrogen bond donors and acceptors.²⁷ It may be noted that each atom in **5** is either a donor (N-H , $\text{Csp}^2\text{-H}$) or an acceptor (C=O , pyrazine N -

atom) and, further all these groups are involved in hydrogen bonding. The structure **5** may be compared with that of pyrazine-2,3-dicarboxylic acid, which crystallizes as a dihydrate.²⁸ The imbalance of the donor–acceptor ratio in the diacid (2:4) is compensated by the inclusion of the two water molecules.

3.6 Cambridge Structural Database Study

From the crystal structures of pyrazinecarboxamide methyl isomers **2–4**, it is evident that the *syn*-N–H of carboxamide makes hydrogen bonds with the carbonyl oxygen of the amide functionality, whereas the *anti*-N–H is hydrogen bonded to the pyrazine N-atom, not to the carbonyl oxygen of the amide group. Crystallographic data were retrieved from the November 2002 (Conquest 1.5, 272066 entries) release of the Cambridge Structural Database²⁹ to verify the recurrence of N–H_a⋯N hydrogen bond. Sub-data base of 36 structures that contain CONH₂ and pyridine moiety were retrieved for the structures with good accuracy (3D coordinates present, no ions and R-factor ≤ 0.10). Of these, 18 entries form the amide–amide homosynthon **I** with the N–H_s⋯O distance and angle range: 1.5–2.4 Å, 130–180°. All the hydrogen atoms involved in non-bonded contact searches were placed in neutron-normalized positions. Out of 18 structures only three structures contain N–H_a⋯N hydrogen bond (Refcode: BOHJIR, PYRZIN and WISZIH).³⁰ 7 entries are involved in N–H_a⋯O hydrogen bond (Refcode: BUDWEC, IACNCA, OFERAS, PEQBES, PYRAZIN01, SEKDOB and XEGPII). Other 8 structures are engaged in an intramolecular N–H_a⋯O, N–H_a⋯N and N–H_a⋯π interactions. Very recently Zaworotko *et.al.*,³¹ have noticed from a database study that nearly 30 % of *anti*-oriented N–H groups are not involved in hydrogen bonding, most commonly because of steric hindrance.

3.7 Conclusions

The crystal chemistry of methyl isomers of pyrazinecarboxamide has been studied. Structures 5-methylpyrazine-2-carboxamide, **2** and 3-methylpyrazine-2-carboxamide, **3** form the more common centrosymmetric amide–amide homosynthon **I**. However, 6-methylpyrazine-2-carboxamide, **4** forms N–H \cdots O hydrogen bonded catemer. In all the three amide structures **2–4**, *anti*-N–H is hydrogen bonded to the pyrazine nitrogen, not to the carbonyl oxygen of amide group. The N–H \cdots N hydrogen bond is a recurring pattern in **2–4**. Database study shows that there are only three such examples in the literature. Crystal structure of 5-methylpyrazine-2-carboxamide, **2** is isostructural to the α -form of pyrazinamide, **1**. Pyrazine-2,3-dicarboxamide, **5** forms a rare staircase type of network.³²

3.8 Experimental Section

Synthesis

Pyrazine carboxamides **2–4** were synthesized by the reaction of NH₄OH with the corresponding methyl esters, which in turn were prepared by esterification of corresponding carboxylic acids. Synthesis of methyl isomers of pyrazine carboxylic acids was described in the previous chapter.

1. Synthesis of 5-methylpyrazine-2-carboxamide, **2**

Methyl 5-methylpyrazine-2-carboxylate: 5-Methylpyrazine-2-carboxylic acid (100 mg, 0.72 mmol) was dissolved in THF at 0 °C. Diazomethane gas was bubbled into the reaction mixture till the solution turns yellow. THF solvent was removed and the resultant methyl ester was purified by column chromatography. Yield: 95 mg (86 %). ¹H-NMR (CDCl₃): δ 2.67 (s, 3H), 4.03 (s, 3H), 8.58 (s, 1H), 9.20 (s, 1H). IR (KBr): 3420, 2965, 1716, 1579, 1485, 1440, 1350, 1284, 1178, 1138, 1033, 788, 723 cm⁻¹.

Similar procedure was applied to prepare methyl 3-methylpyrazine-2-carboxylate and methyl 6-methylpyrazine-2-carboxylate from their respective carboxylic acids.

5-Methylpyrazine-2-carboxamide: To 1 ml of aqueous NH_3 , methyl 5-methylpyrazine-2-carboxylate (50 mg, 0.33 mmol) was added cooled to 0 °C in an ice bath and stirred for one hour. The reaction mixture was filtered and the solid was washed with cold water. The product was recrystallized from 1:1 solvent mixture of hexane and ethyl acetate to obtain single crystals. Yield: 43 mg (95 %). $^1\text{H-NMR}$ (CDCl_3): δ 2.66 (s, 3H), 5.75 (b, 1H), 7.64 (b, 1H), 8.41 (s, 1H), 9.35 (s, 1H). IR (KBr): 3449, 1685, 1581, 1406, 1315, 1033, 570 cm^{-1} . Similar procedure was adopted to synthesize **3** and **4** from their corresponding methyl esters.

2. Synthesis of 3-methylpyrazine-2-carboxamide, **3**

Methyl 3-methylpyrazine-2-carboxylate: $^1\text{H-NMR}$ (CDCl_3): δ 2.91 (s, 3H), 4.05 (s, 3H), 8.51 (s, 1H), 8.62 (s, 1H). IR (KBr): 3412, 2957, 1722, 1427, 1402, 1300, 1213, 1172, 1105 cm^{-1} .

3-Methylpyrazine-2-carboxamide: M.p. 180 °C. $^1\text{H-NMR}$ (CDCl_3): δ 2.98 (s, 3H), 5.70 (b, 1H), 7.80 (b, 1H), 8.42 (s, 1H), 8.65 (s, 1H). IR (KBr): 3400, 3205, 1705, 1601, 1562, 1425, 1379, 1172, 1134, 1080, 873 cm^{-1} . Single crystals were obtained by recrystallization from 1:1 hexane and ethyl acetate solvent mixture.

3. Synthesis of 6-methylpyrazine-2-carboxamide, **4**

Methyl 6-methylpyrazine-2-carboxylate: M.p. 63 °C. $^1\text{H-NMR}$ (CDCl_3): δ 2.68 (s, 3H), 4.03 (s, 3H), 8.58 (s, 1H), 9.20 (s, 1H). IR (KBr): 3412, 2957, 1718, 1579, 1440, 1350, 1284, 1178, 1138, 1033 cm^{-1} .

6-Methylpyrazine-2-carboxamide: M.p. 164 °C. $^1\text{H-NMR}$ (CDCl_3): δ 2.65 (s, 3H), 5.64 (b, 1H), 7.63 (b, 1H), 8.62 (s, 1H), 9.20 (s, 1H). IR (KBr): 3410, 3207, 1660,

1579, 1417, 1367, 1273, 1197, 1143, 1084, 1020 cm^{-1} . Needle shaped crystals were obtained from ethyl acetate.

Pyrazine-2,3-dicarboxamide, 5 was purchased and fine cubic shaped single crystals were obtained from water.

X-ray Crystallography

Dr. Vincent M. Lynch collected the X-ray data for all the amides **2–5** on a Nonius Kappa CCD diffractometer, at University of Texas, Austin, U.S.A. Structure solutions and refinements were performed with SHELXS-97 and SHELXL-97 program packages on Silicon Graphics Octane2 workstations. The relevant crystallographic information is given in the appendix.

3.9 References and Notes

1. G.A. Jeffrey and W. Saenger, *Hydrogen Bonding in Biological Structures*, Springer-Verlag, Berlin, Heidelberg, New York, **1991**.
2. L. Pauling, *The Nature of the Chemical Bond*, Cornell University Press, Ithaca, NY, **1939**.
3. L. Pauling, R.B. Corey and H.R. Branson, *Proc. Nat. Acad. Sci.*, **1951**, 37, 205.
4. J.D. Watson and F.H.C. Crick, *Nature*, **1953**, 171, 737.
5. Y. Tokunaga and J. Rebek Jr., *J. Am. Chem. Soc.*, **1998**, 120, 66.
6. J. Rebek Jr., *Chem. Soc. Rev.*, **1996**, 255.
7. M. Mascal, N.M. Hext, R. Warmuth, M.H. Moore and J.P. Turkenburg, *Angew. Chem., Int. Ed. Engl.*, **1996**, 35, 2204.
8. E. Fan, J. Yang, S.J. Geib, T.C. Stoner, M.D. Hopkins and A.D. Hamilton, *Chem. Commun.*, **1995**, 1251.
9. S.J. Geib, C. Vicent, E. Fan and A.D. Hamilton, *Angew. Chem., Int. Ed. Engl.*, **1993**, 32, 119.

10. J.C. MacDonald and G.M. Whitesides, *Chem. Rev.*, **1994**, 94, 2383.
11. M. Mascal, P.S. Fallon, A.S. Batsanov, B.R. Heywood, S. Champ and M. Colclough, *Chem. Commun.*, **1995**, 805.
12. M.R. Ghadiri, J.R. Granja, R.A. Milligan, D.E. McRee and N. Khazanvoich, *Nature*, **1993**, 366, 324.
13. K.D.M. Harris, *Chem. Soc. Rev.*, **1997**, 26, 279.
14. G.T.R. Palmore and M.R. McBride, *Chem. Commun.*, **1998**, 145.
15. M. Simard, D. Su and J.D. Wust, *J. Am. Chem. Soc.*, **1991**, 113, 4696.
16. R. Kleppinger, C.P. Lillya and C. Yang, *J. Am. Chem. Soc.*, **1997**, 119, 4097.
17. L. Leiserowitz and G.M.J. Schmidt, *J. Chem. Soc., Sect. A*, **1969**, 2372.
18. (a) J.C. MacDonald and G.T.R. Palmore, *The Role of Amides in the Non-covalent Synthesis of Supramolecular Structures in Solution, at Interfaces and in Solids in The Amide Linkage: Selected Structural Aspects in Chemistry, Biochemistry, and Materials Science*; eds., A. Greenberg, C.M. Breneman and J.F. Liebman, John Wiley & Sons, Inc., New York, **2000**, pp.291–336. (b) J. Rebek Jr., *Acc. Chem. Res.*, **1999**, 32, 278. (c) S.S. Kuduva, D. Bläser, R. Boese and G.R. Desiraju, *J. Org. Chem.*, **2001**, 66, 1621. (d) R.E. Meléndez and A.D. Hamilton, *Hydrogen-Bonded Ribbons, Tapes and Sheets as Motifs for Crystal Engineering in Design of Organic Solids*, ed., E. Weber, Springer, Berlin, **1998**, pp.97–130. (e) G.T.R. Palmore, T.M. Luo, M.T. McBride-Wieser, E.A. Picciotto and C.M. Reynoso-Paz, *Chem. Mater.*, **1999**, 11, 3315. (f) G.M. Whitesides, E.E. Simanek, J.P. Mathias, C.T. Seto, D.N. Chin, M. Mammen and D.M. Gordon, *Acc. Chem. Res.*, **1995**, 28, 37. (g) J. Bernstein, M.C. Etter and L. Leiserowitz, *Structure Correlation*, eds., H.-B. Bürgi and J.D. Dunitz, VCH, Weinheim, **1994**, Vol. 2, pp.431–507.
19. F.H. Allen, W.D. Motherwell, P.R. Raithby, G.P. Shields and R. Taylor, *New J. Chem.*, **1999**, 25.

20. (a) Y. Takaki, Y. Sasada and T. Watanabé, *Acta Crystallogr.*, **1960**, *13*, 693, (α -form, CSD Refcode: PYRZIN). (b) R.K. Tiwari, T.C. Patel and T.P. Singh, *Indian J. Phys., Sect. A*, **1982**, *56*, 413, (α -form, PYRZIN14). (c) R.K. Tiwari, N. Deo and T.P. Singh, *J. Sci. Res.*, **1980**, *2*, 161, (α -form, PYRZIN04). (d) G. Rø and H. Sørum, *Acta Crystallogr., Sect. B*, **1972**, *28*, 991, (β -form, PYRZIN01). (e) K. Nakata and Y. Takaki, *Mem. Osaka Kyoiku Univ. Ser.3*, **1987**, *36*, 93, (γ -form, PYRZIN05). (f) C. Tamura and H. Kuwano, *Acta Crystallogr.*, **1961**, *14*, 693, (γ -form, PYRZIN03). (g) G. Rø and H. Sørum, *Acta Crystallogr., Sect. B*, **1972**, *28*, 1677, (δ -form, PYRZIN02).
21. (a) J. Bernstein, *Polymorphism in Molecular Crystals*, Clarendon Press, Oxford, **2002**. (b) R.I. Davey, *Chem. Commun.*, **2003**, 1463. (c) J. Bernstein, R.J. Davey and J.-O. Henck, *Angew. Chem., Int. Ed.*, **1999**, *38*, 3440. (d) T.L. Threlfall, *Analyst*, **1995**, *120*, 2435.
22. G.R. Desiraju, *Science*, **1997**, *278*, 404.
23. P. Vishweshwar, A. Nangia and V.M. Lynch, *J. Org. Chem.*, **2002**, *67*, 556.
24. A. Kálmán and L. Párkányi, *Adv. Mol. Struct. Res.*, **1997**, *3*, 189.
25. A.J. Lough, P.S. Wheatley, G. Ferguson and C. Glidewell, *Acta Crystallogr., Sect. B*, **2000**, *56*, 261.
26. A. Noman, M.M. Rahman, R. Bishop, D.C. Craig, C.E. Marjo and M.L. Scudder, *Cryst. Growth Des.*, **2002**, *2*, 421.
27. (a) M.C. Etter, *Acc. Chem. Res.*, **1990**, *23*, 120. (b) M.C. Etter, *J. Phys. Chem.*, **1991**, *95*, 4601.
28. F. Takusagawa and A. Shimada, *Chem. Lett.*, **1973**, 1121.
29. (a) F.H. Allen, *Acta Crystallogr., Sect. B*, **2002**, *58*, 380. (b) A. Nangia, *CrystEngComm*, **2002**, *4*, 93.

30. (a) M. Takimoto, A. Takenaka and Y. Sasada, *Acta Crystallogr., Sect. C*, **1983**, 39, 73, (CSD Refcode: BOHJIR). (b) Ref. 20a (PYRZIN). (c) M.A.S. Goher and F.A. Mautner, *Polyhedron*, **2000**, 19, 601, (WISZIH).
31. S.G. Fleischman, S.S. Kuduva, J.A. McMahon, B. Moulton, R.D.B. Walsh, N. Rodriguez-Hornedo and M.J. Zaworotko, *Cryst. Growth Des.*, **2003**, 3, ASAP.
32. C. Schmuck, *Angew. Chem., Int. Ed.*, **2003**, 42, 2448.

CHAPTER FOUR

A VERY SHORT O–H···O HYDROGEN BOND: A NEUTRON STUDY

4.1 Introduction

A hydrogen bond may be defined as ‘any cohesive interaction $X-H\cdots A$ where H carries a positive and A a negative charge and the charge on X is more negative than on H’. Hydrogen bonds hold much fascination, and some of the most interesting are the very short (very strong) ones. Desiraju and Steiner have classified hydrogen bonds into three categories:¹ weak hydrogen bonds, in which the proton is confined to the potential well near one atom, strong low barrier hydrogen bonds (LBHB), in which the zero-point vibrational energy (ZPVE) of the hydrogen exceeds the proton transfer barrier, and finally very strong hydrogen bonds, in which hydrogen atoms have sufficient ZPVE to shuttle between the two hydrogen-bonded atoms. Some of the properties of very strong, strong and weak hydrogen bonds are shown in Table 1. Jeffrey has classified these categories as strong, moderate and weak hydrogen bonds based on biological structures.² Very strong hydrogen bonds are formed by unusually activated donors and acceptors, often in an intramolecular situation.³ In general they are formed between an acid and its conjugate base, $X-H\cdots X^-$, or between a base and its conjugate acid, $X^+-H\cdots X$. For a homonuclear O–H···O hydrogen bond very strong hydrogen bonds are believed to exist when the O···O distance is shorter than 2.5 Å. Further decrease of the O···O distance is accompanied by a lengthening of the O–H bond and a shortening of the O···H bond until a symmetrical hydrogen bond may be reached for $d_{O\cdots O} \approx 2.39\text{--}2.40$ Å. Very strong hydrogen bonds have a significant covalent character based on investigations by diverse experimental techniques like infrared spectroscopy⁴ and topological analysis of experimental electron densities.⁵ The substantial covalent character of very strong hydrogen bonds, a result of three-center-four-electron contribution, $O^{\bullet}-H\cdots^{\bullet}O \leftrightarrow O^{\bullet}\cdots H-^{\bullet}O$, is responsible for their

distinctive properties: the near linear angular geometry ($\theta = 175\text{--}180^\circ$), the lengthening of O–H covalent bond⁶ and red shift in IR stretching frequencies.² The strength of very strong hydrogen bonds is comparable to that of the weakest covalent bonds. There is great current interest in the strongest types of hydrogen bonds, in particular in the context of chemical reactivity.^{2,7} Very strong hydrogen bonds have low-energy barrier potential wells in which the position of the proton is very variable hence they are also called as low-barrier or polarization enhanced hydrogen bonds.² Very strong hydrogen bonds have been shown to exist in a high-pressure phase of ice⁸ and have been suggested to play a role in enzyme catalysis.⁹

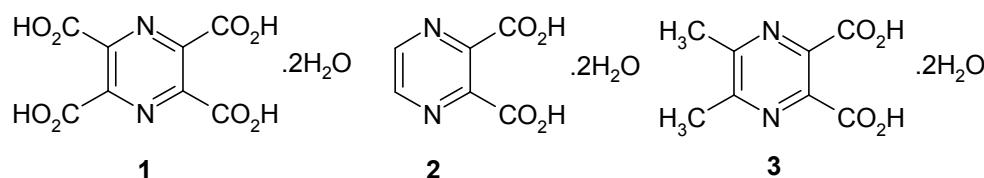
Table 1. Some properties of very strong, strong and weak hydrogen bonds.¹

	Very Strong	Strong	Weak
Bond energy (–kcal/mol)	15–40	4–15	< 4
Bond lengths	$\text{H–A} \approx \text{X–H}$	$\text{H}\cdots\text{A} > \text{X–H}$	$\text{H}\cdots\text{A} \gg \text{X–H}$
Lengthening of X–H (Å)	0.05–0.2	0.01–0.05	≤ 0.01
D(H \cdots A) range (Å)	1.2–1.5	1.5–2.2	2.0–3.0
D(X \cdots A) range (Å)	2.2–2.5	2.5–3.2	3.0–4.0
$\theta(\text{X–H}\cdots\text{A})$ range ($^\circ$)	175–180	130–180	90–180
IR ν , relative shift	> 25%	5–25%	< 5%
^1H chemical shift downfield (ppm)	14–22	< 14	–
Bonds shorter than vdW	100%	Almost 100%	30–80%
Effect on crystal packing	Strong	Distinctive	Variable
Covalency	Pronounced	Weak	Vanishing
Electrostatics	Significant	Dominant	Moderate

Gilli and coworkers¹⁰ have classified the homonuclear O–H···O hydrogen bonds into three classes. (A) There are three classes of very strong hydrogen bonds: (i) (–)CAHB: $\text{–O–H}\cdots\text{O}^-$, negative charge assisted hydrogen bonds.¹¹ (ii) (+)CAHB: $\text{=O–H}^+\cdots\text{O=C}$, positive charge assisted hydrogen bonds.¹² (iii) RAHB: $\text{–O–H}\cdots\text{O=C}$, resonance assisted hydrogen bonds¹³ or π -cooperative hydrogen bonds,¹² where the two oxygen atoms are connected by a π -conjugated system of single and double bonds. (B) One class of strong hydrogen bonds: PAHB, consisting of $\cdots\text{O–H}\cdots\text{O–H}\cdots$ chains of polarization-assisted, or σ -cooperative hydrogen bonds;¹² and (C) one overall class of weak, isolated hydrogen bonds (IHB), which are characterized by being neither charge nor σ - or π -cooperative.

Typical (–)CAHBs [$2.3 \leq \text{D}(\text{O}\cdots\text{O}) \leq 2.50 \text{ \AA}$] are exemplified by intermolecular hydrogen bonds between carboxylic acids and carboxylates. (+)CAHBs [$2.36 \leq \text{D}(\text{O}\cdots\text{O}) \leq 2.43 \text{ \AA}$] are reducible to two identical oxygenated molecules (H_2O , R_2O , Me_2SO , pyridine N-oxide *etc.*), which are bridged by a proton donated by a strong acid. The most common cases of RAHB come from the strong O–H···O hydrogen bonds [$2.39 \leq \text{D}(\text{O}\cdots\text{O}) \leq 2.55 \text{ \AA}$] formed by the heteroconjugated $\cdots\text{O=C–C=C–OH}\cdots$ β -diketone enol group for which a positive synergism between hydrogen bond strengthening and increased π -delocalization of the heterodiene has been described in detail for both intramolecular^{13,14} and intermolecular cases.¹⁵

This chapter describes a very short (carboxyl)O–H···O(water) hydrogen bond observed in the crystal structure of pyrazine-2,3,5,6-tetracarboxylic acid dihydrate **1**. This shortening is attributed to the cumulative stabilization of finite σ - and π -bond cooperativity. This novel hydrogen bond shortening phenomenon is further validated by a variable temperature neutron diffraction (ND) study.



4.2 Cooperativity

The concept that a particular configuration of a single and multiple covalent bonds has a total energy greater than the sum of the energies of the individual bonds is familiar in chemistry. In valence bond theory, this extra energy is called resonance energy, in molecular orbital theory, it is called delocalization energy. The same principle applies to certain patterns of hydrogen bonds, where it is known generally as *nonadditivity* or *cooperativity*.^{1,2} The energy of an array of n interlinked hydrogen bonds is larger than the sum of n isolated hydrogen bonds. This non-additive property arises because the ability of donor and acceptor groups to form hydrogen bonds is further increased by an increase in polarity when the hydrogen bonds form part of a collective ensemble. Two principle mechanisms are responsible for this property and both operate on the mutual polarization of the groups involved.

4.2.1 σ -Bond Cooperativity

If an $X^{\delta-}-H^{\delta+}$ group forms a hydrogen bond $X^{\delta-}-H^{\delta+}\cdots A^{\delta-}$, it becomes more polar. The same is true if it accepts a hydrogen bond, $Y^{\delta-}-H^{\delta+}\cdots X^{\delta-}-H^{\delta+}$. Thus, in a chain with two hydrogen bonds, $Y-H\cdots X-H\cdots A$, *both* the donor and the acceptor become stronger. In other words, functional groups acting simultaneously as hydrogen bond donors and acceptors form extended chains or rings in which the individual hydrogen bonds enhance each other's strengths by mutual polarization. This effect is often called " σ -bond cooperativity", since the charges flow through the $X-H$ σ -bonds, but the terms "polarization-enhanced hydrogen bonding"¹⁶ or

“polarization-assisted hydrogen bonding” have also been proposed.² Model calculations on moderate strength hydrogen bonds yield typical energy gains of around 20 % relative to isolated interactions.¹⁷ The most typical examples are phenols and alcohols, which form infinite chains of single donor–single acceptor $\cdots(\text{R})\text{O}-\text{H}\cdots(\text{R})\text{O}-\text{H}\cdots$ hydrogen bonds which are often remarkably short (*e.g.*, O \cdots O distances 2.660, 2.671 and 2.65 Å in methanol,¹⁸ phenol¹⁹ and *p*-cresol,²⁰ respectively). The σ -bond cooperative stabilization tapers off around 6–7 O–H \cdots O hydrogen bonds.

Harris and co-workers²¹ have reported an exceptionally short and linear C–H \cdots O ($d = 1.96$ Å, $D = 3.02$ Å, $\theta = 169.3^\circ$; $\Delta\nu_{\text{CH}} = 202$ cm^{–1}) hydrogen bond between 1,4-diethynylbenzene and a water molecule in the crystal structure of 4:2:1 complex of Ph₃PO, H₂O and 1,4-diethynylbenzene aggregate (Figure 1). The water molecule is also hydrogen bonded through O–H \cdots O interactions to two molecules of triphenylphosphine oxide (TPPO) oxygen atoms, making it in turn a much stronger acceptor than it normally is. The short C–H \cdots O hydrogen bond is ascribed to the stabilization from σ -bond cooperativity.

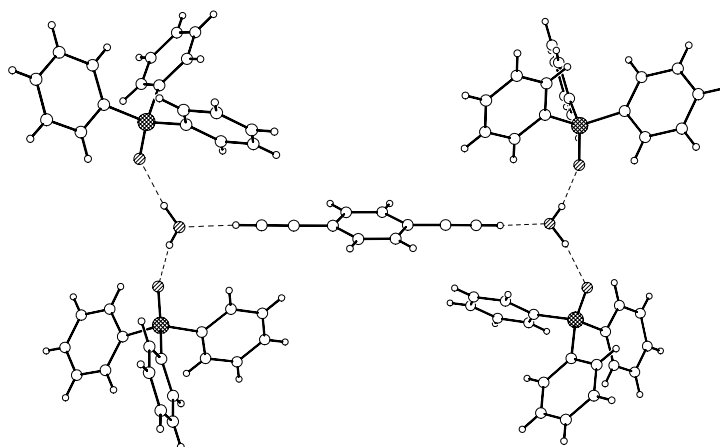
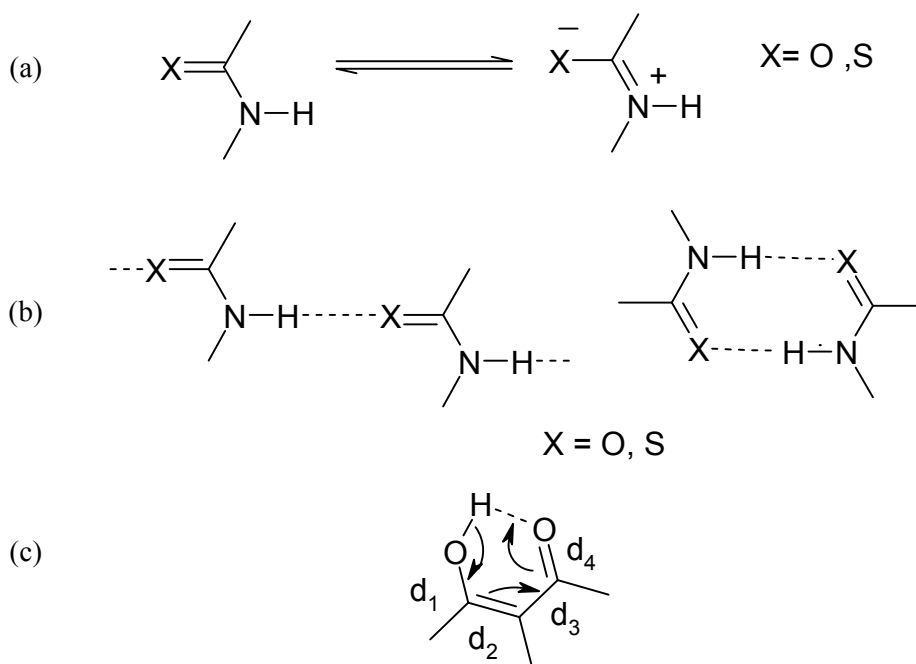


Figure 1. A very short C–H \cdots O hydrogen bond in a chain C \equiv C–H \cdots O_w–H \cdots O=P in the crystal structure of 1,4-diethynylbenzene–water–triphenylphosphine oxide (1:2:4).

4.2.2 π -Bond Cooperativity or Resonance Assisted Hydrogen Bonding (RAHB)

Charge flow in a suitably polarizable π -bond systems increase donor and acceptor strengths. For example, an amide N-H group becomes a stronger donor if the amide O atom accepts a hydrogen bond, $X-H\cdots O=C-N-H$. This is because the zwitterionic resonance form is stabilized (Scheme 1a). The same effect also occurs in thio-amides.¹ Amide units, as a result of their dual donor and acceptor capacity, often form hydrogen-bonded chains or rings (Scheme 1b). Since the polarization occurs through π -bonds, the effect is often called π -bond cooperativity.²



Scheme 1. (a) Resonance forms of amide and thio-amide groups. The neutral form is always dominating, but the weight of the zwitterionic form is increased by accepted as well as by donated hydrogen bonds. (b) Chains and rings as formed by amides and thio-amides through the π -bond cooperativity. (c) The concept of resonance-assisted hydrogen bonding (RAHB) in β -diketone enolates.

On the basis of studies of intramolecular hydrogen bonds in β -diketone enolates Gilli *et. al.* call this effect as “resonance-assisted hydrogen bonding” (RAHB).¹³ A short hydrogen bond in β -diketone enolates is associated with a charge flow through the system of conjugated double bonds (Scheme 1c). The C–O and C–C bonds gain partial double bond character and are shortened, whereas the C=C and C=O bonds are weakened correspondingly. If a delocalization parameter $Q = (d_1 - d_4) + (d_3 - d_2)$ is plotted against the O···O distance, it is seen that the delocalization systematically increases with a shortening of the hydrogen bond distance (Figure 2). In the extreme case of a symmetric position of H atom, Q is zero and the entire fragment becomes symmetric. Completely analogous effects operate in longer chains of conjugated double bonds with intra- and also intermolecular hydrogen bonds. The best-known example is the carboxylic acid dimer.

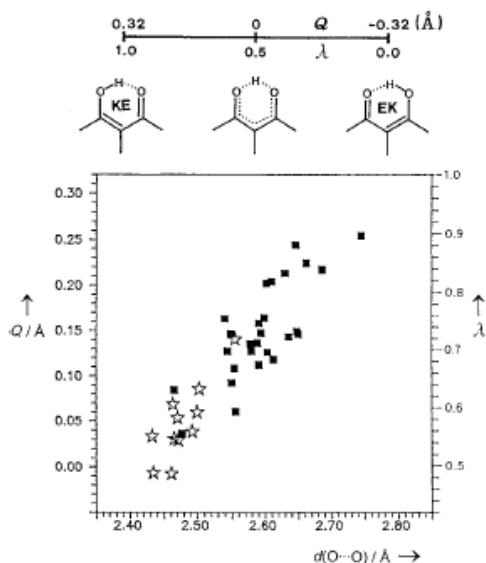
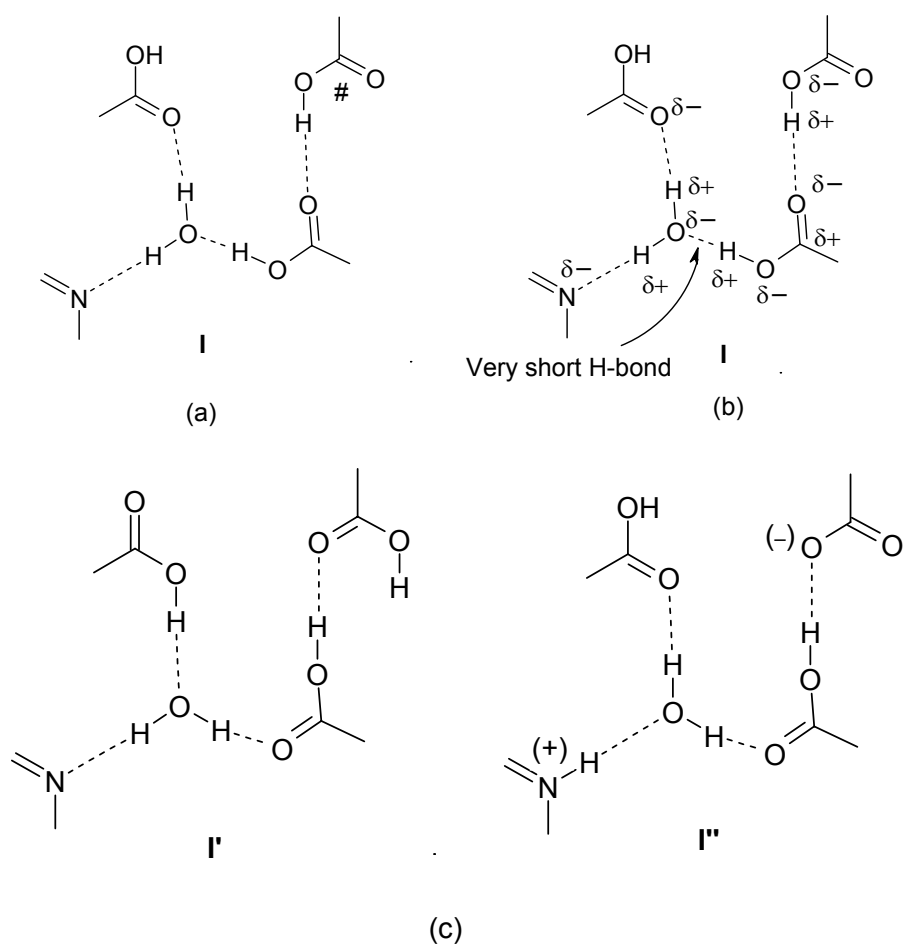


Figure 2. Scatter plot of π -delocalization parameter Q vs the hydrogen bonded O–H···O distances for enolones, showing the degree of π -delocalization decreases with decreasing O···O distance ($Q = 0$ indicates a completely delocalized π -systems, $Q = 0.32$, no delocalization). Stars (☆) represent intramolecular, and squares (■) represent intermolecular hydrogen bonds.

4.3 A Very Short O–H···O Hydrogen Bond in **1**

X-ray diffraction (XRD) quality single crystals of **1** were obtained by recrystallization from dilute HCl. The resulting dihydrate crystallize in the triclinic system and was refined in the centrosymmetric $P\bar{1}$ space group. The molecule resides on an inversion centre. The crystal structure reveals that two carboxylic acid groups are in the plane of the pyrazine ring (torsion angle N5–C4–C3–O2: 9.4°) whereas the other two are out of plane (N5–C6–C7–O8: 80.2°) (Figure 3). The hydration in tetraacid **1** could be because of an imbalance of the donor to acceptor ratio. There are ten acceptor groups whereas only four donors are present in the tetraacid. Water is a donor rich molecule and hence crystallization of the acceptor rich tetraacid **1** as a dihydrate balances the donor/acceptor ratio and stabilizes the crystal packing. It is interesting to note that the carboxylic acid that is coplanar to the pyrazine ring forms a very short (carboxyl)O–H···O(water) [$d = 1.53 \text{ \AA}$, $D = 2.4791(13) \text{ \AA}$, $\theta = 171^\circ$] hydrogen bond (Figure 4). The shortening of (carboxyl)O–H···O(water) hydrogen bond could be because of cooperative array **I** (Scheme 2). Thus, a composite array with σ - and π -bond cooperativity, O–H···O=C–O–H···O_{water}–H···O/N array can shorten an intermolecular O_{acid}–H···O_{water} hydrogen bond into the regime of very short hydrogen bond (O···O < 2.5 \AA). In this very short hydrogen bond both the carboxylic acid O–H donor ability and the water oxygen atom acceptor basicity are simultaneously enhanced through polarization. Such a strong polarizing effect involving water was observed in the complex, Ph₃P=O–1,4-diethynylbenzene–H₂O (4:1:2)²¹ shown in Figure 1. Other O–H···O and O–H···N hydrogen bonds in the crystal are in the short to medium range (Table 2). The present example of very short hydrogen bond is of (i) intermolecular, (ii) not of charge-assisted type,²² (iii) not of the acid–base type²³ and (iv) does not contain highly activated donor and/or acceptor groups.²⁴ The square network structure of **1** is shown in Figure 5.



Scheme 2. (a) Cooperative synthon **I** in tetra-acid **1**. The acid group marked with # is replaced with H₂O in diacids **2** and **3**. (b) Donor and acceptor groups enhanced by polarization in **I**. (c) Tautomer synthons **I'** and **I''** (not observed in **1–3**).

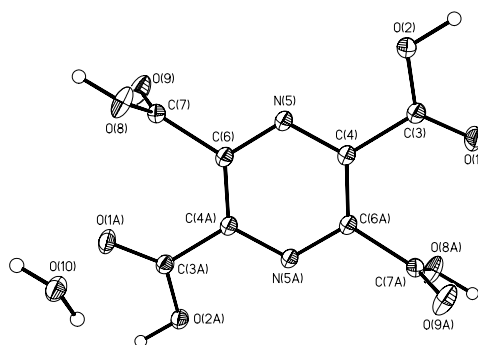


Figure 3. ORTEP drawing of pyrazine-2,3,5,6-tetracarboxylic acid dihydrate **1** showing the atom numbering and 50 % probability ellipsoids for non-hydrogen atoms. Notice the two carboxylic acid groups are co-planar to the pyrazine ring whereas other two are out of plane.

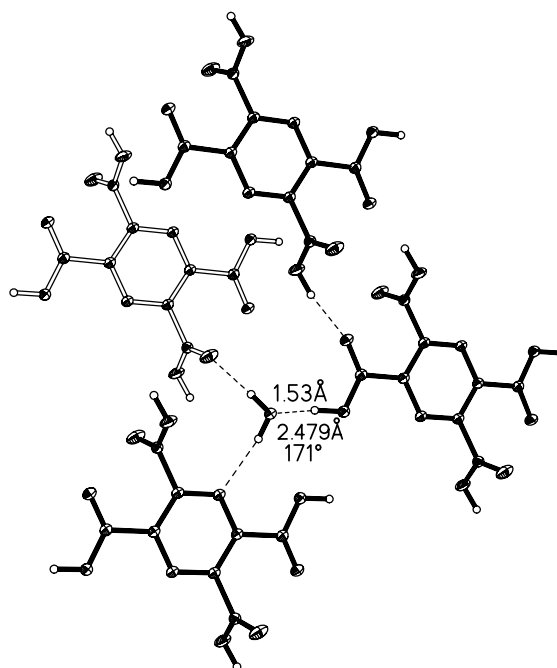


Figure 4. The cooperative array **I** in the crystal structure of **1**. The water molecule forms O–H...O to the carbonyl oxygen of acid of the next layer (shaded differently). Displacement ellipsoids are drawn at 50 % probability level for non-hydrogen atoms. Metrics of very short O–H...O bond are designated.

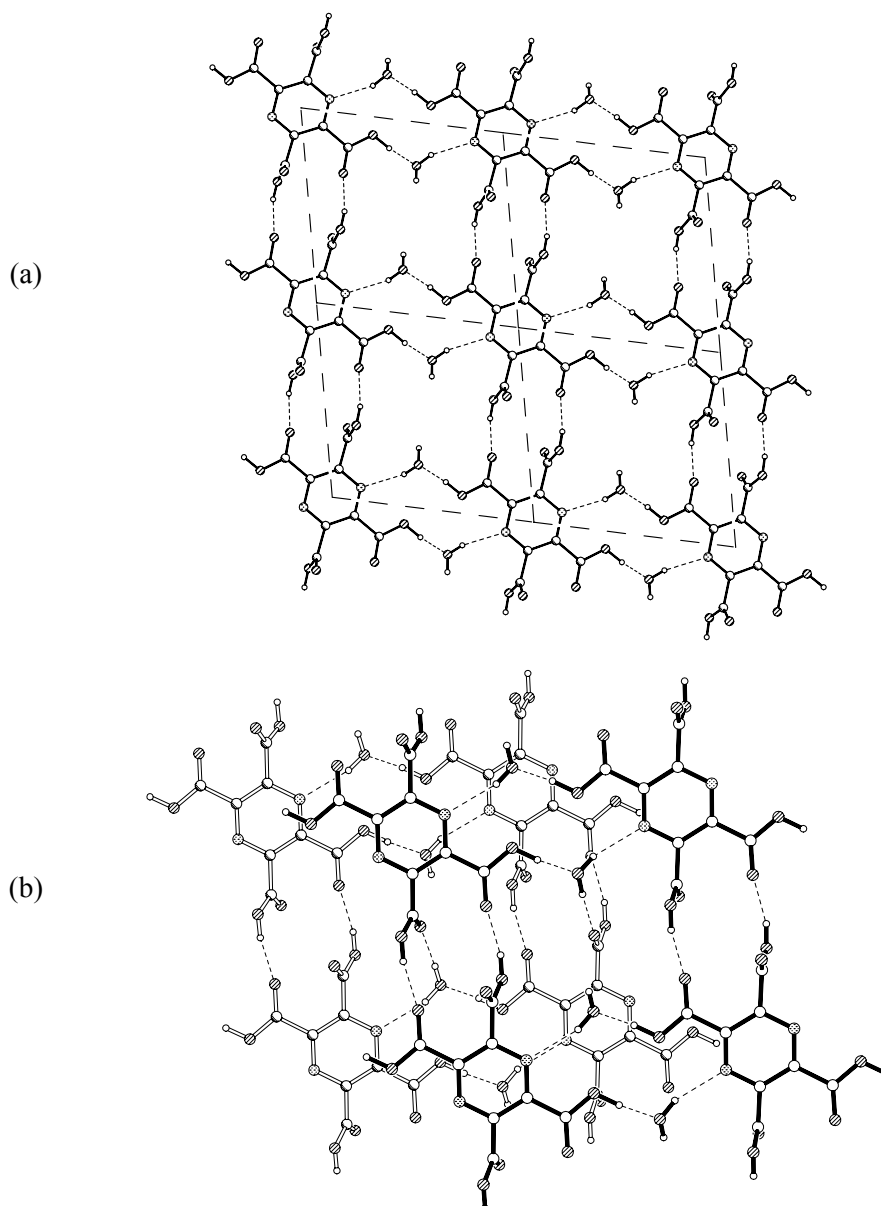


Figure 5. (a) Square network in the crystal structure of pyrazine-2,3,5,6-tetracarboxylic acid dihydrate, **1** with 9.4×9.1 Å dimension. (b) O_{water}–H \cdots O hydrogen bonds connects the square network layers (adjacent layers are shown with different shading).

Table 2. Geometry of O—H \cdots O/ O—H \cdots N hydrogen bonds and C—O bond lengths (X-ray diffraction).

Acid	Hydrogen bond geometry									
	O—H···O				O—H···N				Bond Length	
	O—H /Å	<i>d</i> /Å	<i>D</i> /Å	θ /°	O—H /Å	<i>d</i> /Å	<i>D</i> /Å	θ /°	C—O /Å	C=O /Å
1	0.96(2)	1.53(2)	2.4791(13)	171(2)	0.85(3)	2.14(3)	2.9393(16)	157.6(18)	1.3113(17)	1.2022(15)
	0.91(2)	1.81(2)	2.7010(12)	163.3(18)					1.2957(16)	1.2174(14)
	0.89(2)	1.90(2)	2.7811(12)	172(2)						
2	1.05	1.52	2.5625	170.5	0.73	2.12	2.8402	168.0	1.304	1.208
	0.86	2.14	2.9228	149.1						
3	0.97(2)	1.57(2)	2.5269(12)	167.4(17)	0.87(2)	2.08(3)	2.8963(13)	156.5(18)	1.3143(13)	1.2122(13)
	0.87(2)	2.03(2)	2.8747(12)	163.4(17)						

In order to probe such polarization-induced hydrogen bond shortening in related acids, the crystal structures of pyrazine-2,3-dicarboxylic acid **2** and 5,6-dimethylpyrazine-2,3-dicarboxylic acid **3** were analyzed. The pyrazine diacid **2** was reported as a dihydrate (space group *C2/c*).²⁵ The crystal structure indicates that the carboxylic acid forms a short hydrogen bond with the water molecule (O–H \cdots O: 1.52 Å, 2.5625 Å, 170.5°). Further, the water forms O–H \cdots O and O–H \cdots N hydrogen bonds with carbonyl oxygen of acid and pyrazine N-atom.

4.4 5,6-Dimethylpyrazine-2,3-Dicarboxylic Acid Dihydrate, **3**

The diacid **3** was crystallized as dihydrate in orthorhombic crystal system and refined in the centrosymmetric space group *Pbcn*. The diacid **3** occupies the inversion centre special position. The two adjacent carboxylic acids are out of the plane of pyrazine heterocyclic ring (torsion N–C–C–O: 39.8°). Close examination of the crystal structure reveals that the carboxylic acid O–H donor forms a short O–H \cdots O (1.57 Å, 2.5269(12) Å, 167.4°) hydrogen bond with the water molecule. This is because of polarization of water oxygen since it is forming O–H \cdots O and O–H \cdots N hydrogen bonds with carbonyl oxygen of acid and pyrazine N-atom, respectively (Figure 6). However, O_{acid}–H \cdots O_{water} hydrogen bonds in **2** and **3** are not as short as in **1**. This can be rationalized through differences in their extended arrays: the CO₂H donor (marked # in Scheme 2) in **1** is replaced by H₂O in **2** and **3**. The relative shortness of the O–H \cdots O bond in **3** compared to **2** could be because the donor O–H_{acid} is more polarized by the stronger O_{water}–H \cdots O=C–O–H bond in **3** [O \cdots O: 2.9228 vs 2.8747(12) Å]. The distances should be interpreted with the knowledge that **2** and **3** are X-ray structures determined at different temperatures, but the increase is quite clear. Another reason for the very short O_{acid}–H \cdots O_{water} hydrogen bond in tetra-acid **1** compared to the short hydrogen bond in diacids **2** and **3** is the presence of twice as many electron-withdrawing groups in the former structure. Thus, molecular (four

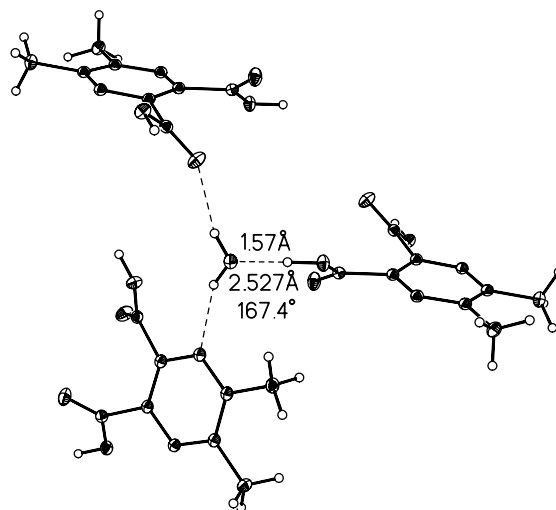


Figure 6. Crystal structure of diacid **3** showing the short (carboxyl)O–H \cdots O(water) hydrogen bond. Metrics of short hydrogen bond are indicated.

CO₂H groups on a pyrazine ring) and supramolecular (extended cooperative array **I**) features act in concert, resulting in the very short O–H \cdots O hydrogen bond in **1**.

In order that the σ - and π -bond cooperative argument through synthon **I** is tenable, the presence of tautomers **I'** and **I''** in tetra-acid **1** must be rigorously excluded, because such motifs would contribute towards resonance stabilization (**I** \leftrightarrow **I'** \leftrightarrow **I''**), and in effect negate the present hypothesis. It is well known that carboxylic acid groups may be characterized as C=O or C–O or as a delocalized carboxylate by their single and double bond lengths.²⁶ A difference of > 0.1 Å implies that a static CO₂H group while a smaller difference (< 0.02 Å) means a resonating or disordered carboxylate. The > 0.1 difference between C=O and C–O bond distances in **1–3** (Table 2) confirms that synthon **I** is present in their crystal structures, and not a resonance-stabilized motif. The protons in **1** and **3** are located from the difference Fourier map and refined isotropically. Since protons are located by XRD, with limited precision, variable temperature ND study of compound **1** was undertaken to locate the

position of protons accurately. The precision in locating proton with XRD is *ca.* 0.01 Å while the accuracy is 0.001 Å with ND.

4.5 X-ray vs Neutron Diffraction

The Cambridge Crystallographic Database (CSD)²⁷ indicates that many crystal structures are determined using XRD with the specific intention of studying the hydrogen bond arrangement. However, the hydrogen atom is a weak X-ray scatterer and can be difficult to locate by XRD. There are large numbers of crystal structures with missing or incomplete tables of hydrogen atom coordinates in the database. The problem is particularly acute for O–H and N–H hydrogen atoms that are of the most interest in the design of molecular solids. Even if the protons are located from the difference Fourier map, the precision with which they are located is comparatively poor. Typical random errors in X-ray O–H or N–H bond lengths are 0.05–0.1 Å,²⁸ by way of comparison, random errors in C–C or N–O distances are usually an order of magnitude smaller. Moreover, X-rays are scattered primarily by electron, and the electron density around a bonded hydrogen atom is distorted along the D–H direction towards the donor atom. Thus, X-ray D–H distances tend to be about 0.1 Å shorter than the true mean internuclear separation. These problems are avoided if ND is used instead of XRD. Neutrons are scattered primarily by atomic nuclei, and D–H distances are therefore measured without serious systematic error. Furthermore, the neutron scattering powers of hydrogen, carbon, oxygen, and nitrogen are all of comparable magnitude. Consequently, O–H and N–H distances are measured almost as precisely as, *e.g.*, C–C or N–O distances (typical random error would be 0.005 Å).

4.6 Variable Temperature ND Structures of Tetra Acid, **1**

Neutrons are used in chemistry, physics and biomolecular sciences, typically for providing accurate anisotropic displacement parameters and accurate hydrogen atom positions and thermal motions. Hydrogen bonds have been studied extensively by ND experiments.²⁹ ND measurements have been made at four different temperatures: 20, 100, 200, and 293 K for tetra acid **1** in order to allow a comparison of the temperature effects on very short $\text{O}_{\text{acid}}\text{--H}\cdots\text{O}_{\text{water}}$ hydrogen bond. Details of experimental ND is given at the end of the chapter. There is no major change in covalent bond distances and angles observed upon cooling the crystal. However, the reduction of thermal motion upon cooling is quite evident from Figures 7. With very short hydrogen bonds, an important point is how sharply the hydrogen atom is located. Table 3 shows that the mean square displacement of the proton in the very short hydrogen bond is small, even smaller than those of the protons of the hydrogen atoms bonded to water and carboxylic acid O–H that is involved in $\text{O--H}\cdots\text{O}=\text{C}$ moderate hydrogen bond. This implies that the proton in the very short hydrogen bond is sharply located. It is notable that in tetra acid **1**, very short hydrogen bond is becoming shorter as temperature decreases from room temperature (293 K) to 20 K (Table 4). Very strong homonuclear $\text{O--H}\cdots\text{O}$ hydrogen bonds are experimentally well accessible, and numerous examples of centered or almost centered geometries have been reliably found by ND experiments.³⁰ Recently Steiner, Majerz and Wilson³¹ have observed the proton migration from phenol oxygen to pyridine nitrogen in the cocrystal of pentachloro phenol and 4-methylpyridine as temperature decreases from room temperature to 20 K. However such proton migration is not observed in tetra acid **1**. From Figure 7 it is very clear that the proton that is involved in very short hydrogen bond is covalently bonded to the carboxylic acid at all temperatures. This supports the present hypothesis of hydrogen bond shortening in **1** through finite σ -

and π -bond cooperativity array **I** and not because of tautomers **I'** or **I''** motifs, which could contribute towards resonance stabilization of hydrogen bond shortening.

Table 3. Mean square displacement parameters (U_{eq}) of protons in tetra acid **1** at different temperatures.

Proton	20 K	100 K	200 K	293 K
O _{acid} –H···O _{water}	0.0167(5)	0.0218(3)	0.0291(6)	0.0371(6)
O _{acid} –H···O _{acid}	0.0205(6)	0.0265(4)	0.0404(7)	0.0515(8)
O _{water} –H···O _{acid}	0.0239(6)	0.0306(4)	0.0415(7)	0.0554(9)
O _{water} –H···N	0.0236(6)	0.0256(4)	0.0348(7)	0.0434(7)

Table 4. Geometrical parameters of neutron data of **1** at variable temperatures.

H-bond	T /K	O–H /Å	<i>d</i> /Å	<i>D</i> /Å	θ /°
O _{acid} –H···O _w	20	1.0721(15)	1.4098(17)	2.4751(11)	171.45(15)
	100	1.0720(13)	1.4113(14)	2.4765(10)	171.46(11)
	200	1.0640(16)	1.4233(18)	2.4807(12)	171.60(16)
	293	1.0550(20)	1.4430(20)	2.4906(16)	171.35(17)
O _{acid} –H···O _{acid}	20	0.9861(17)	1.7393(18)	2.6919(12)	161.28(18)
	100	0.9871(14)	1.7365(14)	2.6931(9)	162.14(13)
	200	0.9895(19)	1.7370(19)	2.6996(14)	163.28(19)
	293	0.9839(19)	1.7490(20)	2.7080(15)	163.70(20)
O _w –H···O _{acid}	20	0.9670(18)	1.8174(19)	2.7794(12)	172.80(20)
	100	0.9670(14)	1.8151(14)	2.7781(10)	173.51(17)
	200	0.9652(20)	1.8231(20)	2.7836(14)	173.03(21)
	293	0.9607(19)	1.8450(20)	2.8001(15)	172.70(30)
O _w –H···N	20	0.9690(20)	1.9982(19)	2.9256(12)	159.56(17)
	100	0.9699(18)	2.0050(17)	2.9340(9)	159.70(12)
	200	0.9630(20)	2.0300(20)	2.9534(13)	159.90(17)
	293	0.9560(20)	2.0600(20)	2.9777(14)	160.28(18)

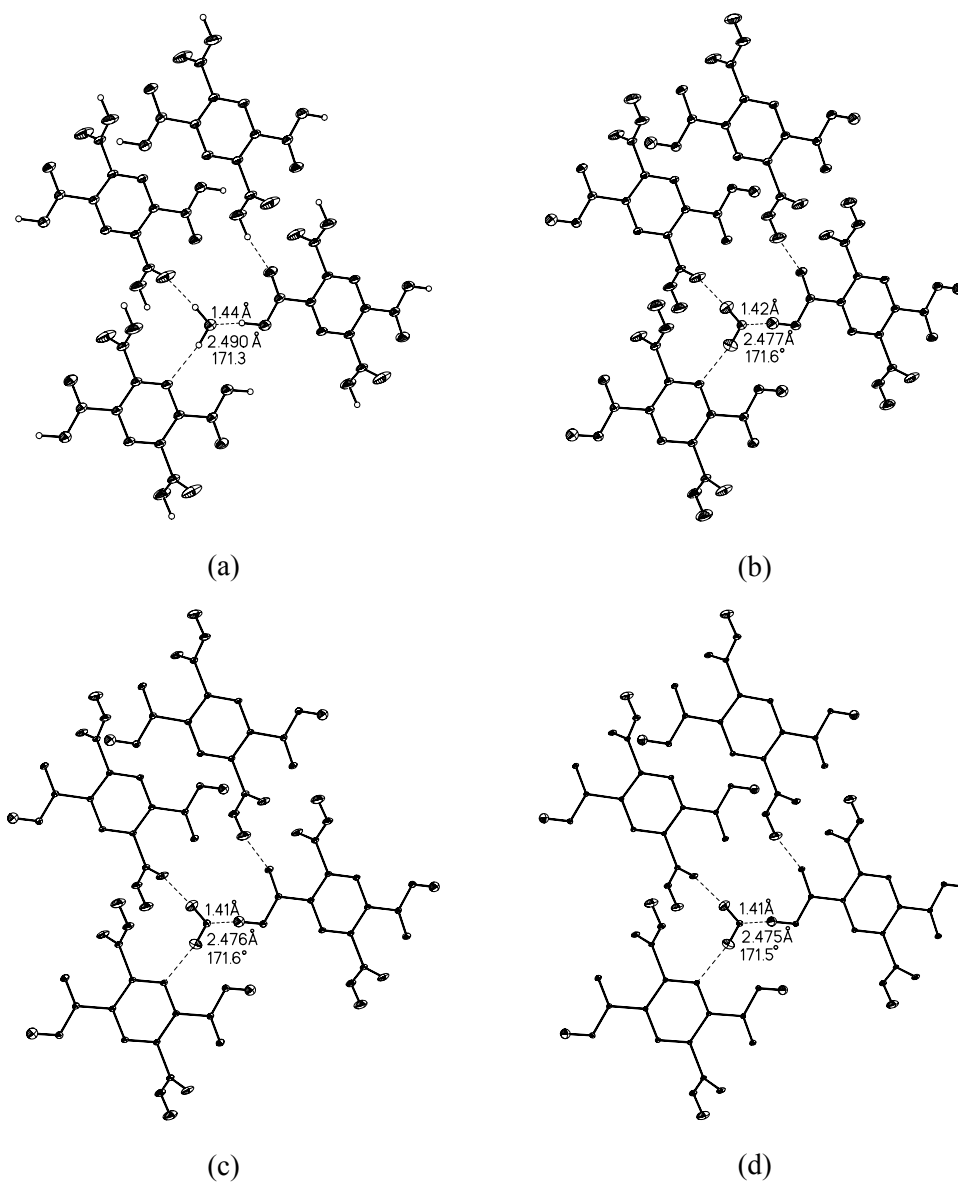


Figure 7. Cooperative array **I** is shown for the variable temperature ND structures of tetra acid **1**. Displacement ellipsoids are drawn at 50 % probability level. (a) at 293 K; (b) 200 K; (c) 100 K; (d) 20 K. Metrics of very short hydrogen bond is indicated. Notice that thermal vibrations of atoms decrease from room temperature to low temperatures. All protons are fully ordered.

Oxalic acid dihydrate structures also have a very short O_{acid}–H···O_{water} hydrogen bond. There are 11 oxalic dihydrate structures with O···O < 2.5 Å for O_{acid}–H···O_{water} hydrogen bond in CSD. In these crystal structures, activation of the donor O–H in the 1,2-dicarboxylic acid moiety results in very short hydrogen bond. The scatter plot, angle vs distance of O_{acid}–H···O_{water} hydrogen bond for 11 oxalic and 5 tetra acid structures (one X-ray and four variable temperature ND) is shown in Figure 8. From the scatter plot it is clear that O_{acid}–H···O_{water} hydrogen bond in **1** is shorter (stronger) than oxalic acid structures. In neutron diffraction category tetra acid **1** is the first example of very short O_{acid}–H···O_{water} hydrogen bond.

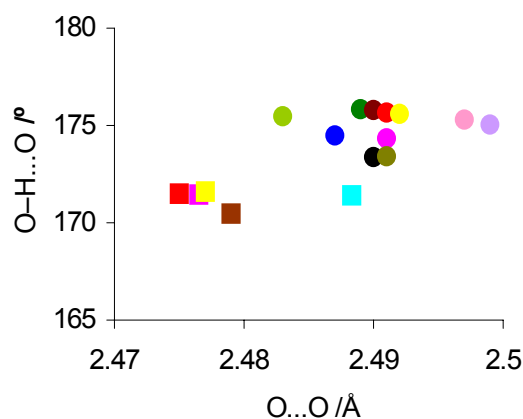


Figure 8. Scatterplot of O–H···O angle vs O···O distances for O_{acid}–H···O_{water} hydrogen bond for 11 oxalic and 5 tetra acid structures. Tetra acid structures are represented as squares (■) and oxalic acid structures as circles (●). Tetra acid ND: (■ 20 K, ■ 100 K, ■ 200 K, ■ 293 K), X-ray ■ 123 K. Oxalic acid: (● 15 K); (●, ●, ● 100 K); (●, ● 130 K); (●, ●, ● 170 K); (●, ● 225 K).

4.7 Conclusions

In general very short hydrogen bonds are formed between charged species and also in resonance stabilized neutral systems. The very short O_{acid}–H···O_{water} hydrogen bond in 2,3,5,6-pyrazine tetracarboxylic acid dihydrate **1** is characterized

by low temperature X-ray diffraction. It has been shown that polarization through a finite σ - and π -bond cooperativity array **I** can also shorten O–H \cdots O bond into the very short regime (O \cdots O < 2.5 Å). The hypothesis of hydrogen bond shortening in **1** is validated by the variable temperature (20, 100, 200 and 293 K) neutron diffraction.

4.8 Experimental Section

Synthesis

The tetra-acid **1** and diacid **3** were synthesized and characterized by the known methods of IR, ^1H -NMR spectroscopy and melting point determinations.

Pyrazine-2,3,5,6-tetracarboxylic acid, **1**³²

A hot solution of 2.28 g (14.4 mmol) of KMnO_4 in 10 ml of water was added drop wise to slurry of 0.2 g (1.11 mmol) of phenazine in 4 ml of hot water containing one pellet of KOH. The mixture was heated on steam bath for 2 hours. After adding few drops of ethanol to destroy the excess KMnO_4 the mixture was filtered and the solid MnO_2 cake was washed with two 10 ml portions of water. The filtrate was concentrated to 10 ml on the hot plate, cooled and acidified drop wise with 36 % HCl. The crude precipitate was washed with hot ethanol and recrystallized from 4 ml of 20% HCl. Yield: 220 mg (77 %), M.p. 202 °C, IR (KBr): 3410, 3234, 1639, 1618, 1398, 1275, 1213, 1134, 831, 748, 613 cm^{-1} .

5,6-Dimethylpyrazine-2,3-dicarboxylic acid, **3**

The diacid **3** was synthesized by the oxidation of 2,3-dimethyl quinoxaline with KMnO_4 , which in turn was obtained by condensation of diacetyl and o-phenylene diamine.

(a) *Preparation of 2,3-dimethyl quinoxaline*: 0.43 g (4 mmol) of o-phenylene diamine was dissolved in 7 ml of water and the solution was heated to 70 °C. With stirring, a

solution of 0.35 ml (4 mmol) of diacetyl in 5 ml of hot water (about 80 °C) was added to the o-phenylene diamine solution. The mixture was allowed to stand for one hour, cooled to room temperature and 1.6 g (19 mmol) of sodium carbonate monohydrate was added. The dimethyl quinoxaline was extracted with ether and dried over anhydrous MgSO₄. Yield: 0.2 g (32 %), M.p. 106 °C, ¹H-NMR (CDCl₃): δ 2.7 (s, 6H), δ 7.7 (m, 2H), δ 8.0 (m, 2H). IR(KBr): 3447, 2995, 2916, 1489, 1396, 1325, 1165, 987, 761, 611 cm⁻¹.

(b) *Synthesis of 3*: In a flask 0.2 g (1.26 mmol) of 2,3-dimethyl quinoxaline and 5 ml of water were placed. With rapid stirring a saturated aqueous solution of 1.17 g (7.4 mmol) of KMnO₄ in 7 ml of hot water was added. The reaction mixture was heated at 70 °C for one hour. After decolorization of KMnO₄ purple colour the solution was filtered to discarded the MnO₂ cake. The filtrate was stirred gently while adding 1 ml of 36 % HCl. The water was removed under reduced pressure until moist cake of solid KCl and compound **3** remains in the flask. To the solid material 1 ml of water and 10 ml of acetone was added and then the mixture was boiled under reflux for 15 minutes then cooled to room temperature and filtered. Evaporation of the acetone filtrate yielded compound **3**. The diacid **3** was recrystallized from the solvent mixture of ethanol and benzene (1:1). Yield: 0.16 g (64 %). M.p. 205 °C. ¹H-NMR (DMSO-d₆): δ 2.6 (s, 6H). IR (KBr): 2910, 1736, 1581, 1439, 1388, 1259, 1194, 1049, 788, 731 cm⁻¹.

X-ray Diffraction

Low-temperature (123 K) X-ray diffraction for compounds **1** and **3** were collected on Nonius Kappa CCD diffractometer by Dr. Vincent M. Lynch, University of Texas, Austin, U.S.A. The incident radiation was Mo-Kα ($\lambda = 0.71073$ Å). The

structures were solved using SHELXS-97 and all the non-hydrogen atoms were refined anisotropically using SHELXL-97.

Neutron Diffraction

A plate-like pale yellow single crystal of 2,3,5,6-pyrazine tetracarboxylic acid dihydrate of dimensions $0.6 \times 1.6 \times 2.8$ mm, calculated volume 3.65 mm^3 , was mounted on a 1 mm diameter vanadium pin using the 2 component glue Kwikfill and sealed in a Displex cryorefrigerator³³ on the instrument D9 at the Institut Laue Langevin. D9 is equipped with an 8 degree \times 8 degree multiwire (32×32) position-sensitive detector and is optimized for accurate neutron intensity measurements at short wavelength. At the chosen wavelength of $0.8397(1) \text{ \AA}$ from a Cu (220) monochromator in transmission, the crystal was cooled carefully at 2 degrees per minute to 20 K, while monitoring a strong low-angle reflection. No change in mosaic was observed. The unique reflections to a 2-theta value of 64° were measured, in several shells of increasing resolution; using omega step scans with step times of 2 to 6 sec. The crystal was then warmed slowly to 100 K, to 200 K and to 293 K and the structure redetermined at each temperature, just as at 20 K. Finally, the crystal was re-cooled to 100 K and additional higher-resolution data to 2-theta values beyond 72° were measured to provide a very accurate data set suitable for possible X–N analysis. Standard reflections were monitored periodically, and showed no significant variation. The space group was at all temperatures consistent with that found in the earlier X-ray work. Bragg intensities were integrated using the ILL program Racer, which employs the method of Wilkinson.³⁴ Precise unit cell dimensions were calculated at all temperatures using the ILL program Rafd9. The integrated intensities were corrected for attenuation by the crystal (calculated $\mu = 1.10 \text{ cm}^{-1}$, typical minimum and maximum transmission coefficients being *e.g.* 0.8515 and 0.9407 at 100 K) with the program Datap, using a Gaussian integration method.³⁵ As a further

check on the attenuation correction, F^2 was measured as a function of ψ , the angle of rotation about the scattering vector, for several strong reflections. The final corrected data are of outstanding quality, typical of D9 measurements at short wavelength, where absorption and extinction effects are minimized. The neutron diffraction experiments were conducted under supervision and support from Dr. Sax A. Mason (ILL, France) and Prof. Judith A.K. Howard (University of Durham, U.K.). The relevant crystallographic information is given in appendix.

4.9 References and Notes

1. G.R. Desiraju and T. Steiner, *The Weak Hydrogen Bond in Structural Chemistry and Biology*, Oxford University Press, Oxford, **1999**.
2. G.A. Jeffrey, *An Introduction to Hydrogen bonding*, Oxford University Press, Oxford, **1997**.
3. (a) G.K.H. Madsen, C. Wilson, T.M. Nymand, G.J. McIntyre and F.K. Larsen, *J. Phys. Chem., Sect. A*, **1999**, *103*, 8684. (b) H. Küppers, F. Takusagawa and T.F. Koetzle, *J. Chem. Phys.*, **1985**, *82*, 5636. (c) M. Currie and J.C. Speakmann, *J. Chem. Soc. A*, **1970**, 1923.
4. C.J. Reid, *J. Chem. Phys.*, **1959**, *30*, 182.
5. (a) P.R. Mallinson, K. Woźniak, G.T. Smith and K.L. McCormack, *J. Am. Chem. Soc.*, **1997**, *119*, 11502. (b) C. Flensburg, S. Larsen and R.F. Stewart, *J. Phys. Chem.*, **1995**, *99*, 10130.
6. (a) T. Steiner, *J. Phys. Chem., Sect. A*, **1998**, *102*, 7041. (b) T. Steiner and W. Saenger, *Acta Crystallogr., Sect. B*, **1994**, *50*, 348.
7. F. Hibbert and J. Emsley, *Adv. Phys. Org. Chem.*, **1990**, *26*, 255.
8. (a) M. Benoit, D. Marx and M. Parrinello, *Nature*, **1998**, *392*, 258. (b) P. Loubeyre, R. LeToullec, E. Wolanin, M. Hanfland and D. Hausermann, *Nature*, **1998**, *397*, 503.

9. (a) A. Warshal, A. Papazyan and P.A. Kollman, *Science*, **1995**, 269, 102. (b) W.W. Cleland, M.M. Kreevoy and P.A. Frey, *Science*, **1995**, 269, 104. (c) W.W. Cleland and M.M. Kreevoy, *Science*, **1994**, 264, 1887. (d) P.A. Frey, S.A. Whitt and I.B. Tobin, *Science*, **1994**, 264, 1927. (e) W.W. Cleland, *Biochemistry*, **1992**, 31, 317.
10. P. Gilli, V. Bertolasi, V. Ferretti and G. Gilli, *J. Am. Chem. Soc.*, **1994**, 116, 909.
11. I. Olovsson, H. Ptasiwicz-Bak, T. Gustafsson and I. Majerz, *Acta Crystallogr., Sect. B*, **2002**, 58, 627.
12. G.A. Jeffrey and W. Saenger, *Hydrogen Bonding in Biological Structures*, Springer-Verlag, Berlin, **1991**.
13. (a) G. Gilli, F. Bellucci, V. Ferretti and V. Bertolasi, *J. Am. Chem. Soc.*, **1989**, 111, 1023. (b) V. Bertolasi, P. Gilli, V. Ferretti and G. Gilli, *J. Am. Chem. Soc.*, **1991**, 113, 4917.
14. P. Gilli, V. Ferretti, V. Bertolasi and G. Gilli, In *Advances in Molecular Structure Research*, eds. I. Hargittai and M. Hargittai, JAI Press, Inc., Greenwich, CT, **1996**, Vol. 2, p. 67.
15. (a) V. Bertolasi, P. Gilli, V. Ferretti and G. Gilli, *Chem. Eur. J.*, **1996**, 2, 925. (b) G. Gilli, V. Bertolasi, V. Ferretti and P. Gilli, *Acta Crystallogr., Sect. B*, **1993**, 49, 564.
16. G.A. Jeffrey, *Crystallogr. Rev.*, **1995**, 3, 213.
17. S. Scheiner, *Hydrogen Bonding. Theoretical Perspective*, Oxford University Press, Oxford, **1997**.
18. K.J. Tauer and W.N. Lipscomb, *Acta Crystallogr.*, **1952**, 5, 606.
19. V.E. Zavodnik, V.K. Bel'skii and P.M. Zorkii, *Zh. Strukt. Khim.*, **1987**, 28, 175.
20. M.T. Vandenborre, H. Gillier-Pandraud, D. Antona and P. Becker, *Acta Crystallogr.*, **1973**, 29, 2488.

21. B.M. Kariuki, K.D.M. Harris, D. Philip and J.M.A. Robinson, *J. Am. Chem. Soc.*, **1997**, *119*, 12679.
22. D. Braga, L. Maini, F. Grepioni, A.D. Cian, O. Fèlix, J. Fischer and M.W. Hosseini, *New J. Chem.*, **2000**, *24*, 547.
23. T. Steiner, A.M.M. Schreurs, M. Lutz and J. Kroon, *Acta Crystallogr., Sect. C*, **2000**, *56*, 577.
24. T. Steiner, C.C. Wilson and I. Majerz, *Chem. Commun.*, **2000**, 1231.
25. F. Takusagawa and A. Shimada, *Chem. Lett.*, **1973**, 1121.
26. D.A. Dieterich, I.C. Paul and D.Y. Curtin, *J. Am. Chem. Soc.*, **1974**, *96*, 6372.
27. F.H. Allen, *Acta Crystallogr., Sect. B*, **2002**, *58*, 380.
28. R. Taylor and O. Kennard, *Acta Crystallogr., Sect. B*, **1983**, *39*, 133.
29. (a) I. Olovsson, H. Ptasiwicz-Bak, T. Gustafsson and I. Majerz, *Acta Crystallogr., Sect. B*, **2001**, *57*, 311. (b) J. Eckert, M. Barthes, W.T. Klooster, A. Albinati, R. Aznar and T.F. Koetzle, *J. Phys. Chem., Sect. B*, **2001**, *105*, 19. (c) J.M. Cole, J.A.K. Howard and G.J. McIntyre, *Acta Crystallogr., Sect. B*, **2001**, *57*, 410. (d) T. Steiner, *J. Phys. Chem., Sect. A*, **2000**, *104*, 433. (e) T. Steiner and S.A. Mason, *Acta Crystallogr., Sect. B*, **2000**, *56*, 254. (f) A.E. Goeta, C.C. Wilson, J.C. Autino, J. Ellena and G. Punte, *Chem. Mater.*, **2000**, *12*, 3342.
30. (a) C.C. Wilson, K. Shankland and N. Shankland, *Z. Kristallogr.*, **2001**, *216*, 303. (b) C.C. Wilson, *Acta Crystallogr., Sect. B*, **2001**, *57*, 435.
31. T. Steiner, I. Majerz and C.C. Wilson, *Angew. Chem., Int. Ed.*, **2001**, *40*, 2651.
32. R.J. Light and C.R. Hauser, *J. Org. Chem.*, **1961**, *26*, 1296.
33. J. Archer and M.S. Lehmann, *J. Appl. Cryst.*, **1986**, *19*, 456.
34. C. Wilkinson, H.W. Khamis, R.F.D. Stansfield and G.J. McIntyre, *J. Appl. Cryst.*, **1988**, *21*, 471.
35. P. Coppens, L. Leiserowitz and D. Rabinovich, *Acta Crystallogr.*, **1965**, *18*, 1035.

CHAPTER FIVE

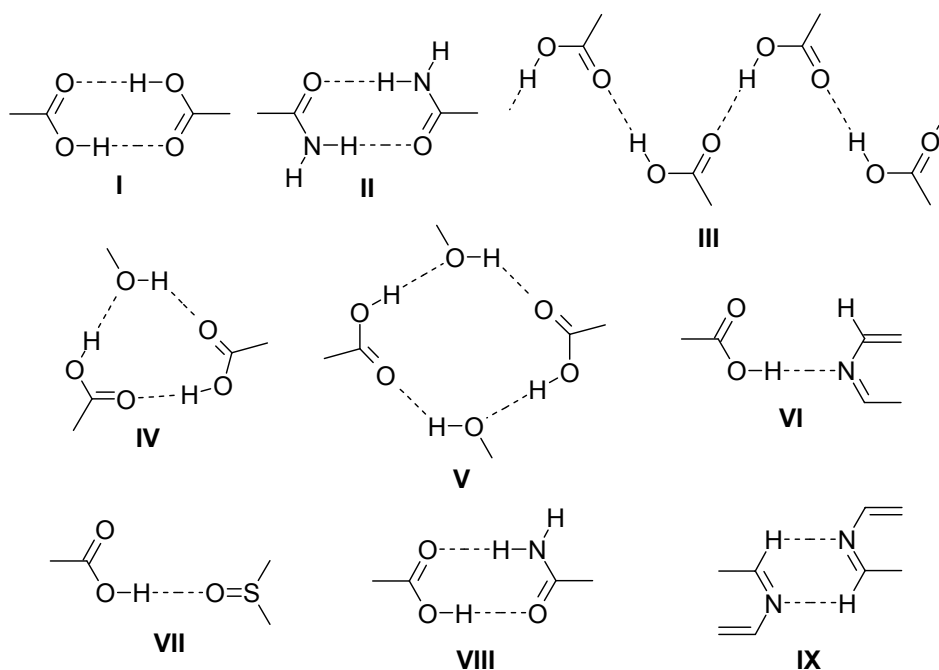
HYDROGEN BONDING IN CARBOXYLIC ACID–ISONICOTINAMIDE COMPLEXES

5.1 Introduction

The design and development of new materials with optical, magnetic or electrical properties suitable for high technology products are of great interest with organic, inorganic, organic–inorganic hybrids where small to large molecular mass is important.¹ A popular method for the design of supramolecular assemblies is to use noncovalent interactions such as hydrogen bonds to guide the construction of smaller molecules into larger organizations. Hydrogen bonding, the master key for molecular recognition, is the most reliable directional interaction in crystal engineering, supramolecular chemistry and biological recognition.² The strong and directional nature of hydrogen bonds is exploited in the organized self-assembly of molecules in solution and the solid-state. Carboxylic acids and amides are two commonly used functional groups in crystal engineering because they generally form robust architectures *via* O–H \cdots O and N–H \cdots O hydrogen bonded dimers.^{3,4} However, the understanding of factors that direct hydrogen bonding motifs when other functional groups are also present in the molecule is still evolving.⁵ The main challenge in carrying out crystal design with multi-functional molecules is that one is unable to predict when a particular functional group (*e.g.* hydroxyl, halogen, pyridine, ester, amide) will perturb the normal hydrogen bond motif of a given functional group (*e.g.* COOH) and in what way the motif will change. The exercise is further complicated because the way in which the hydrogen bond motif changes in a particular system could subtly depend on the molecular structure.^{5f} Therefore, understanding the forces that govern recognition between multi-functional molecules is of fundamental importance in supramolecular chemistry. For the successful implementation of target crystal synthesis it is necessary to understand the synergy, interplay and competition

between different functional groups during self-assembly.⁶ The ultimate goal in crystal engineering is to steer and predict the final crystal structure of the molecular assembly.⁷

Strong and weak hydrogen bonds⁸ ($\text{O}-\text{H}\cdots\text{O}$, $\text{O}-\text{H}\cdots\text{N}$, $\text{N}-\text{H}\cdots\text{O}$, $\text{C}-\text{H}\cdots\text{O}$) have been used for building nanoscale architectures from molecular scaffolds *via* multi-point recognition supramolecular synthons.⁹ Since the energy of hydrogen bonds (2–15 kcal/mol) is an order of magnitude weaker than covalent bonds, statistical trends are a better guide in crystal design than the observed interaction patterns in a subset of structures. A recent survey of the Cambridge Structural Database (CSD)¹⁰ by Allen *et. al.* shows that binary synthons involving even the strong hydrogen bonding functional groups (*e.g.* COOH , CONH_2) have only a modest probability of occurrence in crystals.¹¹ For example, carboxylic acid dimer synthon **I** occurs in *only* 33 % crystal structures and formation of amide dimer **II** is very rare (8 %). In addition to dimer **I**, carboxylic acids hydrogen bond *via* catemer **III** and hydrated motifs **IV**, **V** (Scheme 1). Competition from other good acceptors (COO^- , pyridine-N, CONH_2) is the main reason for the modest reproducibility of acid dimer **I** in the global database. However, it has been shown in a recent database study by Steiner¹² that the success rate of carboxylic acid with complementary functional groups is much higher: for example, acid–pyridine **VI** (91 %), acid–sulfoxide **VII** (78 %) and acid–amide **VIII** (78 %). This study highlights that self-assembly *via* heterosynthons is more reliable than *via* homosynthons. Thus crystal design may be implemented by exploiting the robust recognition in a heterosynthon. Another advantage with heterosynthons is the ability to synthesize binary crystals,¹³ or molecular complexes of two neutral components.



Scheme 1. Hydrogen bond synthons discussed in this chapter.

5.2 Hierarchic Hydrogen Bonding

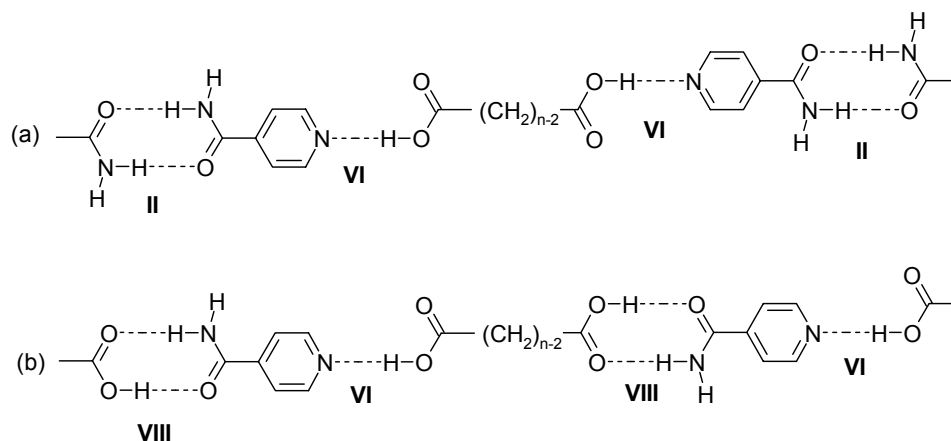
Carboxylic acid–pyridine synthon **VI** has emerged as a robust and recurring theme in crystal engineering.¹⁴ In chapter 2, X-ray crystal structures of pyrazine carboxylic acids were analyzed to understand the role of steric and electronic factors in supramolecular synthon **VI**.^{14a} A modular self-assembly approach to multi-component heteromeric structures is recently proposed by Aakeröy *et al.*¹⁵ based on the occurrence of acid–pyridine synthon **VI** and amide–amide dimer **II** in carboxylic acid•isonicotinamide co-crystals with the idea that predictable target architectures result from the hydrogen bond hierarchy rules formulated by Etter:¹⁶ "the best hydrogen-bond donor (COOH) and the best hydrogen-bond acceptor (pyridine-N) will preferentially form hydrogen bonds to one another"—a consequence of this

statement is that the second best donor will form a hydrogen bond to the second best acceptor (amide dimer), and so forth. The hypothesis provides the synthetic ease of building nanostructures in a modular protocol. However, the factors that control self-assembly in competing hydrogen bond situations are not fully understood. For example, different combinations of O–H \cdots O, O–H \cdots N and N–H \cdots O hydrogen bonds in the carboxylic acid–isonicotinamide system can result in at least four different synthons (**I**, **II**, **VI**, **VIII**; Scheme 1) with the preference order acid–pyridine **VI** > acid–amide **VIII** > amide–amide **II** > acid–acid **I**. However, subtle molecular features, crystallization conditions and small differences in hydrogen bond energy could alter this hierarchy in favour of one motif or another, particularly between heterosynthons **VI** and **VIII**. It is therefore ideal to probe hydrogen bonding in such isoenergetic synthons in X-ray crystal structures with systematic variation of molecular structure.

5.3 Co-crystallization of Isonicotinamide with α,ω -Aliphatic Dicarboxylic Acids

With the above background co-crystallization of isonicotinamide (IN) with homologous α,ω -alkanedicarboxylic acids (HOOC–(CH₂)_{n–2}–COOH): oxalic acid (OA, n = 2), malonic acid (MA, n = 3), succinic acid (SA, n = 4), glutaric acid (GA, n = 5) and adipic acid (AA, n = 6) were undertaken to understand the recognition between multi-functional molecules. The idea of using symmetrical dicarboxylic acid with chemically equivalent COOH groups in a graded p*K*_a scale is to study supramolecular organization in competitive hydrogen bond situations. These five acids afford the expected 1:2 complex of diacid and isonicotinamide stabilized by acid–pyridine **VI** and amide–amide **II** hydrogen bonds, as predicted by the hierarchic model (Scheme 2a). Additionally, glutaric acid and adipic acid co-crystallize in 1:1 stoichiometry with acid–pyridine **VI** and acid–amide hydrogen bond **VIII** (Scheme 2b). In 1:1 co-crystals one of the COOH groups of the symmetrical diacid hydrogen

bonds with pyridine-N (best acceptor) and the other COOH is bonded to amide group (second best acceptor). The occurrence of hydrogen bonds **VI** and **VIII** in binary crystals involving identical COOH group is not predicted by hierarchy rules.¹⁷



Scheme 2. (a) Acid–pyridine **VI** and amide–amide **II** synthons in diacid•(IN)₂ co-crystals ($n = 2$ –6). (b) Acid–pyridine **VI** and acid–amide **VIII** synthons in diacid•IN co-crystals ($n = 5, 6$).

5.4 (Oxalic acid)•(Isonicotinamide)₂

The molecular complex OA•(IN)₂ adopts a centrosymmetric space group *C2/c* in monoclinic crystal system. The asymmetric unit contains half molecule of oxalic acid and one molecule of isonicotinamide. The two COOH groups of oxalic acid hydrogen bond to pyridine nitrogen of isonicotinamide and carboxamide groups aggregate as centrosymmetric dimer (O–H⋯N: 1.58 Å, 179.5°; N–H⋯O: 1.91 Å, 173.8°). Linear tapes of synthons **VI** and **II** are connected *via* N–H⋯O hydrogen bond to acid carbonyl group of inversion-related tapes as shown in Figure 1. Geometrical parameters of hydrogen bonds are given in Table 1.

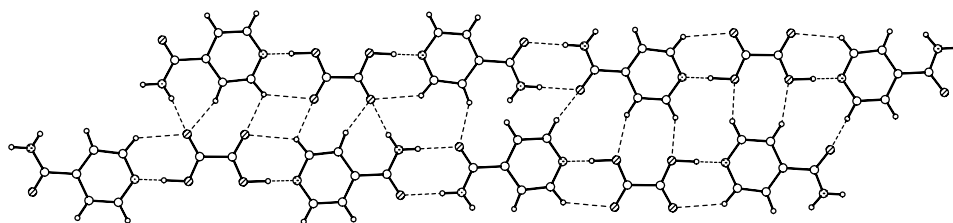


Figure 1. Crystal structure of $\text{OA}\cdot(\text{IN})_2$.

5.4.1 *syn*-Planar Conformation of Oxalic Acid in $\text{OA}\cdot(\text{IN})_2$

Oxalic acid is the smallest member in the series of aliphatic dicarboxylic acids. At room temperature, it exists in two crystalline varieties, the stable orthorhombic α -phase and the metastable monoclinic β -phase.¹⁸ In both crystalline phases, where extensive intermolecular hydrogen bonding occurs, individual molecules were found to be exclusively in a conformation where the $\text{O}-\text{C}-\text{C}-\text{O}$ dihedral angle is 180° , that is, the two carbonyl groups are *trans* to each other, and the two $\text{H}-\text{O}-\text{C}-\text{C}$ dihedral angles assume a *trans* configuration (conformer **tTt**, in Figure 2). In many molecular complexes oxalic acid exists in the *anti* conformation. However, in both gaseous phase and in inert gas matrices at low temperatures, monomeric oxalic acid has been found to exist predominantly in a different conformation, where the two $\text{H}-\text{O}-\text{C}-\text{C}$ dihedral angles adopt the *cis* configuration and are involved in intramolecular hydrogen bonding (form **cTc**).¹⁹ High-level *ab initio* and density functional theory (DFT) calculations predict the existence of six conformers of oxalic acid. The calculations suggest that the **cTc** conformer as corresponding to the most stable form. In the most stable conformer (**cTc**, belonging to the C_{2h} symmetry point group), two intramolecular $\text{O}-\text{H}\cdots\text{O}=\text{C}$ hydrogen bonds are present. The second most stable conformer (**cTt**, C_s point group) shows a single intramolecular $\text{O}-\text{H}\cdots\text{O}=\text{C}$ bond and the most frequently observed conformer in the solid state (**tTt**, C_{2h}) does not exhibit any intramolecular hydrogen bond. The third-

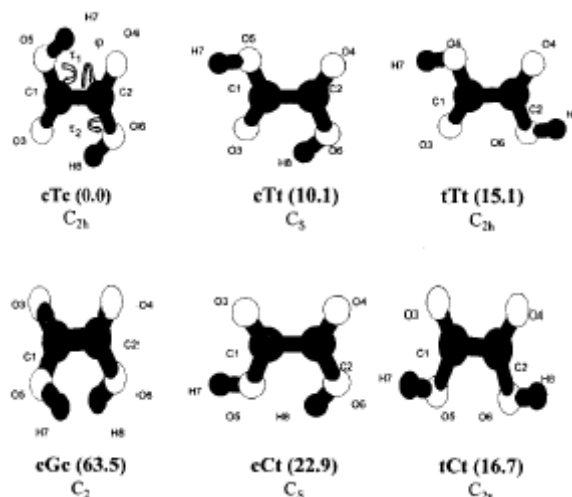


Figure 2. B3LYP/6-31G**-calculated conformers of monomeric oxalic acid.^{20b} The difference in energy (kJ/mol), including zero-point vibrational energy-corrected relative conformational energies to the most stable form, are given in the parenthesis.

and fourth-lowest energy conformers (forms **tTt** and **tCt**) were calculated to have relatively accessible excess energies to the conformational ground state.²⁰

It has been noticed that the oxalic acid does not exist, as is usually found, in the *anti*-planar conformation, but rather in the energetically unfavorable *syn*-planar arrangement in the crystal structure of molecular complex $\text{OA} \cdot (\text{IN})_2$. The oxalic acid molecule resides on the 2-fold rotation axis in *syn*-planar conformation with C=O and O–H groups of diacid pointing in the same direction (Figure 3). The *anti* conformation is more stable than the *syn* conformation by < 0.5 kcal/mol.²¹ There are three other occurrences of *syn* conformation in the literature²² (CSD refcodes: OXLACM, COGREV, FUNCUM) and all these are co-crystals of oxalic acid. The first occurrence of *syn*-OA in the solid-state was reported by Leiserowitz^{22a} in the 1:1 complex with acetamide (OXLACM, space group $A2/a$, there are two molecules of each component in the asymmetric unit). The high-energy *syn* conformation of oxalic acid in $\text{OA} \cdot (\text{IN})_2$ is stabilized by O–H \cdots N and C–H \cdots O hydrogen bonds of synthon

VI together with N–H···O hydrogen bond from CONH₂. The *syn*-planar conformation of OA in its complex with IN is the most planar among published examples, with O=C–C=O torsion angle of 0.13(15)° compared to 2.1° in OA•(acetamide). Table 2 permits a comparison of the geometrical parameters of oxalic acid in OA•(IN)₂ with those of the other three *syn*-planar and *anti*-planar conformation in the published structures. A molecule like oxalic acid can reside either on the inversion center (*anti*-conformation) or on the 2-fold rotation axis (*syn*-conformation) in space group like *C2/c*, *A2/a*. Generally diacids occupy the inversion center special position in a near planar *anti* orientation of C=O groups in the crystal. If the diacid occupies the 2-fold rotation axis the *syn* C=O groups are usually inclined. However, the present case is unique in that OA occupies the 2-fold axis special position in a perfect *syn*-planar conformation. The C=O groups can be in close proximity (O···O 2.76 Å) despite the severe lone-pair repulsion because the oxygen atoms are engaged in extensive hydrogen bonding and this minimizes their repulsion. Similar observation can be seen in the crystal structure of diacetylene dicarboxylic acid²³ (CSD refcode: DACCAH) crystallized in the space group, *I2/c* with four molecules of dihydrate. Space group symmetry requirements could be fulfilled with the molecular centres located at either on crystallographic inversion centres or twofold rotation axis. The X-ray analysis shows unambiguously that the second alternative is adopted. The diacetylene diacid molecules are not planar, instead the two carboxyl groups are mutually rotated about the molecular axis to produce an angle of 57° between them. The coplanarity in *anti*-conformation is due to attractive forces between the various hybridized O atoms. This situation does not exist in *syn*-planar, but nevertheless here too a strong tendency to coplanarity is evident.

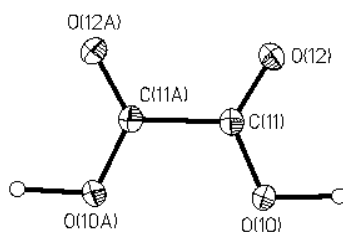


Figure 3: ORTEP drawn at 50 % probability level for non-hydrogen atoms to show the *syn*-planar conformation of oxalic acid in OA•(IN)₂.

Table 1. Geometrical parameters for crystal structures in this study.

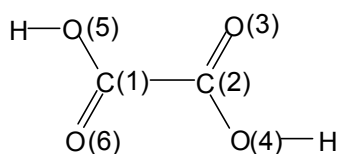
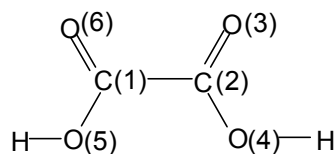
Co-crystal	H-bond	<i>d</i> / Å ^a	<i>D</i> / Å	θ / °
OA•(IN) ₂	O–H···N	1.58	2.5636(13)	179.5
	N–H···O	1.91	2.9168(13)	173.8
	N–H···O	2.00	3.0079(13)	170.9
	C–H···O	2.38	3.2109(13)	132.2
	C–H···O	2.43	3.2853(14)	134.9
	C–H···O	2.48	3.3055(13)	131.6
	C–H···O	2.60	3.5317(14)	143.8
	C–H···O	2.60	3.5317(14)	143.8
MA•(IN) ₂	O–H···N	1.57	2.5475(18)	168.4
	O–H···N	1.57	2.5517(18)	175.9
	O–H···N	1.57	2.5523(20)	172.2
	O–H···N	1.57	2.5545(18)	173.2
	O–H···N	1.59	2.5642(18)	171.9
	N ⁺ –H···O [−]	1.55	2.5559(18)	171.2
	N–H···O	1.86	2.8538(18)	167.9
	N–H···O	1.86	2.8740(20)	175.6
	N–H···O	1.89	2.8697(18)	161.7
	N–H···O	1.89	2.8990(20)	178.2
	N–H···O	1.89	2.9030(20)	175.1
	N–H···O	1.91	2.9095(18)	168.4
	N–H···O	1.92	2.9115(18)	167.1
	N–H···O	1.91	2.9190(20)	175.6
	N–H···O	1.92	2.9119(18)	166.5
	N–H···O	1.95	2.9630(20)	177.3
	N–H···O	1.97	2.9820(20)	175.7
	N–H···O	1.99	2.9644(18)	161.9
	C–H···O	2.17	3.2382(18)	166.0
	C–H···O	2.19	3.2549(18)	166.8

Table 1 *continued*...

SA•(IN) ₂	C–H...O	2.21	3.2843(18)	168.7
	C–H...O	2.24	3.2877(19)	161.4
	O–H...N	1.65	2.6149(14)	165.6
	N–H...O	1.91	2.9211(13)	177.8
	N–H...O	1.97	2.9487(14)	162.5
	C–H...O	2.55	3.4897(15)	144.5
GA•(IN) ₂	C–H...O	2.66	3.4368(16)	127.8
	C–H...O	2.69	3.4356(15)	125.1
	C–H...O	2.70	3.6053(16)	141.0
	O–H...N	1.61	2.5822(18)	168.7
	O–H...N	1.63	2.5957(17)	166.0
	O–H...N	1.68	2.6684(17)	177.2
	O–H...N	1.70	2.6818(17)	174.0
	N–H...O	1.83	2.8341(19)	174.0
	N–H...O	1.84	2.8510(19)	174.6
	N–H...O	1.91	2.9149(19)	174.2
	N–H...O	1.95	2.9607(19)	173.3
	N–H...O	1.98	2.9789(19)	168.3
	N–H...O	1.99	2.9952(18)	170.1
	N–H...O	2.09	3.0725(19)	162.4
AA•(IN) ₂	N–H...O	2.11	3.0871(19)	161.6
	C–H...O	2.22	3.2820(20)	165.1
	C–H...O	2.27	3.3280(20)	163.1
	C–H...O	2.36	3.3570(20)	151.9
	C–H...O	2.37	3.3710(20)	152.9
	O–H...N	1.64	2.6179(15)	170.0
	N–H...O	1.87	2.8794(15)	178.1
	N–H...O	2.04	3.0275(16)	164.6
	C–H...O	2.35	3.4299(19)	172.1
	C–H...O	2.39	3.4304(19)	161.1
	C–H...O	2.46	3.4508(18)	150.6
	C–H...O	2.54	3.5401(19)	153.4
	C–H...O	2.65	3.2665(17)	115.1
	O–H...O	1.64	2.6047(14)	165.4
GA•IN	O–H...N	1.77	2.6710(15)	150.9
	N–H...O	1.85	2.8360(16)	163.5
	N–H...O	1.90	2.9109(17)	173.4
	C–H...O	2.41	3.4844(17)	172.3
	C–H...O	2.41	3.4509(17)	160.5

Table 1 *continued*...

AA•IN	C–H...O	2.45	3.2228(17)	127.3
	O–H...O	1.67	2.6369(16)	167.3
	O–H...N	1.66	2.6344(16)	170.6
	N–H...O	1.91	2.9101(18)	167.6
	N–H...O	1.96	2.9634(17)	170.4
	C–H...O	2.43	3.4396(19)	154.2
	C–H...O	2.45	3.4340(20)	149.6
	C–H...O	2.47	3.2491(18)	127.2

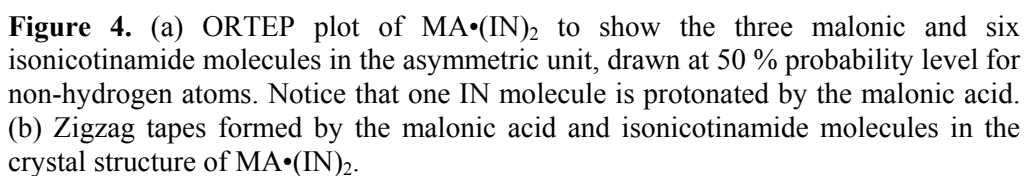
^a O–H, N–H and C–H distances are neutron normalized.**Table 2.** Conformations of oxalic acid in OA•(IN)₂ and some structures in the CSD.*anti-planar**syn-planar*

Bond length /Å	OA•(IN) ₂ ^a	OXLACM ^a	COGREV ^a	FUNCUM ^{a,b}	OXALAC05 ^c
C1–C2	1.5601(14)	1.529(7)	1.534	1.539	1.542
C2=O3	1.2172(13)	1.212(6)	1.199	1.189	1.218
C2–O4	1.2923(13)	1.298(6)	1.298	1.195 1.304	1.303
O4...O5	2.621	2.590	2.574	1.304 2.573	
O3...O6	2.763	2.728	2.754	2.768	
Bond/torsion angle /°					
C1–C2=O3	119.61(9)	119.6(5)	120.248	120.796 121.136	122.07
C1–C2–O4	114.24(9)	114.1(4)	113.169	113.251 113.362	110.89
O3=C2–O4	126.14(10)	126.2(5)	126.581	125.947 125.482	127.04
O3=C2–C1=O6	0.13(15)	2.1	13.81	5.621	180.0

^a *syn*-Planar conformation in co-crystal^b Full molecule in asymmetric unit^c *anti*-Planar conformation in pure oxalic acid

5.5 (Malonic acid)•(Isonicotinamide)₂

The crystal structure of MA•(IN)₂ in triclinic system (space group $P\bar{1}$) has 3 symmetry independent diacid molecules and 6 crystallographic unique IN molecules in the asymmetric unit. Symmetry-independent MA and IN molecules constitute the zigzag tape of acid–pyridine and amide–amide hydrogen bonds, which are in turn connected *via* amide N–H···O hydrogen bonds (Figure 4). Metrics of hydrogen bonds and C–H···O interactions are in the usual range (Table 1). The phenomenon of multiple molecules in the asymmetric unit ($Z' > 1$) continues to interest crystallographers and structural chemists.²⁴ Database analysis have been carried out to understand high Z' structures but the exact reasons are still not fully understood. A database study by Steiner,^{24b} shows that the three Z' values 0.5, 1 and 2 make up 95.3 % of all crystal structures. In organic compounds, $Z' > 1$ occur with a frequency of 10.8 % on average. In several of the crystal structures with high Z' values, all or some of the independent molecules have significantly different conformations, but there are also examples with all molecules having virtually the same conformation. There are even some crystal structures with very high Z' values which are formed by rigid molecules with internal symmetries that would allow crystallization with $Z' < 1$ (*e.g.* CBr₄, $Z' = 4$; selenourea, $Z' = 9$).²⁵ In the present case, the different conformers of the flexible diacid molecule form hydrogen bonded tapes with isonicotinamide using symmetry independent molecules and these aggregates crystallize into larger clusters (layers) without reorganization of the array into a smaller asymmetric unit with a single molecule. O–H···N hydrogen bonds in symmetry-independent occurrences of synthon **VI** are strong with typical O···N distance of *ca.* 2.55 Å (Table 1). Crystallization of multiple conformations of a molecule from solution to the solid state is common in structures stabilized by strong hydrogen bonds (*e.g.* alcohols).



In the crystal structure, SA occupies an inversion centre special position ($Z' = 0.5$) and a full molecule of IN constitutes the asymmetric unit in space group $P\bar{1}$. As expected the packing is typical with linear tapes of acid–pyridine and amide–amide hydrogen bonded synthons along $[1\ -2\ -2]$ vector direction and $N-H\cdots O$, $C-H\cdots O$ bonds between the tapes producing a lamellar sheet parallel to $(2\ 1\ 0)$ plane (Figure

5). The succinic acid adopts more common *trans*-conformation of carboxylic acid functional groups.

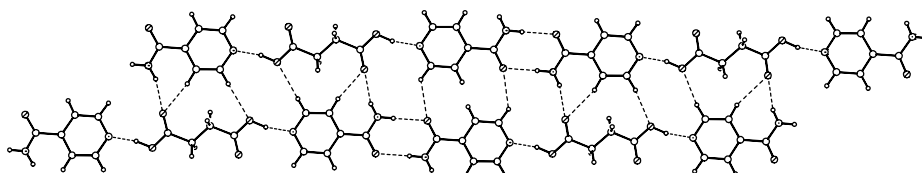


Figure 5. Crystal structure of SA•(IN)₂.

5.7 (Glutaric acid)•(Isonicotinamide)₂

The crystal of GA•(IN)₂ contains two molecules of diacid and four molecules of isonicotinamide in the asymmetric unit (space group $P2_1/n$). The packing is typical with corrugated tapes of acid–pyridine **VI** and amide–amide **II** hydrogen bonded synthons along $[1\ 0\ 2]$ direction and N–H···O, C–H···O bonds between the tapes producing a lamellar sheet parallel to $(2\ 0\ -1)$ plane (Figure 6). In both diacid molecules, one of the O–H···N hydrogen bonds is shorter than the other length (O···N: 2.58, 2.66; 2.59, 2.68 Å). The two molecules of glutaric acid have a *syn*-orientation of carboxylic acid groups ($\text{O}=\text{C}---\text{C}=\text{O} = 4.5^\circ, 6.1^\circ$). There are many occurrences of the *syn* conformer of glutaric acid in the CSD.

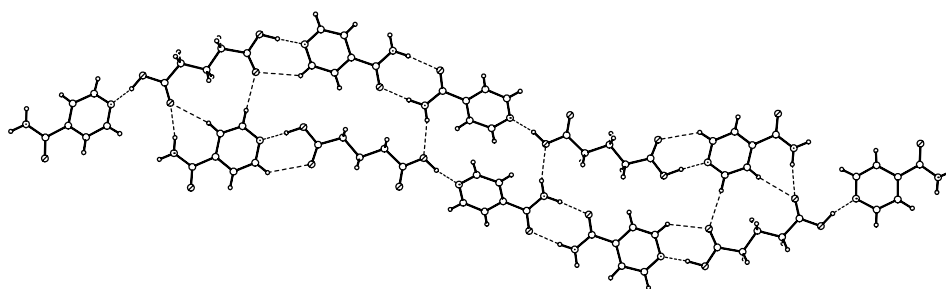


Figure 6. Crystal structure of GA•(IN)₂.

5.8 (Adipic acid)•(Isonicotinamide)₂

AA•(IN)₂ crystallizes in the triclinic system (space group $P\bar{1}$) with half molecule of diacid and one molecule of IN in the asymmetric unit. Molecular aggregation occurs *via* acid–pyridine O–H⋯N and amide–amide N–H⋯O hydrogen bonds. The tapes are extended along [3 1 2] direction. In the crystal structure adipic acid adopts the uncommon folded S-conformation. There are only four other examples with folded conformation in the CSD²⁶ (refcodes: JEWNUU, SOVNIA, XOVPON, ZUKXEI). The S-shaped conformation is stabilized by an intramolecular C–H⋯O hydrogen bond (2.65 Å, 115.1°) in a six-member ring (Figure 7). The folded conformation is more stable than the extended, zigzag conformation by –0.63 kcal/mol, as calculated in *Cerius*² using the Dreiding force field. This is presumably because of stabilization from intramolecular weak C–H⋯O hydrogen bonding in the folded conformation.

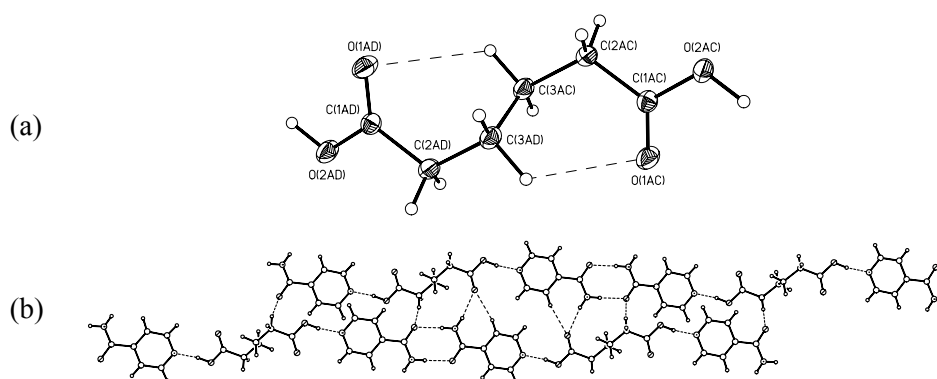


Figure 7. (a) ORTEP showing the folded S-conformation of adipic acid in AA•(IN)₂ stabilized by a six-membered intramolecular C–H⋯O hydrogen bond. (b) Crystal packing of AA•(IN)₂.

5.9 (Glutaric acid)•(Isonicotinamide)

GA•IN crystal structure has one molecule of each GA and IN in the asymmetric unit (monoclinic, $P2_1/c$). It is interesting to note that one of the carboxyl

functional group of glutaric acid forms acid–pyridine synthon **VI** and the other carboxyl group is engaged in the formation of synthon **VIII** with the carboxamide group of IN, resulting a linear tape along $[0\ 1\ 0]$ direction (Figure 8). Such tapes are in turn connected *via* $\text{N-H}\cdots\text{O}$ and $\text{C-H}\cdots\text{O}$ hydrogen bonds to produce a linear sheet parallel to $(1\ 0\ 2)$ plane. Glutaric acid crystallizes with *syn* orientation of carboxylic acid groups ($\text{O}=\text{C}\cdots\text{C}=\text{O} = 2.5^\circ$), as in $\text{GA}\cdot(\text{IN})_2$.

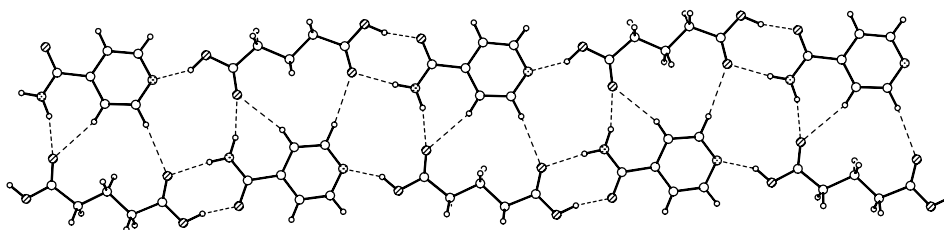


Figure 8. Crystal structure of $\text{GA}\cdot\text{IN}$ (1:1) molecular complex. Notably, glutaric acid is engaged in the formation of acid–pyridine synthon **VI** and acid–amide synthon **VIII** with two isonicotinamide molecules producing a liner tape along $[0\ 1\ 0]$ direction.

5.10 (Adipic acid)•(Isonicotinamide)

$\text{AA}\cdot\text{IN}$ crystallized in monoclinic system with one molecule of each component in the asymmetric unit (Space group $P2_1/c$). Similar to $\text{GA}\cdot\text{IN}$, one of the carboxyl functional group of adipic acid forms acid–pyridine synthon **VI** through $\text{O-H}\cdots\text{N}$ ($1.66\ \text{\AA}$, 170.6°) and $\text{C-H}\cdots\text{O}$ hydrogen bonds and the other carboxyl group is engaged in the formation of synthon **VIII** with the carboxamide group of IN, resulted a linear tape along $[1\ 0\ -1]$ direction (Figure 9). Such tapes are in turn connected *via* $\text{N-H}\cdots\text{O}$ and $\text{C-H}\cdots\text{O}$ hydrogen bonds produced a corrugated sheet. Adipic acid is present in the extended zigzag conformation in $\text{AA}\cdot\text{IN}$ but in the folded S-shaped conformation in $\text{AA}\cdot(\text{IN})_2$.

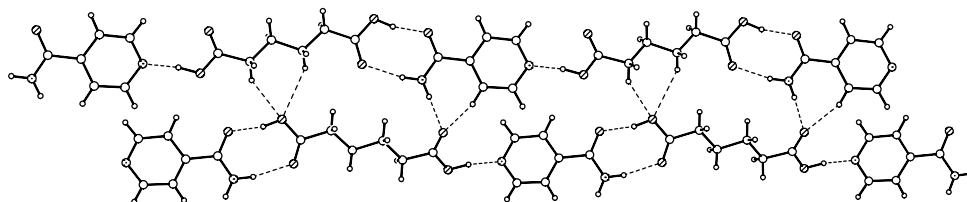


Figure 9. Crystal structure of AA•IN (1:1) co-crystal. Notice that adipic acid forming synthon **VI** and **VIII** with isonicotinamide and it is in zigzag conformation.

5.11 Results and Discussion

The crystal structures of diacid•isonicotinamide 1:2 complexes discussed in this chapter have predictable tapes of synthons **VI** and **II**. There are differences in the way these hydrogen-bonded tapes aggregate as layers and then stack to form the final 3D crystal, but these details are not discussed. The 1:1 co-crystals GA•IN and AA•IN have tapes of acid–pyridine **VI** and acid–amide **VIII** synthons connected *via* N–H···O and C–H···O hydrogen bonds (Figure 8 and 9). Although all strong donor and acceptor groups are engaged in hydrogen bonding, the pairing in 1:1 co-crystals is not in accordance with hierarchy rules.¹⁶ Etter's rules predict that the carboxylic acid donor (best donor) of a diacid (*e.g.* succinic acid, fumaric acid)¹⁵ will hydrogen bond with the pyridine acceptor (best acceptor) of isonicotinamide in a symmetrical motif (1:2 co-crystal). The pK_a , a measure of acidity of COOH group of dicarboxylic acid is identical. It is possible that hydrogen bond of one COOH will slightly alter the acidity of second COOH (*e.g.* in co-crystal of oxalic acid),^{22a} in effect differentiating between the two donor groups. However, such inductive effects will fall off over long range in glutaric acid and adipic acid. Secondly, the change in stoichiometry may not be due to orientation of donor groups^{14c} because 1:1 co-crystals are obtained with even and odd-member diacid. In 1:1 co-crystal, the COOH donor groups hydrogen bonds with the best acceptor (pyridine N) and second best acceptor (CONH₂) *via* different

synthons **VI** and **VIII**. The reasons for alternative crystallization pathways are examined and discussed in the remaining chapter.

Computation-based approach was used to elucidate the formation of 1:2 co-crystals and also explain why 1:1 co-crystals are isolated only in two out of five cases. Carboxylic acid group can hydrogen bond with pyridine or amide moiety of isonicotinamide with $\Delta E_{\text{synthon}}$ values that depend on the strength of COOH group.

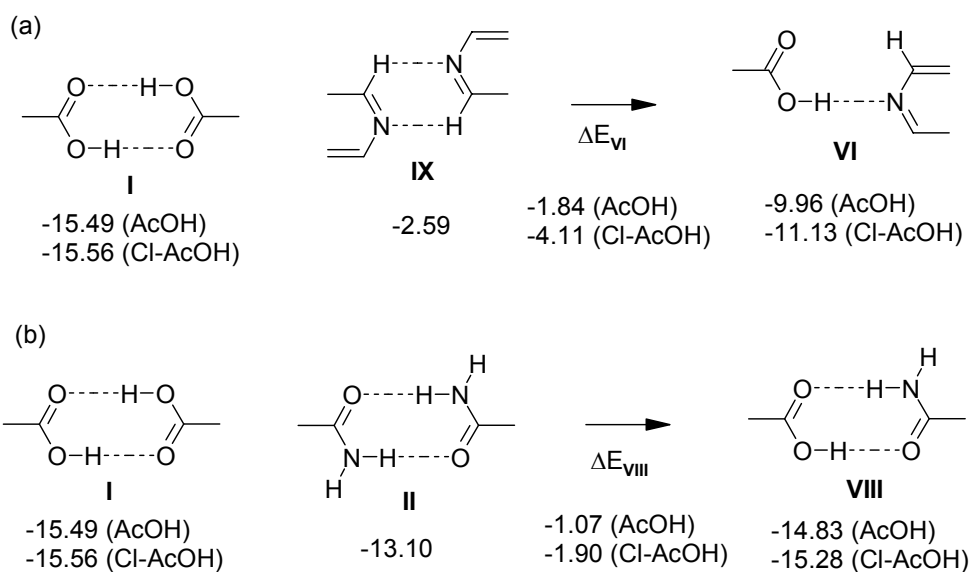
5.11.1 Synthon Energy Computations

Hydrogen bond synthon energies were calculated in *Spartan* using RHF/6-31G** basis set. In order to cover dicarboxylic acids with different strength in the present series (Table 3), chloroacetic acid and acetic acid were taken to represent strong and weak acid, respectively. A reason for selecting Cl-AcOH is that it is a strong acid that hydrogen bonds with isonicotinamide in a neutral co-crystal without transfer of proton.¹⁵ Computed synthon energies on model complexes AcOH•pyridine, AcOH•CH₃CONH₂, Cl-AcOH•pyridine and Cl-AcOH•CH₃CONH₂ (Scheme 3) are used for further discussion of hydrogen bonding in the diacid•isonicotinamide system. E_{synthon} is the energy of hydrogen bond motif and $\Delta E_{\text{synthon}}$ is the energy difference between the heterosynthon and the constituent homosynthons. E_{synthon} values are in the expected range based on the accepted energy of O–H...O, O–H...N, N–H...O and C–H...O hydrogen bonds.⁸ $\Delta E_{\text{synthon}}$ calculations for **VI** and **VIII** show that acid–pyridine and acid–amide heterosynthon is favoured over the constituent homosynthons for both Cl-AcOH and AcOH but the exact energies vary. Values of ΔE_{VI} and ΔE_{VIII} for complexes with Cl-AcOH are quite different (–4.11, –1.90 kcal/mol) but the energy difference for AcOH is small (–1.84, –1.07 kcal/mol). Heterosynthon **VI** is generally favored when COOH, pyridine and CONH₂ groups compete for hydrogen bonding ($\Delta E_{\text{VI}} < \Delta E_{\text{VIII}}$). For strong carboxylic acids **VI** is always formed in preference to **VIII** ($\Delta E_{\text{VI}} - \Delta E_{\text{VIII}} = -2.21$ kcal/mol, Cl-

AcOH) but for weak acids the selectivity is moderate ($\Delta E_{\text{VI}} - \Delta E_{\text{VIII}} = -0.77$ kcal/mol, AcOH).

Table 3. $\text{p}K_a$ (1st step) of carboxylic acids²⁷

Acid	$\text{p}K_a$
Oxalic acid	1.23
Malonic acid	2.83
Succinic acid	4.16
Glutaric acid	4.31
Adipic acid	4.43
Acetic acid	4.75
Chloroacetic acid	2.85



Scheme 3. Energy of hydrogen bond synthons calculated in *Spartan* (RHF/6-31G**, kcal/mol). E_{synthon} refers to the energy of hydrogen bond motif and $\Delta E_{\text{synthon}}$ is the stabilization of heterosynthon compared to homodimers. (a) $\text{CH}_3\text{COOH}\cdot\text{pyridine}$, $\text{ClCH}_2\text{COOH}\cdot\text{pyridine}$; (b) $\text{CH}_3\text{COOH}\cdot\text{CH}_3\text{CONH}_2$, $\text{ClCH}_2\text{COOH}\cdot\text{CH}_3\text{CONH}_2$.

The strength of COOH donor decreases in the series from oxalic acid to adipic acid (pK_a 1.23, 4.43) and so $\Delta E_{\text{synthon}}$ values become nearly equal for the weak, higher homologues. All five diacids give 1:2 co-crystals *via* acid–pyridine and amide–amide hydrogen bonding because for both strong and weak acids the ΔE_{VI} is less than ΔE_{VIII} . Glutaric acid and adipic acid also co-crystallize in 1:1 stoichiometry with acid–pyridine and acid–amide hydrogen bonds because the difference between ΔE_{VI} and ΔE_{VIII} is very small. Thus, hydrogen bond association in 1:1 diacid–isonicotinamide co-crystals is explained by $\Delta E_{\text{synthon}}$ energies even though hierarchy rules predict 1:2 co-crystals in this family.

The dependence of $\Delta E_{\text{synthon}}$ values on acidity can be explained as follows. Acid–pyridine recognition **VI** has a single hydrogen bond (O–H \cdots N) with auxiliary contribution occasionally from weak C–H \cdots O interaction. Hence energy of synthon **VI** decreases for weak carboxylic acid. The O–H \cdots N hydrogen bond in **VI** lengthens with increasing pK_a in 1:2 co-crystals (Table 1, O \cdots N (Å): OA 2.56, MA 2.55, SA 2.61, GA 2.58, 2.67, AA 2.62; e.s.d < 0.002 Å; mean values are quoted for $Z' > 1$). In contrast to **VI**, acid–amide synthon **VIII** is stabilized by two strong hydrogen bonds, O–H \cdots O and N–H \cdots O. With increasing pK_a of COOH, the O–H \cdots O bond lengthens but the N–H \cdots O interaction becomes shorter (because C=O is a better acceptor) and stabilizes the motif. The stronger N–H \cdots O bond makes up for a weaker O–H \cdots O interaction in acid–amide synthon is validated by CSD. O–H \cdots O and N–H \cdots O hydrogen bonds in synthon **VIII** show an inverse correlation, *i.e.* the N–H \cdots O is generally short when the O–H \cdots O contact is long. In some acid•urea complexes with synthon **VIII**, O \cdots O and N \cdots O values are (Å): 2.48, 3.00 (oxalic acid, UROXAL01); 2.50, 3.00 (fumaric acid, TIPWIY01); 2.53, 2.99 (succinic acid, VEJXAJ01); 2.71, 2.84 (glutaric acid, ZODWIY). Such an inverse correlation is absent between O–H \cdots N and C–H \cdots O hydrogen bonds in acid–pyridine synthon **VI**. The energy of acid–amide hydrogen bond **VIII** does not vary much with change in acidity because of

compensation from N–H···O hydrogen bond. The difference in $\Delta E_{\text{synthon}}$ values for **VI** and **VIII** diminishes for weak acid because **VI** weakens with increasing pK_a but the energy of **VIII** is largely invariant.

Entropy is important in these recognition events because they are bimolecular synthons. We assume that enthalpy is an indication of free energy differences. If a product heterosynthon is more stable relative to starting homosynthons then it is more likely to be formed. That such an assumption is reasonable in the present family of crystal structures is corroborated by CSD statistics. In the sub-database of 63 organic crystal structures containing COOH, pyridine (C=N–C) and CONH functional groups, acid–pyridine hydrogen bond is present in 39 hits compared to only 5 hits for acid–amide when O···O and O···N distances within the van der Waals sum were considered.

GA•IN and AA•IN (1:1) are the first examples of binary crystals with acid–pyridine and acid–amide hydrogen bonds in the same structure. What is interesting from the molecular recognition phenomenon is that the same COOH group (identical pK_a) is engaged in two different hydrogen bonded synthons (**VI** and **VIII**). Although such a hydrogen bond pairing is not predicted by hierarchy rules, the observed hydrogen bonding in 1:1 co-crystals is explained through $\Delta E_{\text{synthon}}$ calculations. The strength of acid–pyridine hydrogen bond **VI** is correlated with donor acidity while the strength of heterosynthon **VIII** is determined by the cumulative contribution from O–H···O and N–H···O hydrogen bonds. Energy of synthon **VIII** does not vary much over the pK_a range of organic carboxylic acids. The present study suggests that various contributions to the hydrogen bond energy–acidity of donor, electronegativity of acceptor, cooperative effects, synergy–must be jointly considered to determine which synthon will control crystallization, particularly in multi-functional systems with competitive intermolecular interactions.

Success in co-crystallization depends not only on complementary molecules but also on many other critical factors: similar solubility, size match, correct solvent, temperature, *etc.* Hence the co-crystals isolated in the present experiments represent only a subset of possible combinations. Several attempts to identify 1:1 co-crystal from crystallization experiment with OA, MA and SA gave only 1:2 stoichiometry even when diacid was used in excess.

5.12 Melting Point Alternation

Melting point is a very important physical property of a substance. A comprehensive understanding of enthalpy and entropy during the phase transition can explain the high (or low) melting point of a solid.²⁸

$$T_m = \Delta H_{melt} / \Delta S_{melt}$$

The melting point of a substance is high not only when the enthalpy change is large but also when the entropy of phase transition is small. The earlier work related to the phenomenon of melting point alternation was published in 1877 which deals with α,ω -alkanedicarboxylic acids and fatty acids.²⁹ In this article, Baeyer stated that *“a law which would tell that in a homologous series a compound with odd number of carbon atoms has a relatively lower melting point than those with even number would have considerable interest in molecular physics and ask for investigations if the crystal form, solubility etc., are correlated with the number of carbon atoms.”* Since then the alternation phenomenon is also identified in *n*-alkanes and many of the end-substituted *n*-alkanes.³⁰ The melting point is not the only property that exhibits an alternating trend. Other solid-state properties such as solubility and sublimation enthalpy also display pronounced alternation. The properties related to the liquid state, however, do not show any alternating trend. There is a resurgence of interest in understanding melting point alternation, the change in T_m in a homologous series of molecules. Boese *et.al.*³¹ have studied extensively the melting point alternation in a

homologous *n*-alkanes, α,ω -alkanediols, α,ω -alkanediamines, α,ω -alkanedithiols and α,ω -alkanedicarboxylic acids. T_m alternation is easily explained when crystal density alternates, *i.e.* if even C molecules have higher density than odd C molecules. However, when melting and density are not correlated, as in α,ω -alkanedicarboxylic acids, differences in packing motif and molecular conformation in crystals provide a satisfactory answer. The higher melting point of even diacids compared to odd members is understood by analyzing the crystal structures of individual molecules. Molecules of odd diacids have energetically unfavourable conformations in crystals. Even diacids close pack in a parallelogram shape but odd diacids pack as trapezoids with small voids. This explains the lower melting point of odd diacids because the energy required for solid-to-liquid phase transition is lower.^{31a} Very recently, Bond has observed the melting point alternation in the co-crystals of pyrazine and higher homologous of *n*-alkyl carboxylic acids. In addition, this was correlated with the alternating crystal density.³²

The observed melting point (by DSC) and density, packing fraction (from X-ray structure) in the family of diacid•(IN)₂ co-crystals and the corresponding pure diacids are displayed in Figure 10. All co-crystals have higher melting point than the corresponding pure diacids (Table 4) because strong hydrogen bonds and efficient close packing stabilize the structures of molecular complexes. T_m of co-crystals with *n* = 2, 3, 4, 5 and 6 carbon atoms show the expected alternation of even series being higher than odd members. Correlation of melting point with crystal density (D_{calc}) and/or packing fraction (C_k^*) is reasonable because these parameters are an indicator of how closely packed the molecules are in the solid-state. Both D_{calc} and C_k^* values alternate in these co-crystals, though the correlation is to some extent superior with packing fraction. Inasmuch as enthalpy considerations determine melting point in this family of crystal structures, D_{calc} (or C_k^*) is correlated with T_m .

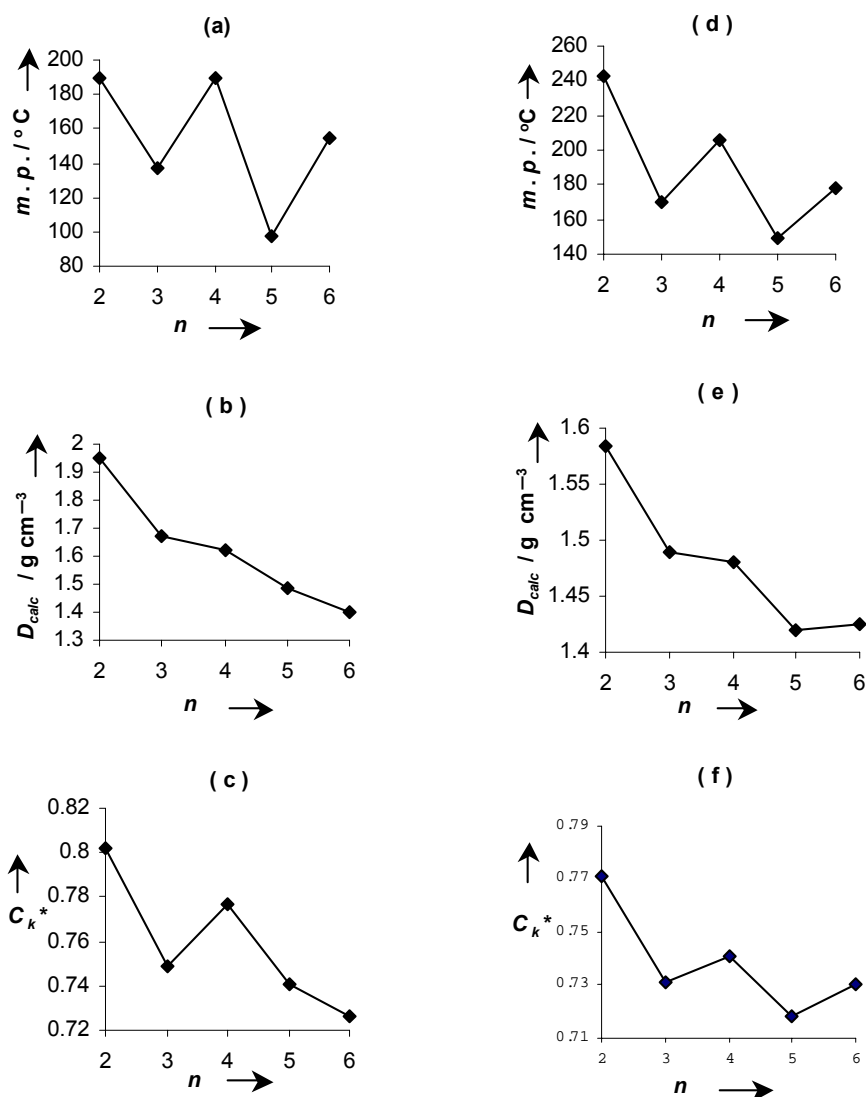


Figure 10. Melting point (a), crystal density (b), and packing fraction (c) for α,ω -alkanedicarboxylic acids using data taken from ref. 31a. Melting point (d), crystal density (e), and packing fraction (f) for diacid•(IN)₂ co-crystals. Note that melting point alternation in co-crystals correlates with D_{calc} and C_k^* values.

Table 4. Melting point of α,ω -aliphatic dicarboxylic acids and their 1:2 co-crystals with isonicotinamide, diacid•(IN)₂.

Dicarboxylic acid	M.P. of diacid / °	M.P. of co-crystal / °
Oxalic acid	190	243
Malonic acid	137	170
Succinic acid	193	206
Glutaric acid	98	149
Adipic acid	155	178

5.13 Conclusions

The carboxylic acid–isonicotinamide supramolecular system in a family of homologous α,ω -alkanedicarboxylic acids were examined to better understand competition and interplay between the heterosynthons, acid–pyridine **VI** and acid–amide **VIII**. Five co-crystals of diacid•IN with 1:2 stoichiometry are isolated and characterized by low temperature X-ray diffraction. Hydrogen bonding in these five structures obeys hierarchy rules. Furthermore, two co-crystals with 1:1 composition are characterized in which hydrogen bonding does not follow from the best donor–best acceptor order. The reason for alternative crystallization pathway in acid–isonicotinamide complexes is explained by a combination of synthon energy and structural database derived arguments. Acid–pyridine synthon **VI** is clearly favored over acid–amide **VIII** for strong carboxylic acid but the preference is marginal for weak acid. The rules for selecting carboxylic acid with a specific pK_a and molecular structure depending on the hydrogen bonding required in the co-crystal is a useful guide in crystal engineering. The observed melting point alternation in diacid•(IN)₂ co-crystals is correlated with change in crystal density and packing coefficient.

5.14 Experimental Section

Crystallization

In all experiments the components were well ground and dissolved in appropriate solvents. Melting point is recorded on Fisher–Johns apparatus and also from the onset temperature of endotherm in DSC.

OA•(IN)₂: Oxalic acid dihydrate (26 mg, 0.2 mmol) and isonicotinamide (50 mg, 0.4 mmol) were dissolved in hot water–ethanol (1:1) mixture. Colourless cube-like crystals were formed after a few days upon evaporation of the solvent. M.p. 241–243 °C; IR (KBr): 3385, 3161, 1686, 1404, 1236, 1032, 852, 653 cm⁻¹.

MA•(IN)₂: A 1:2 mixture of malonic acid (21 mg, 0.2 mmol) and isonicotinamide (50 mg, 0.4 mmol) was dissolved in hot ethanol. Needle-like colourless crystals were obtained after a few days. M.p. 167–170 °C; IR (KBr): 3389, 3178, 1722, 1392, 1153, 1055, 856, 650 cm⁻¹.

SA•(IN)₂: Succinic acid (24 mg, 0.2 mmol) was dissolved in a hot ethyl acetate–methanol (1:1) together with isonicotinamide (50 mg, 0.4 mmol). Colourless crystals were formed after one week upon evaporation of the solvent. M.p. 205–206 °C; IR (KBr): 3395, 3171, 1686, 1413, 1317, 1184, 1063, 1014, 798, 619 cm⁻¹.

GA•(IN)₂: Light-brown plate-like crystals of the complex were obtained upon crystallization of 1:2 mixtures of glutaric acid (27 mg, 0.2 mmol) and isonicotinamide (50 mg, 0.4 mmol) from hot methanol solution. M.p. 148–149 °C; IR (KBr): 3410, 3175, 1682, 1556, 1418, 1387, 1283, 1182, 1016, 852, 642 cm⁻¹.

AA•(IN)₂: A powdered mixture of adipic acid (30 mg, 0.2 mmol) and isonicotinamide (50 mg, 0.4 mmol) was dissolved in hot methanol. Needle-shaped crystals were obtained after few days. M.p. 177–178 °C; IR (KBr): 3399, 3158, 2957, 1686, 1410, 1258, 1016, 852, 804, 754, 644 cm⁻¹.

GA•IN: A 1:1 mixture of glutaric acid (54 mg, 0.4 mmol) and isonicotinamide (50 mg, 0.4 mmol) were dissolved in hot methanol. Light-brown crystals were collected after a few days. M.p. 134–135 °C; IR (KBr): 3391, 3194, 1701, 1589, 1545, 1414, 1281, 1186, 1065, 1005, 883, 858, 756, 638 cm⁻¹.

AA•IN: Adipic acid (60 mg, 0.4 mmol) and isonicotinamide (50 mg, 0.4 mmol) were dissolved in hot methanol. Needle-shaped crystals were formed after a few days. M.p. 163–165 °C; IR (KBr): 3354, 3169, 2932, 1705, 1601, 1555, 1501, 1466, 1412, 1269, 1186, 1063, 1016, 941, 854 cm⁻¹.

X-ray Crystallography

X-ray data were collected by Dr. Vincent M. Lynch at University of Texas, Austin, U. S. A., on Nonius Kappa CCD diffractometer at 153(2) K with incident X-ray radiation Mo-K α (λ = 0.71073 Å). The crystals were cooled with an Oxford Cryosystem device attached to CCD machine. Data reductions were performed using DENZO–SMN.³³ Structures were solved by direct methods using SHELXS-97 program and refined by full-matrix least squares refinement on F^2 with anisotropic displacement parameters for the non-H atoms using the SHELXL-97.³⁴ Geometrical analysis was carried out in PLATON³⁵ on Silicon Graphics Octane2 workstation.

Computations

Spartan program³⁶ was used to calculate hydrogen bond energy in RHF/6-31G** basis set on Pentium PC. Energy of the conformations was calculated in the *Cerius*² suite of programs³⁷ with Dreiding force field.

Crystallography Database

The Cambridge Structural Database (CSD),¹⁰ ConQuest version 1.5 (November 2002 update, 272066 entries) operating on Pentium PC was used for

statistical analysis. Searches were carried out on organic crystal structures with standard distance and angle cut-off criteria.

Differential Scanning Calorimetry

DSC was recorded on Perkin Elmer DSC4 at a scan rate of 10° per min.

5.15 References and Notes

1. (a) J.-M. Lehn, *Proc. Natl. Acad. Sci., U.S.A.*, **2002**, 99, 4763. (b) G.M. Whitesides and M. Boncheva, *Proc. Natl. Acad. Sci., U.S.A.*, **2002**, 99, 4769.
2. (a) J.W. Steed and J.L. Atwood, *Supramolecular Chemistry*, Wiley, Chichester, **2000**. (b) G.A. Jeffrey and W. Saenger, *Hydrogen Bonding in Biological Structures*, Springer-Verlag, Berlin, **1991**. (c) G.R. Desiraju, *Crystal Engineering: The Design of Organic Solids*, Amsterdam, Elsevier, **1989**.
3. (a) L. Leiserowitz, *Acta Crystallogr., Sect. B*, **1976**, 32, 775. (b) J. Bernstein, M.C. Etter and L. Leiserowitz, in *Structure Correlation, Vol. 2*, eds. H.-B. Bürgi and J.D. Dunitz, VCH, Weinheim, **1994**, pp. 431–507. (c) S.V. Kolotuchin, E.E. Fenlon, S.R. Wilson, C.J. Loweth and S.C. Zimmerman, *Angew. Chem., Int. Ed. Engl.*, **1995**, 34, 2654. (d) R.K.R. Jetti, F. Xue, T.C.W. Mak and A. Nangia, *J. Chem. Soc., Perkin Trans. 2*, **2000**, 1223.
4. (a) L. Leiserowitz and G.M.J. Schmidt, *J. Chem. Soc., Sect. A*, **1969**, 2372. (b) L. Leiserowitz and M. Tuval, *Acta Crystallogr., Sect. B*, **1978**, 34, 1230. (c) R.E. Meléndez and A.D. Hamilton, *Top. Curr. Chem.*, **1998**, 198, 97. (d) G.T.R. Palmore and J.C. MacDonald, in *The Amide Linkage: Selected Structural Aspects in Chemistry, Biochemistry, and Materials Science*, eds. A. Greenberg, C.M. Breneman and J.F. Liebman, Wiley, New York, **2000**, pp. 291–336.
5. (a) L. Leiserowitz and F. Nader, *Acta Crystallogr., Sect. B*, **1977**, 33, 2719. (b) P.L. Wash, E. Maverick, J. Chiefari and D.A. Lightner, *J. Am. Chem. Soc.*, **1997**,

- 119, 3802. (c) Y. Chang, M. West, F.W. Fowler and J.W. Lauher, *J. Am. Chem. Soc.*, **1993**, *115*, 5991. (d) S.S. Kuduva, D.C. Craig, A. Nangia and G.R. Desiraju, *J. Am. Chem. Soc.*, **1999**, *121*, 1936. (e) J.N. Moorthy, R. Natarajan, P. Mal and P. Venugopalan, *J. Am. Chem. Soc.*, **2002**, *124*, 6530. (f) P.W. Baures, J.R. Rush, A.V. Wiznycia, J. Desper, B.A. Helfrich and A.M. Beatty, *Cryst. Growth Des.*, **2002**, *2*, 653.
6. (a) G.R. Desiraju, *Angew. Chem., Int. Ed. Engl.*, **1995**, *34*, 2311. (b) A. Nangia and G.R. Desiraju, *Top. Curr. Chem.*, **1998**, *198*, 57.
7. (a) G.R. Desiraju, *Nature Materials*, **2002**, *1*, 77. (b) A. Gavezzotti, *Acc. Chem. Res.*, **1994**, *27*, 309.
8. For monographs on hydrogen bonding see: (a) G.A. Jeffrey, *An Introduction to Hydrogen Bonding*, Oxford University Press, Oxford, **1997**. (b) G.R. Desiraju and T. Steiner, *The Weak Hydrogen Bond in Structural Chemistry and Biology*, Oxford University Press, Oxford, **1999**.
9. Some recent papers are: (a) V.S.S. Kumar, A. Nangia, A.K. Katz and H.L. Carrell, *Cryst. Growth Des.*, **2002**, *2*, 313. (b) M.R. Edwards, W. Jones and W.D.S. Motherwell, *Cryst. Eng.*, **2002**, *5*, 25. (c) P. Vishweshwar, R. Thaimattam, M. Jaskólski and G.R. Desiraju, *Chem. Commun.*, **2002**, 1830. (d) V.S.S. Kumar, A. Nangia, M.T. Kirchner and R. Boese, *New J. Chem.*, **2003**, *27*, 224.
10. (a) F.H. Allen, *Acta Crystallogr., Sect. B*, **2002**, *58*, 380. (b) A. Nangia, *CrystEngComm*, **2002**, *4*, 93.
11. F.H. Allen, W.D.S. Motherwell, P.R. Raithby, G.P. Shields and R. Taylor, *New J. Chem.*, **1999**, *23*, 25.
12. T. Steiner, *Acta Crystallogr., Sect. B*, **2001**, *57*, 103.
13. (a) B. Moulton and M.J. Zaworotko, *Chem. Rev.*, **2001**, *101*, 1629. (b) R.D.B. Walsh, M.W. Bradner, S. Fleishman, L.A. Morales, B. Moulton, N. Rodríguez-

- Hornedo and M.J. Zaworotko, *Chem. Commun.*, **2003**, 186. (c) S.C. Fleischman, S.S. Kuduva, J.A. McMahon, B. Moulton, R.D.B. Walsh, N. Rodriguez-Hornedo and M.J. Zaworotko, *Cryst. Growth Des.*, **2003**, 3, ASAP. (d) K.K. Arora and V.R. Pedireddi, *J. Org. Chem.*, **2003**, 68, ASAP.
14. (a) P. Vishweshwar, A. Nangia and V.M. Lynch, *J. Org. Chem.*, **2002**, 67, 556. (b) B.R. Bhogala, P. Vishweshwar and A. Nangia, *Cryst. Growth Des.*, **2002**, 2, 325. (c) N. Shan, A.D. Bond and W. Jones, *Cryst. Eng.*, **2002**, 5, 9. (d) C.B. Aakeröy, A.M. Beatty, M. Tremayne and D.M. Rowe, *Cryst. Growth Des.*, **2001**, 1, 377. (e) E. Batchelor, J. Klinowski and W. Jones, *J. Mater. Chem.*, **2000**, 10, 839. (f) G.T.R. Palmore, T.-J.M. Luo, M.T. McBride-Wieser, E.A. Picciotto and C.M. Reynoso-Paz, *Chem. Mater.*, **1999**, 11, 3315. (g) V.R. Pedireddi, W. Jones, A.P. Chorlton and R. Docherty, *Chem. Commun.*, **1996**, 997. (h) C.V.K. Sharma and M.J. Zaworotko, *Chem. Commun.*, **1996**, 2655. (i) J.J. Kane, R.-F. Liao, J.W. Lauher and F.W. Fowler, *J. Am. Chem. Soc.*, **1995**, 117, 12003.
15. C.B. Aakeröy, A.M. Beatty and B.A. Helfrich, *J. Am. Chem. Soc.*, **2002**, 124, 14425.
16. (a) M.C. Etter, *Acc. Chem. Res.*, **1990**, 23, 120. (b) M.C. Etter, *J. Phys. Chem.*, **1991**, 95, 4601.
17. Ternary crystals of isonicotinamide with two different carboxylic acids contain synthons **VI** and **VIII** as predicted by hierarchy rules: the best donor (stronger COOH) hydrogen bonds with the best acceptor (pyridine) and the second best donor (weaker COOH) hydrogen bonds with the second best acceptor (amide). C.B. Aakeröy, A.M. Beatty and B.A. Helfrich, *Angew. Chem., Int. Ed.*, **2001**, 40, 3240.
18. J.L. Derissen and P.H. Smit, *Acta Crystallogr., Sect. B*, **1974**, 30, 2240.

19. (a) J. Nieminen, M. Räsänen and J. Murto, *J. Phys. Chem.*, **1992**, 96, 5303. (b) L.R. Redington and T.E. Redington, *J. Mol. Struct.*, **1978**, 48, 165. (c) B.C. Stace and B.C. Oralratmanee, *J. Mol. Struct.*, **1973**, 18, 339.
20. (a) P.D. Godfrey, M.J. Mirabella and R.D. Brown, *J. Phys. Chem., Sect. A*, **2000**, 104, 258. (b) J. Higgins, X. Zhou, R. Liu and T.T.-S. Huang, *J. Phys. Chem., Sect. A*, **1997**, 101, 2702.
21. (a) E.M.S. Maçôas and R. Fausto, *J. Phys. Chem., Sect. A*, **2000**, 104, 6956. (b) P.D. Godfrey, M.J. Mirabella and R.D. Brown, *J. Phys. Chem., Sect. A*, **2000**, 104, 258. (c) J. Nieminen, M. Räsänen and J. Murto, *J. Phys. Chem.*, **1992**, 96, 5303.
22. (a) L. Leserowitz and F. Nader, *Angew. Chem., Int. Ed.*, **1972**, 11, 514. (b) J. Zukerman-Schpector, E.E. Castellano, G. Oliva, A.C. Massabni and A.D. Pinto, *Can. J. Chem.*, **1984**, 62, 725. (c) R.J. Doedens, G.P. Meier and L.E. Overman, *J. Org. Chem.*, **1988**, 53, 685.
23. (a) J.D. Dunitz, *Chem. Eur. J.*, **1998**, 4, 745. (b) J.D. Dunitz and J.M. Robertson, *J. Chem. Soc.*, **1947**, 1145.
24. (a) J.W. Steed, *CrystEngComm*, **2003**, 5, 169. (b) T. Steiner, *Acta Crystallogr., Sect. B*, **2000**, 56, 673. (c) C.P. Brock and J.D. Dunitz, *Chem. Mater.*, **1994**, 6, 1118. (d) N. Padmaja, S. Ramakumar and M.A. Viswamitra, *Acta Crystallogr., Sect. A*, **1990**, 46, 725.
25. (a) M. More, F. Baert and J. Lefebvre, *Acta Crystallogr., Sect. B*, **1977**, 33, 3681. (b) J.S. Rutherford and C. Calvo, *Z. Kristallogr.*, **1969**, 128, 229.
26. (a) Z.-G. Sun, Y.-P. Ren, L.-S. Long, R.-B. Huang and L.-S. Zheng, *Inorg. Chem.*, **2002**, 5, 629. (b) V.R. Pedireddi, S. Chatterjee and A. Ranganathan, *Tetrahedron*, **1998**, 54, 9457. (c) R.-F. Liao, J.W. Lauher and F.W. Fowler, *Tetrahedron*, **1996**, 52, 3153. (d) F. Garcia-Tellado, S. Goswami, S.K. Chang, S.J. Geib and A.D. Hamilton, *J. Am. Chem. Soc.*, **1990**, 112, 7393.

27. *CRC Handbook of Chemistry and Physics*, 65th edition, CRC Press, Boca Raton (Florida), p. D-165, **1984**.
28. A. Gavezzotti, *J. Chem. Soc., Perkin Trans. 2*, **1995**, 1399.
29. A. Baeyer, *Ber. Chem. Ges.*, **1877**, 10, 1286.
30. F.L. Breusch, *Fortschr. Chem. Forsch.*, **1969**, 12, 119.
31. (a) V.R. Thalladi, M. Nüsse and R. Boese, *J. Am. Chem. Soc.*, **2000**, 122, 9227.
 (b) V.R. Thalladi, R. Boese and H.-C. Weiss, *J. Am. Chem. Soc.*, **2000**, 122, 1186. (c) V.R. Thalladi, R. Boese and H.-C. Weiss, *Angew. Chem., Int. Ed.*, **2000**, 39, 918. (d) V.R. Thalladi and R. Boese, *New J. Chem.*, **2000**, 24, 579. (e) R. Boese, H.-C. Weiss and D. Bläser, *Angew. Chem., Int. Ed.*, **1999**, 38, 988.
32. A.D. Bond, *Chem. Commun.*, **2003**, 250.
33. Z. Otwinowski and W. Minor, DENZO-SMN, in *Methods in Enzymology, Macromolecular Crystallography*, Part A, Vol. 276, eds. C.W. Carter Jr. and R.M. Sweet, Academic Press, New York, **1997**.
34. G.M. Sheldrick, SHELX-97, Program for the Solution and Refinement of Crystal Structures, University of Göttingen, Germany, **1997**.
35. A.L. Spek, PLATON, Bijvoet Center for Biochemical Research, Vakgroep Kristal-en Structure-Chemie, University of Utrecht, The Netherlands.
36. *Spartan Pro 1.0*, Wave Function Inc., 18401 von Karman Avenue, Suite 370, Irvine, CA 92612.
37. *Cerius²*, Accelrys Ltd., 334 Cambridge Science Park, Cambridge CB4 0WN, U.K.

CHAPTER SIX

HYDROGEN BOND SYNTHONS IN PHENOL–ISONICOTINAMIDE COMPLEXES

6.1 Introduction

Organic crystal engineering¹ relies on hydrogen bonds intermolecular interactions that are weak and moderately directional in comparison with covalent bonds.² Hydrogen bonds, because of their strength and directionality, play a decisive role in controlling the self-assembly of many molecular crystals and biopolymers. Crystal engineering of organic solids using strong hydrogen bonding interactions of the O–H \cdots O, O–H \cdots N and N–H \cdots O types is widely practiced.³ The strength and directionality of these interactions confers enormous predictability in many systems. The majority of supramolecular synthons comprise complementary or self-complementary hydrogen bonding units and, therefore, functional groups able to participate in hydrogen bonds play a crucial role in the self-organization of molecular building blocks into one-, two- or three-dimensional networks.⁴ It is difficult to predict (anticipate) the crystal packing when multiple functional groups are present.

The O–H \cdots N hydrogen bond is a robust and versatile synthon in crystal engineering.⁵ Phenols (pK_a 8–11) are more acidic than alcohols (pK_a 15–17), the O–H \cdots N hydrogen bonds formed between phenols and tertiary or aromatic amines are expected to be stronger than those formed between alcohols and amines. Crystallization of phenol with pyridine (O–H \cdots N hydrogen bond) has been examined to build structures with intricate supramolecular architectures,⁶ for non-linear optics,⁷ to synthesize host–guest complexes⁸ and as supramolecular template to direct topochemical reactions. MacGillivray and co-workers⁹ have described a method involving a linear template, based on resorcinol to enforce topochemical alignment of olefins in the solid state by way of robust O–H \cdots N hydrogen bonds such that they undergo [2 + 2] photoreaction. Steiner *et. al.*, have studied proton transfer in a very

short heteronuclear O–H⋯N hydrogen bond in the complex pentachlorophenol–4-methylpyridine with variable temperature neutron diffraction.¹⁰ Some examples of predictable supramolecular organization mediated by strong and directional O–H⋯N hydrogen bond in co-crystals of phenol molecules with pyridine derivatives are shown in Table 1.

Table 1. Examples of hydroquinone, resorcinol and phloroglucinol co-crystals with pyridine bases found in the CSD.¹¹

Phenol	Base	Refcode
Hydroquinone	Phenazine	FOQHEY
	Urotropine	HMTHQU
	1,2- <i>bis</i> (4-Pyridyl)ethane	MEKWUU
Resorcinol	<i>trans</i> -1,2- <i>bis</i> (4-Pyridyl)ethylene	ABEKUN
	1,2,3,4- <i>tetrakis</i> (4-Pyridyl)cyclobutane	ABELAU
	<i>trans</i> -1,2- <i>bis</i> (2-Pyridyl)ethylene	ABELIC
	1,2- <i>bis</i> (4-Pyridyl)ethane	ACOYOG
	Urotropine	RSHMTA
Phloroglucinol	4-Methylpyridine	HIMGAL
	2,4-Dimethylpyridine	HIMGEP
	2,2'-Bipyridine	PUVMIC
	Urotropine	RAWDIC
	4,4'-Bipyridine	TEKKOJ

This chapter deals with the study of X-ray crystal structures of molecular complexes (hydroquinone)_{0.5}•(isonicotinamide) **1**, (resorcinol)•(isonicotinamide)₂ **2**, (phloroglucinol)•(isonicotinamide)₂•(H₂O)₂ **3**, and (4-hydroxybenzoic acid)•(isonicotinamide) **4**. These complexes are studied to obtain a better understanding of recognition between multifunctional groups. It has been anticipated

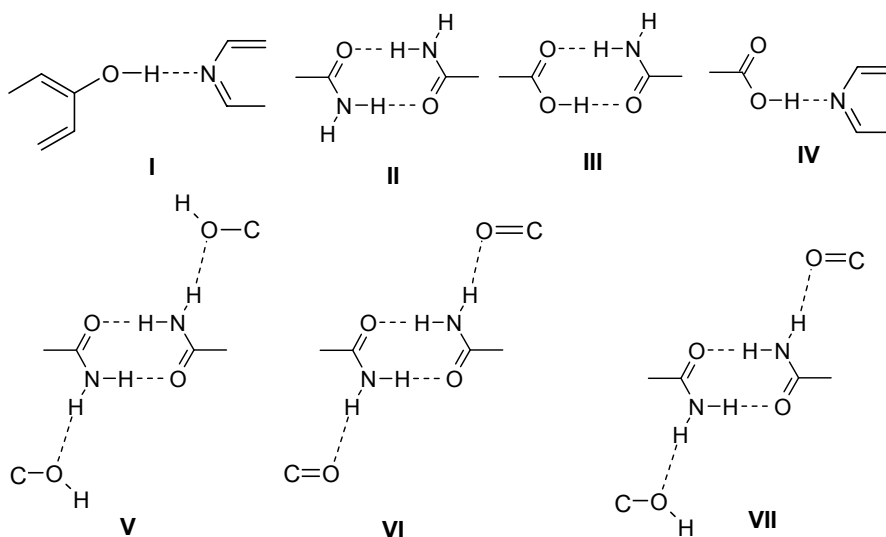
that *bis*- and *tris*-phenols would hydrogen bond with the pyridine moiety of isonicotinamide through synthon **I** and the amide group will extend the hydrogen bond aggregate *via* dimer synthon **II**. Systematic study of phenol–isonicotinamide co-crystals will shed light on competition and interplay between O–H⋯O, O–H⋯N and N–H⋯O hydrogen bonds in binary systems.

1: (Hydroquinone)_{0.5}•(Isonicotinamide)

2: (Resorcinol)•(Isonicotinamide)₂

3: (Phloroglucinol)•(Isonicotinamide)₂•(H₂O)₂

4: (4-Hydroxybenzoic acid)•(Isonicotinamide)



Scheme 1. Hydrogen bonded synthons discussed in this chapter.

6.2 (Hydroquinone)_{0.5}•(Isonicotinamide), **1**

In the crystal structure of **1** hydroquinone resides at an inversion centre in monoclinic crystal system (space group $P2_1/c$). The molecules aggregate as linear tapes along $[1\ -2\ 1]$ through O–H⋯N hydrogen bond **I** (1.73 Å, 2.693(2) Å, 165.1°)

and centrosymmetric amide N–H···O dimer **II** (1.93 Å, 2.932(2) Å, 171.7°), as shown in Figure 1. The metrics of hydrogen bonds are shown in Table 2. The primary amide does not extend through the normal 5.1 Å translation¹² but instead hydrogen bonds with the phenol oxygen atom of screw axis related tape *via* N–H···O (2.11 Å, 3.110(2) Å, 169.1°) hydrogen bond. A search of the Cambridge Structural Database (CSD)¹³ for motif **V**, (Scheme 1) wherein the amide dimer is hydrogen bonded to OH group shows that is present in five crystal structures (Refcodes: CERNIW, JIXCOI, OHPHXD, RUJVAT, WEGYEM)¹⁴ and motif **VI** occurs in one structure (MEGLOZ).¹⁵ Similarity of hydrogen bonding in **1** with 4-hydroxybenzamide monohydrate is notable (CSD refcode: JIXCOI, $P2_1/a$).¹⁶ In this structure also the amide dimers hydrogen bond with the OH group of 2₁-related molecule through N–H···O bonds.

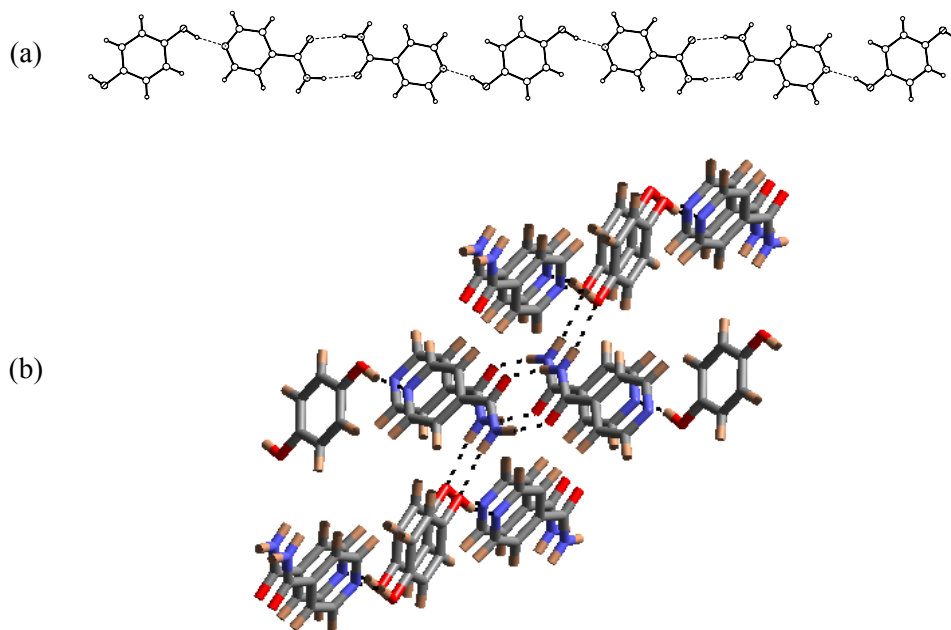


Figure 1. (a) Linear tapes of O–H···N synthon **I** and amide dimer **II** in **1** along [1 $\bar{2}$ 1] direction. (b) N–H···O_{phenol} hydrogen bond between the tapes is shown.

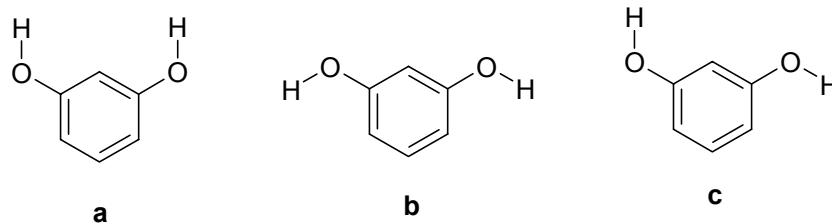
Table 2. Geometrical parameters of hydrogen bonds

Co-crystal	H-bond	<i>d</i> (Å) ^a	<i>D</i> (Å)	θ (°)
1	O–H⋯N	1.73	2.6936(16)	165.1
	N–H⋯O	1.93	2.9321(19)	171.7
	N–H⋯O	2.11	3.1100(20)	169.1
	C–H⋯O	2.30	3.3270(20)	156.9
	C–H⋯O	2.51	3.1370(20)	115.5
2	O–H⋯N	1.75	2.7225(14)	168.7
	O–H⋯N	1.78	2.7198(15)	159.0
	N–H⋯O	1.87	2.8764(15)	176.2
	N–H⋯O	1.95	2.8657(15)	149.8
	N–H⋯O	2.02	3.0208(15)	168.6
	N–H⋯O	2.14	3.1202(15)	162.4
	C–H⋯O	2.36	3.2262(17)	135.4
	C–H⋯O	2.67	3.5682(17)	140.1
3	O–H⋯O	1.65	2.6275(14)	173.0
	O–H⋯O	1.81	2.7899(15)	170.3
	O–H⋯O	1.81	2.7967(14)	178.2
	O–H⋯O	1.83	2.8172(14)	175.3
	O–H⋯O	1.94	2.8878(14)	160.1
	O–H⋯N	1.77	2.7555(14)	174.5
	O–H⋯N	1.81	2.7953(14)	179.2
	N–H⋯O	1.91	2.9128(15)	174.1
	N–H⋯O	1.92	2.9292(15)	176.2
	N–H⋯O	2.14	3.0464(16)	148.5
	N–H⋯O	2.48	3.3096(16)	138.6
	C–H⋯O	2.44	3.2249(16)	128.4
	C–H⋯O	2.48	3.5438(17)	166.9
	C–H⋯O	2.65	3.4998(17)	134.5
	C–H⋯N	2.48	3.2895(17)	130.2
	C–H⋯N	2.67	3.4132(16)	125.6
4	O–H⋯O	1.61	2.5796(15)	168.5
	O–H⋯N	1.78	2.7459(17)	165.2
	N–H⋯O	1.98	2.9760(17)	168.2
	N–H⋯O	2.46	3.2931(17)	139.3
	N–H⋯O	2.47	3.1334(17)	122.6
	C–H⋯O	2.44	3.2060(20)	126.8
	C–H⋯O	2.51	3.5050(20)	152.4
	C–H⋯O	2.61	3.4670(20)	135.0

^a O–H, N–H and C–H distances are normalized to standard neutron values.

6.3 (Resorcinol)•(Isonicotinamide)₂, 2

The crystal structure of **2** (space group $P\bar{1}$, $Z = 2$) contains one molecule of resorcinol and two molecules of isonicotinamide in the asymmetric unit. Of the three possible conformations of resorcinol OH groups (Discrete dimer **a**, Linear chain **b**, Zigzag chain **c**), the divergent form that leads to linear tape is present in **2** [synthon **I**: (i) 1.78 Å, 2.719(2) Å, 159.0°; (ii) 1.75 Å, 2.722(2) Å, 168.7°]. Symmetry-independent isonicotinamide molecules extend the chain along $[2\ 1\ -1]$ via dimer **II** [N–H···O: (iii) 1.87 Å, 2.876(2) Å, 176.2°; (iv) 2.02 Å, 3.020(2) Å, 168.6°] (Figure 2). The *anti*- N–H of amide groups hydrogen bonds with amide carbonyl and phenol oxygen atoms of inversion-related tapes [N–H···O_{amide} (v) 1.95 Å, 2.865(2) Å, 149.8°; N–H···O_{phenol} (vi) 2.14 Å, 3.120(2) Å, 162.4°] to produce 2D sheet parallel to $(-1\ 2\ 0)$ plane. The amide donor with shorter N–H···O bond in synthon **II** (iii) has a longer second contact (vi) and vice versa (iv and v). There are no examples in the CSD of primary amide with symmetry-independent dimers **II** that hydrogen bond to different acceptor groups, C=O and OH (motif **VII**). Generally, carbonyl oxygen is the preferred acceptor for H atom in primary amides. The cooperative hydrogen bond array^{3,17} in motif N–H···O_{phenol}–H···N perhaps polarizes the acceptor and makes it comparable to amide C=O group.



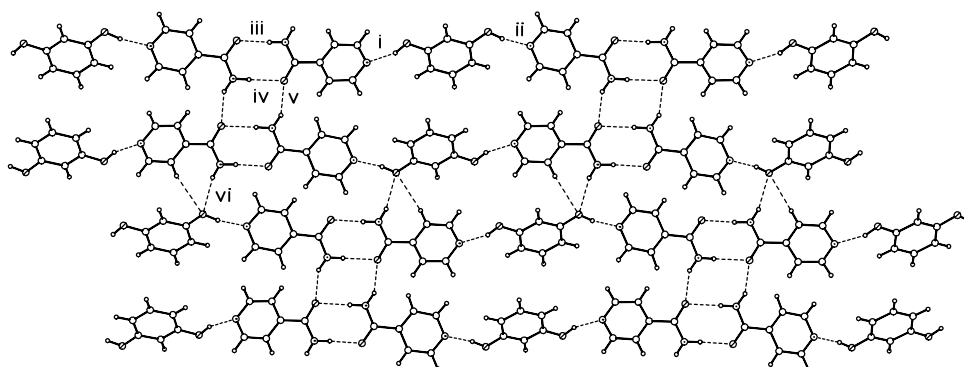


Figure 2. Linear tapes of O–H···N synthon **I** and amide dimer **II**, in the crystal structure of **2**. The amide synthon **II** is between the symmetric independent molecules of isonicotinamide. The tapes are connected *via* N–H···O_{amide} and N–H···O_{phenol} hydrogen bonds into 2D sheets parallel to (1 $\bar{2}$ 0) plane.

6.4 (Phloroglucinol)•(Isonicotinamide)₂•(H₂O)₂, **3**

Crystallization of phloroglucinol and isonicotinamide in 1:3 ratio afforded dihydrate **3**. There is one phloroglucinol, two isonicotinamide and two water molecules in the asymmetric unit (triclinic crystal system, space group $P\bar{1}$). Six component self-assembly involving two phloroglucinol and four isonicotinamide molecules result in stacked dimer of 1:2 stoichiometry (Figure 3a). Two phenol groups are hydrogen bonded with symmetry independent isonicotinamide molecules [O–H···N **I**: (i) 1.77 Å, 2.755(2) Å, 174.5°; (ii) 1.81 Å, 2.795(2) Å, 179.2°] that are in turn bonded *via* symmetry-independent amide dimer **II** [N–H···O: (iii) 1.92 Å, 2.929(2) Å, 176.2°; (iv) 1.91 Å, 2.912(2) Å, 174.1°]. These stacked dimer units constructed from inversion-related phloroglucinol and isonicotinamide molecules are hydrogen bonded along [0 1 2] *via* the third phenol and two water molecules. Phenol to water hydrogen bond [O–H···O: (v) 1.65 Å, 2.627(2) Å, 173.0°] is shorter than H-bonds from water [(vi) 1.81 Å, 2.796(2) Å, 178.2°; (vii) 1.81 Å, 2.789(2) Å, 170.3°]. Two phenol and four water molecules form a supramolecular chair cyclohexane with

O–H···O hydrogen bonds (Figure 3b).¹⁸ The six oxygen atoms are related by a centre of symmetry, the most common (81 %) torsion in R6 water clusters.^{18a} The *anti*-amide N–H hydrogen bond with phenol and water oxygen acceptors [N–H···O_{phenol}: 2.48 Å, 3.309(2) Å, 138.6°; N–H···O_{water}: 2.14 Å, 3.046(2) Å, 148.5°] through interactions at the long distance range. It may be noted that N–H_a···O_{amide} hydrogen bond from dimer aggregate is replaced by N–H_a···O_{phenol/water} in this series of co-crystals. **1** and **2** are forming infinite chains whereas in **3** phenol–isonicotinamide recognition results in finite stacked dimers of synthons **I** and **II** that extend *via* the third O–H group of phloroglucinol as the dihydrate. However, phloroglucinol crystallizes in 2:3 stoichiometry with 4,4'-bipyridine.^{11j} In this structure three hydroxyl groups are hydrogen bonded to the pyridine groups *via* O–H···N hydrogen bonds. Two phloroglucinol molecules and two bipyridines forms a stacked dimers of synthon **I** that extend *via* the O–H···N hydrogen bond formed between third hydroxyl group of phloroglucinol with bipyridine.

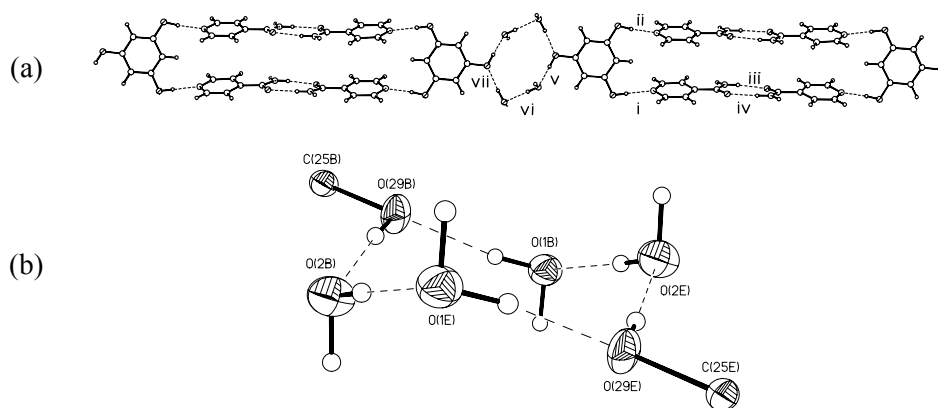


Figure 3. (a) Six component self-assembly in **3** through eight hydrogen bonds of synthon **I** and **II**. The third OH of phloroglucinol is hydrogen bonded to water molecules. (b) Supramolecular ‘chair cyclohexane’ of O–H···O hydrogen bonds from two phenols and four water molecules. The ORTEP is drawn at 50 % probability level for non-hydrogen atoms.

6.5 (4-Hydroxybenzoic acid)•(Isonicotinamide), **4**

The 1:1 co-crystal of 4-hydroxybenzoic acid and isonicotinamide, **4** (monoclinic, space group $P2_1/n$) is a multi-functional system to study hydrogen bond competition between phenol, acid, pyridine and amide groups. Phenol–pyridine and acid–amide synthons **I** and **III** [$\text{O} \cdots \text{H} \cdots \text{N}$: 1.78 Å, 165.2°; $\text{O} \cdots \text{H} \cdots \text{O}$: 1.61 Å, 168.5°; $\text{N} \cdots \text{H} \cdots \text{O}$: 1.98 Å, 168.2°] assemble *n*-glide related molecules as zigzag tapes (Figure 4).

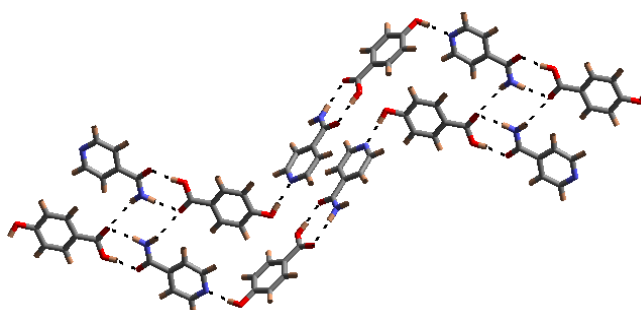


Figure 4. Zigzag tapes of alternating synthon **I** and acid–amide synthon **III** in **4**. The tapes are connected by $\text{N} \cdots \text{H}_a \cdots \text{O}_{\text{acid}}$ hydrogen bonds. Notably the crystal structure is stabilized exclusively through heterosynthons.

Thus, competition between four functional groups in co-crystallization of **4** results in zigzag tapes of phenol–pyridine $\text{O} \cdots \text{H} \cdots \text{N}$ hydrogen bond **I** and acid–amide heterodimer **III**. Such inversion related tapes are connected by amide-to-acid $\text{N} \cdots \text{H}_a \cdots \text{O}$ hydrogen bond [2.46 Å, 3.293(2) Å, 139.3°] and weak $\text{C} \cdots \text{H} \cdots \text{O}$ interactions (Table 2). There are at least two other supramolecular organization modes possible in **4**. (1) In the crystal structure of $(3,5\text{-dihydroxybenzoic acid})_2 \cdot (4,4'\text{-bipyridine})_3$ (space group $P\bar{1}$)^{6d} both phenol OH and COOH groups are hydrogen bonded to pyridine acceptor *via* $\text{O} \cdots \text{H} \cdots \text{N}$ hydrogen bonds **I** and **IV** (Figure 5).

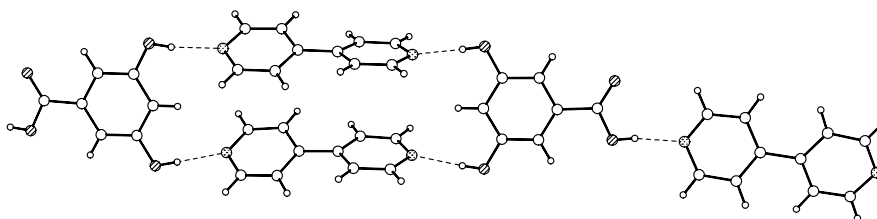


Figure 5. Crystal structure of (3,5-dihydroxybenzoic acid)₂•(4,4'-bipyridine)₃. Notice that two hydroxyl and carboxylic acid groups are hydrogen bonded to the pyridine group.

(2) The crystal structure of (3-hydroxybenzoic acid)•(isonicotinamide) (1:1 co-crystal, *C2/c*)¹⁹ is stabilized by acid–pyridine and amide–amide hydrogen bonds **IV** and **II** (Figure 6).

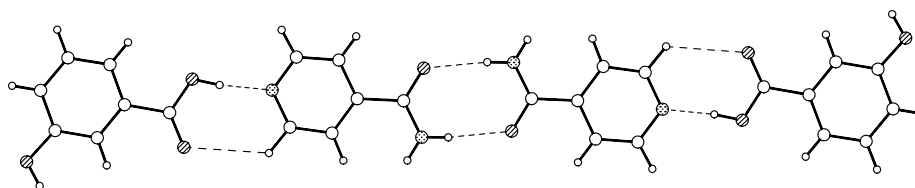


Figure 6. Crystal structure of (3-hydroxybenzoic acid)•(isonicotinamide).

The occurrence of different combinations of synthons **I–IV** are present in a given adduct involving the same hydrogen bonding functional groups implies that their energy is perhaps comparable. Co-crystal **4** is the first example of carboxylic acid–isonicotinamide adduct with phenol–pyridine and acid–amide synthons **I** and **III**. On the other hand, Aakeröy and co-workers have published many crystal structures with acid–pyridine and amide–amide synthons **IV** and **II** using isonicotinamide as a co-crystallizing agent for carboxylic acids.^{19,20} In the previous chapter it has been shown that glutaric and adipic acids co-crystallize with isonicotinamide in 1:2 and also in 1:1 stoichiometry. In 1:2 complexes, both the

carboxylic acid groups hydrogen bonds to pyridine groups, in accordance with the hierarchy of hydrogen bonding. However, in 1:1 complexes one acid group hydrogen bonds to pyridine and the other to amide moiety.²¹ The fact that synthon **I** prevails in the presence of COOH group in structure **4** establishes that phenol–pyridine is specific and strong hydrogen bond and provides yet another example of acid–amide hydrogen bonding in the presence of pyridine moiety.

Three types of supramolecular organizations are possible for 1,3/1,4-*bis*- and 1,3,5-*tris*-phenols: infinite chain,^{6f} finite dimer^{6d} and trigonal motif.^{6c} When π – π stacking stabilizes the strong hydrogen bond assembly, finite dimers are preferred over infinite chains in adducts with resorcinol.^{9a} The placement of electronegative Cl atom in resorcinol steers infinite chain motif towards finite stacked dimer.^{11e} In light of these observations perhaps the weak π – π stacking (3.9–4.0 Å) of pyridyl rings appears to tip the structure towards discrete dimer in **3** compared to infinite chain in **2**. The fact that numerous hydrogen bonds (O–H \cdots O, O–H \cdots N, N–H \cdots O) and weak C–H \cdots O and van der Waals interactions stabilize these structures, it is difficult to further dissect the reason for 1D chain in **2** and 0D dimer in **3**. The phenol–pyridine pairs can form neutral or ionic co-crystal depending on the acidity of the phenols and basicity of the pyridines. When the pK_a difference of the pyridine and phenols is equal to or greater than 2.95, the hydroxy proton of the phenols may transfer to the pyridine nitrogen atom of the pyridines and form phenoxide–pyridinium salts.⁷ However, the present co-crystal crystal structures reveal that the proton transfer does not occur. The protons in these complexes are located from difference Fourier map.

6.6 Conclusions

Crystal engineering with complementary multi-functional systems requires a proper understanding of the factors that control supramolecular organization when different hydrogen bond synthons are in competition. Crystal structures **1–3** of phenol–isonicotinamide adducts have recurring O–H \cdots N synthon **I** and amide dimer **II**. The OH group of phenol/water appears to be a better hydrogen bond acceptor for the *anti*- amide N–H than C=O, perhaps because of cooperative effect in the former motif. The change from infinite chain to stacked dimer pattern in **2** and **3** is ascribed to stabilization from weak $\pi\cdots\pi$ stacking in the latter structure. The adduct **4** provides the first example of carboxylic acid–isonicotinamide co-crystal with acid–amide synthon **III** without acid–pyridine recognition **IV**. Phenol–pyridine synthon **I** is a persistent recognition pattern in the present family of co-crystals.

6.7 Experimental Section

Chemicals were purchased from Lancaster and used as such for the crystallization without further purification. In all co-crystallization experiments the components were finely ground manually and dissolved in appropriate solvents in the stoichiometry mentioned below.

Crystallization

(Hydroquinone)_{0.5}•(Isonicotinamide), **1**

Hydroquinone (0.022 g, 0.20 mmol) and isonicotinamide (0.05 g, 0.40 mmol) were dissolved in hot EtOH. Colourless, needle-shaped crystals were formed after a few days upon evaporation of the solvent. M.p: 155 °C.

(Resorcinol)•(Isonicotinamide)₂, **2**

A 1:2 mixture of resorcinol (0.025 g, 0.23 mmol) and isonicotinamide (0.055 g, 0.46 mmol) was dissolved in hot EtOAc. Needle shaped, light brown crystals were obtained after a few days. M.p: 155 °C.

(Phloroglucinol)•(Isonicotinamide)₂•(H₂O)₂, 3

Phloroglucinol (0.017 g, 0.14 mmol) and isonicotinamide (0.05 g, 0.42 mmol) were ground and dissolved in acetone. Colourless crystals of the dihydrate were obtained the next day after evaporation of solvent. M.p: 144 °C.

(4-Hydroxybenzoic acid)•(Isonicotinamide), 4

Colourless, plate like crystals of the 1:1 complex were obtained upon crystallization of 4-hydroxybenzoic acid (0.028 g, 0.205 mmol) and isonicotinamide (0.025 g, 0.205 mmol) from hot MeOH. M.p: 195 °C.

X-ray Diffraction

Reflections were collected on Nonius Kappa CCD diffractometer at 153(2) K using incident X-ray radiation MoK α (λ = 0.71073 Å) by Dr. Vincent M. Lynch at University of Texas, Austin, U.S.A. Crystals were cooled with Oxford Cryosystem device attached to the CCD machine. Data reductions were performed using DENZO–SMN. Structures were solved by direct methods using SHELXS-97 and refined by full-matrix least-squares refinement on F^2 with anisotropic displacement parameters for non-H atoms using SHELXL-97. Geometrical analysis was carried out in PLATON. Hydrogen bond metrics are neutron normalized because H atom is located with limited accuracy by X-ray diffraction (Table 2).

6.8 References and Notes

1. G.R. Desiraju, *Crystal Engineering: The Design of Organic Solids*, Elsevier, Amsterdam, **1989**.
2. G.R. Desiraju and T. Steiner, *The Weak Hydrogen Bonding in Structural Chemistry and Biology*, Oxford University Press, Oxford, **1999**.
3. G.A. Jeffrey, *An Introduction to Hydrogen Bonding*, Oxford University Press, New York, **1997**.
4. (a) D.N. Chin, J.A. Zerkowski, J.C. MacDonald and G.M. Whitesides, in *Organised Molecular Assemblies in the Solid State*, ed., J.K. Whitesell, Wiley, Chichester, **1999**, ch. 5. (b) J.R. Fredericks and A.D. Hamilton, in *Comprehensive Supramolecular Chemistry*, eds., J.L. Atwood, J.E.D. Davis, D.D. MacNicol and F. Vögtle, Pergamon, Oxford, **1996**, Vol. 9, ch. 16. (c) J.C. MacDonald and G.M. Whitesides, *Chem. Rev.*, **1994**, 94, 2383.
5. (a) G.R. Desiraju, *Angew. Chem., Int. Ed. Engl.*, **1995**, 34, 2311. (b) E. Fan, C. Vincent, S.J. Geib and A.D. Hamilton, *Chem. Mater.*, **1994**, 6, 1113. (c) S. Subramanian and M.J. Zaworotko, *Coord. Chem. Rev.*, **1994**, 137, 357.
6. (a) A.C. Bényei, P.I. Coupar, G. Ferguson, C. Glidewell, A.J. Lough and P.R. Meehan, *Acta Crystallogr., Sect. C*, **1998**, 54, 1515. (b) T.L. Nguyen, A. Scott, B. Dinkelmeier, F.W. Fowler and J.W. Laughier, *New J. Chem.*, **1998**, 22, 129. (c) K. Biradha and M.J. Zaworotko, *J. Am. Chem. Soc.*, **1998**, 120, 6431. (d) P.S. Wheatley, A.J. Lough, G. Ferguson and C. Glidewell, *Acta Crystallogr., Sect. C*, **1999**, 55, 1489. (e) G. Ferguson, C. Glidewell, R.M. Gregson and E.S. Lavender, *Acta Crystallogr., Sect. B*, **1999**, 55, 573. (f) E. Corradi, S.V. Meille, M.T. Messina, P. Metrangolo and G. Resnati, *Angew. Chem., Int. Ed.*, **2000**, 39, 1782. (g) C.M. Zakaria, G. Ferguson, A.J. Lough and C. Glidewell, *Acta Crystallogr., Sect. C*, **2002**, 58, o1.

7. K.-S. Huang, D. Britton, M.C. Etter and S.R. Byrn, *J. Mater. Chem.*, **1997**, 7, 713.
8. (a) M.R. Caira, A. Horne, L.R. Nassimbeni and F. Toda, *J. Mater. Chem.*, **1997**, 7, 2145. (b) G. Ferguson, C. Glidewell, A.J. Lough, G.D. McManus and P.R. Meehan, *J. Mater. Chem.*, **1998**, 8, 2339. (c) L.R. MacGillivray, J.L. Reid and J.A. Ripmeester, *CrystEngComm*, **1999**, 1. (d) L.R. MacGillivray, J.L. Reid and J.A. Ripmeester, *Chem. Commun.*, **2001**, 1034. (e) B.-Q. Ma, Y. Zhang and P. Coppens, *Cryst. Growth Des.*, **2001**, 1, 271. (f) J. Scott, M. Asami and K. Tanaka, *New J. Chem.*, **2002**, 26, 1822. (g) B.-Q. Ma, Y. Zhang and P. Coppens, *Cryst. Growth Des.*, **2002**, 2, 7. (h) S. Hoger, D.L. Morrison and V. Enkelman, *J. Am. Chem. Soc.*, **2002**, 124, 6734.
9. (a) L.R. MacGillivray, J.L. Reid and J.A. Ripmeester, *J. Am. Chem. Soc.*, **2000**, 122, 7817. (b) L.R. MacGillivray, *CrystEngComm*, **2002**, 4, 37.
10. T. Steiner, I. Majerz and C.C. Wilson, *Angew. Chem., Int. Ed.*, **2001**, 40, 2651.
11. (a) V.R. Thalladi, T. Smolka, R. Boese and R. Sustmann, *CrystEngComm*, **2000**, 17, (CSD refcode: FOQHEY). (b) T.C.W. Mak, C.-S. Tse, Y.-H. Chong and F.-C. Mok, *Acta Crystallogr., Sect. B*, **1977**, 33, 2980, (HMTHQU). (c) Ref. 6f (MEKWUU). (d) Ref. 9a (ABEKUN, ABELAU, ABELIC). (e) G.S. Papaefstathiou and L.R. MacGillivray, *Org. Lett.*, **2001**, 3, 3835, (ACYOYOG). (f) M.M. Mahmoud and S.C. Wallwork, *Acta Crystallogr., Sect. B*, **1979**, 35, 2370, (RSHMTA). (g) Ref. 6c (HIMGAL, HIMGEP). (h) E.S. Lavender, C. Glidewell and G. Ferguson, *Acta Crystallogr., Sect. C*, **1998**, 54, 1637, (PUVMIC). (i) P.I. Coupar, C. Glidewell and G. Ferguson, *Acta Crystallogr., Sect. B*, **1997**, 53, 521, (RAWDIC). (j) P.I. Coupar, G. Ferguson and C. Glidewell, *Acta Crystallogr., Sect. C*, **1996**, 52, 2524, (TEKKOJ).
12. (a) L. Leiserowitz and G.M.J. Schmidt, *J. Chem. Soc., Sect. A*, **1969**, 2372. (b) L. Leiserowitz and M. Tuval, *Acta Crystallogr., Sect. B*, **1978**, 34, 1230.

13. F.H. Allen, *Acta Crystallogr., Sect. B*, **2002**, 58, 380.
14. The CSD (ConQuest 1.5, November 2002 update, 272066 entries) contains 225 hits with CONH₂ and COH fragments having $R \leq 0.10$ and 3D coordinates determined. Of these, 27 crystal structures contain amide dimer **II**, among these 27 entries five structures contain motif **V** and one structure has motif **VI** in distance–angle range $1.5 < \text{H}\cdots\text{O} < 2.4 \text{ \AA}$ (HNORM) and $130 < \angle \text{N-H}\cdots\text{O} < 180^\circ$. (a) J. Zukerman-Schpector, E.E. Castellano, G. Oliva and G. Carvajal, *Acta Crystallogr., Sect. C*, **1984**, 40, 685, (CSD Refcode: CERNIW). (b) S. Kashino, S. Tateno, H. Tanabe, M. Haisa and Y. Katsube, *Acta Crystallogr., Sect. C*, **1991**, 47, 2236, (JIXCOI). (c) E.E. Castellano, J.Z. Schpector and G. Carvajal, *Acta Crystallogr., Sect. B*, **1981**, 37, 284, (OHPHXD). (d) G. Quinkert, S. Scherer, D. Reichert, H.-P. Nastler, H. Wennemers, A. Ebel, K. Urabahns, K. Wagner, K.-P. Michaelis, G. Wiech, G. Prescher, B. Bronstert, B.-J. Freitag, I. Wicke, D. Lisch, P. Belik, T. Crecelius, D. Hoerstermann, G. Zimmermann, J. W. Bats, G. Duerner and D. Rehm, *Helv. Chim. Acta*, **1997**, 80, 1683, (RUJVAT). (e) F. Aqiino, H. Pauling, W. Walther, D.A. Plattner and W. Bonrath, *Synthesis*, **2000**, 731, (WEGYEM).
15. M.A. Walters and A.L. Rheingold, *Private Communication*, **2000**, (MEGLOZ).
16. S. Kashino, S. Tateno, H. Tanabe, M. Haisa and Y. Katsube, *Acta Crystallogr., Sect. C*, **1991**, 47, 2236.
17. (a) P. Vishweshwar, A. Nangia and V.M. Lynch, *Chem. Commun.*, **2001**, 179. (b) B.R. Bhogala, P. Vishweshwar and A. Nangia, *Cryst. Growth Des.*, **2002**, 2, 325.
18. (a) L. Infantes and S. Motherwell, *CrystEngComm*, **2002**, 454. (b) R. Ludwig, *Angew. Chem., Int. Ed.*, **2001**, 40, 1808. (c) R. Custelcean, C. Afloroaei, M. Vlassa and M. Polverejan, *Angew. Chem., Int. Ed.*, **2000**, 39, 3094. (d) J.N. Moorthy, R. Natarajan and P. Venugopalan, *Angew. Chem., Int. Ed.*, **2002**, 41,

3417. (e) K.-M. Park, R. Kuroda and T. Iwamoto, *Angew. Chem., Int. Ed.*, **1993**, 32, 884.
19. C.B. Aakeröy, A.M. Beatty and B.A. Helfrich, *J. Am. Chem. Soc.*, **2002**, 124, 14425.
20. (a) C.B. Aakeröy, A.M. Beatty and B.A. Helfrich, *Angew. Chem., Int. Ed.*, **2001**, 40, 3240 (b) C.B. Aakeröy, A.M. Beatty, B.A. Helfrich and M. Nieuwenhuyzen, *Cryst. Growth Des.*, **2003**, 3, 159.
21. P. Vishweshwar, A. Nangia and V.M. Lynch, *Cryst. Growth Des.*, **2003**, 3, ASAP.

CHAPTER SEVEN

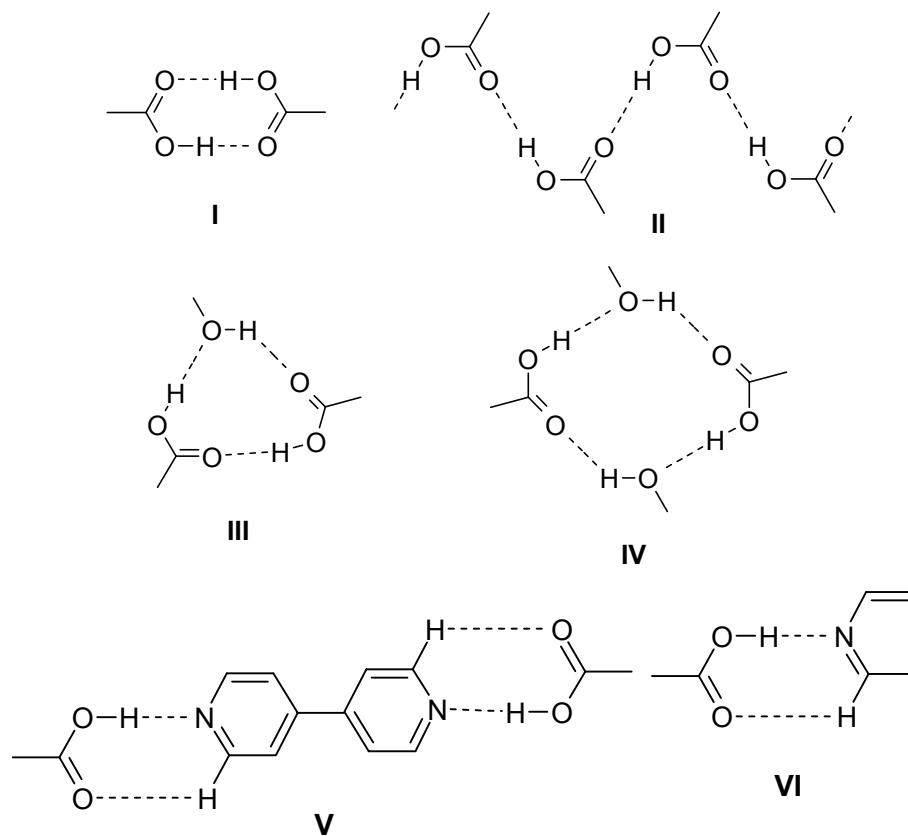
HYDROGEN BOND NETWORKS IN CYCLOHEXANE-1, 3*cis*, 5*cis*-TRICARBOXYLIC ACID

7.1 Introduction

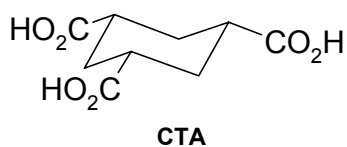
The description of crystal structures in terms of networks is a promising and systematic approach for the analysis of crystal structures in a precise fashion. Wells has excellently described this technique in his well-known book “*Structural Inorganic Chemistry*”.¹ The design and synthesis of infinite two dimensional and three dimensional network structures using non-covalent soft bonds such as hydrogen bonds and strong metal-ligand coordination bonds is a current goal of crystal engineering.² In the application of network theory to organic structures, the molecular residues are taken as nodes and the supramolecular bonds are taken as node connectors.³ The topology or connectivity of a given network is represented in terms of the general symbol (n, p) , where n is the number of nodes in the smallest closed circuits in the net and p is the number of connections to neighboring nodes that radiate from any centre or node. Conventional hydrogen bonds like O–H \cdots O, O–H \cdots N and N–H \cdots O have been extensively used to generate three-dimensional network structures because of their strength and directionality.⁴

This chapter deals with the crystal structures of cyclohexane-1, 3*cis*, 5*cis*-tricarboxylic acid (CTA) monohydrate and its complex with 4,4'-bipyridine. The present work describes how robust heterosynthons are useful for the design of network structures. CTA represented a novel trigonal scaffold for crystal engineering at the time of this study, though over 19 structures are now published to date. As mentioned in the previous chapters the carboxylic acid group is an important hydrogen bonding functional group in crystal engineering.⁵ Carboxylic acids are well known to form centrosymmetric dimer **I**, catemer **II**, and bridged motifs **III** and **IV**

(Scheme 1). The supramolecular synthons⁶ **II**, **III** and **IV** are nonetheless rare and the reported high frequency of dimer **I** formation⁷ suggests that carboxylic acids are attractive candidates for controlling short-range crystal packing.



Scheme 1. Hydrogen bonded synthons discussed in this chapter.



It has been anticipated that the supramolecular diversity and complexity of hydrogen bonded hexagonal networks could be expanded if trimesic acid (TMA) is replaced by the conformationally flexible and non-planar cyclohexane-1, 3*cis*, 5*cis*-tricarboxylic acid. The strategy is based on the control of crystalline architecture by the same supramolecular synthon despite small changes in the carbon skeleton of the molecular scaffold.

7.2 A Pseudo–Honeycomb Network in CTA•H₂O

Cyclohexane-1, 3*cis*, 5*cis*-tricarboxylic acid crystallizes as a monohydrate in the monoclinic crystal system with one molecule of each CTA and water in the asymmetric unit (space group *C2/c*). In the crystal structure of CTA•H₂O, two carboxylic acids form the expected centrosymmetric dimer **I** (O–H...O: 1.65 Å, 178.4°; 1.67 Å, 176.6°) and the third acid group aggregates with another CO₂H group using the water molecule through synthon **IV** (O–H...O_w: 1.63 Å, 169.5°; O_w–H...O: 1.82 Å, 172.6°) (Table 1). Thus, six CTA and four water molecules form a pseudo-hexagonal network stabilized by synthons **I** and **IV** (Figure 1). The perfect hexagonal symmetry observed in the network of TMA is distorted to pseudo-hexagonal in CTA because two of the carboxylic acid groups aggregate *via* synthon **I**, while the third one forms motif **IV**. The “chicken-wire” grid of CTA•H₂O is shown in Figure 2. Three identical hydrogen bonded networks thread through the 15 × 11 Å size of voids of this (6,3) net almost perpendicular to the 2D corrugated sheet of the original framework resulting in the four-fold inclined interpenetrated network (Figure 3). These interweaving nets, inclined at an angle of 87°, are connected by O_w–H...O hydrogen bonds. The near identity in the topology, connectivity, and interpenetration mode of the (6,3) nets in the crystal structures of TMA⁸ and CTA•H₂O is noteworthy. Hydration (solvation) of carboxylic acids by one or two water (alcohol) molecules as open or cyclic hydrogen bond motifs is a common phenomenon during

crystallization.^{7,9} The role of water in this crystal structure may be rationalized as providing a strong $O_w-H\cdots O$ hydrogen bond link between the interweaving networks. The role of water has been aptly described as a “gluing factor” in organic crystals.¹⁰

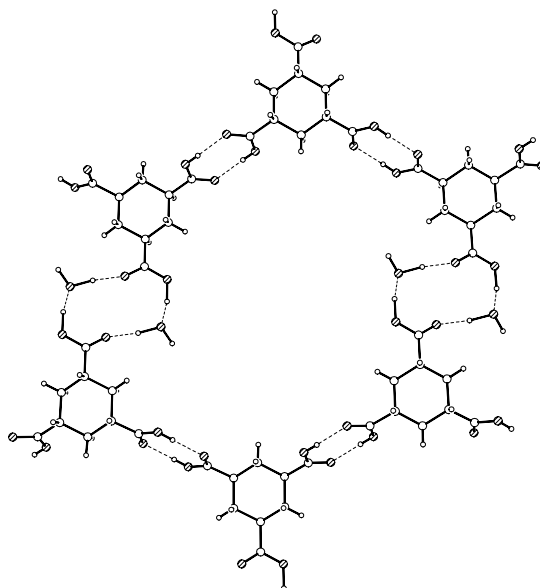


Figure 1. Pseudo-honeycomb open network of $CTA\cdot H_2O$ stabilized by hydrogen bond synthons **I** and **IV**. The cavity size is 15×11 Å.

Table1. Geometrical parameters of hydrogen bonds

Co-crystal	H-bond	d (Å) ^a	D (Å)	θ (°)
CTA•H ₂ O	O–H \cdots O	1.64	2.612(3)	169.5
	O–H \cdots O	1.65	2.636(3)	178.4
	O–H \cdots O	1.68	2.662(3)	176.6
	O–H \cdots O	1.82	2.799(3)	172.6
	O–H \cdots O	1.87	2.845(3)	168.6
	C–H \cdots O	2.54	3.558(4)	155.5
	C–H \cdots O	2.60	3.602(4)	152.5
	C–H \cdots O	2.62	3.625(4)	153.9
	C–H \cdots O	2.63	3.617(4)	150.9
CTA•bipyridine•H ₂ O	O–H \cdots O	1.60	2.570(2)	169.8

Table 1, *continued*...

O—H...O	1.89	2.855(2)	166.9
O—H...N	1.65	2.635(2)	176.6
O—H...N	1.66	2.632(2)	170.6
O—H...N	1.67	2.651(2)	170.6
O—H...N	1.68	2.633(2)	162.1
O—H...N	1.68	2.658(2)	169.6
O—H...N	1.78	2.753(2)	168.2
C—H...O	2.26	3.336(2)	173.2
C—H...O	2.37	3.409(2)	160.1
C—H...O	2.37	3.453(2)	176.9
C—H...O	2.43	3.375(2)	145.2
C—H...O	2.46	3.278(2)	131.0
C—H...O	2.47	3.349(2)	137.2
C—H...O	2.47	3.481(2)	155.0

^a O—H and C—H distances are normalized to standard neutron values.

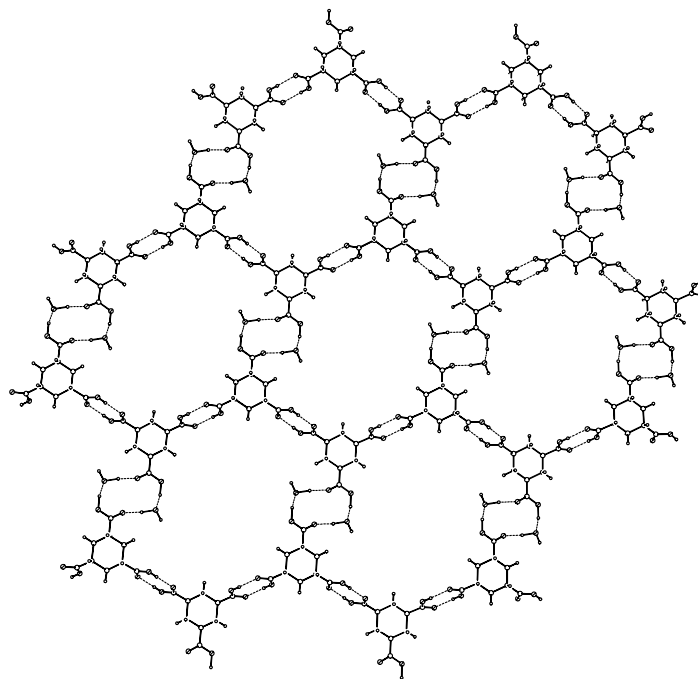


Figure 2. The basic “chicken-wire” motif—a two-dimensional network of CTA•H₂O.

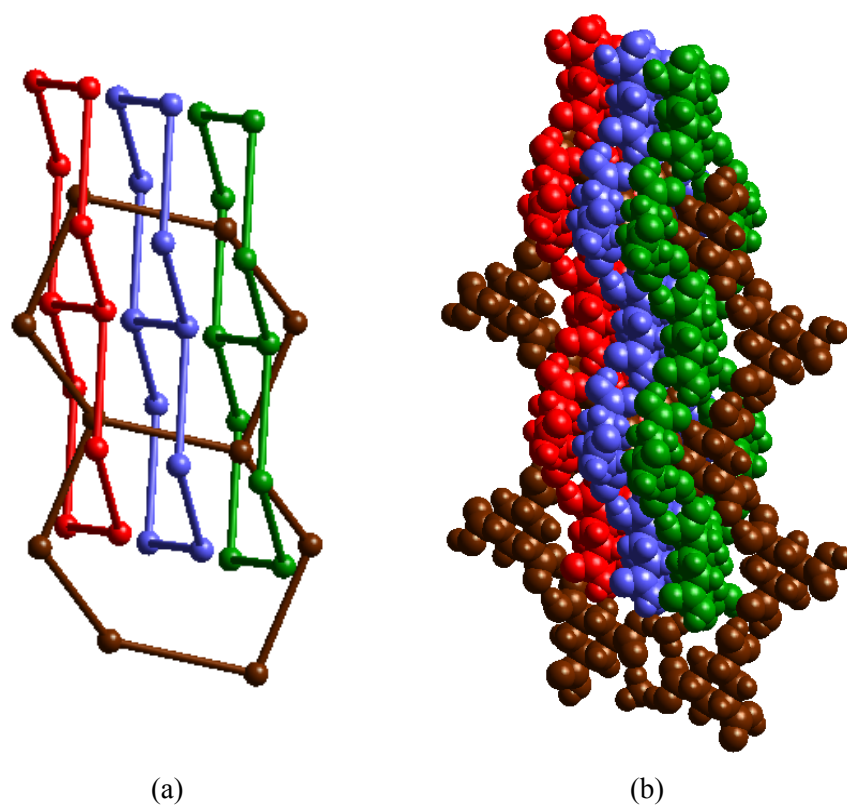


Figure 3. Four-fold inclined interpenetrated (6,3) networks in CTA•H₂O. (a) Ball and stick model. Three-connected nodes represent the centres of CTA and hydrogen bonds are shown as sticks. (b) Space filling model to show the hexagonal void filled with interpenetrating networks.

Ermer and coworkers¹¹ reported that when CTA crystallized from [18]crown-6 (CRO) in a 2:1 ratio from ethanol solvent gave the crystals of the composition (CTA)₂•CRO•(H₂O)₅. The fifth water molecule is positionally disordered. The two carboxylic groups of CTA molecules form zigzag chains in the crystal held together by synthon **I**. The third carboxylic acid groups of CTA not engaged in the zigzag chains donate their hydrogen atoms to hydrogen bonds directed towards the oxygen atom of a water molecule of CRO tetrahydrate ensembles. Thus, CTA zigzag chains

linked by $\text{CRO} \cdot (\text{H}_2\text{O})_4$ spacers through the carboxyl–water hydrogen bonds produced a distorted, puckered honeycomb network (Figure 4). These three-connected honeycomb sheets are highly porous, but they do not interpenetrate and have their cavities filled by CRO molecules of neighboring sheets.

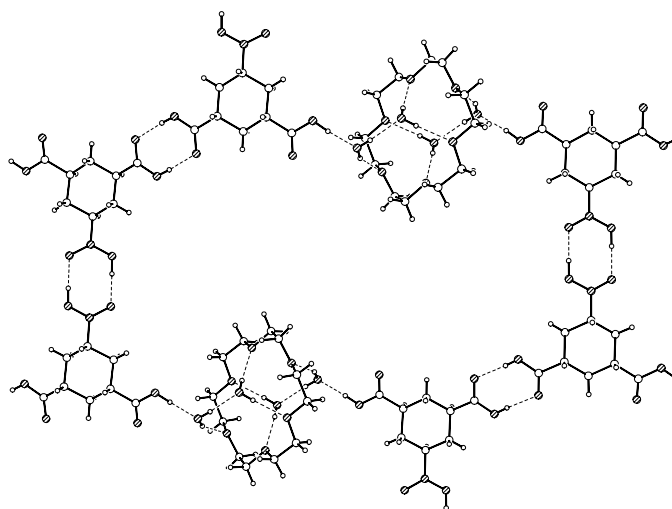


Figure 4. Three-connected puckered and distorted honeycomb network of $(\text{CTA})_2 \cdot \text{CRO} \cdot (\text{H}_2\text{O})_5$.

Very recently Jones and co-workers¹² have shown the crystal structure of pseudo-hexagonal network formed by CTA molecule with acetonitrile solvent. Crystal structure reveals that extended zigzag supramolecular acid tapes are formed by hydrogen bonds within a carboxylic acid dimer **I**. These tapes are linked by acetonitrile molecules *via* $\text{O}-\text{H} \cdots \text{N}$ and $\text{C}-\text{H} \cdots \text{O}$ interactions to create a two-dimensional supramolecular network, similar to that found in $\text{CTA} \cdot \text{H}_2\text{O}$ structure. Cavities are formed that are approximately $14 \times 10 \text{ \AA}$ in size (Figure 5), with the puckered honeycomb open network filled by interpenetration of four independent networks similar to that of $\text{CTA} \cdot \text{H}_2\text{O}$ structure (Figure 6). This interpenetration, running approximately perpendicular to the plane of the cavity, is facilitated by

puckering of the pseudo-honeycombs that form the networks. The hexagons resemble the 'chair' conformation of cyclohexane.

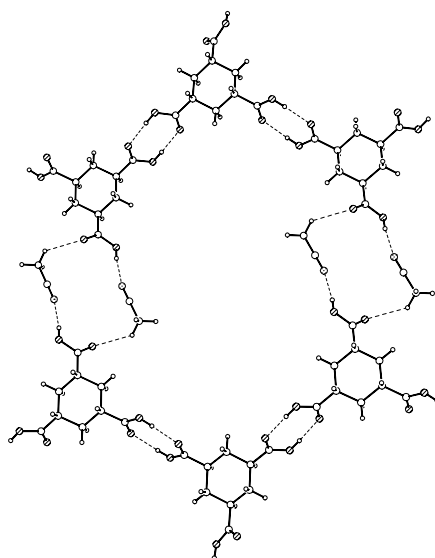


Figure 5. A 14×10 Å size pseudo-honeycomb network formed in the crystal structure of CTA•Acetonitrile. Notice the similarity with the pseudo-honeycomb network in Figure 1.

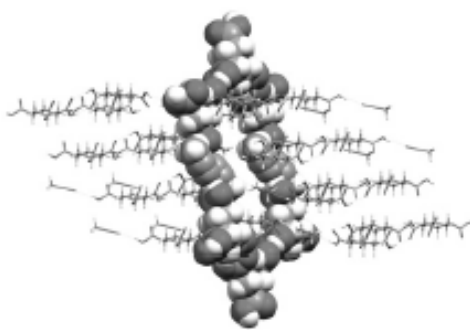


Figure 6. Four-fold inclined interpenetration in the crystal structure of CTA•Acetonitrile.

Since CTA crystallizes along with solvent or water molecule, the structure of unsolvated CTA was solved by Jones and Motherwell¹³ using powder X-ray diffraction. There are two CTA molecules in the asymmetric unit. Five of six CO₂H groups form synthon **I** with neighboring CO₂H groups. The motifs connect molecules to form pseudo-hexagonal, ten-member rings that fuse into supramolecular buckled honeycomb sheets, which stack and are linked by O–H...O hydrogen bonds (Figure 7). Despite the large cross section of hexagonal channels *ca.* 30 × 13 Å, no interpenetration of sheets is observed in the crystal structure. The ten-molecule units in the pseudo-hexagonal grid adopt supramolecular ‘chair’ conformation (Figure 8).

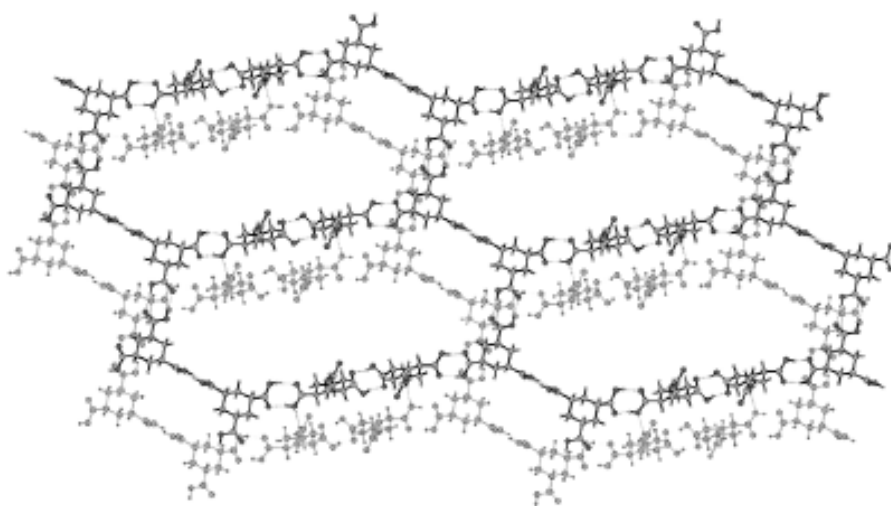


Figure 7. The stacking of super pseudo-honeycomb networks in the crystal structure of CTA.

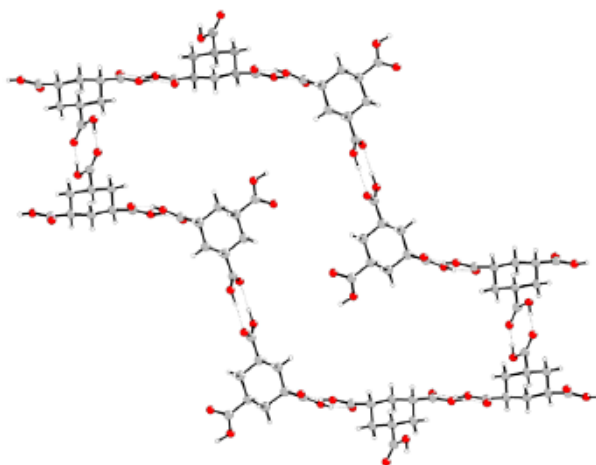


Figure 8. The supramolecular ‘chair’ formation of super pseudo-honeycomb network of ten molecules connected through synthon I.

7.3 Super Pseudo–Honeycomb Network of $(\text{CTA})_2 \cdot (4,4'\text{-bipyridine})_3 \cdot \text{H}_2\text{O}$

We have anticipated that the pseudo-honeycomb CTA network can also be extended to generate larger voids and channels for guest inclusion and/or interpenetration like in the case of TMA honeycomb network. CTA was crystallized with bipyridine in 2:3 molar ratio from *iso*-propanol/benzene (3:1) solvent mixture. X-ray diffraction of a single crystal structure showed it to have the composition $\text{CTA} \cdot 4,4'\text{-bipyridine} \cdot \text{H}_2\text{O}$ of 2:3:1 (space group $P\bar{1}$). The bipyridine spacer extends synthon I linearly to motif V with robust acid–pyridine synthon VI. The cavity size expands from $15 \times 11 \text{ \AA}$ to $27 \times 27 \text{ \AA}$ dimension without changing the network topology. There are two CTA (A1, A2), three bipyridine (B1, B2, B3) and one water molecule in the asymmetric unit. Two CO_2H groups of both A1 and A2 molecules are hydrogen bonded to different bipyridine molecules (B1, B2) *via* $\text{O}-\text{H} \cdots \text{N}$ bonds, which in some cases are stabilized by auxiliary $\text{C}-\text{H} \cdots \text{O}$ interactions, *i.e.*, synthon VI ($\text{O}-\text{H} \cdots \text{N}$: $1.6\text{--}1.7 \text{ \AA}$, $160\text{--}175^\circ$; $\text{C}-\text{H} \cdots \text{O}$: $2.4\text{--}2.6 \text{ \AA}$, $120\text{--}130^\circ$). The third CO_2H group of A1 is hydrogen bonded through the water molecule (synthon IV: $\text{O}-\text{H} \cdots \text{O}_w$:

1.59 Å, 169.7°; O_w–H...O: 1.88 Å, 166.9°) resulting in the super pseudo-honeycomb network as shown in Figure 9. The cavity in CTA•4,4'-bipyridine•H₂O has an area of 27 × 27 Å², over four times the void size in CTA•H₂O. The acid–acid homodimer synthon **I** in CTA•H₂O structure is replaced by the robust acid–pyridine heterosynthon **VI** in CTA•4,4'-bipyridine•H₂O, while synthon **IV** with a strong O–H...O_w hydrogen bond carries over from the CTA•H₂O structure to the bipyridine complex. The O–H...O bonds of the dimer synthon **I** is weaker than that of hydrated synthon **IV**, and it is the former CO₂H groups that dissociates and reform to synthon **VI** in the bipyridine complex. This indicates that the synthon **IV** is marginally more robust than synthon **I** presumably because of cooperative stabilization,¹⁴ even though both synthons are assembled with O–H...O hydrogen bonds. The interpenetration in CTA•4,4'-bipyridine•H₂O is of the parallel type akin to that observed in the TMA•4,4'-bipyridine complex (2:3).¹⁵ Three identical hydrogen bonded (6,3) nets interlock by parallel threading along the *a*-axis (Figure 10), which are in turn connected to *b*-translated nets by acid–bipyridine and water–bipyridine hydrogen bonds involving the third CO₂H group of A2, B3 and water molecules (O–H...N: 1.65 Å, 176.5°; 1.78 Å, 168.2°). Thus the bipyridine ligand acts as a spacer between the CO₂H groups and also functions as bridge between the networks in the 2D corrugated sheet.

Jones and co-workers¹⁶ reported the crystal structure of closely related CTA•4,4'-bipyridine (1:1) complex. Two CO₂H groups of CTA form zigzag tape *via* acid–pyridine synthon **VI** that are in turn connected through the third CO₂H group into corrugated sheets. This 1:1 CTA•4,4'-bipyridine structure does not exhibit interpenetration.

The notable feature of this work is that the interpenetration characteristics of the parent acid CTA, and its bipyridine complex, follow that of the corresponding

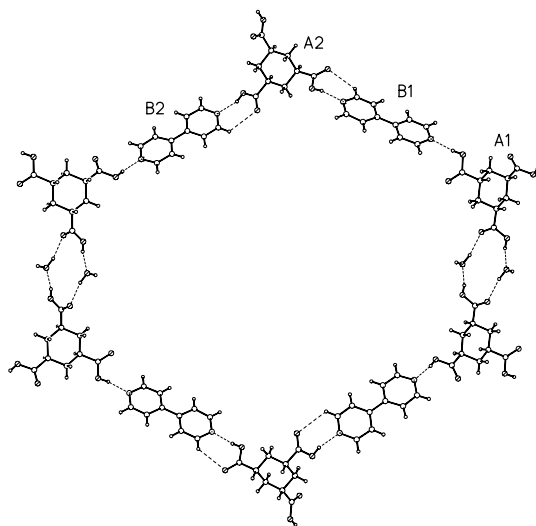


Figure 9. Super pseudo-honeycomb open network in $(\text{CTA})_2 \cdot (4,4'\text{-bipyridine})_3 \cdot \text{H}_2\text{O}$ stabilized by hydrogen bond synthons **IV** and **VI**. Notice that the void has expanded over four times compared to Figure 1.

TMA structures in most respects. Unlike coordination polymers, organic crystal structures can be very fragile to changes in the molecular structure¹⁷ because hydrogen bonds are an order of magnitude weaker than metal–ligand bonds (7–15 kcal/mol vs 40–80 kcal/mol).¹⁸ Further, there are numerous examples of coordination polymers and metal–organic crystals that exhibit interpenetration, interlocked systems built from purely organic molecules are rare.¹⁹ In the category of 2D inclined 4-fold interpenetrated (6,3) nets, TMA and $\text{CTA} \cdot \text{Acetonitrile}$ are the only two examples of an all organic molecules. There are three organic structures with 3-fold parallel interpenetrated (6,3) nets. Furthermore, the ready solubility of CTA compared to TMA is advantageous in crystal engineering.

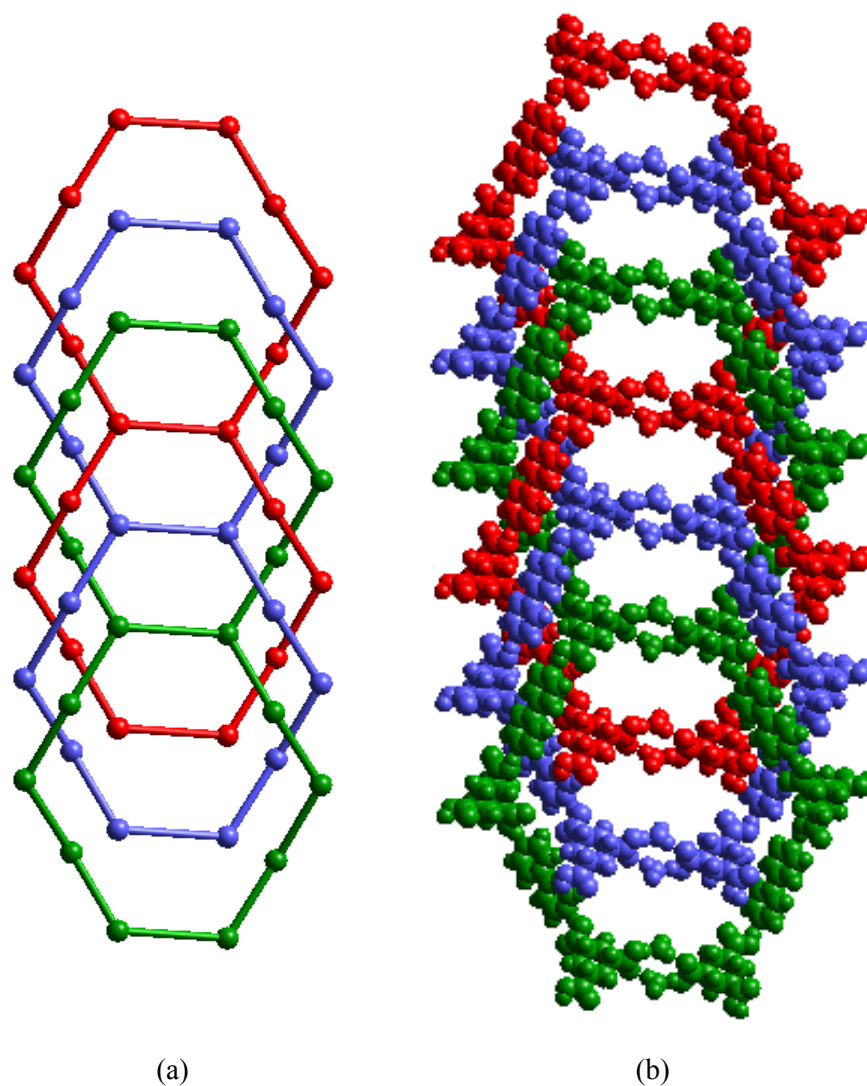


Figure 10. Three-fold parallel interpenetrated (6,3) networks in $(\text{CTA})_2 \cdot (4,4'\text{-bipyridine})_3 \cdot \text{H}_2\text{O}$. (a) Ball and stick model. Three-connected nodes represent the centres of CTA molecules, two-connected nodes are the midpoints of 4,4'-bipyridine molecules, and hydrogen bonds are shown as sticks. (b) Space filling model showing the larger pseudo-hexagonal cavities filled with interpenetration.

7.4 Conclusions

A (6,3) pseudo-honeycomb network formed by cyclohexane-1, 3*cis*, 5*cis*-tricarboxylic acid monohydrate with 4-fold inclined interpenetration is described. Crystallization of CTA with 4,4'-bipyridine provides the complex, (CTA)₂•(4,4'-bipyridine)₃•H₂O, which has 3-fold interweaving (6,3) network with parallel interpenetration. In (CTA)₂•(4,4'-bipyridine)₃•H₂O complex, the 15 × 15 Å pseudo-honeycomb cavity of CTA•H₂O is expanded to 27 × 27 Å size with 4,4'-bipyridine, acting as a spacer to the homosynthon **I**. The striking similarity of these hydrogen bond networks to those found in the crystal structures of TMA and its complex with 4,4'-bipyridine indicates that such interpenetrated network structures may be engineered using retrosynthetic strategies.

7.5 Experimental Section

Crystallization

(a) CTA•H₂O

Cyclohexane-1, 3*cis*, 5*cis*-tricarboxylic acid was purchased from Aldrich and crystallized from ethanol solvent without further purification. Nice needle shaped crystals were obtained after a few days. M.p. 216–217 °C. IR (KBr): 3400, 2974, 1697, 1419, 1290, 1200, 1167, 1128, 906 cm⁻¹.

(b) (CTA)₂•(4,4'-bipyridine)₃•H₂O

A 2:3 mixture of cyclohexane-1, 3*cis*, 5*cis*-tricarboxylic acid (30 mg, 139 mmol) and 4,4'-bipyridine (32.5 mg, 208 mmol) were dissolved in 3:1 solvent mixture of *iso*-propanol and benzene at room temperature, plate-shaped crystals appeared after a few days. M.p. 206 °C. IR (KBr): 3472, 2945, 2469, 1921, 1697, 1599, 1408, 1257, 1190, 1001, 808, 623 cm⁻¹.

X-ray Crystallography

Reflections on the crystals $\text{CTA}\cdot\text{H}_2\text{O}$ and $(\text{CTA})_2\cdot(4,4'\text{-bipyridine})_3\cdot\text{H}_2\text{O}$ were collected on Bruker SMART 1000 CCD diffractometer at 93 K by Dr. Judy-Flippen-Anderson and Jeff Deschamps, Naval Research Laboratory, Washington DC, U.S.A. The incident radiation is $\text{Mo-K}\alpha$ X-ray ($\lambda = 0.71073$). Data reduction was performed using Bruker SAINT v6.02a.²⁰ The structure solutions and refinements of both the crystal structures were performed with the SHELX-97. All the geometrical analysis was carried out with PLATON on Silicon Graphics Octane2 workstation.

7.6 References and Notes

1. A.F. Wells, *Structural Inorganic Chemistry*, 5th ed.; Oxford University Press, Oxford, **1984**.
2. G.R. Desiraju, *Crystal Engineering. The Design of Organic Solids*, Elsevier, Amsterdam, **1989**.
3. (a) G.R. Desiraju, *Chem. Commun.*, **1997**, 1475. (b) M.J. Zaworotko, *Chem. Commun.*, **2001**, 1.
4. J.P. Glusker, *Topics in Current Chemistry*, Vol. 198, E. Weber (ed.), Springer-Verlag, Berlin, **1998**, pp.1–56.
5. (a) L. Leiserowitz, *Acta Crystallogr., Sect. B*, **1976**, 32, 775. (b) J. Bernstein, M.C. Etter and L. Leiserowitz, In *Structure Correlation*, eds. H.-B. Bürgi and J.D. Dunitz, VCH, Weinheim, Vol. 2, **1994**.
6. G.R. Desiraju, *Angew. Chem., Int. Ed. Engl.*, **1995**, 34, 2311.
7. S.V. Kolotuchin, E.E. Fenlon, S.R. Wilson, C.J. Loweth and S.C. Zimmerman, *Angew Chem., Int. Ed. Engl.*, **1995**, 34, 2654.

8. (a) D.J. Duchamp and R.E. Marsh, *Acta Crystallogr., Sect. B*, **1969**, 25, 5. (b) F.H. Herbstein, in *Comprehensive Supramolecular Chemistry*, eds. D.D. MacNicol, F. Toda and R. Bishop, Pergamon, Oxford, **1996**, Vol. 6, pp 61–83.
9. (a) A. L. Gillon, N. Feeder, R. J. Davey and R. Storey, *Cryst. Growth Des.*, **2003**, 3, ASAP. (b) F.A.A. Paz, A.D. Bond, Y.Z. Khimyak and J. Klinowski, *New J. Chem.*, **2002**, 26, 381. (c) P. Vishweshwar, A. Nangia and V.M. Lynch, *Chem. Commun.*, **2001**, 179. (d) F.H. Herbstein, M. Kapon and V. Shteiman, *Acta Crystallogr., Sect. B*, **2001**, 57, 692.
10. T.M. Krygowski, S.J. Grabowski and J. Konarski, *Tetrahedron*, **1998**, 54, 11311.
11. O. Ermer and J. Neudörfl, *Chem. Eur. J.*, **2001**, 7, 4961.
12. N. Shan, A.D. Bond and W. Jones, *New J. Chem.*, **2003**, 27, 365.
13. H. Nowell, N. Shan, J.P. Attfield, W. Jones and W.D.S. Motherwell, *Cryst. Eng.*, **2003**, 6, 57.
14. G.A. Jeffrey, *An Introduction to Hydrogen Bonding*, Oxford University Press, New York, **1997**.
15. C.V.K. Sharma and M.J. Zaworotko, *Chem. Commun.*, **1996**, 2655.
16. N. Shan, A.D. Bond and W. Jones, *Cryst. Eng.*, **2002**, 5, 9.
17. S. Aitipamula, P.K. Thallapally, R. Thaimattam, M. Jaskólski and G.R. Desiraju, *Org. Lett.*, **2002**, 4, 921.
18. D. Braga and F. Grepioni, *Acc. Chem. Res.*, **2000**, 33, 601.
19. Current examples of interpenetration are updated on the website of Dr. S.R. Batten, Monash University (www.chem.monash.edu.au). Out of the 500 or so examples of interpenetration documented in the pdf file current up to January 15, 2002, only 10 % are organic crystal structures.
20. Bruker SAINT v6.02A, Bruker AXS, Inc., Madison, Wisconsin, U.S.A., **2000**.

LIST OF PUBLICATIONS

1. Pyrazine-2,3-dicarboxamide.
Peddy Vishweshwar, Ashwini Nangia and Vincent M. Lynch
Acta Crystallogr., Sect. C, **2000**, *56*, 1512–1514.
2. Cooperative Assistance in a Very Short O–H···O Hydrogen Bond. Low temperature X-ray Crystal Structures of 2,3,5,6-Pyrazinetetracarboxylic Acid and Related Acids.
Peddy Vishweshwar, Ashwini Nangia and Vincent M. Lynch
Chem. Commun., **2001**, 179–180.
3. Recurrence of Carboxylic acid–Pyridine Supramolecular Synthons in the Crystal Structures of Some Pyrazine Carboxylic Acids.
Peddy Vishweshwar, Ashwini Nangia and Vincent M. Lynch
J. Org. Chem., **2002**, *67*, 556–565.
4. Four-fold Inclined Interpenetrated and Three-fold Parallel Interpenetrated Hydrogen bonded Networks in 1,3,5-Cyclohexanetricarboxylic Acid Hydrate and its Molecular Complex with 4,4'-Bipyridine.
Balakrishna R. Bhogala, **Peddy Vishweshwar** and Ashwini Nangia
Cryst. Growth Des., **2002**, *2*, 325–328.
5. Supramolecular Synthon Based on N–H···N and C–H···O Hydrogen Bonds. Crystal Engineering of a Helical Structure with 5,5-Diethyl Barbituric Acid.
Peddy Vishweshwar, Ram Thaimattam, Mariusz Jaskólski and Gautam R. Desiraju
Chem. Commun., **2002**, 1830–1831.
6. Searching for a Polymorph: Second Crystal Form of 6-Amino-2-Phenylsulfonylimino-1,2-dihydropyridine.
Ram K. R. Jetti, Roland Boese, Jagarlapudi A. R. P. Sarma, L. Sreenivas Reddy, **Peddy Vishweshwar** and Gautam R. Desiraju
Angew. Chem., **2003**, *115*, 2008–2012; *Angew. Chem., Int. Ed.*, **2003**, *42*, 1963–1967.
7. Supramolecular Synthons in Phenol–Isonicotinamide Adducts.
Peddy Vishweshwar, Ashwini Nangia and Vincent M. Lynch
CrystEngComm, **2003**, *5*, 164–168.

8. Molecular Complexes of Homologous Alkanedicarboxylic Acids with Isonicotinamide: X-ray Crystal Structures, Hydrogen Bond Synthons and Melting Point Alternation.
Peddy Vishweshwar, Ashwini Nangia and Vincent M. Lynch
Cryst. Growth Des., **2003**, 3, ASAP.
9. Self-assembly of Interpenetrated Diamondoid Network from C3 Symmetry Tecton.
Peddy Vishweshwar, Balakrishna R. Bhogala and Ashwini Nangia (manuscript in preparation).
10. The Role of σ - and π -Bond Cooperativity in a Very Short O–H \cdots O Hydrogen Bond. Variable Temperature Neutron Diffraction Analysis of 2,3,5,6-Pyrazinetetracarboxylic Acid Dihydrate.
Peddy Vishweshwar, Ashwini Nangia, Sax A. Mason, Charlotte K. Broder and Judith A.K. Howard (manuscript in preparation).

ABOUT THE AUTHOR

Peddy Vishweshwar was born in Pipri, a village in Nizamabad district of Andhra Pradesh, India, in 1975. He received his elementary and secondary school education in Ramagundam, Armoor and Nirmal. After completion of B.Sc. and M.Sc. degrees from Osmania University, Hyderabad, he joined the School of Chemistry, University of Hyderabad for M.Phil. in 1997 and continued for his Ph.D. degree in 1998.

*To
My Parents*

APPENDIX

Table 1. Salient Crystallographic details of the compounds discussed in this thesis.

	<i>Chapter 2</i>			
	2	3	4	11
Empirical formula	C ₆ H ₆ N ₂ O ₂	C ₆ H ₆ N ₂ O ₂	C ₆ H ₆ N ₂ O ₂	C ₆ H ₄ N ₂ O ₄ ·(H ₂ O) ₂
Formula wt.	138.13	138.13	138.13	204.14
Crystal system	Monoclinic	Monoclinic	Orthorhombic	Triclinic
Space group	<i>P</i> 2 ₁ / <i>n</i>	<i>P</i> 2 ₁ / <i>c</i>	<i>Pca</i> 2 ₁	<i>P</i> $\bar{1}$
<i>a</i> [Å]	4.1037(8)	5.0546(2)	14.494(3)	5.2101(2)
<i>b</i> [Å]	11.597(2)	13.2795(6)	3.8090(8)	6.8261(2)
<i>c</i> [Å]	13.556(3)	9.1067(4)	11.269(2)	6.8713(2)
α [deg]	90	90	90	119.144(2)
β [deg]	93.34(3)	95.315(3)	90	99.808(2)
γ [deg]	90	90	90	99.927(2)
<i>Z</i>	4	4	4	1
Volume [Å ³]	644.0(2)	608.64(5)	622.1(2)	200.85(1)
<i>D</i> _{calc} [g/cm ³]	1.425	1.507	1.475	1.688
<i>T</i> [K]	293(2)	123(2)	173(2)	153(2)
<i>F</i> (000)	288	296	288	106
2 θ range	4.62–59.92	7.60–54.98	7.24–55.06	6.9–54.86
Index ranges	0 ≤ <i>h</i> ≤ 5	−6 ≤ <i>h</i> ≤ 6	−18 ≤ <i>h</i> ≤ 18	−6 ≤ <i>h</i> ≤ 5
	0 ≤ <i>k</i> ≤ 16	−17 ≤ <i>k</i> ≤ 16	−4 ≤ <i>k</i> ≤ 4	−8 ≤ <i>k</i> ≤ 7
	−18 ≤ <i>l</i> ≤ 18	−11 ≤ <i>l</i> ≤ 11	−14 ≤ <i>l</i> ≤ 14	−8 ≤ <i>l</i> ≤ 8
N-total	1870	8509	3793	1268
N-independent	1870	1392	1399	875
N-observed	1265	1174	1346	781
Parameters	113	115	115	80
<i>R</i> ₁	0.063	0.040	0.027	0.032
<i>wR</i> ₂	0.176	0.114	0.070	0.091
GOF	1.058	1.056	1.055	1.052

Table 1. *Continued...*

<i>Chapter 3</i>				<i>Chapter 4</i>
2	3	4	5	3
C ₆ H ₇ N ₃ O	C ₆ H ₇ N ₃ O	C ₆ H ₇ N ₃ O	C ₆ H ₆ N ₄ O ₂	C ₈ H ₈ N ₂ O ₄ · (H ₂ O) ₂
137.15	137.15	137.15	166.15	232.19
Monoclinic	Monoclinic	Orthorhombic	Triclinic	Orthorhombic
<i>P</i> 2 ₁ / <i>n</i>	<i>P</i> 2/ <i>c</i>	<i>Pna</i> 2 ₁	<i>P</i> $\bar{1}$	<i>Pbcn</i>
3.7758(8)	24.451(2)	8.3253(9)	5.0250(3)	12.6454(3)
6.7508(14)	3.7361(4)	15.6581(17)	7.0977(3)	9.0812(3)
25.289(5)	14.3545(12)	4.9806(5)	10.1196(5)	8.8800(3)
90	90	90	70.826(3)	90
93.09(3)	104.989(6)	90	81.868(3)	90
90	90	90	81.163(3)	90
4	8	4	2	4
643.7(2)	1266.7(2)	649.26(12)	335.25(3)	1019.74(5)
1.415	1.438	1.403	1.646	1.512
153(2)	123(2)	153(2)	153(2)	123(2)
288	576	288	172	488
6.2–55.0	5.8–55.0	7.2–55.0	6.28–60.04	7.18–54.96
$-4 \leq h \leq 4$	$-30 \leq h \leq 30$	$-10 \leq h \leq 10$	$-7 \leq h \leq 7$	$-16 \leq h \leq 16$
$-7 \leq k \leq 8$	$-4 \leq k \leq 4$	$-20 \leq k \leq 20$	$-9 \leq k \leq 9$	$-11 \leq k \leq 11$
$-32 \leq l \leq 32$	$-18 \leq l \leq 18$	$-6 \leq l \leq 6$	$-14 \leq l \leq 13$	$-11 \leq l \leq 11$
2405	4194	1287	2623	2132
1409	2648	1287	1868	1161
1202	1820	1180	1754	1059
119	237	119	133	97
0.038	0.071	0.038	0.035	0.031
0.104	0.203	0.094	0.101	0.086
1.10	1.02	1.08	1.058	1.069

Table 1. Continued...

Chapter 4				
1 (X-ray)	1 (Neutron)	1 (Neutron)	1 (Neutron)	1 (Neutron)
$\text{C}_8\text{H}_4\text{N}_2\text{O}_8 \cdot$	$\text{C}_8\text{H}_4\text{N}_2\text{O}_8 \cdot$	$\text{C}_8\text{H}_4\text{N}_2\text{O}_8 \cdot$	$\text{C}_8\text{H}_4\text{N}_2\text{O}_8 \cdot$	$\text{C}_8\text{H}_4\text{N}_2\text{O}_8 \cdot$
$(\text{H}_2\text{O})_2$	$(\text{H}_2\text{O})_2$	$(\text{H}_2\text{O})_2$	$(\text{H}_2\text{O})_2$	$(\text{H}_2\text{O})_2$
292.16	292.16	292.16	292.16	292.16
Triclinic	Triclinic	Triclinic	Triclinic	Triclinic
$P\bar{1}$	$P\bar{1}$	$P\bar{1}$	$P\bar{1}$	$P\bar{1}$
5.4409(3)	5.4361(10)	5.4385(10)	5.4606(10)	5.4950(10)
6.4041(3)	6.3699(10)	6.3885(10)	6.4133(10)	6.4410(10)
8.6995(3)	8.6672(10)	8.6809(10)	8.7164(10)	8.7670(10)
98.572(3)	97.911(5)	98.381(5)	98.962(5)	99.393(6)
107.374(3)	107.546(5)	107.406(5)	107.408(5)	107.565(7)
105.519(3)	105.718(5)	105.573(5)	105.348(5)	105.174(7)
1	1	1	1	1
269.97(2)	267.48(7)	268.72(7)	271.57(7)	275.44(8)
1.797	1.813	1.804	1.785	1.761
123(2)	20(1)	100(1)	200(1)	293(1)
150	100	100	100	100
6.82–54.88	6.0–64.18	6.0–80.28	5.98–64.22	6.0–64.2
$-7 \leq h \leq 7$	$-1 \leq h \leq 6$	$-1 \leq h \leq 8$	$-1 \leq h \leq 6$	$-1 \leq h \leq 6$
$-8 \leq k \leq 8$	$-8 \leq k \leq 7$	$-9 \leq k \leq 9$	$-8 \leq k \leq 7$	$-8 \leq k \leq 7$
$-11 \leq l \leq 11$	$-10 \leq l \leq 10$	$-13 \leq l \leq 12$	$-10 \leq l \leq 10$	$-10 \leq l \leq 10$
2300	1333	3123	1297	1295
1219	1123	1915	1123	1122
1125	1088	1762	1034	1040
107	135	135	135	135
0.030	0.019	0.023	0.020	0.021
0.082	0.043	0.046	0.048	0.046
1.082	1.222	1.168	1.128	1.120

Table 1. *Continued...*

<i>Chapter 5</i>				
OA•(IN)₂	MA•(IN)₂	SA•(IN)₂	GA•(IN)₂	AA•(IN)₂
(C ₂ H ₂ O ₄) _{0.5} · (C ₆ H ₆ N ₂ O)	(C ₃ H ₄ O ₄) ₃ · (C ₆ H ₆ N ₂ O) ₆	(C ₄ H ₆ O ₄) _{0.5} · (C ₆ H ₆ N ₂ O)	(C ₅ H ₈ O ₄) ₂ · (C ₆ H ₆ N ₂ O) ₄	(C ₆ H ₁₀ O ₄) _{0.5} · (C ₆ H ₆ N ₂ O)
167.15	1044.95	181.17	752.74	195.20
Monoclinic	Triclinic	Triclinic	Monoclinic	Triclinic
<i>C</i> 2/ <i>c</i>	<i>P</i> $\bar{1}$	<i>P</i> $\bar{1}$	<i>P</i> 2 ₁ / <i>n</i>	<i>P</i> $\bar{1}$
11.7466(2)	11.9420(2)	6.8198(2)	14.0439(2)	5.2522(1)
10.0164(2)	14.8580(2)	7.0650(2)	10.9859(1)	9.1180(2)
12.1967(2)	15.6820(2)	9.0971(3)	23.0238(4)	10.4487(3)
90	65.6990(6)	80.509(1)	90	104.473(1)
102.395(1)	85.5740(6)	77.614(1)	97.5560(5)	103.477(1)
90	67.3070(6)	72.838(1)	90	100.811(1)
8	2	2	4	2
1401.60(4)	2328.62(6)	406.62(2)	3521.4(12)	454.824(19)
1.584	1.490	1.480	1.420	1.425
153(2)	153(2)	153(2)	153(2)	153(2)
696	1092	190	1584	206
5.96–54.96	5.82–54.94	6.08–54.98	5.82–54.96	5.82–54.96
–15 ≤ <i>h</i> ≤ 15	–15 ≤ <i>h</i> ≤ 15	–8 ≤ <i>h</i> ≤ 7	–18 ≤ <i>h</i> ≤ 18	–6 ≤ <i>h</i> ≤ 6
–12 ≤ <i>k</i> ≤ 12	–15 ≤ <i>k</i> ≤ 19	–9 ≤ <i>k</i> ≤ 8	–14 ≤ <i>k</i> ≤ 12	–10 ≤ <i>k</i> ≤ 11
–15 ≤ <i>l</i> ≤ 15	–20 ≤ <i>l</i> ≤ 20	–11 ≤ <i>l</i> ≤ 11	–29 ≤ <i>l</i> ≤ 29	–10 ≤ <i>l</i> ≤ 13
2980	16180	2738	13721	3003
1596	10660	1818	7966	2012
1428	6898	1565	5020	1582
137	748	154	647	171
0.032	0.046	0.034	0.043	0.039
0.091	0.101	0.088	0.099	0.094
1.064	1.031	1.048	0.982	1.052

Table 1. Continued...

Chapter 5		Chapter 6		
GA•IN	AA•IN	1	2	3
(C ₅ H ₈ O ₄) · (C ₆ H ₆ N ₂ O)	(C ₆ H ₁₀ O ₄) · (C ₆ H ₆ N ₂ O)	(C ₆ H ₆ O ₂) _{0.5} · (C ₆ H ₆ N ₂ O)	(C ₆ H ₆ O ₂) · (C ₆ H ₆ N ₂ O) ₂	(C ₆ H ₆ O ₃) · (C ₆ H ₆ N ₂ O) ₂ · (H ₂ O) ₂
254.24	268.27	177.18	354.36	406.40
Monoclinic	Monoclinic	Monoclinic	Triclinic	Triclinic
<i>P</i> 2 ₁ / <i>c</i>	<i>P</i> 2 ₁ / <i>c</i>	<i>P</i> 2 ₁ / <i>c</i>	<i>P</i> $\bar{1}$	<i>P</i> $\bar{1}$
9.8980(3)	13.6429(4)	14.2811(4)	7.0307(1)	7.4967(1)
16.7520(6)	9.6159(2)	5.4136(2)	10.7052(2)	8.8748(1)
7.3150(5)	9.8215(2)	11.9110(3)	11.9562(2)	15.2793(3)
90	90	90	87.755(1)	95.1886(6)
95.479(2)	97.562(1)	111.934(1)	82.735(1)	97.4790(6)
90	90	90	73.835(1)	105.7701(7)
4	4	4	2	2
1207.37(10)	1277.26(5)	854.21(5)	857.36(2)	961.50(3)
1.399	1.395	1.378	1.373	1.404
153(2)	153(2)	153(2)	153(2)	153(2)
536	568	372	372	428
5.82–54.96	5.82–54.96	6.16–54.94	6.08–61.04	5.82–55.04
–12 ≤ <i>h</i> ≤ 12	–17 ≤ <i>h</i> ≤ 17	–18 ≤ <i>h</i> ≤ 18	–9 ≤ <i>h</i> ≤ 9	–9 ≤ <i>h</i> ≤ 9
–21 ≤ <i>k</i> ≤ 18	–10 ≤ <i>k</i> ≤ 12	–6 ≤ <i>k</i> ≤ 7	–15 ≤ <i>k</i> ≤ 14	–11 ≤ <i>k</i> ≤ 11
–9 ≤ <i>l</i> ≤ 9	–12 ≤ <i>l</i> ≤ 12	–15 ≤ <i>l</i> ≤ 15	–16 ≤ <i>l</i> ≤ 16	–15 ≤ <i>l</i> ≤ 19
4619	4705	3354	7843	6903
2710	2803	1933	4462	4275
1966	2235	1277	3324	3583
221	236	154	307	350
0.039	0.039	0.044	0.041	0.036
0.090	0.109	0.113	0.115	0.098
1.049	1.060	1.040	1.070	1.051

Table 1. *Continued...*

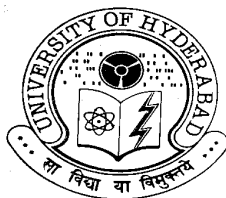
<i>Chapter 6</i>	<i>Chapter 7</i>	
4	CTA•H₂O	CTA•bipy
(C ₇ H ₆ O ₃) · (C ₆ H ₆ N ₂ O)	(C ₉ H ₁₂ O ₆) · (H ₂ O)	(C ₉ H ₁₂ O ₆) ₂ · (C ₁₀ H ₈ N ₂) ₃ · (H ₂ O)
260.25	234.20	918.94
Monoclinic	Monoclinic	Triclinic
<i>P</i> 2 ₁ / <i>n</i>	<i>C</i> 2/ <i>c</i>	<i>P</i> $\bar{1}$
6.0729(1)	22.255(14)	10.5609(4)
9.4013(2)	6.890(4)	14.2226(6)
20.6723(4)	16.204(12)	16.9229(7)
90	90	113.293(1)
95.287(1)	118.34(3)	102.553(1)
90	90	93.852(1)
4	8	2
1175.23(4)	2187(2)	2245.41(16)
1.471	1.423	1.359
153(2)	93(2)	93(2)
544	992	968
5.86–54.98	4.16–49.44	2.72–56.56
$-7 \leq h \leq 7$	$-23 \leq h \leq 26$	$-14 \leq h \leq 12$
$-12 \leq k \leq 12$	$-8 \leq k \leq 8$	$-18 \leq k \leq 18$
$-26 \leq l \leq 26$	$-19 \leq l \leq 18$	$-22 \leq l \leq 22$
4946	6482	18003
2684	1862	10662
1952	1708	7970
221	201	804
0.041	0.040	0.044
0.105	0.107	0.116
1.029	1.02	1.03

SYNOPSIS
of the thesis entitled

HETEROSYNTHONS IN CRYSTAL ENGINEERING

To be submitted for the Degree of
Doctor of Philosophy

By
P. VISHWESHWAR



Thesis Supervisor: Prof. Ashwini Nangia

School of Chemistry
University of Hyderabad
Hyderabad 500 046
India

The thesis entitled “**Heterosynthons in Crystal Engineering**” consists of seven chapters. Chapter 1 gives an overview of crystal engineering and supramolecular chemistry. Chapter 2 describes the recurrence of carboxylic acid–pyridine supramolecular synthon in the crystal structures of some pyrazine mono carboxylic acids. Pyrazine di- and tetracarboxylic acids crystallize as hydrates. Crystal structures of methyl isomers of pyrazinecarboxamide are discussed in Chapter 3. Chapter 4 deals with the occurrence of very short (strong) O–H \cdots O hydrogen bond in pyrazine-2,3,5,6-tetracarboxylic acid ascribed to the cumulative stabilization from the σ - and π - bond cooperativity. Hydrogen bond recognition motifs in molecular complexes of α , ω -aliphatic dicarboxylic acids with isonicotinamide are discussed in Chapter 5. Chapter 6 deals with the study of supramolecular synthons in phenol–isonicotinamide adducts. Interpenetrated hydrogen bond networks in the crystal structures of cyclohexane-1,3,5-tricarboxylic acid monohydrate and its complex with 4,4'-bipyridine are described in Chapter 7.

CHAPTER ONE

CRYSTAL ENGINEERING

Modern organic chemistry finds itself at the onset of a fascinating new period in which interest is directed beyond the covalent bond, towards the construction of organized systems of cooperative molecules in which each molecule has its distinct location and specific role. Crystal engineering is one of the promising fields in this new endeavor, offering routes to the rational design of functional solids. The term ‘crystal engineering’ was first coined by Schmidt in 1971 in the context of organic solid-state photochemical reactions of cinnamic acids.¹ A broad definition of crystal engineering² was suggested by Desiraju as *"the understanding of intermolecular interactions in the context of crystal packing and the utilization of such understanding in the design of new solids with desired physical and chemical properties"*. The aim of crystal engineering is to establish rigorous connections between molecular structure and supramolecular architecture *via* intermolecular interactions. Crystal engineering is a rapidly growing field because it lies at the intersection of ‘top down’ and ‘bottom up’ technologies for supramolecular materials.³

Rationalization, analysis, design and prediction are the key elements in crystal engineering. In this context, the supramolecular synthon⁴ concept simplifies the rationalization and non-covalent synthesis of crystal structures. Analysis means examination of various intermolecular interactions that govern the crystal packing. This is mainly carried out by the analysis of structural data archived in the Cambridge Structural Database (CSD)⁵ and through computational methods. Design involves the utilization of the knowledge thus gained in the synthesis of novel structures. However, success in design and synthesis is often hindered by polymorphism⁶, i.e. the different ways in which molecules are arranged in a crystal structure.

Crystal engineering is an inter-disciplinary field that seeks to develop protocols for predicting and controlling the structure and thus the functional properties of solids. Such properties range from the commonplace (colour, melting point) to those of great relevance to materials scientists and physicists (polarity, porosity, conductivity) and pharmaceutical development (active drug form, bioavailability). Some of the key research areas under the purview of crystal engineering include:⁷ catalysis, optical, conducting and magnetic materials, nanotechnology, electronic materials and sensors, protein-receptor binding, nano and microporous materials, supramolecular devices, molecular modeling and drug design.

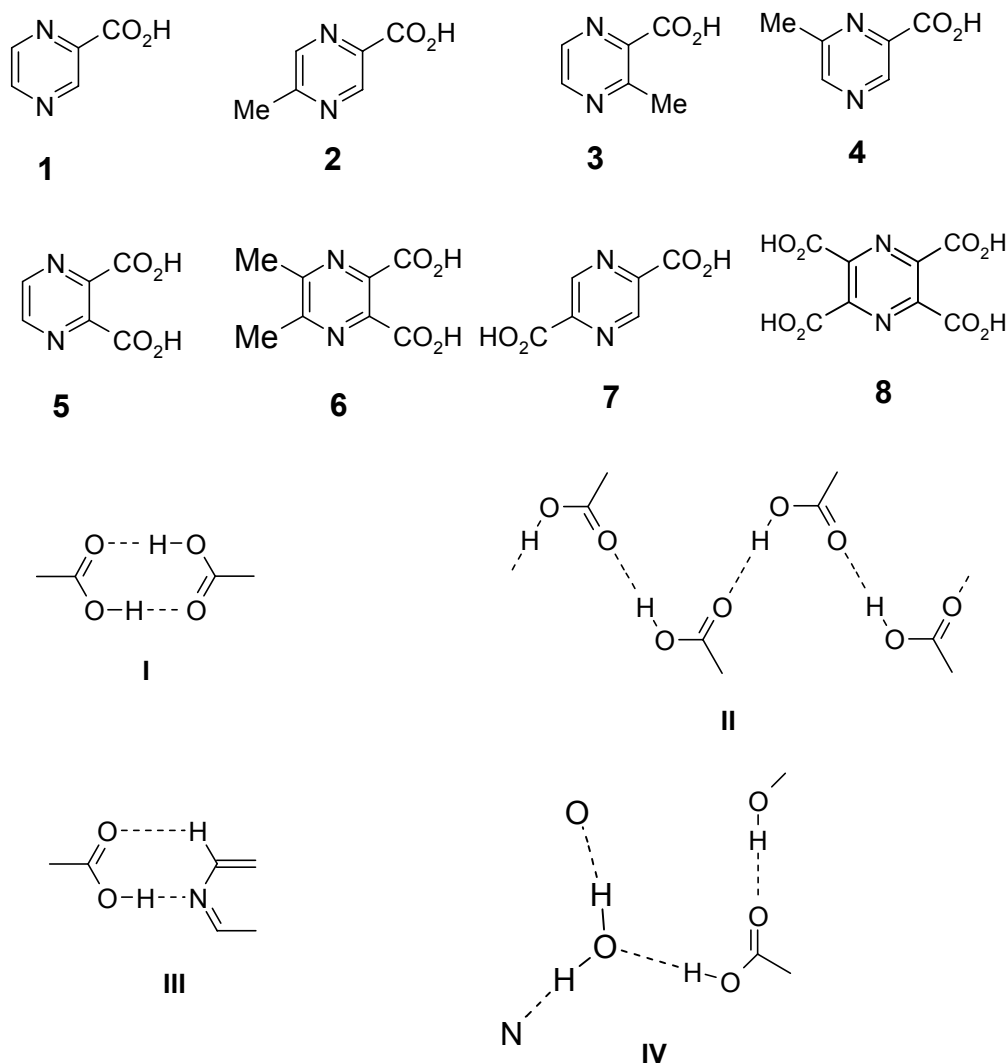
This thesis mainly deals with the self-assembly of target architectures from molecular scaffolds mediated by hydrogen bonding between unlike functional groups, defined as heterosynthon (Chapters 2, 5, 6 and 7). Chapters 3 and 4 deal with homosynthons and very short (strong) hydrogen bonds in pyrazine–amides and acids, respectively.

CHAPTER TWO

CARBOXYLIC ACID–PYRIDINE SUPRAMOLECULAR SYNTHON

Carboxylic acids are among the best-investigated hydrogen bonded functionalities in crystal engineering.⁸ Carboxylic acids are well known to form cyclic dimer synthon **I** and open catemer **II**. The crystal packing patterns of various carboxylic acids have been examined in depth and thus they are considered as the most important building block in crystal design. A recent survey of the CSD⁹ shows that aggregation of O–H group of

carboxylic acids with heteroatoms (pyridine N, S=O, P=O, COO⁻) are more pronounced compared to dimer **I** and catemer **II** motifs with itself and that acid–acid aggregation generally does not form when competing acceptor groups are present in the system. Thus, crystal design may be predictably implemented by exploiting the robust recognition in a heterosynthon (e.g. synthon **III**)¹⁰



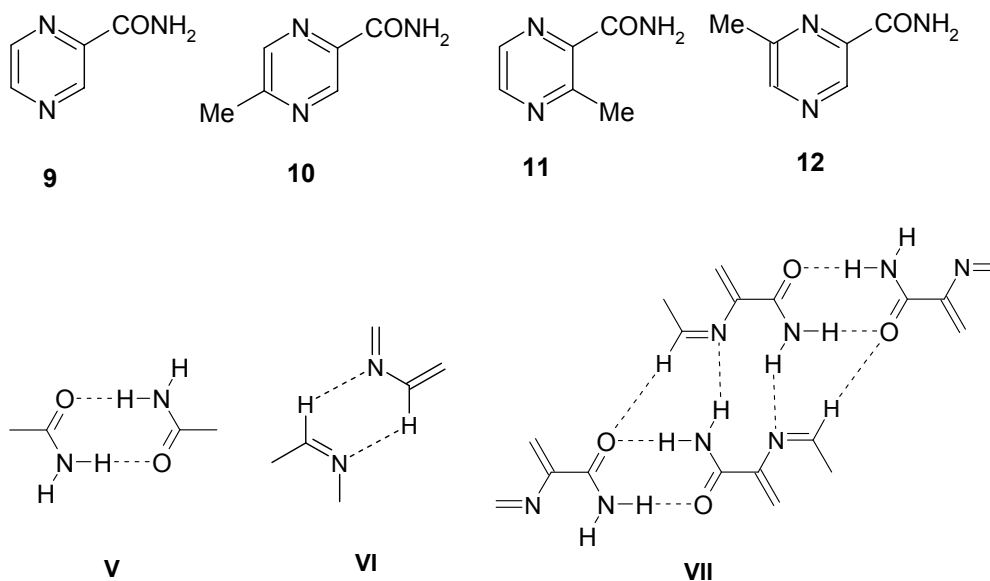
In the present study, X-ray crystal structures of pyrazinic acid **1** and isomeric methylpyrazine carboxylic acids **2–4** are analyzed to examine the robustness of synthon **III** in these heterocyclic acids. In all the pyrazine mono-carboxylic acids **1–4**, carboxylic acids forms synthon **III** through (carboxyl)O–H···N(pyridine) and (pyridine)C–H···O(carbonyl) hydrogen bonds. The recurrence of acid–pyridine heterosynthon **III**

compared to the more common acid–acid homodimer **I** in these crystal structures has been explained by energy computations with the RHF/6-31G* basis set. Both the O–H···N and C–H···O hydrogen bonds in synthon **III** result from activated acidic donor and basic acceptor atoms in **1–4**. Pyrazine dicarboxylic acids **5**, **6**, **7** and tetracarboxylic acid **8** crystallize as dihydrate with a (carboxyl)O–H···O(water) hydrogen bond (synthon **IV**), a recurring pattern in pyrazine di- and tetracarboxylic acids.

CHAPTER THREE

SUPRAMOLECULAR SYNTHONS IN PYRAZINE CARBOXAMIDES

The role of the carboxamide group in crystal packing and molecular recognition is well studied.¹¹ The most common pattern is the centrosymmetric dimer **V**, formed with the *syn*-N–H of amide. The *anti*-oriented N–H group forms either a linear tape with a 5.1 Å translation or one-dimensional catemer where adjacent molecules are related by glide plane or 2₁ axis. Pyrazinecarboxamide **9** an antituberculosis drug is a rare example of a compound with five different polymorphic forms.¹² The occurrence of polymorphism can also be explained in terms of supramolecular synthons. If a functional group can form more than one synthon this would lead to the possibility of polymorphism. In pyrazinecarboxamide the same dimer synthon **VI**, is formed from chemically distinct locations of the molecule leading to polymorphism.

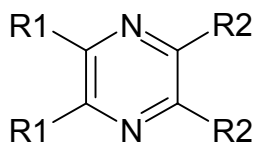


In this chapter, the crystal chemistry of a family of methyl pyrazine carboxamides **10–12** are examined. 5-methylpyrazine-2-carboxamide **10** and 3-methylpyrazine-2-carboxamides **11** form the centrosymmetric amide dimer **V**. Such dimers are not connected *via* the 5.1 Å short axis, instead the *anti* N–H group of amide connects to the pyrazine nitrogen through N–H \cdots N hydrogen bond (motif **VII**) with short axis of 7.7 and 7.4 Å in **10** and **11** respectively. The crystal structure of 5-methylpyrazine-2-carboxamide is similar to the α -polymorph of pyrazinecarboxamide. 6-methylpyrazine-2-carboxamide **12** forms a catemer motif through N–H \cdots O hydrogen bonds. Some features common to the polymorphs of pyrazinenamide are observed in the methyl isomers of pyrazinecarboxamide.

CHAPTER FOUR

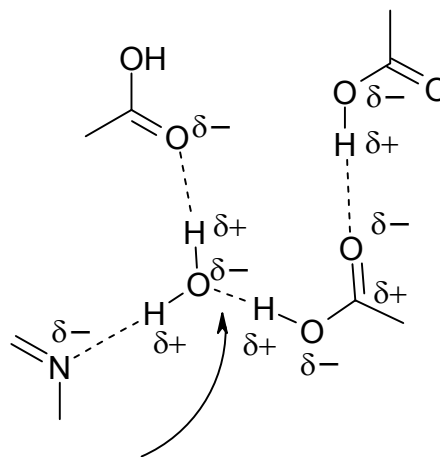
VERY SHORT O–H \cdots O HYDROGEN BOND: A NEUTRON STUDY

Hydrogen bonds may be classified as very strong, strong and weak.¹³ Very strong hydrogen bonds are formed by unusually activated donors and acceptors, often in an intra molecular situation.¹⁴ In general they are formed between an acid and its conjugate base, O–H \cdots O[–], or between a base and its conjugate acid, O⁺–H \cdots O. With H \cdots O distances in the range 1.2–1.5 (O \cdots O: 2.2–2.5 Å), very strong hydrogen bonds have a significant covalent character and have energies in the range of 15–40 kcal/mol. The substantial covalent character of very strong hydrogen bonds, a result of three-center-four-electron contribution, O \cdot –H \cdots O \cdot \leftrightarrow O \cdot \cdots H \cdot –O, is responsible for their distinctive properties: the near linear angular geometry ($\theta = 170$ – 180°), the lengthening of O–H covalent bond, and the red shift in IR stretching frequencies (up to 2000 cm^{–1}). Very strong hydrogen bonds are also called as low-barrier or polarization enhanced hydrogen bonds.¹⁵ Very strong intermolecular hydrogen bonds are generally observed when there is charge-assistance (CAHB: O–H \cdots O[–], O⁺–H \cdots O) like in carboxylic acids or in the neutral β -diketone enol fragment \cdots O=C–C=C–OH \cdots wherein resonance-assistance (RAHB) through π -bonds results in unusual bond shortening.¹⁶



13: R1 = R2 = CO₂H

14: R1 = CH₃, R2 = CO₂H



Very short H-bond

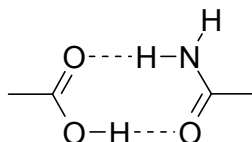
VIII

The present chapter describes a very short intermolecular O–H···O hydrogen bond formed between carboxylic acid and water molecule in the crystal structure of pyrazine-2,3,5,6-tetracarboxylic acid dihydrate **13**. In contrast to the role of charge- and resonance-assistance in very strong hydrogen bonds, a very short O_{acid}–H···O_{water} [*d* = 1.50 Å, *D* = 2.4791(13) Å, θ = 170.3°] hydrogen bond is ascribed to the cumulative stabilization from σ - and π - bond cooperativity. In this very short hydrogen bond, both the carboxylic acid O–H donor and water oxygen atom acceptor basicity are simultaneously enhanced through polarization as shown above. There is no proton transfer from acid to water oxygen as all the protons are located from the difference Fourier map. Crystal structure of 5,6-dimethylpyrazine-2,3-dicarboxylic acid **14**, is also studied in order to probe such polarization-induced hydrogen bond shortening. However, in **14**, the O_{acid}–H···O_{water} [*d* = 1.55 Å, *D* = 2.5269(12) Å, θ = 167.2°] hydrogen bond is of moderate length. Since X-ray cannot locate the proton position very precisely, neutron diffraction has been carried out to locate the proton positions accurately. Variable temperature neutron diffraction (at 20, 100, 200 and 293 K) confirms that there is no proton migration from acid to water oxygen, thus supporting the hypothesis of hydrogen bond shortening in a finite cooperative array of σ - and π -bonds (motif **VIII**).

CHAPTER FIVE

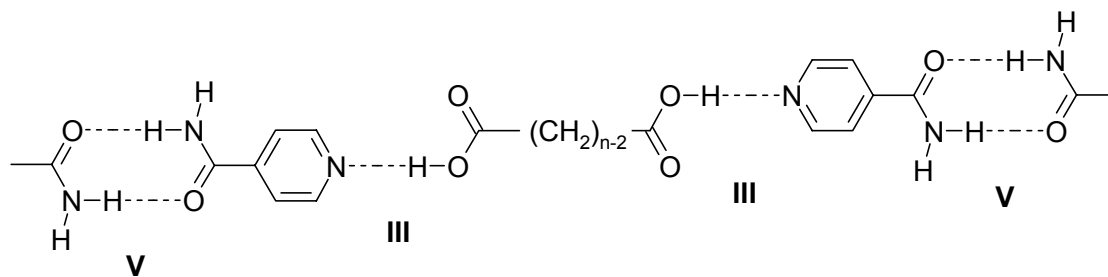
HYDROGEN BONDING IN CARBOXYLIC ACID–ISONICOTINAMIDE COMPLEXES

Hydrogen bond is the most reliable directional interaction in molecular recognition and its significance in crystal engineering, supramolecular chemistry and biological recognition is by now well established. As mentioned in the previous chapters carboxylic acids and amides are two commonly used functional groups in crystal engineering because they generally form robust architectures *via* O–H...O and N–H...O hydrogen-bonded dimers. However, the understanding of the factors that direct hydrogen-bonding motifs when other functional groups are also present in the molecule is not properly understood. The main challenge in carrying out crystal design with multi-functional molecules is that one is unable to predict when a particular functional group (e.g. pyridine, amide, hydroxyl) will perturb the normal hydrogen bond motif of a given functional group (e.g. CO₂H) and in what way the motif will change.

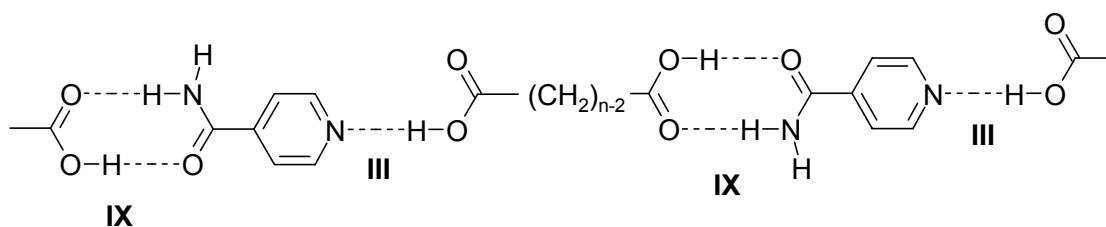


IX

In this background, crystallization of α,ω -alkanedicarboxylic acids with isonicotinamide (IN) are carried out and their X-ray structures determined. Five co-crystals of (diacid)•(IN)₂ composition (diacid = oxalic acid, malonic acid, succinic acid, glutaric acid and adipic acid) form tapes of acid–pyridine and amide–amide synthons **III** and **V**, as predicted by the hierarchic model of Etter,¹⁷ the best donor (COOH) and best acceptor (pyridine N) hydrogen bond as acid–pyridine synthon **III** and the second best donor-acceptor group (CONH₂) aggregates as amide dimer **V**. However, glutaric and adipic acids co-crystallize in 1:1 stoichiometry also (diacid)•(IN) with acid–pyridine **III** and acid-amide **IX** synthons. Synthon energy computations (Spartan, RHF/6-31G**) have been utilized to explain why 1:1 co-crystals are obtained for the weaker glutaric and adipic acids. Furthermore, melting point alternation in five homologous (diacid)•(IN)₂ co-crystals is correlated with the changes in crystal density and packing fraction.



Dicarboxylic acid: IN (1:2); $n = 2-6$

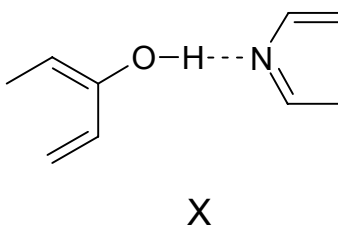


Dicarboxylic acid: IN (1:1); $n = 5, 6$

CHAPTER SIX

HYDROGEN BOND SYNTHONS IN PHENOL–ISONICOTINAMIDE COMPLEXES

Crystal engineering with multi-functional systems requires a proper understanding of the factors that control supramolecular organization when different hydrogen bond synthons are in competition. Crystallization of phenol with pyridine (O–H \cdots N hydrogen bond) has been carried out to build structures with intricate supramolecular architectures,¹⁸ non-linear optics,¹⁹ to synthesize host-guest complexes,²⁰ and as supramolecular template to direct topochemical reactions.²¹ Proton transfer in a very short O–H \cdots N hydrogen bond in pentachlorophenol–4-methylpyridine has been studied by variable temperature neutron diffraction.²²



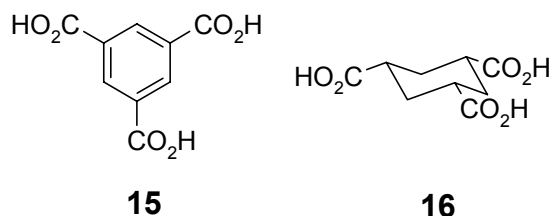
Chapter 6 describes the molecular complexes of four phenols (hydroquinone, resorcinol, phloroglucinol and 4-hydroxybenzoic acid) with isonicotinamide (IN). Study

of phenol–isonicotinamide co-crystals gives a better understanding of hydrogen bond competition and interplay between O–H...O, O–H...N and N–H...O hydrogen bonds in binary systems. It was anticipated that bis- and tris-phenols would hydrogen bond with the pyridine moiety of isonicotinamide through O–H...N hydrogen bond **X** and the amide functional group will extend the hydrogen bond aggregate *via* amide dimer motif **V**. As expected (hydroquinone)_{0.5}•(IN) and (resorcinol)•(IN)₂ have tapes of O–H...N and amide N–H...O dimer synthons. In (phloroglucinol)•(IN)₂•(H₂O)₂, six component self-assembly results in stacked dimer with four O–H...N and four N–H...O hydrogen bonds. The structure (4-hydroxybenzoic acid)•(IN) establishes the robustness of phenol–pyridine hydrogen bonding in the presence of carboxylic acid group. This is the first example of carboxylic acid–isonicotinamide co-crystal with acid–amide motif without acid–pyridine synthon.

CHAPTER SEVEN

HYDROGEN BOND NETWORKS IN CIS,CIS-1,3,5-CYCLOHEXANETRICARBOXYLIC ACID

One conceptual approach to building frameworks can be carried out by representing molecules as points or nodes and the intermolecular interactions as node connectors. The network structures formed by coordination polymers have been studied extensively in recent years. The exercise of generating network structures with new organic molecules will expand their scope and diversity. 1,3,5-benzenetricarboxylic acid (trimesic acid, TMA) **15** is an important building block in crystal engineering due its predictable honeycomb network in the crystal through acid–acid dimer synthon **I**. The α -polymorph of trimesic acid contains hexagonal rings made of TMA molecules with a diameter of approximately $14 \times 14 \text{ \AA}$.²³ The honeycomb grid in **15** is puckered and the cavities are filled by 4-fold inclined interpenetration. Zaworotko *et al.*,²⁴ have reported the crystal structure of (15)₂•(bipyridine)₃ complex stabilized by acid–pyridine synthon **III**. The hexagonal cavity of $35 \times 26 \text{ \AA}$ is filled by the 3-fold parallel interpenetration of independent networks.



The present chapter deals with the mode of interpenetration in the crystal structures of cyclohexane-1,3,5-tricarboxylic acid **16** and its co-crystal with bipyridine. The monohydrate of **16** forms a pseudohoneycomb network with voids of dimensions 15×11 Å. Such independent (6,3) nets interweave almost perpendicular to the 2D corrugated sheet of the original framework resulting in the 4-fold inclined interpenetrated network. The crystal structure of **16** (anhydrous form) determined by powder X-ray diffraction pattern was reported very recently.²⁵ It was anticipated that the network in **16** can be extended to generate larger cavities by employing the modular self-assembly approach. As expected the 15×11 Å cavity of **16** is expanded to 27×27 Å size when bipyridine is used as a spacer. **16**•bipyridine•H₂O (2:3:1) has 3-fold interweaving (6,3) networks with parallel interpenetration. There is a striking similarity of these hydrogen bond networks to those found in the crystal structures of trimesic acid and its complex with bipyridine.

List of Publications

1. Pyrazine-2,3-dicarboxamide.

Peddy Vishweshwar, Ashwini Nangia and Vincent M. Lynch

Acta Crystallogr., Sect. C, **2000**, 56, 1512–1514.

2. Cooperative Assistance in a Very Short O–H···O Hydrogen Bond. Low temperature X-ray Crystal Structures of 2,3,5,6-Pyrazinetetracarboxylic Acid and Related Acids.

Peddy Vishweshwar, Ashwini Nangia and Vincent M. Lynch

Chem. Commun., **2001**, 179–180.

3. Recurrence of Carboxylic acid–Pyridine Supramolecular Synthons in the Crystal Structures of Some Pyrazine Carboxylic Acids.
Peddy Vishweshwar, Ashwini Nangia and Vincent M. Lynch
J. Org. Chem., **2002**, 67, 556–565.
4. Four-fold Inclined Interpenetrated and Three-fold Parallel Interpenetrated Hydrogen bonded Networks in 1,3,5-Cyclohexanetricarboxylic Acid Hydrate and its Molecular Complex with 4,4'-Bipyridine.
Balakrishna R. Bhogala, **Peddy Vishweshwar** and Ashwini Nangia
Cryst. Growth Des., **2002**, 2, 325–328.
5. Supramolecular Synthons Based on N–H···N and C–H···O Hydrogen Bonds. Crystal Engineering of a Helical Structure with 5,5-Diethyl Barbituric Acid.
Peddy Vishweshwar, Ram Thaimattam, Mariusz Jaskólski and Gautam R. Desiraju
Chem. Commun., **2002**, 1830–1831.
6. Searching for Polymorph: Second Crystal Form of 6-Amino-2-Phenylsulfonylimino-1,2-dihydropyridine.
Ram K. R. Jetti, Roland Boese, Jagarlapudi A. R. P. Sarma, L. Sreenivas Reddy, **Peddy Vishweshwar** and Gautam R. Desiraju
Angew. Chem., **2003**, 115, 2008–2012; *Angew. Chem., Int. Ed.*, **2003**, 42, 1963–1967.
7. Supramolecular Synthons in Phenol–Isonicotinamide Adducts.
Peddy Vishweshwar, Ashwini Nangia and Vincent M. Lynch
CrystEngComm, **2003**, 5, 164–168.
8. Molecular Complexes of Homologous Alkanedicarboxylic Acids with Isonicotinamide: X-ray Crystal Structures, Hydrogen Bond Synthons and Melting Point Alternation.
Peddy Vishweshwar, Ashwini Nangia and Vincent M. Lynch
Cryst. Growth Des., (In Press)

References

1. G. M. J. Schmidt, *Pure Appl. Chem.*, **1971**, 27, 647.
2. G. R. Desiraju, *Crystal Engineering: The Design of Organic Solids*, Elsevier: Amsterdam, **1989**.
3. (a) M. R. Bryce (ed.), *J. Mat. Chem.*, Special Issue on Molecular Assemblies and Nanochemistry, **1997**, 7, 1069–1290. (b) D. N. Reinhoudt (ed.), *Perspectives in Supramolecular Chemistry*, Vol. 4, Supramolecular Materials and Technologies, Wiley, Chichester, **1999**. (c) M. A. Hillmeyer and J. S. Moore, *J. Phys. Org. Chem.*, Special Issue on Materials for the 21st Century, **2000**, 13, 765–879.
4. (a) G. R. Desiraju, *Angew. Chem., Int. Ed. Engl.*, **1995**, 34, 2311. (b) A. Nangia and G. R. Desiraju, *Top. Curr. Chem.*, **1998**, 198, 57.
5. (a) F. H. Allen, *Acta Crystallogr., Sect. B*, **2002**, 58, 380. (b) A. Nangia, *CrystEngComm*, **2002**, 4(17), 93.
6. J. Bernstein, *Polymorphism in Molecular Crystals*, Clarendon, Oxford, **2002**.
7. (a) C. V. K. Sharma, *Cryst. Growth Des.*, **2002**, 2, 465. (b) I. Weissbuch, M. Lahav and L. Leiserowitz, *Cryst. Growth Des.*, **2003**, 3, 125.
8. (a) S. S. Kuduva, D. C. Craig, A. Nangia and G. R. Desiraju, *J. Am. Chem. Soc.*, **1999**, 121, 1936. (b) Z. Berkovitch-Yellin and L. Leiserowitz, *J. Am. Chem. Soc.*, **1982**, 104, 4052. (c) L. Leiserowitz, *Acta Crystallogr., Sect. B*, **1976**, 32, 775.
9. T. Steiner, *Acta Crystallogr., Sect. B*, **2001**, 57, 103.
10. N. Shan, A. D. Bond and W. Jones, *Cryst. Eng.*, **2002**, 5, 9.
11. (a) S. S. Kuduva, D. Bläser, R. Boese and G. R. Desiraju, *J. Org. Chem.*, **2001**, 66, 1621. (b) J. C. MacDonald and G. M. Whitesides, *Chem. Rev.*, **1994**, 94, 2383. (c) L. Leiserowitz and G. M. Schmidt, *J. Chem. Soc. A*, **1969**, 2372.
12. G. R. Desiraju, *Science*, **1997**, 278, 404.
13. G. R. Desiraju and T. Steiner, *The Weak Hydrogen Bond in Structural Chemistry and Biology*, Oxford University Press, Oxford, **1999**.
14. V. Bertolasi, P. Gilli, V. Ferretti and G. Gilli, *J. Am. Chem. Soc.*, **1991**, 113, 4917.
15. G. A. Jeffrey, *An Introduction to Hydrogen bonding*, OUP, Oxford, **1997**.
16. V. Bertolasi, P. Gilli, V. Ferretti and G. Gilli, *Chem. Eur. J.*, **1996**, 2, 925.

17. (a) M. C. Etter, *Acc. Chem. Res.*, **1990**, 23, 120. (b) M. C. Etter, *J. Phys. Chem.*, **1991**, 95, 4601.
18. E. Corradi, S. V. Meille, M. T. Messina, P. Metrangolo and G. Resnati, *Angew. Chem., Int. Ed.*, **2000**, 39, 1782.
19. K.-S. Huang, D. Britton, M. C. Etter and S. R. Bryn, *J. Mater. Chem.*, **1997**, 7, 713.
20. S. Hoger, D. L. Morrison and V. Enkelman, *J. Am. Chem. Soc.*, **2002**, 124, 6734.
21. L. R. MacGillivray, *CrystEngComm*, **2002**, 4, 37.
22. T. Steiner, I. Majerz and C. C. Wilson, *Angew. Chem., Int. Ed.*, **2001**, 40, 2651.
23. (a) D. J. Duchamp and R. E. Marsh, *Acta Crystallogr., Sect. B*, **1969**, 25, 5. (b) F. H. Herbstein, *Top. Curr. Chem.*, **1987**, 140, 107.
24. C. V. K. Sharma and M. J. Zaworotko, *Chem. Commun.*, **1996**, 2655.
25. H. Nowell, N. Shan, J. P. Attfield, W. Jones and W. D. S. Motherwell, *Cryst. Eng.*, **2003**, 6, 57.